Cerebral Blood Flow Regulation, Aging, and Cerebral Vessel Anatomy in Humans

By

Kathleen Byrne Miller

A dissertation submitted in partial fulfillment

of the requirements for the degree of

Doctor of Philosophy

(Kinesiology)

At the

UNIVERSITY OF WISCONSIN-MADISON

2021

Date of final oral examination: 06/18/2021

The dissertation is approved by the following members of the Final Oral Committee:

Jill Barnes, Assistant Professor, Kinesiology

Dane Cook, Professor, Kinesiology

Sterling Johnson, Professor, Geriatrics

Oliver Wieben, Professor, Medical Physics and Radiology

Marlowe Eldridge, Professor, Pediatrics

ACKNOWLEDGEMENT

To my advisor, Dr. Jill Barnes. Jill, thank you for your unwavering support and dedication to my mentorship. When I started in the lab, one of your former students told me how lucky I was to have you as a mentor. They were absolutely right. Under your guidance, working in your laboratory has been a transformative, unique, and wonderful experience. It is hard for me to put into words how thankful I am. I look up to you in so many ways and will carry your teachings with me for my entire life.

To my dissertation committee, Dr. Oliver Wieben, Dr. Sterling Johnson, Dr. Dane Cook and Dr. Marlowe Eldridge, thank you for your patience, guidance, and support of my dissertation projects and your flexibility during the pandemic. Dr. Wieben, thank you for your mentorship with the MRI techniques and welcoming me into the ADRD imaging group. Dr. Johnson, thank you for welcoming and facilitating our collaborations with the ADRC. Dr. Cook, thank you for your continued mentorship on my dissertation projects and my fellowship application. Dr. Eldridge, thank you for your mentorship over the years and even allowing me to do some experiments in your laboratory with your students who have become lifelong friends.

To the members of the Barnes Laboratory, Anna Howery, Adam Corkery, Nicole Eisenmann and Andrew Pearson, I am incredibly thankful for my experiences working with you all and I am not sure what I am going to do without you. I will always cherish our friendships and times together, even when we got stuck in Orlando Florida. I also want to thank the undergraduates I have worked with throughout the years who have been

tremendously helpful. One of my greatest joys has been seeing what you have all gone onto accomplish after your time in the lab.

To the students, faculty, and staff in the Department of Kinesiology. Thank you for creating an environment that was my home for almost 10 years. To Dr. Schrage and Dr. Diffee, I think I took every class you have both ever offered and thoroughly enjoyed them all. To the other graduate students in the department, thank you for your lifelong friendships. To Laura, Kristin, Angie and Joe, I know that wherever we are in the world I can always count on a plate of nachos to share. To Neda, Brianna, and Jess, I can always count on you all to be cheering the good times and during the pandemic, anti-cheering to the not so good times.

To my family, thank you for your love and support. To my mom, Nancy, who has taught me that the most important thing to be is kind. To my dad, Steven, who reminds me not to take life too seriously. To my brother Evan, who inspires me to travel and try new things. To my grandparents, Donald and Marlyce, for their continued attention to my life. To my late grandparents, John and Joyce, for their emphasis on the importance of education.

To Brodan, my partner who has been with me every step of the way. I feel so incredibly grateful to have gone through this experience with you by my side. Thank you for accepting me as I am and inspiring me to be my best self. I can't wait for what our future has in store.

To all who have made this experience possible, I cannot thank you enough.

~Kathleen Miller, June 2021

ABSTRACT

As the global population continues to age, understanding how cerebral blood flow changes with healthy aging is important to determine physiology from pathology. However, the study of cerebral blood flow (CBF) regulation in humans is complex as the encapsulation of the brain in the skull makes the brain's vasculature difficult to image. Furthermore, studies of cerebrovascular anatomy suggest that over 50% of humans do not have standard anatomical configurations. Thus, inferences regarding CBF regulation in an individual with the standard anatomical configuration may not translate to others. This dissertation will describe 1) the effect of aging on cerebrovascular function 2) the age-related changes in CBF in adults with a cerebral anatomical variation (vertebral artery hypoplasia) and 3) the prevalence of vertebral artery hypoplasia in a larger cohort of cognitively unimpaired adults with enriched risk for Alzheimer's disease. Using *in vivo* standard (transcranial Doppler ultrasound) and novel (4D flow phase contrast MRI) imaging techniques, the results from these studies suggest that there are age-related differences in cerebrovascular function. In addition, an anatomical variation in the posterior circulation (vertebral artery hypoplasia) impacts the age-related differences in regional cerebral blood flow. Furthermore, vertebral artery hypoplasia is associated with lower global cerebral blood flow even after adjusting for vascular risk factors. Taken together, these findings suggest that cerebral anatomical variations may affect the age-related changes in cerebral blood flow regulation and could be considered a risk factor for cerebral hypoperfusion.

TABLE OF CONTENTS

LIST OF FIGURES

LIST OF TABLES

LIST OF APPENDICES

LIST OF ABBREVIATIONS

[^{15}O]: Oxygen 15 labeled water

ACA: Anterior cerebral artery

ACOM: Anterior communicating artery

AD: Alzheimer's disease

ADRC: Alzheimer's Disease Research Center

AIx: Aortic augmentation index

ANOVA: Analysis of variance

APOE: Apolipoprotein E

ASL: Arterial spin labeling

ATP: Adenosine triphosphate

BA: Basilar artery

BOLD: Blood oxygenation level dependent

CBF: Cerebral blood flow

CBFv: Cerebral blood flow velocity

cfPWV: Carotid-femoral pulse wave velocity

CO: Cardiac output

CO_2: Carbon dioxide

COPD: Chronic obstructive pulmonary disease

COX: Cyclooxygenase

CPP: Cerebral perfusion pressure

CSA: Cross-sectional area

CSF: Cerebral spinal fluid

CTA: Computed tomography angiography

CVC: Cerebrovascular conductance

CVCi: Cerebrovascular conductance index

CVR: Cerebrovascular reactivity

ECG: Electrocardiogram

EDV: End-diastolic velocity

$ETCO_2$: end-tidal carbon dioxide

fMRI: functional magnetic resonance imaging

FOV: Field of view

GM: Gray matter

HR: Heart rate

ICA: Internal carotid artery

ICP: Intracranial pressure

IMT: Intima-media thickness

MAP: Mean arterial pressure

MCA: Middle cerebral artery

MCAv: middle cerebral artery velocity

MCI: Mild cognitive impairment

MET: Metabolic equivalent

MRA: Magnetic resonance angiography

MRI: Magnetic resonance imaging

NO: Nitric oxide

NOS: Nitric oxide synthase

NVU: Neurovascular unit

O_2: oxygen

OA: Ophthalmic artery

PC: Phase contrast

PCA: Posterior cerebral artery

PCO_2: Partial pressure of carbon dioxide

PCOM: Posterior communicating artery

PET: Positron emission tomography

PI: Pulsatility index

PICA: Posterior inferior cerebellar arteries

PSV: Peak systolic velocity

SD: Standard deviation

SNA: Sympathetic nervous system activity

SPO_2: Peripheral capillary oxygen saturation

TCD: Transcranial Doppler ultrasound

TOF: Time of flight

VA: Vertebral artery

VAH: Vertebral artery hypoplasia

Venc: Velocity encoding

VO_2max: Maximal oxygen uptake

VSMC: Vascular smooth muscle cell

WM: White matter

CHAPTER 1

1. GENERAL INTRODUCTION

"Perhaps no other organ of the body is less adapted to an experimental study of its circulation than the brain" Carl J Wiggers, 1905.

Encapsulated in the skull lies the brain, the most complex organ, and the center of human life. Though the brain is only three pounds, it is responsible for regulating the organ systems, integrating and interpreting stimuli from the outside world, and embodying intelligence, personality, memory, creativity, and emotion. The brain has an extensive and exquisite circulatory system required for supporting its connections of 86 billion neurons. It relies on this system for consistent and adequate blood flow delivery. Loss of blood flow to the brain can cause irreversible damage in a matter of seconds (Lipton, 1999).

The study of the brain's circulation has challenged humans for centuries. The skull provides adequate protection such that blood vessels in the brain cannot be easily imaged or experimentally manipulated. In addition, despite detailed drawings of the cerebral vessel anatomy dating back to the 17th century, it is estimated that up to 50% of humans do not have these "standard" configurations of cerebral anatomy (Alpers et al., 1959). Thus, inferences regarding cerebral blood flow (CBF) regulation in an individual with a certain anatomical configuration may not translate to others.

The population is aging, and in the United States, the people over the age of 65 are expected to grow to over 21% of the population by 2040 (Sidney et al., 2019). With the increase in age comes an increase in prevalence of neurodegenerative diseases including dementia (Wu et al., 2017). Studies of the etiology of dementia, or cognitive decline, have revealed an intersection

between age-related neurodegeneration and vascular degeneration (Kisler et al., 2017). Thus, to improve the understanding of this neurovascular organ, insight into the brain's circulatory system, and its ability to regulate blood flow, is essential.

This dissertation employs *in vivo* human studies to describe 1) the effect of aging on cerebrovascular function 2) age-related changes in CBF in adults with a cerebral anatomical variation (vertebral artery hypoplasia) and 3) the prevalence of vertebral artery hypoplasia in a larger cohort of cognitively unimpaired adults with enriched risk for Alzheimer's disease.

The dissertation is comprised of five chapters. The first chapter describes the specific aims of the studies, the background literature, and the significance of the aims. The second chapter describes the first experimental study and results, the third chapter describes the second experimental study and results, and the fourth chapter describes the third experimental study and results. The fifth chapter provides a synthetized discussion and conclusion.

1.2 THESIS OBJECTIVE AND HYPOTHESIS

The central aim of this thesis is to evaluate CBF regulation of large intracranial vessels in aging humans. The overarching hypothesis is that there will be age-related differences in CBF regulation and a regional cerebral anatomical variation, vertebral artery hypoplasia, will influence CBF regulation. The specific aims and hypotheses for each experimental study will be outlined in upcoming chapters.

1.3 INTRODUCTION AND SPECIFIC AIMS

Adequate cerebral blood flow regulation is essential for brain function. The brain utilizes 20% of the body's total oxygen and cardiac output despite being only 3% of the total body weight (Lassen, 1959). As the functional unit of the brain is the neurovascular unit, the vasculature is important to consider regarding cognitive function (Guo and Lo, 2009; Iadecola, 2017). In a healthy brain, blood flow is regulated to areas of the brain with high neuronal activity to match increased demands for oxygen and glucose (Girouard and Iadecola, 2006). In conditions with poor cerebral vascular function, areas of high metabolic demand may be under perfused and undergo neuronal death (Lipton, 1999). Importantly, reductions in CBF and cerebral vascular function may precede neurodegenerative pathology and adverse changes in cognitive function (Iadecola, 2004).

As the population in the world ages, the prevalence of cerebrovascular disease is projected to rise 25% by the year 2030 (Wu et al., 2017). It is becoming increasingly clear that vascular pathology contributes to the etiology of cognitive decline. For example, over 50% of Alzheimer's disease (AD) cases display vascular pathology upon post-mortem evaluation, regardless of the dementia diagnosis (Azarpazhooh et al., 2018; Santisteban and Iadecola, 2018; Schneider et al., 2009). Thus, understanding the regulation of CBF and how it changes with advancing age is important for distinguishing what is considered normal compared to what is pathologic.

It is important to note that the age-related changes in CBF may be regionally specific. Though many studies suggest age-related differences in CBF are more prominent in the anterior circulation (Matsuda et al., 1984; Melamed et al., 1980; Pagani et al., 2002), recent studies suggest that the relative age-related difference in CBF is greater in the posterior circulation (Albayrak et al., 2007; Dörfler et al., 2000; Olesen et al., 2019). In addition, evaluating the CBF response to a stimulus, compared to evaluating CBF at rest, may provide necessary insight into cerebrovascular

function (Willie et al., 2012). Many studies only report blood flow; however, further investigation into the rheology of the flow, such as dissecting the flow waveform into systolic and diastolic components and calculating cerebral pulsatility index (PI) (Gosling and King, 1974), may add information regarding the resistance of the cerebral microvessels. For example, higher cerebral PI is associated with distal vascular resistance (Giller et al., 1990), and cerebral PI increases with progression through the AD trajectory (Rivera-Rivera et al., 2016).

The brain is highly sensitive to changes in the partial pressure of carbon dioxide, as a decrease in pH in the perivascular space sets off a cascade of cellular events that augments CBF in order to wash out the hydrogen ions (Tominaga et al., 1976). Thus, the CBF response to hypercapnia is a common stimulus used to measure the function of the cerebral vessels, termed cerebrovascular reactivity (Xie et al., 2006). The impact of aging on cerebrovascular reactivity is controversial, with some studies showing no change (Braz and Fisher, 2016; Coverdale et al., 2017; Galvin et al., 2010; Madureira et al., 2017) and others showing age-related differences in reactivity to hypercapnia with age (Bailey et al., 2013; Barnes et al., 2012; Flück et al., 2014; Jaruchart et al., 2016; Kastrup et al., 1998; Oudegeest-Sander et al., 2014) (see Table 3 of Hoiland 2019 for review) (Hoiland et al., 2019). Discrepancies between studies may be due to the inclusion of adults with various vascular risk factors, methodical differences in both measuring CBF and administrating the CO_2 stimulus, and control of sex hormones.

Importantly, previous cross-sectional studies on cerebrovascular reactivity and aging included participants with various physical activity habits, exercise training history and cardiorespiratory fitness levels. For example, studies by Barnes et al., 2013 and Bailey et al., 2013 demonstrated a positive association between cerebrovascular reactivity and cardiorespiratory fitness in older adults. These results suggest that the age-related differences in cerebrovascular

reactivity may be attenuated by habitual exercise participation (Bailey et al., 2013; Barnes et al., 2013). Indeed, in our previous study, middle-aged healthy adults who were habitual exercisers (performed at least 150 minutes of moderate intensity aerobic exercise per week) had similar cerebrovascular reactivity compared with young adults (Miller et al., 2018). A recent meta-analysis found that cardiorespiratory fitness positively affects cerebrovascular function; however, the effect of an exercise intervention on cerebral blood flow characteristics is unclear (Smith et al., 2021). Therefore, habitual exercise status is important to consider when evaluating the effect of primary aging on cerebrovascular reactivity.

An additional consideration for studying cerebrovascular reactivity is the methodology used to evaluate cerebral blood flow. Transcranial Doppler ultrasound (TCD) is a common technique used to measure cerebral blood velocity through the middle cerebral artery (MCA). TCD relies on low frequency Doppler ultrasound and despite its high temporal resolution, this device has low special resolution and cannot measure the vessel diameter. Importantly, recent evidence suggests that the large intracranial vessels are in fact vasoactive in response to hypercapnia (Al-Khazraji et al., 2019; Brothers and Zhang, 2016; Coverdale et al., 2017; Hoiland and Ainslie, 2016; Verbree et al., 2014) proposing that measurements of blood flow velocity through TCD may be underestimating blood flow. The age-related changes in cerebrovascular reactivity to hypercapnia have not been studied using a technology that measures blood flow and vessel diameter simultaneously.

The lack of spatial resolution of the TCD presents an additional barrier to CBF research. The ultrasound probe can insonate only one vessel at a time, but the user cannot determine specifics of the intracranial anatomy. This is important, because it is possible that over 50% of people do not have “standard” intracranial vascular anatomy (Alpers et al., 1959), which likely impacts blood

flow regulation. For example, vertebral artery hypoplasia (VAH), a relatively common variation where one of the intracranial vertebral arteries is smaller than the other accompanied with low flow (Kulyk et al., 2018; Thierfelder et al., 2014), has been associated with cerebral hypoperfusion and increased risk of posterior stroke (Chuang et al., 2006; Hu et al., 2013; Mitsumura et al., 2016; Park et al., 2007). Despite its relatively high reported prevalence (15-35%) in healthy populations (Ogeng'o et al., 2014; Park et al., 2007; Peterson et al., 2010; Thierfelder et al., 2014; Zhang et al., 2016), CBF regulation in adults with VAH are understudied. Common techniques to detect VAH include ultrasound and angiographic MRI; however, determination of VAH using a technology that measures blood flow and vessel diameter simultaneously has not been employed. In addition, CBF regulation in adults with VAH are understudied, especially in non-stroke populations.

To address the gaps in the literature, this dissertation employs both traditional (TCD) and novel (4D flow MRI) techniques to measure CBF regulation in humans. It includes prospective studies of cross-sectional aging in a healthy cohort, as well as leverages existing data from a cohort of middle-aged and older adults that are risk-enriched for Alzheimer's disease. Collectively, these aims provide essential information to determine the age-related changes in CBF regulation and the impact of VAH. These studies provide rationale for longitudinal studies evaluating the impact of chronic reductions of CBF on cognitive function.

Specific Aim 1: To evaluate the impact of aging on cerebrovascular reactivity to hypercapnia using two imaging techniques.

- Hypothesis 1: There will be no age-related differences in cerebrovascular reactivity to hypercapnia in healthy, habitually exercising adults when evaluating cerebral blood velocity with TCD.

- Hypothesis 2: Older adults will have lower cerebrovascular reactivity to hypercapnia compared with young adults when evaluating cerebral blood flow using 4D flow MRI.
- Hypothesis 3: The middle cerebral artery will increase in cross-sectional area in response to hypercapnia in young adults, but not older adults.

Specific Aim 2: To determine the impact of VAH on the age-related differences in regional blood flow in the large intracranial arteries.

- Hypothesis 1: In healthy adults without VAH, age-related differences in CBF will be greater in posterior vessels compared with anterior vessels at rest and during hypercapnia.
- Hypothesis 2: In healthy adults with VAH, age-related differences in CBF will be greater in anterior vessels compared with posterior vessels at rest and during hypercapnia.
- Exploratory Hypothesis: Older adults will demonstrate higher cerebral pulsatility index in the large intracranial anterior and posterior vessels compared with young adults in both groups with and without VAH.

Specific Aim 3: To evaluate the impact of VAH on resting cerebral hemodynamics in a cohort of cognitively unimpaired adults with enriched risk for Alzheimer's disease.

- Hypothesis 1: The prevalence of VAH in this cohort will be comparable to previously reported values (15-35%).
- Hypothesis 2: Adults with VAH will have lower global CBF and lower blood flow in the major intracranial arteries compared with controls without VAH.
- Hypothesis 3: Adults with VAH will have higher global cerebral pulsatility index and higher pulsatility in the major intracranial arteries compared with controls without VAH.

1.4 BACKGROUND

1.4.1 CEREBRAL VASCULAR ANATOMY

Overview of Cerebral Vascular Anatomy

Shuttling energy rich blood to match the demand of 86 billion neurons requires a sophisticated and dynamic vascular system. The cerebrovascular system forms a 400-mile long vascular network (Begley and Brightman, 2003) with multiple roles including oxygen and substrate delivery to tissues, removal of waste products and acid-base balance. The cerebral vascular tree has three main components. The first component includes arteries and arterioles, which are tasked with delivering blood to the tissues. The arterial cerebrovascular system arises from the aorta and progressively divides into smaller arteries and arterioles that eventually enter into the skull and penetrate brain tissue (Jones, 1970). The second component of the cerebral vascular tree includes venules and veins, which are responsible for draining blood from the tissues. The cerebral venous system is comprised of both large surface veins and penetrating deep veins (Kiliç and Akakin, 2008). The third component is the capillary bed, which connects the arterial and venous systems and is essential for gas exchange and forming the blood brain barrier. Together, these three components are essential for the control of blood flow and maintenance of the brain's homeostatic environment. Of note, the brain's circulatory system does not only include blood vessels. Neurons and glial cells in close proximity to blood vessels are involved in blood flow regulation, termed the neurovascular unit (NVU). In the following sections, the anatomical configuration of the arterial and venous cerebral circulations, as well as the anatomy of the NVU, will be described.

Cerebral Anatomical Configuration

The closed loop nature of the cardiovascular circulation was first described by Dr. William Harvey in the early 1600's (Ribatti, 2009). Then, more accurate descriptions of the cerebral anatomy were illustrated by Casserius in his book *Tabulae anatomicae* in 1645 and Veslingius in his book *Syntagma Anatomica* in 1651 (Traystman, 2004). Later, much of the work detailing the cerebral circulation came from Thomas Willis's *Cerebri Anatome*, published in Latin in 1664 (O'Connor, 2003). Willis published his accounts describing cerebral anatomy through autopsy observations and injection of dies into the vasculature in humans and animals. He importantly described how blockage of one of the four major cerebral arteries did not lead to unconsciousness (O'Connor, 2003) and the identification of the brain's circular arterial system was his namesake, "the Circle of Willis". The following section is informed by *Gray's Anatomy, 39th edition: The Anatomical Basis of Clinical Practice* (Neuroradiology, 2005).

Blood flow into the cranium starts at the heart. The left ventricle ejects blood through the aortic arch. Branching off of the aortic arch is the brachiocephalic artery which splits into posteriorly into the right subclavian artery and anteriorly into the right common carotid artery. On the left side, both the left common carotid artery and the left subclavian artery branch directly off of the aortic arch (Figure 1). The right and left subclavian arteries branch to form the vertebral arteries which travel through the transverse foramina of the cervical vertebrae. The vertebral arteries enter the skull through the foramen magnum and unite as the basilar artery. The right and left common carotid arteries bifurcate to form the internal carotid artery and the external carotid artery. The internal carotid arteries enter the cranium through the brain carotid canal (Figure 1) and supply the majority of the anterior circulation whereas the external carotid arteries supply the majority of the blood flow to the face.

The intracranial circulation is derived from four major vessels, the right and left ICAs, supplying the majority of the anterior circulation and ~70% total CBF, and the right and left vertebral arteries (VAs), supplying the majority of the posterior circulation and ~30% total CBF. The vertebral arteries and their branches (the vertebro-basilar system) supply blood to the upper spinal cord, brainstem, cerebellum, and the posterior cerebral hemisphere. The posterior inferior cerebellar arteries (PICA) and the anterior spinal artery branch off of the vertebral arteries before they merge into the basilar artery on the midline of the ventral side of the brain. There are multiple branches off of the basilar artery including the Labyrinthine (internal auditory) artery, anterior inferior cerebellar artery, the pontine arteries, and the superior cerebellar arteries. Caudally to the pons, the basilar artery branches into the posterior cerebral arteries. The internal carotid arteries are the major suppliers to the anterior circulation, the eyes, and are responsible for connecting the anterior and posterior circulations via the Circle of Willis (Figure 2). At the level of the optic chiasm, the internal carotid artery splits into the anterior cerebral artery, supplying blood to the frontal lobes, and the middle cerebral artery, supplying blood to the parietal, temporal, and frontal lobes. The anterior cerebral arteries are connected by the anterior communicating artery. The ophthalmic arteries are also derived from the internal carotid arteries supplying blood flow to the ipsilateral eye. Rostral from the middle cerebral arteries, other branches of the internal carotid arteries include the anterior choroidal artery and the posterior communicating artery, which connects to the posterior cerebral artery. The posterior cerebral arteries, posterior communicating arteries, anterior cerebral arteries, and anterior communicating artery form the Circle of Willis (Figure 2). The function of the Circle of Willis is to supply blood to all areas of the brain; thus, the structure is built in such a way that if one or more of the major arteries that supply the brain (VAs

or ICAs) are compromised, another could support the area that would be otherwise ischemic (Riggs and Rupp, 1963).

To drain blood from the cerebral circulation, there are both superficial and deep systems. The primary superficial sinus is the superior sagittal sinus which runs along the sagittal plane of the entire cerebrum to the confluence of sinuses. At the confluence of sinuses, the right and left transverse sinus travel laterally around the superior cerebellum. The inferior branch of the transverse sinus forms the sigmoid sinus, which ultimately drains into the jugular veins. The jugular veins travel parallel to the carotid arteries and empty into the superior vena cava. The deep venous system is formed by veins in the deep structures of the brain. These include the inferior sagittal sinus and the straight sinus, which converges with the superior sinus system at the confluence of sinuses (Figure 3).

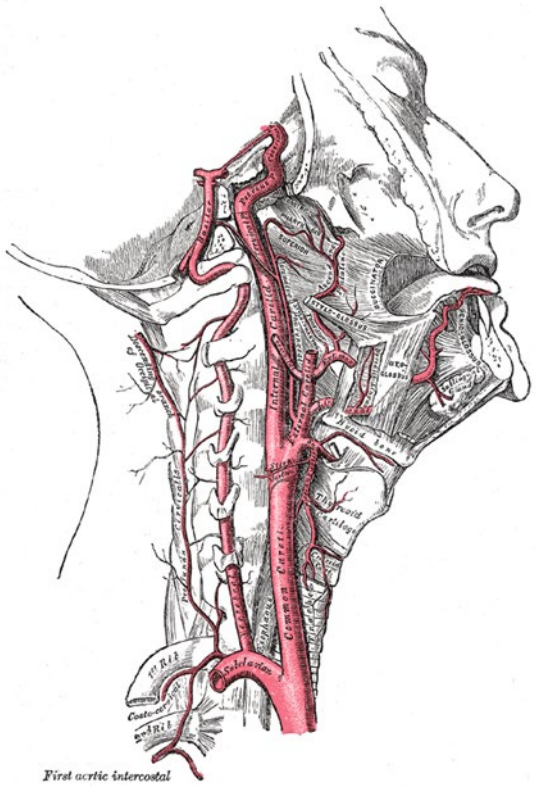

Figure 1. Large intracranial arteries of the head and neck viewed from the right side.

Shown are the subclavian artery, the vertebral artery, the common carotid artery, the internal carotid artery, and the external carotid artery.

Figure information:

Reproduction of a lithograph plate from Gray's Anatomy, originally published in 1918. It is not copyrightable in the United States as per Bridgeman Art Library v. Corel Corp. Neuroradiology, A.S. of (2005). Gray's Anatomy, 39th Edition: The Anatomical Basis of Clinical Practice. American Journal of Neuroradiology 26, 2703–2704.

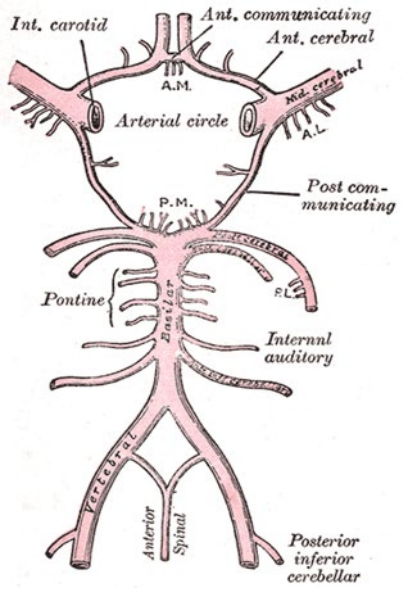

Figure 2. The arteries on the base of the brain that form the Circle of Willis.

Shown are the vertebral arteries and its branches, the anterior spinal artery and the posterior inferior cerebellar artery, the basilar artery and its branches, the internal auditory artery, the pontine arteries, the superior cerebellar arteries and the posterior cerebral arteries, the posterior communicating artery, the internal carotid arteries and its branches, the middle cerebral artery, the anterior communicating artery, and the anterior cerebral arteries. The posterior cerebral, posterior communicating, middle cerebral, anterior communicating and the anterior cerebral arteries make up the Circle of Willis.

Figure information:

Reproduction of a lithograph plate from Gray's Anatomy, originally published in 1918. It is not copyrightable in the United States as per Bridgeman Art Library v. Corel Corp. Neuroradiology, A.S. of (2005). Gray's Anatomy, 39th Edition: The Anatomical Basis of Clinical Practice. American Journal of Neuroradiology 26, 2703–2704.

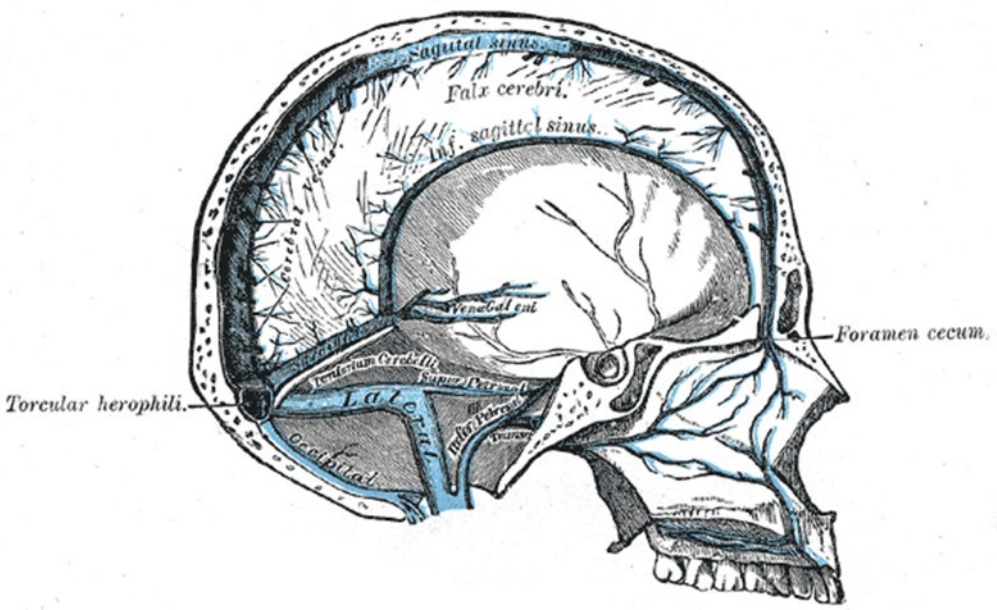

Figure 3. Sagittal section of the skull showing the sinuses of the dura and superficial cortical veins.

Shown are the sagittal sinus, the straight sinus, the inferior sagittal sinus, the lateral sinus also known as the transverse sinus and the occipital sinus. The sinuses converge at the torcular herophili, also known as the confluence of sinuses.

Figure information:

Reproduction of a lithograph plate from Gray's Anatomy, originally published in 1918. It is not copyrightable in the United States as per Bridgeman Art Library v. Corel Corp. Neuroradiology, A.S. of (2005). Gray's Anatomy, 39th Edition: The Anatomical Basis of Clinical Practice. American Journal of Neuroradiology 26, 2703–2704.

The Neurovascular Unit and the Blood Brain Barrier

The large intracranial vessels described above eventually branch into intracerebral arteries that penetrate into brain tissue. These blood vessels are surrounded by neurons and glial cells. Though the cerebrovascular system has historically been studied independent of neurons, there was a paradigm shift in 2001. Instead of studying and describing brain tissues and the brain's vascular system as separate entities, the concept of the neurovascular unit (NVU) was formed by the Stroke Progress Review group meeting of the National Institute of Neurological Disorders and Stroke of the National Institutes of Health (Iadecola, 2017). The NVU describes functional unit of the brain as the integration of multiple cellular components including neurons, glial cells, and vascular cells. Specifically, the NVU contains endothelium, pericytes, vascular smooth muscle cells (VSMC), astrocytes, microglia, oligodendroglia, and neurons (Guo and Lo, 2009). The anatomy of the NVU is described in the following section.

Pial arteries lie beneath the dura and run through the subarachnoid space containing cerebral spinal fluid. From the pial arteries branch the intracerebral arteries. These arteries penetrate the brain parenchyma forming the NVU. The structure of the NVU changes throughout the vascular tree (Kisler et al., 2017) (Figure 4). At the level of the penetrating arteries, the lumen of the blood vessels is surrounded by endothelial cells. The endothelial cells are surrounded by layers of VSMC and ensheathed by a layer of pia mater. Adjacent to the blood vessel are astrocytic end-feet. The space between the astrocytes and the blood vessel is called the Virchow-Robin space and it contains cerebral spinal fluid. Both the VSMC and the astrocytes are innervated by neurons (Figure 4, b). As the penetrating arteries move deeper into the cortex, they form arterioles. This is the level where flow is controlled. Arterioles only have one layer of endothelial cells surrounding the lumen. The endothelial cells are then wrapped by a single layer of VSMC. The VSMC are

surrounded by astrocyte end-feet and innervated by neurons. Occasionally, pericytes will appear at this layer (Figure 4, c). At the capillary level, there is an endothelial cell layer as well as a pericyte layer. These layers share a basement membrane. Astrocytic end-feet cover both the endothelial and the pericyte layers. Both the astrocytes and pericytes are innervated by neurons.

The blood brain barrier is formed at the level of the capillaries. The endothelial cells that form the blood brain barrier are connected by tight junctions and are non-fenestrated. Astrocytes and pericytes that surround the endothelial cells provide structural and chemical support to the barrier. This system creates a semipermeable border that allows for some molecules to passively diffuse while restricting the passage of pathogens and large, hydrophilic molecules into the cerebral spinal fluid (Begley and Brightman, 2003). The blood brain barrier is essential for protection of the central nervous system and regulation of brain homeostasis.

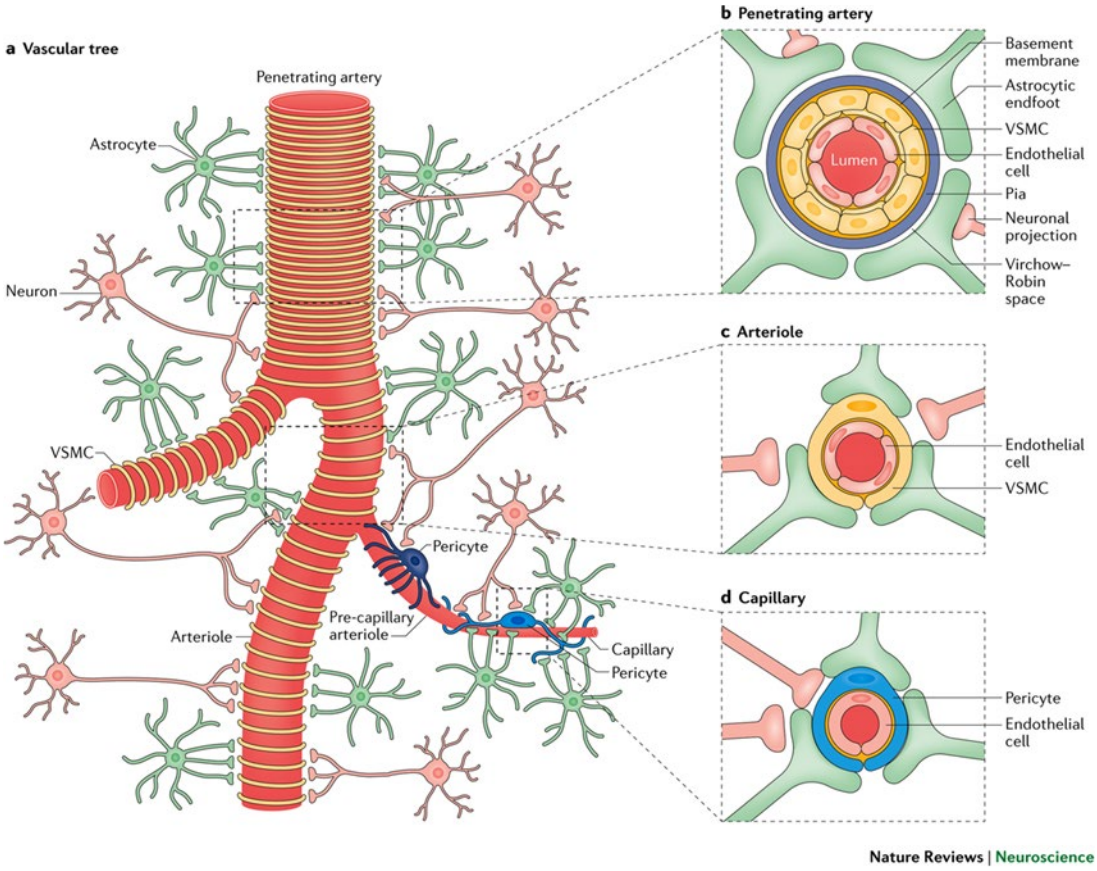

Figure 4. A schematic representation of the neurovascular unit.

A) overview of the vascular tree showing the penetrating artery and surrounding glial cells. B) structural anatomy of the penetrating artery and surrounding glial cells C) structural anatomy of the arteriole and surrounding glial cells D) structural anatomy of the capillary and surrounding glial cells.

Figure information:

Figure reused with permission. License number: 4954861059663. Kisler, K., Nelson, A.R., Montagne, A., and Zlokovic, B.V. (2017). Cerebral blood flow regulation and neurovascular dysfunction in Alzheimer disease. Nat. Rev. Neurosci. *18*, 419–434.

Distribution of Blood Flow in Large Intracranial Vessels

The following section briefly describes the distribution of blood flow in the large intracranial vessels in individuals with "standard" anatomy. However, it is important to note that anatomical variations of the Circle of Willis and other large intracranial vessels are relatively common (~50%) (Alpers et al., 1959; Iqbal, 2013). Anatomical variations and their effect on blood flow distribution are discussed in the section regarding "Anatomical Variations and Vertebral Artery Hypoplasia".

Using phase contrast MRI, distribution of blood flow in large intracranial vessels has been determined in 15 cerebral (Zarrinkoob et al., 2015; Zhao et al., 2007) and 6 extracerebral arteries (Zarrinkoob et al., 2015) in over 80 young and older healthy adults. Four main vessels supply the intracranial circulation. The right and left ICAs supply the anterior circulation and the left and right VAs supply the posterior circulation (Figure 5). The ratio between the anterior and posterior contribution to total CBF is approximately 3:1.

In adults without anatomical variations, the right and left ICAs account for approximately 72 ± 4% of total CBF. The difference between the contribution of the right and left ICA is often minimal (Zarrinkoob et al., 2015). The blood flow from the ICAs is distributed to the right and left MCAs (approximately 70%), right and left ACAs (approximately 30%) and 1-2% to the right and left ophthalmic arteries (Zarrinkoob et al., 2015). The VAs account for approximately 29 ± 5% of blood flow. Two-thirds of blood flow is distributed to the BA with the remaining third allocated to the posterior inferior cerebellar artery (Zarrinkoob et al., 2015). Differences in the distribution between right and left flow of the VA is not negligible, with reports of over 40% of individuals demonstrating left side flow dominance (Schöning et al., 1994) possibly because of vertebral artery hypoplasia, a relatively common anatomical variation where one of the vertebral arteries is narrowed and accompanied with low flow.

Summary of Cerebral Vascular Anatomy

The circulatory system of the brain is uniquely suited to match the brain's large metabolic need. The major suppliers of the brain's anterior circulation are the ICAs, and the major suppliers of the brain's posterior circulation are the VAs. Large intracranial vessels form a cerebral anastomosis, the Circle of Willis, connecting the anterior and posterior cerebral circulations. The surface arteries branch into smaller pial vessels that penetrate into the cortex. The NVU is formed by intracerebral vessels, neurons, and glial cells. Unique to the brain's circulatory system is the formation of the blood brain barrier that includes non-fenestrated capillaries surrounded by glial cells. A summary of the large intracranial arteries is provided in Table 1.

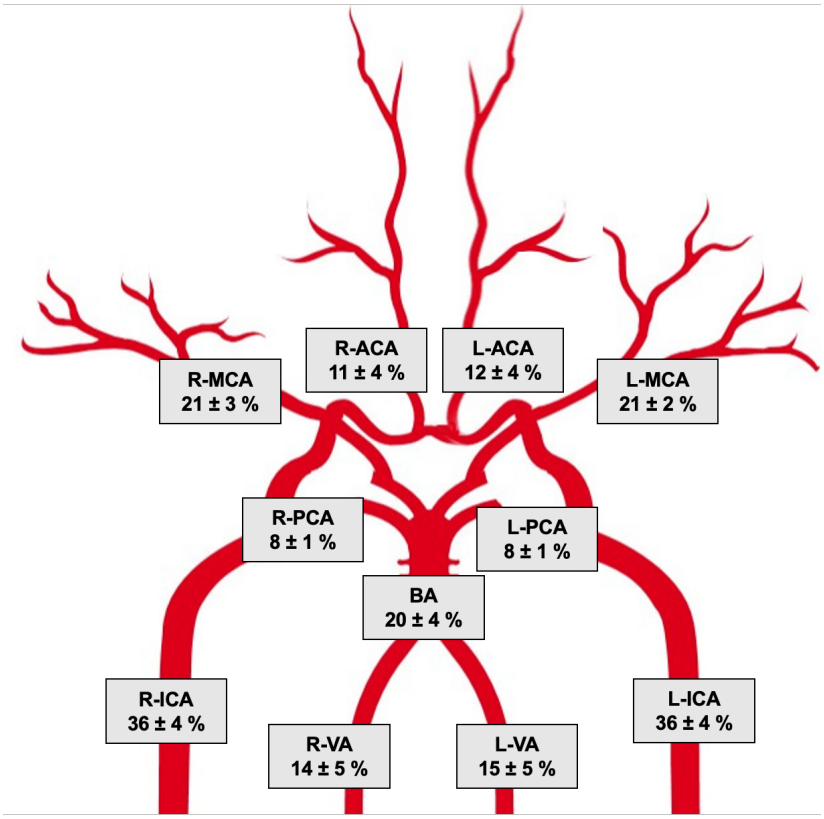

Figure 5. Distribution of total cerebral blood flow in the larger intracranial arteries.

This figure describes the distribution of total cerebral blood flow (tCBF) in percentage for each cerebral artery in 94 subjects with normal anatomical configurations. ACA, anterior cerebral artery; BA, basilar artery; ICA, internal carotid artery; L, left; MCA, middle cerebral artery; PCA, posterior cerebral artery; R, right; VA, vertebral artery.

Figure information:

Figure adapted from Zarrinkoob, L., Ambarki, K., Wåhlin, A., Birgander, R., Eklund, A., and Malm, J. (2015). Blood flow distribution in cerebral arteries. J Cereb Blood Flow Metab 35, 648–654.

Table 1. Summary of large intracranial arteries and their abbreviations

Side	Blood Vessel	Vessel Abbreviation	Circulation	% of total CBF	Region of the brain it supplies
Right	Internal Carotid Artery	ICA	Anterior	36 ± 4	Anterior circulation of brain
Left	Internal Carotid Artery	ICA	Anterior	36 ± 4	Anterior circulation of the brain
Right	Middle Cerebral Artery	MCA	Anterior	21 ± 3	Temporal and parietal lobes of the cerebrum
Left	Middle Cerebral Artery	MCA	Anterior	21 ± 2	Temporal and parietal lobes of the cerebrum
Right	Anterior Cerebral Artery	ACA	Anterior	11 ± 4	Frontal lobe of the cerebrum
Left	Anterior Cerebral Artery	ACA	Anterior	12 ± 4	Frontal lobe of the cerebrum
Right	Ophthalmic Artery	OA	Anterior	2 ± 1	Eyes
Left	Ophthalmic Artery	OA	Anterior	2 ± 1	Eyes
Right	Vertebral Artery	VA	Posterior	14 ± 5	Posterior circulation of the brain
Left	Vertebral Artery	VA	Posterior	15 ± 5	Posterior circulation of the brain
	Basilar Artery	BA	Posterior	20 ± 4	Brain stem. Sends branches to the cerebellum
Right	Posterior Cerebral Artery	PCA	Posterior	8 ± 1	Posterior cerebrum and brain stem
Left	Posterior Cerebral Artery	PCA	Posterior	8 ± 1	Posterior cerebrum and brain stem

Table 1 shows the major large intracranial vessels, their abbreviations, whether they are part of the anterior of posterior cerebral circulation, the distribution of blood flow to that vessel as a percentage of total cerebral blood flow (CBF), and the region of the brain that the vessel supplies. Percentage of total cerebral blood flow is based on 94 subjects without cerebral anatomical variations, adapted from Zarrinkoob et. al., 2015 (Zarrinkoob et al., 2015).

1.4.2 QUANTIFYING CEREBRAL BLOOD FLOW

Overview of Cerebral Blood Flow Quantification

Because the brain is encapsulated by skull, the measurement of cerebral perfusion and metabolism remains difficult. Studies of the brain's circulation started as detailed anatomical illustrations. It was not until the 19th century that the pial window technique, a highly surgically-invasive craniotomy procedure, allowed one to observe the pial microcirculation in the brain of experimental animals (Traystman, 2004). Following, a seminal study by Kety and Schmidt in 1945 described how to quantify blood flow in conscious humans (Kety and Schmidt, 1945, 1946, 1948a). Their technique cleverly used the principles of the Fick equation, where flow is equal to the quantity of a substance added or removed over time divided by the difference between the arterial and venous concentrations of the substance, to measure CBF via inhaled low dose nitrous oxide. Arterial and venous blood concentrations of nitrous oxide were sampled after 10-15 minutes of inhalation and compared to steady-state conditions. Using this technique, Kety and Schmidt estimated that global CBF in healthy young men was approximately 54 ± 12 ml/100g/min (Kety and Schmidt, 1945). This number has since been reproduced using modern MRI and ultrasound techniques (Traystman, 2004). The Kety and Schmidt method however has some short comings. It has no ability to separate the extra-cranial circulation from the intra-cranial circulation, it is invasive in nature, and the time delay makes it difficult to measure transient changes in blood flow. Thus, although the studies using the Kety and Schmidt technique are important to consider in the study of CBF regulation, this technique is no longer frequently used. Imaging devices including ultrasound and magnetic resonance imaging (MRI) have since expanded the understanding of human CBF. The following sections describe modern techniques to measure CBF in awake humans.

Ultrasound Methods

To address the limitation of the invasive nature of the Kety and Schmidt technique, Doppler ultrasound is used to estimate CBF by measuring blood velocity in the carotid arteries (Miyazaki and Kato, 1965). However, high temporal resolution imaging of the intracranial vessels was not realized until 1982, when Aaslid and colleagues demonstrated that blood velocity in the large intracranial arteries could be imaged by penetrating the skull using a range-gated, pulsed-Doppler ultrasonic beam of 1-2 MHz (Aaslid et al., 1982). This technique, transcranial Doppler ultrasound (TCD), allows for in vivo measurement of beat-to-beat blood velocity through an intracranial vessel (middle cerebral, anterior cerebral, posterior cerebral and basilar arteries). The TCD technique is based on the Doppler shift, by which an ultrasound beam at a known frequency contacts moving red blood cells that cause a shift in the returning frequency (Aaslid et al., 1982). TCD operates under a few assumptions including the flow through the vessel is laminar, the diameter of the vessel does not change, and the viscosity of the blood remaining constant. Due to the low frequency necessary to penetrate the skull, the arterial diameter of the intracranial vessels cannot be imaged. Despite these assumptions being a potential limitation for using the device, its high signal to noise ratio and high temporal resolution makes it an attractive candidate for *in vivo* CBF measurement. The MCA is commonly insonated and its use has many experimental advantages including its high flow volume, importance in supplying blood to the frontal cortex, and anatomical location allowing for clear imaging on most humans (Markwalder et al., 1984). Thus, TCD is used frequently for dynamic measurement of blood velocity in humans in various postures and in various environmental conditions (Willie et al., 2014). It has also been used in clinical populations to assess vasoreactivity and stroke (Wijman et al., 1998).

Duplex ultrasound of extracranial vessels has also been used to describe CBF (Furuhata et al., 1983). The advantages of using duplex ultrasound of extracranial vessels over TCD are that the device allows for acquisition of arterial diameter in brightness mode (B-mode) and blood velocity in pulse wave mode. Like TCD, duplex ultrasound has high temporal resolution because it can measure beat-by-beat blood velocity, though its spatial resolution is limited. It can only insonate the extracranial portions of the common carotid, internal carotid, and vertebral arteries. Duplex ultrasound requires technically skilled user placement of the probe (Thomas et al., 2015a) and has other technical limitations including unknown velocity profiles, as parabolic flow is assumed (Iooss et al., 2002) and non-uniform insonation of the blood vessels by the ultrasound beam (Evans, 1985).

PET & MRI Methods

Other imaging techniques, such as positron emission tomography (PET), arterial spin labeling (ASL) MRI, and blood-oxygen level dependent imaging (BOLD) MRI have also greatly enhanced the understanding of CBF. Specifically, [^{15}O]-water positron emission tomography utilizes [^{15}O]-water as a tracer that enters into cerebral tissue but is not metabolized. After a few minutes have passed, the PET signal reflects the perfusion brain's perfusion status (Herscovitch et al., 1983; Raichle et al., 1983). However, to utilize this technique, a cyclotron is necessary due to the short half-life of [^{15}O] and blood flow values over 65 ml/ (min x 100g) can be underestimated due to the limitation of brain permeability to water (Raichle et al., 1983). In addition, this technique is invasive as it requires arterial cannulation and tracer injection. ASL is an MRI technique that uses water as an endogenous tracer. Separate labeled and control images are acquired so that the resulting signal difference can be used to determine CBF values (Fan et al., 2016). Because

endogenous water is used as the tracer, anything that effects hydration status and hematocrit levels including diet and diurnal cycles may cause variability in the measurement (Wen et al., 2019). In addition, compared with PET imaging, regional CBF measured by ASL may be over-estimated in the gray matter as much as 29% (Zhang et al., 2014). Importantly, low CBF can reduce the signal to noise ratio in ASL which complicates using ASL to study how CBF changes with aging or disease (Kilroy et al., 2014). BOLD imaging is most commonly used to assess neuronal activation or functional MRI. It relies on the basis that an increase in neural activation is accompanied with an increase in CBF. BOLD imaging does not require a tracer (Kim and Ogawa, 2012). It measures the ratio of oxygenated to de-oxygenated blood with the assumption the change in blood flow reflects neuronal activity (Forster et al., 1998). Because deoxygenated hemoglobin is paramagnetic, it attenuates the T2* signal strength in surrounding tissues. If the cerebral metabolic rate of oxygen is constant, concentrations of deoxygenated hemoglobin will be low, and the bold signal will be high. BOLD imaging involves multiple neurochemical, metabolic and hemodynamic factors, and is complicated by the inability to localize BOLD contrast to neuronal activity relative to draining veins (Kinahan and Noll, 1999; van Zijl et al., 1998). Despite its limitations, BOLD imaging has a higher signal-to-noise ratio, spatial and temporal resolution compared with PET imaging (Kinahan and Noll, 1999). Thus, it has been frequently used to measure CBF at rest and in response to gas challenges (Donahue et al., 2014; Mandell et al., 2008; Mikulis et al., 2005; Sam et al., 2015). However, BOLD lacks specificity of measurement if the experimental question requires direct measurements of blood flow or blood velocity.

Another commonly used MRI method to measure blood flow in large vessels is phase contrast MRI. Phase contrast scans are common for cardiac imaging but have become more popular to use in other vascular beds such as the brain (Khan et al., 2017). Phase contrast imaging

of blood flow measures the phase shifts of moving and non-moving parts to compute velocity components of flow along each direction. Scans can be gated with an electrocardiogram to measure pulsatile blood flow (Sträter et al., 2018). 2D scans require the manual placement of measurement planes along the axis of the vessel and can only measure one vessel at a time. This works well with major central blood vessels like the aorta but proves difficult when trying to image a more complicated vascular system with multiple vessels like the Circle of Willis. In that case, 3D, or time-resolved 3D, often termed 4D flow MRI, may be a superior alternative. High resolution 4D flow MRI can image both blood flow and angiographic data in the large intracranial vessels with high special and temporal resolution in one scan acquisition and no contrast agent. Shorter scan times are possible due to radial under sampling of the k-space (Schrauben et al., 2014). Current sequences require 5-7 minutes for acquisition, making them clinically feasible. Vessel segmentation can occur post-scan acquisition, so as many as 11 or more intracranial vessels can be imaged simultaneously. This technique is however limited to measuring blood flow in large intracranial arteries and veins and requires longer scanning and post-processing times.

Summary of Cerebral Blood Flow Quantification

A summary of common techniques used to measure cerebral blood flow in humans is shown in Table 2. Because of the confines of the skull, CBF is difficult to measure. Multiple techniques have been utilized to measure CBF in awake humans. Early techniques were invasive in nature; however, most modern techniques employ non-invasive imaging. Ultrasound imaging is frequently used to measure either the extracranial vessels of the neck, or intracranial vessels that can be imaged through the skull. MRI techniques measure global or regional CBF or blood flow through the large intracranial vessels. There is no gold standard technique, as each technique has

strengths and limitations. In general, ultrasound techniques have excellent temporal resolution with the ability to measure beat by beat blood flow. However, ultrasound lacks spatial resolution as it can only image one vessel at a time. Conversely, MRI techniques can image the entire brain, but temporal resolution is low compared to ultrasound. Thus, the severity of the limitations of each technique will depend on the research question and the experimental protocol. Importantly, most of the strengths and limitations of each device have been considered in the context of measuring CBF at rest. When a stimulus is presented, such as a hypercapnic gas challenge, there are other limitations to each technique that arise. These are discussed in future sections “Cerebrovascular Reactivity to Hypercapnia” and “Change in MCA diameter during Cerebrovascular Reactivity to Hypercapnia”.

Table 2. Summary of common techniques used to measure cerebral blood flow in un-anesthetized humans

Method	Description	Strengths	Limitations
Inert gases: Kety-Schmidt Technique	• Bulk CBF is calculated from the area between arterial and venous washout curves from a diffusible tracer (commonly nitrous oxide).	• Volumetric flow measurement.	• Requires invasive cannulation. • No ability to separate extracranial and intracranial flow. • Time (15-20 minutes) required for tracer steady state and washout.
Ultrasound: Transcranial Doppler Ultrasound (TCD)	• Velocity though an intracranial vessel is calculated from a Doppler shift.	• High temporal resolution, can measure beat-by-beat data. • Noninvasive. • Portable.	• No volumetric flow measurement. Only velocity. • No angiographic data. • One vessel at a time.
Ultrasound: Duplex Ultrasound	• Duplex imaging (Doppler and brightness mode (B-mode)) allows velocity and structural data acquisition to measure volumetric flow of extracranial vessels.	• High temporal resolution. • Noninvasive. • Volumetric flow measurement.	• Extracranial measurements only. • Measurements limited to number of probes. • Technical expertise required for probe placement.
Positron Emission Tomography (PET)	• PET signal reflects perfusion as radioactive tracer is injected (commonly [^{15}O]-water) that is freely diffusible but not metabolized by brain tissue.	• Global and regional measurements.	• Requires invasive cannulation. • Requires tracer injection. • Brain has limited permeability to water. • Requires cyclotron.
MRI: Arterial Spin Labeling (ASL)	• MRI technique that measures differences in signal from control image to magnetically tagged water image to infer blood flow.	• Water is an endogenous tracer. • Global and regional measurements.	• Low signal-to-noise compared with other MRI methods. • Hydration status is confounding variable.

MRI: Blood Oxygen Level Dependent (BOLD) Imaging	• MRI technique that measures ratio of oxygenated to de-oxygenated hemoglobin to infer blood flow.	• Non-invasive. • Global and regional measurements. • Higher signal-to-noise ratio than PET imaging.	• Indirect measurement of flow. • Relies on adequate neurovascular coupling. • Cannot be localized relative to veins.
MRI: 2D Phase Contrast	• MRI technique that measures phase shifts of move and non-moving parts to compute velocity through an intracranial blood vessel.	• Volumetric flow measurement of intracranial vessels. • Relatively short scan times (~1 minute per vessel).	• Requires manual placement of measurement planes orthogonal to flow. • Low temporal resolution compared with Doppler methods (cannot measure beat-by-beat data).
MRI: Time resolved 3D (4D) Phase Contrast	• MRI technique that expands on 2D PC by adding three directional velocity encoding and time-resolution. Allows for imaging of flow in larger 3D volumes.	• Volumetric flow measurement of intracranial vessels. • Multiple vessels can be imaged simultaneously.	• Low temporal resolution compared with Doppler methods (cannot measure beat-by-beat data). • Requires post-processing vessel segmentation.

Table 2 shows a summary of common techniques that are used to quantify cerebral blood flow in un-anesthetized humans. Similar tables have been published (Fantini et al., 2016; Hoiland et al., 2019; Wintermark et al., 2005). CBF, cerebral blood flow. MRI, magnetic resonance imaging.

1.4.3 CEREBRAL BLOOD FLOW REGULATION

Overview of Cerebral Blood Flow Regulation

The brain is a highly vascularized organ with high metabolic activity. Unlike other organs, matching blood supply to metabolic demand in the brain is complex because the brain lacks any type of storage for its fuel. The brain requires approximately 20-30% of the total cardiac output at a given time. This is despite the brain being only 2-3% of the body's total weight (Williams and Leggett, 1989). This amounts to approximately one liter of blood per minute under resting conditions (Kety and Schmidt, 1946). Because there is no substrate storage in the brain, blood flow needs to precisely match metabolic need to the correct physical location and with the appropriate amount, preventing both hyperperfusion and hypoperfusion. Regulation of brain blood flow is multifarious and involves both local and systemic factors. In general, the integrative factors regulating CBF on a global level are brain metabolism, blood pressure, neurogenic factors, cardiac output, and chemical factors including arterial partial pressure of O_2 and arterial partial pressure of CO_2. An overview of how these factors influence CBF are presented in Figure 6. The following sections describes how each of these factors influence CBF in more detail.

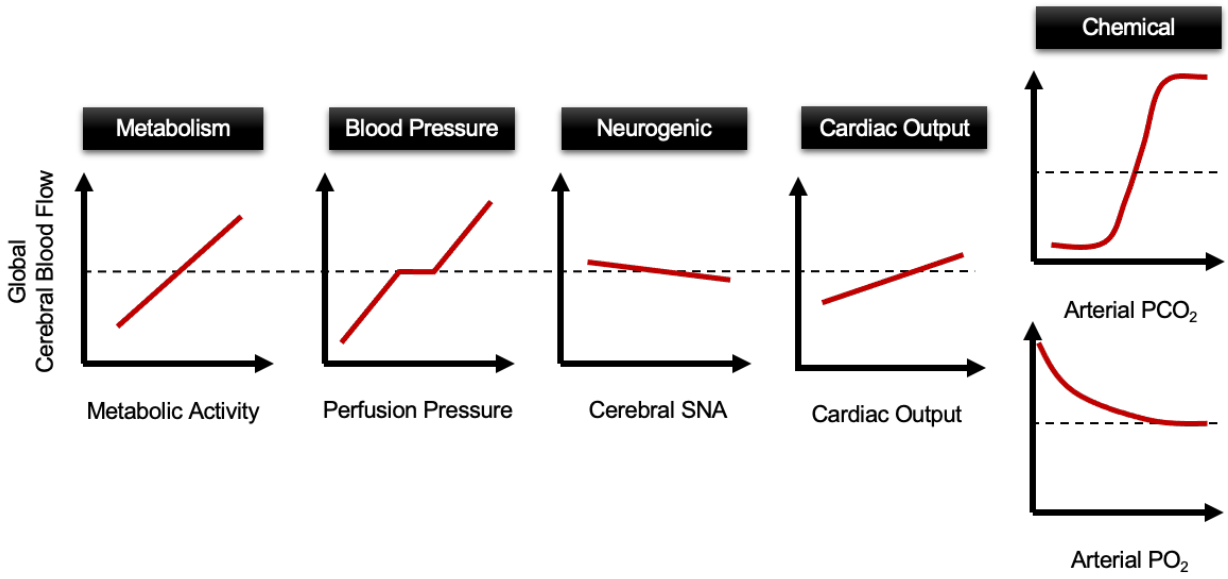

Figure 6. Overview of factors that regulate global cerebral blood flow.

Graphs show approximate directional responses to changes in brain metabolic activity, blood pressure, cerebral sympathetic nerve activity (SNA), cardiac output, and partial pressures of arterial carbon dioxide (PCO_2) and arterial oxygen (O_2).

Figure information:

Figure adapted from Smith, K.J., and Ainslie, P.N. (2017). Regulation of cerebral blood flow and metabolism during exercise. Experimental Physiology 102, 1356–1371.

Factors that Regulate Cerebral Blood Flow: Metabolism

The coupling of blood flow to the brain's metabolic activity was first described in humans the late 19th century. Italian physiologist Angelo Mosso was studying an individual with a skull defect that allowed Mosso to measure changes in his brain volume though a hole in his skull. When Mosso asked the individual to solve a math problem, the brain swelled, suggesting there was in increase in CBF (Mosso, 1880). Following this insight from Mosso, Roy and Sherrington did a series of experiments in mammals where they also recorded brain volume changes, this time in specific areas. They found that changes in CBF were specific to the regions of the brain that were most metabolically active (Roy and Sherrington, 1890). These seminal experiments provided the foundation of the understanding in how neural activation can illicit changes in blood flow. The coupling of CBF to cerebral metabolic demand is called neurovascular coupling. Neurovascular coupling is the basis of many modern functional neuroimaging techniques such as BOLD MRI. However, despite the importance and relevance of neurovascular coupling, the exact mechanisms linking neuronal activity to blood flow are unclear.

Neurovascular coupling requires the coordination of the entire neurovascular unit, including neurons, glial cells, and vascular cells. In short, the firing of action potentials in neurons causes three main effects: release of neurotransmitters, increase in adenosine triphosphate (ATP) consumption and increase in oxygen and glucose utilization (Adachi et al., 1994; Liu et al., 2012a). The blood flow response to neuronal activation is regulated by both feed forward (increased glutamatergic signaling) and feedback (increase in metabolic by products and drops in the partial pressure of O_2 in the tissues) mechanisms (Cox et al., 1993; Hosford and Gourine, 2019). There is also some evidence that communication between capillary pericytes is implicated in the neurovascular coupling response (Hall et al., 2014; Longden et al., 2017). A common test of

neurovascular coupling in humans is the blood flow response to visual stimulation or cognitive challenge. For example, when presented with a visual stimulus, an increase in blood velocity of 20-30% was observed in the PCA, the artery that supplies the occipital cortex (Rosengarten et al., 2001, 2003). Ultimately, it has been suggested that the relationship between the brain's metabolic activity and blood flow is linear (Figure 6), though this has been based on mostly *in vitro* and *in vivo* animal models, as these reviews discuss (Hamel, 2006; Iadecola, 2004, 2017).

Factors that Regulate Cerebral Blood Flow: Blood Pressure

The physical factors that govern flow are based on fundamental laws of physics, particularly Ohm's law which states that voltage is equal to the current multiplied by the resistance (Eq. 1).

$$V = IR$$

In regard to fluid flow, voltage is analogous to pressure, current is analogous to flow and resistance is analogous to the resistance to the flow. Resistance is determined by multiple factors including the fluid viscosity, the length of the tube, and radius of the tube to the fourth power. This is known as Poiseuille's law (Eq. 2) which states that the pressure difference between two ends of a tube is equal to 8 times the viscosity (μ) multiplied by the length of the tube (L) and the volumetric flow rate (Q) divided by pi times the radius (R) to the fourth power (Eq. 2).

$$\Delta p = \frac{8\mu LQ}{\pi r^4}$$

These basic physical principles can be applied to the cerebral circulation, under the assumptions that flow is laminar, the fluid is Newtonian, and the tubes are rigid cylinders. In the brain, the driving pressure of the system is the cerebral perfusion pressure (CPP), which is the pressure gradient across the brain and equal to the mean blood pressure (MAP) minus the intracranial pressure (ICP). In healthy adults, intracranial pressure is approximately 5-15 mmHg (Rangel-

Castillo and Robertson, 2006), and is about 4 mmHg lower in the seated position compared with the supine position (Ng et al., 2004). Experimentally, ICP is frequently referred to as negligible because of its small proportion compared with MAP. Thus, CPP is commonly estimated as the MAP. The resistance is termed cerebrovascular resistance (CVR) and follows the principles of Poiseuille's law. Thus, the simplified equation governing cerebral blood flow's relationship with pressure is below (Eq. 3).

$$CBF = \frac{CPP}{CVR}$$

And Poiseuille's law, related to cerebrovascular resistance is below (Eq. 4).

$$CVR = 8L\eta * \pi r^4$$

Together, the equation for CBF is below (Eq. 5).

$$CBF = \frac{(CPP * \pi r^4)}{8L\eta}$$

Of note, because flow is proportional to the vessel radius to the fourth power, adjustments to vascular resistance have the greatest influence on global CBF. The above equations offer general guidelines relating the control of CBF to physical principles; however, using these equations rely on various assumptions as stated above. Importantly, the anatomical configuration of the cerebral circulation does not lend itself to be viewed as a singular circular tube. Rather, it is more likely a collection of syndicate vessels with its flow represented as the sum of parallel vessels, with calculations of vessel diameter and blood viscosity necessary for each individual vessel (Secomb and Pries, 2013). In addition, flow through cerebral blood vessels may not always be laminar, and turbulence can decrease flow at any given perfusion pressure. In addition, higher pulsatility index, defined as the average between the maximum and minimum blood flow velocity normalized to the average velocity, requires greater pressure for a given flow. Thus, the calculations of pressure,

flow and resistance in cerebral hemodynamics are part of a complex and dynamic system that are difficult to model, and many non-linear analysis have been attempted (Gadda et al., 2018; Henley et al., 2017; Marmarelis et al., 2016).

As described above, cerebral perfusion pressure (CPP) is the driving pressure force that influences CBF. Importantly, cerebral perfusion pressure is largely determined by arterial blood pressure. The relationship between arterial blood pressure and CBF was indicated in early studies (1890's) by Roy and Sherrington (Roy and Sherrington, 1890) and again in the 1930's by M. Fog. Fog observed that the cerebral pial arterioles of anesthetized cats changed in diameter when blood pressure was experimentally manipulated. He noted that "the muscular tonus of the pial arteries was controlled by intravascular pressure, hypertension causing augmentation and hypotension diminution of the tone" (Fog, 1938). He also describes the blood pressure and blood flow relationship as "having certain limits" (Fog, 1938). This idea set the stage for future studies in humans by Lassen, where he derived the cerebral autoregulatory curve (Lassen, 1959). Lassen described cerebral autoregulation as the ability to maintain CBF throughout a range of perturbations in mean arterial pressure. Through his experiments manipulating blood pressure using pharmacological agents in patients or studying patients with pathologically high or low blood pressure, he derived the frequently referenced cerebral autoregulation curve that suggests CBF is maintained when MAP is within the range of 60-150 mmHg (Lassen, 1959). These findings were expanded by Heistad in dogs, where he experimentally increased blood pressure to over ~150 mmHg and found that CBF was still maintained (Heistad et al., 1978a). However, the curve derived from Lassen's early experiments in humans and Heistad's experiments in dogs has since been challenged. Recent studies with more advanced imaging techniques (including transcranial Doppler ultrasound) suggested the range of the plateau in humans is likely ~15 mmHg rather than

the ~90 mmHg described by Lassen (Hori et al., 2017; Lucas et al., 2010; Numan et al., 2014; Tan, 2012), shown in (Figure 6). Mechanisms controlling cerebral autoregulation are not entirely understood and likely rely on a combination of elements including metabolic, neurogenic and myogenic factors (Hamner and Tan, 2014). Importantly, innate autoregulatory mechanisms may be overridden during other challenges to the cerebrovascular system such as perturbations in blood gases (Häggendal and Johansson, 1965; Harper and Glass, 1965). Thus, it is important to consider mean arterial pressure when interpreting changes in CBF.

Because blood pressure can influence blood flow, blood flow data is often expressed as conductance (Lautt, 1989; Stark, 1968). Conductance is calculated as blood flow / MAP. If blood velocity is measured, conductance index is quantified as blood velocity / MAP. In the case of the cerebral circulation, it is termed cerebrovascular conductance or cerebrovascular conductance index (CVCi), when measuring blood flow or blood velocity respectively. Measurements of conductance are especially important when challenges to assess blood flow or blood velocity responses elicit changes in MAP (Claassen et al., 2007).

Factors that Regulate Cerebral Blood Flow: Neurogenic

The autonomic nervous system is the main unconscious control system in the body regulating bodily functions via feedback loops from the periphery to the central nervous system. There are two divisions of the autonomic nervous system, the sympathetic nervous system, known for controlling the “fight or flight” bodily responses and parasympathetic nervous system known for controlling the “rest or digest” bodily responses. The sympathetic nervous system can influence blood pressure and blood flow by directly innervating blood vessels, with higher sympathetic nervous system activity (SNA) causing vasoconstriction of blood vessels. This has been well

described in the periphery (Joyner et al., 2015; Thomas and Segal, 2004); however, the influence of SNA on the cerebral circulation is controversial. Anatomically, neurogenic structures including sympathetic nervous system fibers and adrenoreceptors are present in the cerebral circulation. This has been described by imaging the nerve plexus of human brains during postmortem evaluation (Bleys et al., 1996). In addition, the density of fibers and receptors is location specific. For example, the anterior cerebral circulation (internal carotid arteries) appears to have denser sympathetic innervation compared with the posterior cerebral circulation (vertebrobasilar system) (Hamel, 2006) and the density of different adrenoreceptors (α-1, α-2, β) appears to change throughout cerebrovascular tree (Sercombe et al., 1990). Despite the presence of the sympathetic nervous system structures in the cerebral circulation, its function in regulating CBF has not yet been elucidated.

There are two major difficulties in understanding the impact of SNA on CBF regulation in humans. The first is the difficulty of performing controlled, human studies (Brassard et al., 2017) and the second is the profound differences in SNA structures between animal and human models rendering results from animal studies difficult to translate (Heistad et al., 1978b). The main approaches to human studies have either been studying patients with a ganglionectomy, which is the removal of sympathetic ganglion as a treatment for a clinical condition, or by performing ganglionic blockade of sympathetic ganglia or adrenoreceptors in healthy humans (Brassard et al., 2017). In the ganglionectomy studies, CBF was increased after removal of the ganglion, suggesting the SNA is responsible for regulating basal CBF (Jeng et al., 1999; Shenkin, 1969; Suzuki et al., 1975). However, ganglia blockade studies have yielded conflicting results, with some studies showing increased CBF after ganglia blockade (Ide et al., 2000; Linden, 1955; Treggiari et al., 2003; Umeyama et al., 1995) and others observing no change in CBF (Harmel and Hafkenschiel,

1949; Ohta et al., 1990; Scheinberg, 1950). The systemic effects of SNA blockade such as changes in blood pressure and cardiac output further add to the difficult of interpretation of results.

Ultimately, the presence of sympathetic structures in the cerebral circulation, coupled with limited human data suggesting that removal or blockade of those structures can change CBF, support the hypothesis that SNA is an important regulator of CBF. The relationship between SNA and CBF appears to be linear with increases in SNA eliciting decreases in CBF, as shown in Figure 6. However, more work needs to be done in humans to better understand the physiological mechanisms behind the relationship between cerebral SNA and CBF.

Factors that Regulate Cerebral Blood Flow: Cardiac Output

Cardiac output by definition is the amount of blood that the heart is pumping through the circulatory system each minute. In general, the relative distribution of cardiac output to a certain organ depends on that organ's metabolic rate. However, perfusion, as noted in Ohm's law above, also depends on the pressure driving the system, which is arterial blood pressure in this case, as well as the resistance capacitance of the organ's vasculature. Thus, both metabolism, pressure and vascular resistance will determine the amount of cardiac output going to an organ. The brain receives a high percentage of cardiac output (approx. 20% of total) relative to its weight (approx. 2% of total) (Williams and Leggett, 1989). The relationship between acute changes in cardiac output and CBF are more complex. In order to study the isolated effect of cardiac output on CBF, the experimental design needs to account for reflex changes in other physiological variables that may also influence CBF, such as changes in blood pressure, changes in blood gases, or changes in brain metabolism. Nonetheless, many studies have assessed the relationship between cardiac output and CBF by attempting to acutely change cardiac output in un-anesthetized, healthy

humans. For example, lower body negative pressure, a condition which causes the central blood volume to move out of the thorax thus decreasing cardiac output, caused a decrease in cerebral blood velocity in a linear manner (Brown et al., 2003; Guo et al., 2006; Levine et al., 1994; Ogawa et al., 2007; Ogoh et al., 2005). Acute increases in cardiac output, via leg tensing while standing (van Lieshout et al., 2001) albumin infusion (Ogoh et al., 2005) or saline infusion (Ogawa et al., 2007) resulted in increased CBF. Based on the cumulative results from these data regarding acute increases and decreases in cardiac output, a 30% change in cardiac output independently results in an approximate 10% change CBF (Meng et al., 2015). This relationship appears to be linear, as shown in Figure 6.

Factors that Regulate Cerebral Blood Flow: Chemical

Blood gasses, particularly oxygen (O_2) and carbon dioxide (CO_2), are independent, potent regulators of global and regional CBF. A seminal study describing this relationship was by Wolff and Lennox in 1930. These experiments involved measuring pial artery diameter in anesthetized cats using the pial window technique before and during inhalation of various gas mixtures and the injection of acid and alkali. Decreases in CO_2 levels in the blood resulted in a moderate decrease in pial artery diameter. In contrast, higher CO_2 levels in the blood resulted in approximately 40% increase in pial artery diameter. When O_2 levels were increased, pial artery diameters decreased. Conversely, low O_2 levels resulted in pial artery vasodilation (Wolff et al., 1930). The results from this study showed the potency of both O_2 and CO_2 in regulating the intracranial circulation, with high CO_2 resulting in the greatest change in pial artery diameter. Another experiment by Lennox and colleagues in 1934 in un-anesthetized humans reported that blood flow in the jugular vein was increased after inhaled hypoxic gas caused drops in arterial O_2 tension. Furthermore, increased

arterial CO_2 by elevated CO_2 inhalation caused an even more marked change in jugular vein flow than the O_2 experiments (Gibbs et al., 1935). The experiments in un-anesthetized humans were expanded in the late 1940s by Kety and Schmidt (Kety and Schmidt, 1948b). Using the Kety and Schmidt method to determine CBF, they reported an average increase of 75% in CBF after inhalation of 5 or 7% CO_2 and an approximate increase of 35% in CBF after inhalation of 10% O_2. Taken together, the early experiments in animals and humans suggest that both O_2 and CO_2 are important regulators of CBF, with higher levels of arterial CO_2 (hypercapnia) experimentally having the most profound impact on global CBF. Figure 6 shows a summary of the relationships between arterial O_2, arterial CO_2 and CBF. These relationships are described in further detail in the following sections.

Arterial O_2

As described in the experiments in the 1930's and 1940's, the arterial levels of O_2 can impact CBF globally. In general, reductions in arterial oxygen content that could jeopardize cerebral oxygen delivery are met with vasodilation of the cerebral vessels to increase blood flow and the delivery of O_2. Arterial O_2 content can be estimated in heathy humans by measuring O_2 saturation, which refers to the percentage of hemoglobin binding sites occupied by O_2. In healthy humans at sea level, O_2 saturation is usually between 96-99% and changes within that range are generally not a threat to cerebral oxygenation. However, in certain disease states such as chronic obstructive pulmonary disease (COPD), chronic reductions in O_2 saturation may be below <95% (Dalbak et al., 2015). Indeed, individuals with COPD demonstrate elevated CBF and there is a dose response relationship depending on the level of hypoxemia (Albayrak et al., 2006). Chronic changes in O_2 saturation have also been documented in individuals that sojourn or live in high altitude (Ainslie

and Subudhi, 2014; Severinghaus et al., 1966). Acute changes in O_2 levels can also elicit changes in CBF. Experimentally, hypoxia, or acute reductions in O_2, are typically induced by inhaling 10% oxygen in order to bring arterial O_2 saturation down to approximately 80%. Using this technique, studies have reported an approximate 0.5-2.5% increase in CBF per percent reduction in arterial O_2 saturation (Cohen et al., 1967; Querido et al., 2013; Shapiro et al., 1970; Willie et al., 2012). Similar reductions in blood flow have been observed in individuals with obstructive sleep apnea during intermittent hypoxic episodes experienced during sleep (Reichmuth et al., 2009). Taken together, both chronic and acute reductions in arterial O_2 content can increase global CBF.

Hyperoxia, or high levels of O_2, can also cause reductions in global CBF. The use of supplemental oxygen in healthy men has been associated with cerebral hypoperfusion (Floyd et al., 2003; Kety and Schmidt, 1948b). However, studying the effect of hyperoxia in insolation from changes in CO_2 are difficult. Induction of hyperoxia can cause hyperventilation, thereby reducing arterial CO_2 and resulting in cerebrovascular constriction (Easton et al., 1986). Similarly, hyperoxia can cause constriction in vascular beds and decrease local perfusion, paradoxically increasing the risk of hypoxic stress in the tissues (Iscoe and Fisher, 2005). Thus, overall findings suggest that hyperoxia causes a reduction in global CBF, but results may be confounded by changes in arterial CO_2 levels.

The mechanisms by which arterial oxygen levels influence CBF are complex. Regarding hypoxia, the CBF response depends on the magnitude and duration of hypoxic exposure, the interaction between changes in acid-base levels, changes in hemoglobin concentration and saturation, and the local vasodilatory response of the cerebrovasculature (Hoiland et al., 2015). In general, hypoxia induced vasodilation of the cerebral vessels is likely due to multiple cellular events including neurovascular coupling caused by decreases in tissue oxygen, acidosis of the

extracellular space due to increases in neural anaerobic metabolism, and direct effects on the vasculature (Willie et al., 2014). In addition, deoxygenated hemoglobin from red blood cells may release signaling molecules such as ATP or COX that induce vasodilation (Hoiland et al., 2015). In summary, arterial levels of O_2 can cause chronic and acute changes in CBF. Hypoxia elicits an increase in CBF and hyperoxia elicits a decrease in CBF, though results from hyperoxia experiments may be confounded by changes in arterial CO_2.

Arterial CO_2

Many of the early experiments on the relationship between CBF and blood gases in humans noted the profound impact of CO_2. In healthy humans, CO_2 has said to be the most potent regulator of cerebrovascular tone and consequently, CBF. Hypercapnia induced vasodilation causes an approximate increase of 3-5% of middle cerebral artery blood velocity per mmHg increase in arterial CO_2 above resting values (Xie et al., 2006). In other words, a 20-mmHg change in arterial CO_2 above resting values can increase CBF velocity approximately 100%. The positive association between arterial CO_2 and CBF has been replicated in multiple studies in humans using multiple different methods to administer CO_2 and measure CBF (Fierstra et al., 2013; Kety and Schmidt, 1948b). Measuring the blood flow or blood velocity response to CO_2 is the basis of the measurement of cerebrovascular reactivity, which is a test of the vasodilatory function of the cerebral vessels. Cerebrovascular reactivity is described in further detail in the section "Cerebrovascular Reactivity to Hypercapnia". Based on data from both human and animal studies, the relationship between arterial CO_2 and CBF appears to be sigmoidal, as shown in Figure 6. However, the response is linear within arterial CO_2 ranges that are able to be achieved in un-anesthetized, awake humans (Battisti-Charbonney et al., 2011; Harper and Glass, 1965).

Hypocapnia, or reductions in arterial CO_2 below resting levels, causes vasoconstriction and a reduction in cerebral blood volume (Ito et al., 2004). Experimentally, hypocapnia can be induced in humans by hyperventilation. Taken together, CO_2 is a potent controller of global CBF with hypercapnia causing an increase in CBF and hypocapnia causing a decrease in CBF.

The mechanisms that underlie the CBF response to changes in arterial CO_2 are mediated through the action of hydrogen ions on the cerebral arteries, rather than CO_2 itself. During hypercapnia, the increase in arterial CO_2 causes change in cerebrospinal fluid pH (via the increase in H+) in the perivascular spaces; thus, with proper vasomotor function, pial vessels in the healthy brain will quickly vasodilate and augment CBF to ensure removal of CO_2 and maintain homeostasis (Tominaga et al., 1976). The changes in extracellular pH may also be sensed in the ventrolateral medulla (Brian et al., 1996) causing systemic physiological responses such as chemoreflex activation and increases in sympathetic system nervous activity.

The increases in arterial CO_2 elicit vasodilation of the cerebral vessels. Hypercapnia mediated cerebral vasodilation likely occurs as a result of three main mechanisms: endothelial derived vasodilation, direct action of the hydrogen ions on the VSMC, and decreased pH and increase in shear stress causing ATP release from red blood cells (Ainslie and Duffin, 2009). Many of the studies that evaluate the direct effect of CO_2 or H+ ions on the VSMC, (Harper and Bell, 1963; Lambertsen et al., 1961; Wahl et al., 1970) as well as the effects of hypercapnia mediated ATP release from red blood cells (Bergfeld and Forrester, 1992; Ellsworth et al., 1995) have been conducted in animal or *in vitro* models. Studies in humans have suggested that endothelial derived prostaglandins are large contributors to hypercapnic mediated cerebral vasodilation. Prostaglandins can effect K+ channel conductance causing K+ efflux and subsequent hyperpolarization relaxation of the VSMC (Kitazono et al., 1995). Cyclooxygenase (COX) is one

of the main enzymes that converts arachidonic acid to prostaglandins. Human studies that blocked COX using indomethacin demonstrated ~50% reduction in the CBF response to hypercapnia (Barnes et al., 2012; Eriksson et al., 1983; Kastrup et al., 1999; Xie et al., 2006). This may be specific to indomethacin as the same reduction was not observed with other COX inhibitors ketorolac and naproxen (Hoiland et al., 2016). Endothelial derived nitric oxide is another potential contributor to hypercapnic mediated cerebral vasodilation, though evidence in humans has been controversial. For example, nitric oxide synthase (NOS) blockade resulted in a blunted CBF response to CO_2 (Schmetterer et al., 1997); however, other studies reported no effect of a NOS blockade on the CBF response to CO_2 (Ide et al., 2007; Wang et al., 1992; White et al., 1998). In summary, hypercapnia causes vasodilation of the cerebral vessels via multiple mechanisms. The most evidence in humans suggests a large role of endothelial derived release of prostaglandins.

Summary of Factors that Regulate Cerebral Blood Flow

In summary, CBF is regulated by various integrative factors. A summary of these factors is shown in Figure 6. In general, global CBF increases linearly with increases in metabolic activity. Increases in perfusion pressure also elicit increases in CBF, though CBF is maintained with a range of ~15 mmHg. Because influence of blood pressure on blood flow, flow data is often expressed as conductance, which is calculated as flow or velocity divided by MAP. Cerebral SNA appears to cause vasoconstriction in cerebral vessels thus decreasing CBF, though evidence in humans is sparse. Cardiac output appears to increase CBF in a positive, linear manner. Decreases in arterial O_2 increase CBF; however, evidence for hyperoxia mediated vasoconstriction is less clear. Arterial CO_2 is a potent regulator of CBF, with hypercapnia increasing CBF and hypocapnia decreasing CBF. The curve is sigmoidal; however, CO_2 levels on the linear portion of the curve can be

obtained in awake, un-anesthetized humans. Although this dissertation does not test CBF regulation by each of these factors, it is important to keep them in mind when analyzing and designing experiments to test CBF regulation.

1.4.4 CEREBRAL HEMODYNAMICS AND VASCULAR STIFFNESS

Overview of Cerebral Hemodynamics and Vascular Stiffness

Blood flow throughout the cerebrovascular system is impacted by both the structure and function of the blood vessels. In the human cardiovascular system, the heart acts as a pump resulting in perfusion pressure and blood flow throughout the body to be pulsatile. Pressure is highest during the contractile phase of the heart (systole) and lowest during the relaxation phase of the heart (diastole). The measured pressure waveform is a combination of the forward and reflected wave, and it can be dissected to determine the contribution of each. Measuring the speed by which the pulse is traveling can give an idea regarding the stiffness of the vasculature, as a faster pulse wave velocity would indicate a stiffer vessel (Attinger, 1965). Similarly, dissecting the flow waveforms in the brain into their systolic and diastolic components and calculating cerebral pulsatility index may reflect the amount of distal vascular resistance in that vascular bed.

Vascular Stiffness

The shape of the pressure and flow waveform changes as blood moves from the aorta and central arteries to the peripheral arteries and though different vascular beds (Attinger, 1965). The aorta, the largest central vessel that arises from the left ventricle, acts to buffer and dampen the pulse. However, with advancing age, the aorta becomes less elastic and loses buffering capacity (Vaitkevicius et al., 1993). This is manifested as higher systolic blood pressure, a widening of the arterial pulse pressure, an increase in wave reflection, a reduction in arterial compliance and a concordant increase in arterial stiffness (Kelly et al., 1989; O'Rourke, 1976). Because of the reduction in buffering capacity of the aorta, mechanical forces caused by cardiac pumping can be translated into distal vascular beds, especially high flow vascular beds such as the brain (Mitchell,

2008). It is possible that elevations in central arterial stiffness may have a negative impact on the vasculature of the brain. The gold standard of central arterial stiffness measurement is carotid-femoral pulse wave velocity (cfPWV), where faster pulse wave velocity is reflective of higher vascular stiffness. CfPWV is related to white matter brain damage (Maillard et al., 2017) and elevated cfPWV is associated with reduced cognitive function (Mitchell et al., 2011; Stone et al., 2015). Therefore, stiffening of the large central vessels can negatively impact brain vascular structure, and elevated central arterial stiffness is associated with reduced cognitive function.

Cerebral Pulsatility Index

Investigating the rheological parameters of blood flow in the intracranial vessels may provide further insight regarding cerebral vascular function. A common measurement derived from flow or velocity measurements in the brain is Gosling's pulsatility index (PI), which is calculated as the difference between the systolic and diastolic flow or velocity divided by the mean flow or velocity. An example of cerebral PI quantified from an MCA velocity waveform is shown in Figure 7. Cerebral PI is often interpreted as a descriptor of distal cerebrovascular resistance. For example, a greater PI may reflect higher resistance distally to the location of the flow or velocity measurement (Giller et al., 1990). Others have suggested that cerebral PI may also represent intracranial pressure (Bellner et al., 2004). For example, a greater cerebral PI may represent higher intracranial pressure, as when intracranial pressure is increased, diastolic flow decreases from increased distal resistance. In addition, cerebral PI may reflect proximal stenosis, as ICA stenosis is associated with lower cerebral PI in the MCA (Bill et al., 2020). Cerebral PI in the MCA is positively associated with vascular risk factors, such as age (Bill et al., 2020; Tegeler et al., 2013), carotid plaque burden, acute ischemic brain lesion, and cerebral small vessel disease (Kidwell et al., 2001). Finally,

cerebral PI has been positively associated with increasing severity of dementia (Foerstl et al., 1989; Rivera-Rivera et al., 2016). Taken together, cerebral PI may represent distal cerebrovascular resistance, or something else that is related to the structure of the cerebral microvessels. Likely it represents a combination of factors. Regardless, higher cerebral PI is associated with disrupted cerebrovascular hemodynamics and other unfavorable outcomes.

Summary of Cerebral Hemodynamics and Vascular Stiffness

Blood pressure and blood flow throughout the cardiovascular system is pulsatile. Pulse components can be dissected to understand the system hemodynamics. A faster carotid-femoral pulse wave velocity is reflected as higher central arterial stiffness, which increases with aging. Central arterial stiffness may reduce the buffering capacity of the aorta, allowing translation of high mechanical forces into the microvascular beds of the brain. Indeed, cfPWV is associated with white matter damage and cognitive impairment. Gosling's Pulsatility index can be derived from the flow or velocity waveforms of large intracranial arteries such as the MCA. Higher cerebral PI may be reflective of increased distal resistance. Furthermore, cerebral PI in the brain is positively associated with vascular risk factors and dementia severity.

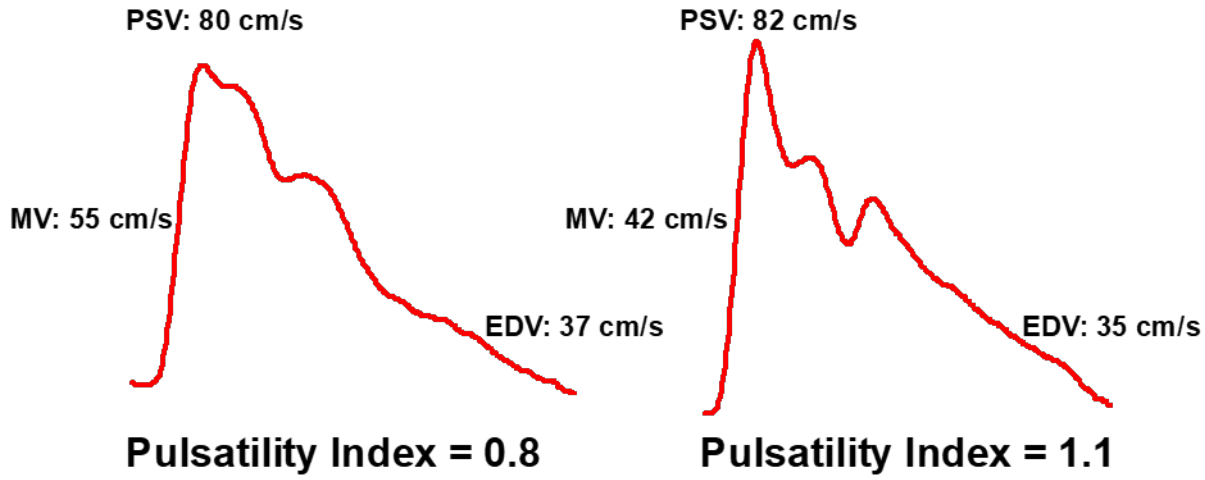

Figure 7. Example quantification of cerebral pulsatility index from a velocity waveform

This figure shows two tracings of the middle cerebral artery velocity (MCAv) from two different participants. These tracings were acquired using a transcranial Doppler ultrasound. The waveform on the left is an example of a pulsatility index of 0.8. The waveform on the right is an example of the pulsatility index of 1.1. Pulsatility index is calculated using the following equation: Pulsatility index = (Peak systolic velocity (PSV) – End diastolic velocity (EDV)) / Mean velocity (MV).

Figure information:

Figure created using unpublished data from our laboratory.

1.4.5 CONSEQUENCES OF POOR CEREBRAL BLOOD FLOW REGULATION

Overview of Consequences of Poor Cerebral Blood Flow Regulation

Though robust, the cerebrovascular system is not perfect and the consequences of inadequate blood flow supply both acutely and chronically are severe. For example, complete loss of blood flow to neuronal tissue can cause tissue death in less than five minutes. In addition, many cellular processes including protein synthesis, aerobic metabolism, and overall glucose metabolism are inhibited with reductions in global CBF below 25 ml/100g/min (Mies et al., 1991). This is unique to neural tissue, as other tissues such as cardiac myocytes or kidney cells can tolerate 20-40 minutes of ischemia before irreversible damage occurs (Silver and Erecińska, 1990). In the instance of occlusion of a large intracranial vessel, such as a stroke, the resulting ischemia can cause permanent brain damage and even death (Thomas et al., 2015b). Acute hypoperfusion may cause dizziness, headache and lack of consciousness (Smith et al., 2011). Hyperperfusion can also cause vascular damage, as the skull does not allow for much expansion of extracellular fluid or tissue (van Mook et al., 2005). Chronically low blood flow, or inadequate matching of blood supply to metabolic demand in the brain, may have long term cognitive consequences. For example, chronic hypoperfusion may manifest as neuronal injury in vulnerable areas that are often associated with cognitive impairment (Johnson et al., 2005). In addition, there is evidence to suggest that cerebrovascular dysfunction may be part of the etiology of dementia and interact with Alzheimer's disease pathology, which is described in the following section in further detail. Thus, adequate CBF is necessary for the survival of brain tissue, optimal brain health and cognitive function.

Relevance of Cerebral Blood Flow to Dementia

There is increasing evidence that vascular dysfunction may be part of the etiology of dementia. Vascular risk factors increase the risk for developing dementia at least two-fold. This has been demonstrated in multiple large population based studies (Alonso et al., 2009, 2009; Breteler et al., 1994; Freitag et al., 2006; Gottesman et al., 2017; Kivipelto et al., 2001). The term dementia refers to progressive decline in cognition and is typically associated with aging, independent of pathology. The leading diagnosis of dementia is Alzheimer's disease. However, the diagnosis of vascular dementia, a high load of vascular-related brain pathology and evidence of cognitive decline, accounts for approximately 20% of dementia diagnoses (Gorelick et al., 2011). While it is becoming increasingly clear that the health of the cerebrovascular system is important for cognitive health, the integration of vascular dementia and Alzheimer's disease related pathologies are still being elucidated.

The index case for "Alzheimer's disease" (AD) described by Aloys Alzheimer, identified neurofibrillary tangles in nerve cells and senile plaques in the cerebral cortex of a woman with severe cognitive impairment (Jellinger, 2006). The plaques, later identified as parenchymal and vascular amyloid deposits, became the hallmark pathology of AD. Interestingly, in the early 1900's, dementia was thought to be caused by the "hardening of the arteries" and most of its studies were related to vascular factors (Bowler, 2007). It was not until the late 1980's when an important discovery led to the amyloid hypothesis defining dementia research. The amyloid beta peptide was identified as the main component of amyloid deposits or senile plaques (Glenner and Wong, 1984; Kang et al., 1987) and subsequent studies of its genome found that the amyloid precursor protein (APP) gene was associated with multiple pedigrees of early-onset familiar AD (St George-Hyslop et al., 1987). Much of the research on AD since has been focused on the idea that the development

of multiple brain pathologies (neurofibrillary tangle formation, synapse loss and neuronal cell death) are a consequence of the imbalance between the generation and clearance of Aβ (Bowler, 2007). Clinical diagnosis still reflects this idea, with majority of dementia cases being classified as AD. Yet, the neuropathology is more complex, with only 24% of dementia cases featuring exclusively AD pathology. The remaining cases feature vascular pathology, a mix of vascular and AD pathology, or other pathology (Santisteban and Iadecola, 2018). Thus, it is possible that the interaction between vascular pathology and typical AD pathology is multifarious. Vascular and AD pathology may be working independently or synergistically. The "two-hit vascular hypothesis" is an example of synergistic pathology. This hypothesis suggests that multiple factors including genetic, vascular, and environmental cause primary vascular damage on blood vessels in the brain and subsequently the neurovascular unit, leading to Aβ accumulation in the brain. The second hit is then caused by the Aβ accumulation, accelerating the Aβ-dependent pathway of neurodegeneration and preventing washout since blood vessels are damaged (Kisler et al., 2017).

Importantly, the timing of the two pathologies may also be crucial for the movement through the latent, to prodromal, to disease phase of AD. It has been suggested that reduced CBF is a biomarker of clinical AD (Hays et al., 2016) and that declines in CBF occur before common neurological biomarkers such as changes in Aβ or brain volume (Iturria-Medina et al., 2016). In addition, reductions in cerebrovascular reactivity have been reported in patients with mild-cognitive impairment (Lim et al., 2018; Shim et al., 2015; Silvestrini et al., 2006) and other cross-sectional studies have shown an association between hypoperfusion and mild cognitive impairment (Johnson et al., 2005). A study by Wolters et al., prospectively evaluated the association between CBF and cognition in participants of the Rotterdam Study without dementia. They found that cerebral hypoperfusion was associated with accelerated cognitive decline and increased risk of

dementia in the overall group. In addition, when global CBF was divided into quartiles (Q1=<50 mL/100mL/min, Q2=50-55 mL/100mL/min, Q3=56-62 mL/100mL/min, Q4=>62 ml/100mL/min), the hazard ratio for all-cause dementia increased 2-fold in the lowest quartile group compared with the highest. Those in the lowest quartile group who additionally had severe white matter hyperintensity damage incurred another 2-fold hazard ratio increase for all-cause dementia (Wolters et al., 2017). These results suggest that not only is global perfusion associated with all-cause dementia, those with cerebral hypoperfusion may be more effected by microvascular damage. In patients with mild cognitive impairment (MCI), ICA and MCA mean flow values, measured using 4D flow MRI, were associated with a performance of executive function, such that participants with lower flow values performed worse on the cognitive test. In addition, ICA flow was also associated with amyloid positivity (Berman et al., 2017). Furthermore, in a cross-sectional study of 314 subjects, mean global CBF decreased while global cerebral PI increased as disease progressed from healthy control to MCI to AD (Rivera-Rivera et al., 2016). Taken together, these findings further supported a role of cerebral hypoperfusion in the pathophysiology of dementia. This is evident in pre-clinical phases, where neuropathological and cognitive symptoms could not yet be detected, and as well as in clinical phases, when symptoms and pathology are present. Despite this evidence, the nature of the relationship between vascular pathology and neuronal pathology in the development of dementia requires further study.

Summary of Consequences of Poor Cerebral Blood Flow Regulation

Without adequate blood flow, the brain cannot optimally function. A functional cerebrovascular system is necessary to adequately regulate blood flow. Acute reductions in blood flow cause damage to neural tissues within minutes. Other symptoms of acute reductions in blood flow include

dizziness and loss of consciousness. Chronic reductions in blood flow may have cognitive consequences. Vascular pathology in the brain, including reductions in blood flow and cerebrovascular dysfunction have been linked to dementia. It is possible that brain vascular dysfunction is part of the etiology of Alzheimer's disease, though the connection between neuronal pathology and vascular pathology has yet to be elucidated.

1.4.6 CEREBRAL BLOOD FLOW AND AGING

Overview of Cerebral Blood Flow and Aging

Aging itself is defined as the passing of time, and with the passing of time comes a progressive loss of cellular integrity, impaired cellular function and increased vulnerability to pathologies (López-Otín et al., 2013). Age-related differences in CBF have been noted by multiple investigators utilizing different techniques to measure CBF, though cellular mechanisms responsible for a decline in CBF with aging have not been elucidated. Notably, using the Kety-Schmidt technique to measure CBF (Kety, 1956), Kety concluded that cerebral blood flow declines steeply from childhood to adolescence. Physical maturation is followed by a gradual decline in CBF throughout the lifespan. This was later replicated by Melamed et. al using the 133 Xenon inhalation method to measure CBF (Melamed et al., 1980) and other techniques including ASL (Cavuşoğlu et al., 2009; Chen et al., 2011; Liu et al., 2012b; Zou et al., 2009), PET imaging (Leenders et al., 1990; Martin et al., 1991; Pantano et al., 1984), and phase-contrast MRI (Buijs et al., 1998; Lu et al., 2011; Zarrinkoob et al., 2015). Additionally, using color duplex ultrasound to measure blood flow through the carotid and vertebral arteries, Scheel et. al. estimated that the age-related difference in global CBF of 78 adults was approximately 3 ml/min/year (Scheel et al., 2000). In a population based study of 1720 participants, the age-related differences in MCA velocity measuring using TCD was approximately 0.5 cm/s per year (Bakker et al., 2004). Regardless of technique, most large studies report an approximate age-related difference in global CBF of -5% per decade, which is similar to the reduction in metabolic rates for oxygen and glucose (Leenders et al., 1990; Petit-Taboué et al., 1998). The brain atrophies with age; however, rates of atrophy are not linear, with larger age-related differences in volume occurring after the 7th decade of life, and they may be heterogeneous across regions (Scahill et al., 2003). Importantly, age-

related differences in CBF appear to be independent of gray matter atrophy (Chen et al., 2011; Itoh et al., 1990) . Thus, aging is associated with the decline in global CBF, and this association been described using multiple techniques to measure CBF. Age-related differences in CBF appear to be analogous, but independent, from age-related brain atrophy.

Regional Cerebral Blood Flow and Aging

In addition to global reductions in CBF observed with aging, it is possible that certain brain regions are more vulnerable to age-related declines in CBF. Early studies using 133 Xenon inhalation to measure CBF observed that age-related differences were more prominent in frontal regions supplied by the anterior circulation, particularly in the left hemisphere, compared with other regions in adults aged 19-79 (Melamed et al., 1980). Using the same technique to measure CBF, a study of 105 participants age 19-80 found that age-related differences were more prominent in the MCA distribution areas, reflective of the anterior circulation, though they did not observe hemispheric differences (Matsuda et al., 1984). A study using PET imaging of 50 healthy subjects aged 31-78 found that age-related differences in CBF were greater in the left hemisphere, and significantly greater in left frontotemporal cortex and temporocingulate cortex; however, regional CBF actually increased with age in central structures (Pagani et al., 2002). Observations from the Dallas Lifespan Brian Study with 226 subjects aged 20-89 suggest that the largest age-related differences were present in the anterior circulation within rostral areas of the brain. Age-related differences were also more prominent in the right hemisphere (Lu et al., 2011). Other studies have observed significant differences in regions that are not related to the default mode network, suggesting that default mode network areas are preserved with age at the expense of other areas (Beason-Held et al., 2009; Chen et al., 2011; Lee et al., 2009; Leenders et al., 1990). Taken

together, these studies suggest that there is variability in the regional locus of age-related differences in global CBF. Many studies suggest that age-related differences in CBF may be more pronounced in anterior regions. However, this may be due to the scale of blood flow directed to anterior regions, as 70% of total flow is directed to anterior regions as opposed to 30% directed to posterior regions.

There are a few studies that evaluated blood flow in the large intracranial arteries that suggest posterior brain regions demonstrate greater relative age-related differences in CBF compared with anterior regions. In a study of 48 adults aged 20 to 80, age-related differences in ICA flow was approximately 13% over the lifespan, whereas age-related differences in VA flow was approximately 32% over the lifespan (Dörfler et al., 2000). Using Doppler sonography to measure CBF in 180 healthy adults, the relationship between CBF and age was stronger in the ICAs compared with the VAs. However, the relative age-related difference in ICA flow was 16% on average whereas the relative age-related difference in VA flow was 25% on average (Albayrak et al., 2007). In a cross-sectional of 22 young (age = 24) and 11 elderly adults (age = 70), blood flow in the ICAs was approximately 10% lower in older adults compared with young adults. Yet, VA blood flow was approximately 37% lower in older adults compared with young adults (Olesen et al., 2019). A study using 2D phase contrast quantitative MR angiography also found larger age-related differences in CBF in the posterior circulation. When comparing the youngest to the oldest age groups, age-related differences in CBF of the BA was approximately 28% and difference in CBF in the left ICA was 25% (Zhao et al., 2007). However, a separate study that measured CBF using ultrasound in the extracranial vessels in 78 men and women without carotid plaque formation, ICA flow significantly was significantly lower with age but the difference in flow with age in the sum of the VAs was not significant (Scheel et al., 2000). Thus, these studies suggest

age-related differences in the blood flow of the ICAs are between 10-25% and age-related differences in the blood flow of the BA or VAs are between 25-37%. Difference in the technique used to measure CBF, as well as the inclusion of one or both of the vessels on the right or left side may contribute to the variability in the results.

In summary, it appears that the trajectory of age-related differences in CBF may vary by region. Studies of CBF of the entire brain using PET or MRI techniques suggest that differences in blood flow with aging is more prominent in the anterior regions of the brain. However, when evaluating blood flow in the large intracranial arteries, the evidence suggests that the posterior circulation is potentially the most affected by aging. It is important to consider that the discrepancy in the literature may be the way that CBF is quantified, either relative to the entire brain or relative to each region. In addition, there are other factors that may influence the trajectory, and the region, of age-related differences in CBF. These include anatomical variations, biological sex, vascular risk factors, and exercise training or cardiorespiratory fitness.

Influence of Cardiorespiratory Fitness on Cerebral Blood Flow and Aging

The age-related differences in resting CBF may be influenced by regular aerobic exercise. For example, in prospective study by Bailey et al., 81 healthy adults were assigned to groups according to their age and lifetime physical activity levels. Individuals with higher physical activity levels had attenuated the age-related differences in resting cerebral blood velocity. Though the measure of lifetime physical activity was self-report, which could be considered a limitation to the way they categorized participants into groups, they also had an objective measure of fitness. All participants also underwent an incremental exercise test to determine their maximal cardiorespiratory fitness levels (VO_2max). Results from this analysis showed a linear relationship between resting cerebral

blood velocity and VO_2max in older adults (Bailey et al., 2013). Using ASL to measure CBF in 55 older adults, estimated cardiorespiratory fitness mediated the effects of aging on CBF in gray matter (Zimmerman et al., 2014). In a study of master athletes and sedentary older adults, master athletes demonstrated higher perfusion in both the posterior cingulate and the precuneus regions compared with age-matched adults who were sedentary (Thomas et al., 2013). Our previous work suggests that young and middle-aged adults who perform habitual exercise did not demonstrate age-related differences in MCA velocity (Miller et al., 2018). In addition, sedentary older adults who underwent a 3 month aerobic exercise intervention demonstrated elevated perfusion in the anterior cingulate region after the intervention (Chapman et al., 2013). However, a study of 47 middle-aged to older adults aged 64-78 years did not report an improvement in cerebral perfusion measured by ASL after a 6 month aerobic exercise training intervention (Flodin et al., 2017). Taken together, the results from these studies suggest that the trajectory of the age-related declines in CBF may be modified by habitual exercise status and associated with cardiorespiratory fitness. However, this effect is not conclusive and may be more relevant for certain brain regions.

Influence of Sex on Cerebral Blood Flow and Aging

The trajectory of age-related changes in CBF may be sex specific. Both men and women experience fluctuations in hormones throughout the lifespan, with significant hormonal changes in women occurring during the menopausal transition. During the menopausal transition, women experience a loss of estrogen availability. Estrogen is often referenced as “cardioprotective”. Thus, reducing estrogen availability may explain why women experience an acceleration of risk for cardiovascular events after menopause (Reckelhoff and Fortepiani, 2004). Sex-specific etiologies and outcomes of diseases have also been reported in the brain. For example, postmenopausal

women have a higher incidence of stroke (Haast et al., 2012) white matter lesions, and cognitive impairment (Breteler et al., 1994) compared with age matched men. Not only do women have higher risk, the cognitive performance of postmenopausal women diagnosed with Alzheimer's disease decline faster than age-matched men (Tschanz et al., 2011). Despite the observed sex differences in cardiovascular risk, there have only been a few studies that have evaluated the influence of sex on age-related declines in CBF. For example, in 115 men and women aged 20-83, women demonstrated greater CBF compared with age-matched men until age 60, where there were no sex differences present (Martin et al., 1994). Similar findings were reported in a study of 364 healthy men and women age 18-80 where MCA velocity was higher in women until approximately age 60 (Tegeler et al., 2013) and in a large, population based study with over 1,000 participants where women demonstrated greater MCA velocity compared with age-matched men until age 80 (Bakker et al., 2004). Taken together, these results suggest that women may experience accelerated age-related decline in CBF after menopause. It is possible that sex differences in the age-related trajectory of CBF decline may contribute to some of the variability in the rates of decline that are reported. In addition, sex differences in CBF may have implications for sex differences in brain disease prognosis and outcomes.

Summary of Cerebral Blood Flow and Aging

In summary, the amounting evidence suggests that CBF declines with age. However, the trajectory of decline may vary by region and be influenced by confounding factors. For example, some studies suggest that age-related differences in CBF are more prominent in anterior brain regions. However, the magnitude of differences in CBF relative to the blood flow distribution to each region may be more pronounced in the posterior circulation. Cardiorespiratory fitness and habitual

exercise have positive effect on resting cerebral blood flow and may attenuate age-related differences, though the magnitude of this effect, as well as the influence of other physical activity and lifestyle behaviors such as smoking, sedentary time, and diet are unknown. Trajectory of declines in CBF may also be sex-specific, as women experience greater declines in CBF after the 6^{th} decade of life, which corresponds to the menopausal transition. Further research is necessary to understand how CBF changes with advancing age, and the extent that factors such as cardiorespiratory fitness and sex impact age-related changes in CBF.

1.4.7 CEREBROVASCULAR REACTIVITY TO HYPERCAPNIA

Overview of Cerebrovascular Reactivity to Hypercapnia

Quantifying the CBF response to a stimulus may be more telling of health of the cerebral vessels compared with measuring CBF at rest. The cerebral circulation is uniquely sensitive to changes in arterial CO_2. Because of this, CO_2 is an excellent stimulus to test the vasomotor function of the cerebral vessels. Thus, the CBF response to hypercapnia, termed cerebrovascular reactivity, is commonly used in many laboratory settings to quantify cerebral vasomotor function in humans (Iliff et al., 1974). In the range where the relationship between CBF and arterial CO_2 is linear, changes in CBF (via changes in blood flow velocity and blood vessel diameter) can be associated with changes in arterial CO_2 to determine a reactivity slope. An example of this relationship is shown in Figure 8. In this example, subject 1 has a greater cerebrovascular reactivity slope which would suggest a more robust CBF or cerebral blood velocity response to the CO_2 stimulus and perhaps better cerebrovascular function compared with subject 2.

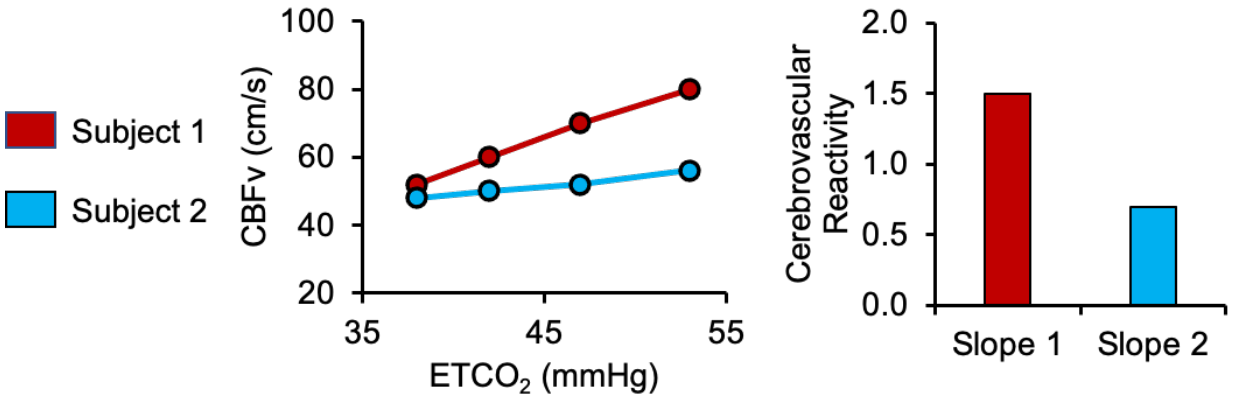

Figure 8. Example quantification of cerebrovascular reactivity.

This example uses representative data. Subject 1 is shown in red and subject 2 is shown in blue. The graph on the left shows the cerebral blood velocity (CBFv) response to stepwise increases in end-tidal CO_2 ($ETCO_2$). The graph on the right shows the slope of the line from graph 1, calculated as the slope of the relationship between $ETCO_2$ and CBFv. In this case, subject 1 (red) demonstrated a greater cerebral blood velocity response to CO_2, as indicated by a larger slope compared with subject 2. This would suggest that subject 1 has a greater cerebral vasodilator capacity and perhaps better cerebral vasomotor function compared with subject 2.

Figure information:

Figure created using unpublished data from our laboratory.

Association between Reduced Cerebrovascular Reactivity and Other Outcomes

Reductions in cerebrovascular reactivity to hypercapnia have been implicated in multiple pathological conditions that are associated with reduced cerebral vasomotor function. For example, reduced cerebrovascular reactivity is evident in patients with a history of concussions (Churchill et al., 2019), a history of traumatic brain injury (Amyot et al., 2018), metabolic syndrome (Viticchi et al., 2015) diabetes (Dandona et al., 1978; Tchistiakova et al., 2014), sleep apnea (Buterbaugh et al., 2015; Prilipko et al., 2014) and hypertension (Haight et al., 2015; Lipsitz et al., 2000). In addition, reduced cerebrovascular reactivity may precede other brain pathologies including white matter damage (Kearney-Schwartz et al., 2009), stroke (Gupta et al., 2012; Markus and Cullinane, 2001; Portegies et al., 2014), and amyloid-beta deposition (Smith and Greenberg, 2009). Cerebrovascular reactivity is progressively worse in AD patients with more pronounced cognitive decline (Richiardi et al., 2015; Shim et al., 2015; Silvestrini et al., 2006), is lower in patients with AD compared with cognitively normal adults (Silvestrini et al., 2006) and has been suggested as a biomarker to predict dementia risk (Hays et al., 2016; Iadecola, 2004; Urbanova et al., 2018). Taken together, reduced cerebrovascular reactivity may indicate reduced cerebral vasomotor function, and may precede other brain pathologies and cognitive decline.

Experimental Considerations for Cerebrovascular Reactivity to Hypercapnia

Multiple approaches have been used to administer CO_2 for cerebrovascular reactivity testing. Although the goal of all methods is to produce a vasoactive response, they differ in administration, output, and reproducibility within and between subjects (Fierstra et al., 2013). The main methods to induce hypercapnia include breath holds and re-breathing, administration of acetazolamide,

inhalation of gases at fixed concentrations (~3-10% CO_2) or inhalation of CO_2 with targeted CO_2 levels above resting values (~+5 to +10 mmHg).

Acetazolamide administration produces acidosis in both the extracellular and intracellular space causing maximal vasodilation of the VSMC (Vorstrup et al., 1986). However, the variability in the dosing between subjects and response to a given dose within subjects prevents a reproducible stimulus (Dahl et al., 1995). Acetazolamide administration is further complicated by side effects of large doses and mild but uncomfortable symptoms at low doses (Saito et al., 2011). Breath hold index as a way to assess cerebrovascular function has been praised by its convenience and lack of invasiveness (Markus and Harrison, 1992) though its output can be difficult to reproduce leading to inaccurate interpretation of results (van Beek et al., 2011; Palazzo et al., 2013). Similar issues arise with rebreathing techniques (Berkenbosch et al., 1989).

Administration of CO_2 by gas inhalation has proved to be a safe and effective alternative to other methods. The main concern with inhaling CO_2 at a fixed concentration is that it may not elicit a constant end-tidal CO_2, i.e. some participants may increase end-tidal CO_2 levels more than others (Fisher, 2016). It is also important to note that end-tidal CO_2 is commonly used as an estimate of arterial CO_2 when arterial blood sampling is not available. In order to address this limitation, multiple levels of CO_2 at steady-state can be administered. A reactivity slope can then be determined that describes the change in CBF per 1 mmHg increase in end-tidal CO_2 as employed by (Berkenbosch et al., 1989; Xie et al., 2006).

There are also multiple methods to measure CBF during cerebrovascular reactivity to hypercapnia. Common methods including BOLD MRI, TCD, Duplex Ultrasound and phase contrast MRI (Hoiland et al., 2019). In addition to the strengths and limitations for each method to measure CBF at rest, additional limitations for these methods arise when employing a hypercapnic

challenge to measure cerebrovascular reactivity. Although BOLD MRI can determine regional reactivity non-invasively, BOLD MRI lacks a volumetric flow measurement. In addition, when measuring reactivity to hypercapnia, BOLD MRI has a lack of specificity of the measurement as it is largely influenced by the cerebral metabolic rate of oxygen. Advantages of duplex ultrasound include the ability to measure velocity and vessel diameter. With multiple probes on the large intracranial vessels, global CBF can be estimated. However, measurements must be done extracranially. For intracranial measurements, TCD is commonly employed. Typically, the MCA or PCA is insonated by TCD to provide an estimate of the anterior or posterior blood flow response to CO_2. However, TCD can only measure velocity and is constrained to one vessel per probe. Importantly, recent evidence suggests that TCD may underestimate cerebrovascular reactivity of the MCA as the MCA may vasodilate during the hypercapnic stimulus. This evidence is described in further detail in the following section. To address this limitation, phase contrast MRI may be a sufficient alternative. Phase contrast MRI can measure both velocity and angiograph data in the large intracranial vessels. Individual arteries or veins are measured by placing cut planes perpendicular to the vessel (2D phase contrast) or by imaging the entire brain (3D or 4D phase contrast). Though it cannot assess beat-by-beat blood flow, phase contrast MRI can assess steady-state blood flow response to stimuli even if the large intracranial vessels are changing diameter.

In summary, multiple approaches have been used to measure cerebrovascular reactivity including various ways to administer CO_2 and various ways to measure CBF. The studies in this dissertation use the steady-state inhalation technique to elicit hypercapnia and determine reactivity as a slope. They use TCD as well as 4D flow MRI to measure cerebral blood velocity and CBF respectively.

Change in MCA diameter during Cerebrovascular Reactivity to Hypercapnia

One of the key assumptions using the TCD is that the blood velocity measured is reflective of blood flow. This requires that the vessel diameter does not change during measurement. Holding this assumption true is especially important during a physiological perturbation when the goal is trying to assess a blood flow response as an indicator of the health of the cerebral vessels. This concept has been a topic of debate in the Journal of Physiology – cross talk (Brothers and Zhang, 2016; Hoiland and Ainslie, 2016). Recent studies using high field MRI have shown vasodilation of the MCA during hypercapnia. A study of 11 young adults that underwent a 3T MRI scan demonstrated an 8% change in MCA diameter with a T2 fast spin echo sequence during a 6% CO_2 stimulus (Coverdale et al., 2015). Subsequent studies using 7T MRI have reported similar findings. In a study by Verbree et al., 10 healthy young adults underwent a 7T MRI scan where MCA diameter was assessed during hypocapnia, normocapnia and two levels of hypercapnia (+7.5 and +10mmHg). The authors reported a 6.8% increase in MCA diameter in response to +10 mmHg compared with baseline. However, there were no significant changes in the other conditions (Verbree et al., 2014). In a study by Al-Khazraji et al., 8 young adults underwent a 7T MRI scan and measured MCA diameter using a T1-weighted 3D SPACE pulse sequence during 5% CO_2 stimulus. The authors described a 11% increase in MCA cross-sectional area compared to the normocapnic conditions (Al-Khazraji et al., 2019). However, in a study of 8 young adults, no significant change in MCA cross-sectional area was observed when participants underwent a 3T MRI scan and 4D flow was used to evaluate the MCA during an increase of ~4 mmHg, though the authors credit the lower CO_2 levels compared with previous studies as the reason for no observed changes in MCA diameter (Mikhail Kellawan et al., 2016). Only one study has reported on MCA diameter changes during hypercapnia in older adults using a T2 fast spin echo sequence during a

3T MRI scan (Coverdale et al., 2017). Their results in 10 older adults suggest heterogeneous changes in MCA during a 6% CO_2 stimulus, as some participants demonstrated increases in MCA cross-sectional area, and some demonstrated decreases MCA cross-sectional area. Overall, the increase in MCA cross-sectional area was approximately 4%.

It is important to note that the aforementioned studies provide evidence against classic dogma suggesting that the MCA is stable during a hypercapnic perturbation (Aaslid et al., 1982; Claassen et al., 2007; Serrador et al., 2000) . For example, 6 participants underwent a 1.5 T MRI scan to measure MCA diameter using black blood magnetic resonance angiography at rest and during 6% CO_2 inhalation (Serrador et al., 2000). They reported that the MCA did not change during the hypercapnic stimulus. However, the MCA values were approximately 2.5 mm, which is approximately 0.5 mm less than typically reported values for men and women of that age (Müller et al., 1991). In addition, studies detecting changes in MCA diameter during hypercapnia report data from low subject numbers, utilize different MRI techniques which require manual delineation of the vessel, and do not consider how elevated mean arterial pressure during the stimulus may impact the MCA diameter. Thus, the extent of the vasoactive nature of the MCA during hypercapnia is still controversial, especially as it applies to different subject populations besides young, healthy adults.

Cerebrovascular Reactivity to Hypercapnia and Aging

Though it has been established using multiple techniques that global CBF declines with advancing age, the age-related changes in the cerebrovascular response to a hypercapnic stimulus are less clear. Dozens of studies have evaluated the age-related differences in either the blood velocity or the blood flow response to hypercapnia (see Table 3 of Hoiland 2019). Many of the findings

suggest age-related differences in cerebrovascular reactivity. For example, in a population based study of approximately 1700 participants, the MCA velocity response to hypercapnia measured using TCD was lower across the lifespan with the greatest age-related differences in MCA velocity occurring after 65 years of age (Bakker et al., 2004). An age-related reduction in cerebrovascular reactivity to hypercapnia has been observed in other studies also using TCD (Bailey et al., 2013; Barnes et al., 2012; Jaruchart et al., 2016; Kastrup et al., 1998; Oudegeest-Sander et al., 2014), as well as in studies using other techniques to measure CBF such as PET imaging (Ito et al., 2004), 133 Xenon inhalation (Lu et al., 2011) and BOLD MRI (Thomas et al., 2013, 2014). In contrast, some studies using TCD have reported similar cerebrovascular reactivity (no decline with age) in healthy adults. For example, a study by Madureira et al., suggested that age was not related to cerebrovascular reactivity to hypercapnia in 58 adults aged 20-80, though this study did not exclude for hypertension, and did not take hypercapnia induced changes in arterial blood pressure into account of their measurement of cerebrovascular reactivity (Madureira et al., 2017). A study by Galvin et. al., reported a similar reactivity between young and older age groups; however, the CO_2 stimulus also included 95% O_2, which could lead to a blunted vasodilatory response (Galvin et al., 2010). Thus, the majority of the evidence suggests that there are age-related differences in cerebrovascular reactivity to hypercapnia, although there are some exceptions that could be explained by consideration of hypercapnia-induced changes in mean arterial blood pressure or the method of CO_2 administration. However, similar to age-related differences in resting CBF, it is possible that the trajectory of age-related changes in cerebrovascular reactivity to hypercapnia may be influenced by other factors such as sex hormones, habitual exercise participation or cardiorespiratory fitness.

Influence of Cardiorespiratory Fitness on Cerebrovascular Reactivity

There have been conflicting reports on the influence of habitual exercise participation or cardiorespiratory fitness on cerebrovascular reactivity to hypercapnia. In our previous study, middle-aged healthy adults who performed habitual exercise (at least 150 minutes of moderate intensity aerobic exercise per week) had similar cerebrovascular reactivity to hypercapnia compared with young adults (Miller et al., 2018). This suggests that the age-related differences in cerebrovascular reactivity may be attenuated by habitual exercise participation. A study by Murrell et. al., observed an increase in cerebrovascular reactivity to hypercapnia after 12 weeks of aerobic exercise training regardless of age (Murrell et al., 2013). Other studies have reported that cerebrovascular reactivity to hypercapnia is positively associated with cardiorespiratory fitness (Bailey et al., 2013; Barnes et al., 2013). However, studies of Master's athletes have reported higher (Zhu et al., 2013) or lower (Thomas et al., 2013) cerebrovascular reactivity compared with age-matched, sedentary peers. In addition, Braz et. al., reported no differences in cerebrovascular reactivity to hypercapnia in trained and untrained men (Braz et al., 2017). Thus, the effect of habitual exercise and cardiorespiratory fitness on cerebrovascular reactivity to hypercapnic is unclear. It is important to note that apart from the study by Thomas et al., all the previous studies utilized TCD to measure the MCA velocity response to hypercapnia. If the MCA vasodilates during hypercapnia, it is unknown if habitual exercise or cardiorespiratory fitness impacts the degree of dilation, and this may contribute to some of the variability in the literature.

Influence of Sex on Cerebrovascular Reactivity

Many of the previous studies on cerebrovascular reactivity to hypercapnia and aging did not consider potential sex differences in cerebrovascular function. Aging elicits a milieu of hormones

changes in both men and women. In women, fluctuations in hormones due to the timing of the menstrual cycle, as well as the use of exogenous hormones as menopausal hormone therapy may influence the cerebral vasculature. Thus, the trajectory of age-related changes in cerebrovascular reactivity to hypercapnia may vary by sex.

There are conflicting reports in the literature on whether or not sex differences exist in cerebrovascular reactivity to hypercapnia in pre-menopausal women and age-matched men. For example, premenopausal women have a higher cerebral blood velocity response to acetazolamide administration compared with age-matched men (Karnik Ronald et al., 1996; Oláh et al., 2000). Similarly, using inhaled CO_2 as the hypercapnic stimulus, there have been reports of women demonstrating higher cerebrovascular reactivity (Kastrup et al., 1998, 1997, 1999). However, another study that utilized inhaled CO_2 to +10 mmHg above baseline levels as the hypercapnic stimulus observed no difference between sexes (Peltonen et al., 2015). The timing of the menstrual cycle may contribute to the discrepancy in findings. For example, elevated estradiol during the late follicular phase in young women may influence the bioavailability of vasodilators like NO or prostaglandins. Indeed, premenopausal women demonstrated a higher breath hold index compared with age-matched men during the late follicular phase, despite no sex difference reported during the early follicular phase (Diomedi et al., 2001). In response to acetazolamide administration, the blood flow response in the common carotid and ICAs was significantly associated with ovarian hormone concentrations (estrogen and progesterone) (Krejza et al., 2013). It was also noted that the cerebral blood velocity response to hypercapnia after indomethacin administration was linearly related to responses before indomethacin administration, suggesting that vasodilating prostaglandins may contribute to the sex differences observed (Kastrup et al., 1999). However, another study that evaluated the cerebral blood velocity response to hypercapnia did not find any

difference in cerebrovascular reactivity throughout the menstrual phases nor did they find unique contributions of prostaglandins by sex (Peltonen et al., 2016). In summary, sex differences in cerebrovascular reactivity to hypercapnia in pre-menopausal women and age-matched men are still unclear. Many studies suggest pre-menopausal women demonstrate greater reactivity compared with young men, though these results are not conclusive. Furthermore, the vasodilatory stimulus, as well the timing of menstrual cycle likely contributes to the variability in the literature.

There is also conflicting data describing if cerebrovascular reactivity is different between sexes in older adults. In 344 participants older than 70, postmenopausal women demonstrated a higher cerebral blood velocity response to hypercapnia compared with age-matched men (Deegan et al., 2011). However, other studies have reported no differences between postmenopausal women and age-matched men (Kastrup et al., 1997; Oláh et al., 2000), or lower cerebrovascular reactivity to hypercapnia in postmenopausal women compared with men (Bakker et al., 2004; Matteis et al., 1998). The inclusion of post-menopausal women taking menopausal hormone therapy may also contribute to the variability in the literature. For example, in a cross-sectional study, the most prominent age-related difference in cerebrovascular reactivity was in the fifth decade of life; however, this difference was attenuated in women who had taken menopausal hormone therapy (Kastrup et al., 1998). In a separate study, after 3 years of cessation of treatment, women who had taken menopausal hormone therapy had a marginally greater cerebrovascular reactivity to inhaled CO_2 compared with those who had taken a placebo (Barnes et al., 2019). However, menopausal hormone therapy did not alter the cerebral blood velocity response to acetazolamide administration (Bain et al., 2004). Taken together, sex differences in cerebrovascular reactivity to hypercapnia in older adults are unclear. There may be some influence of exogenous hormones, but further study

is needed to determine the impact of menopausal hormone therapy on cerebrovascular reactivity to hypercapnia.

In summary, there are reports of both higher and lower cerebrovascular reactivity in women compared with men. Furthermore, the timing of the menstrual cycle, as well as the use of exogenous hormones for menopausal hormone therapy, may further add to the controversy in the literature. It appears that there may be an influence of menstrual cycle hormones or exogenous hormones; however, more studies are needed to determine their impact. Importantly, the question regarding if the trajectory of age-related change in cerebrovascular reactivity varies by sex remains unanswered.

Summary of Cerebrovascular Reactivity to Hypercapnia

Cerebrovascular reactivity to hypercapnia is a common laboratory test of cerebral vasomotor function where the cerebral blood flow response to a change in CO_2 is quantified. Reductions in cerebrovascular reactivity to hypercapnia have been described in many clinical conditions and may precede cognitive decline. There are multiple methods that can be used to elicit hypercapnia and to measure CBF. Common CO_2 administration methods include steady-state inhalation of fixed CO_2 levels or using end-tidal CO_2 targeting. Common CBF measurement techniques for cerebrovascular reactivity to hypercapnia include duplex or transcranial Doppler ultrasound, as well as BOLD or phase contrast MRI. TCD is commonly used to measure intracranial blood flow velocity. However, this technique is limited if the vessel changes in diameter during the gas perturbation, and this has been observed in recent studies. In general, much of the evidence suggests there are age-related differences in cerebrovascular reactivity to hypercapnia. This would propose that aging is associated with a reduction in cerebral vasomotor function. However, sex,

habitual exercise, or cardiorespiratory fitness may impact the trajectory of the age-related changes in cerebral vasomotor function.

1.4.8 ANATOMICAL VARIATIONS AND VERTEBRAL ARTERY HYPOPLASIA

Overview of Anatomical Variations and Vertebral Artery Hypoplasia

In a perfect system, the intracranial arteries anastomose around the Circle of Willis to provide collateral flow in case of a blockage. Importantly, the configuration of the cerebrovascular system, especially the Circle of Willis, is highly variable. Approximately 50% of human brains display the typical anatomical layout, leaving half of human brains to have some form of anatomical variations (Alpers et al., 1959). Anatomical variations include vessels that are hypoplastic, duplicated, fenestrated or even absent entirely. Based on post-mortem study of fatal fetal aneurysms, it is likely that anatomical variations are determined genetically and persist through maturation (Crompton, 1962). Many anatomical variations are benign; however, they may increase the frequency and severity of stroke and aneurysm. For example, if a stroke were to occur and the collateral nature of the Circle of Willis is compromised, the effective ischemic area may be more severe (Bogousslavsky and Regli, 1990). In addition, aneurysm typically occurs in areas where there are branches or bifurcations, which may increase with additional anatomical variations (Riggs and Rupp, 1963). Cerebral anatomical variations may also influence the distribution of CBF. For example, blood flow distribution in individuals with common anatomical variations including fetal-type posterior cerebral arteries and a missing or hypoplastic A1 segment of the anterior cerebral artery can affect the distribution of CBF on both the ipsilateral and contralateral sides (Zarrinkoob et al., 2015). Thus, cerebral anatomical variations are relatively common and may affect brain blood flow regulation.

There are many commonly reported cerebral anatomical variations, especially ones that are associated with the Circle of Willis. For example, incidence rates of common variations include fetal-type posterior cerebral arteries (PCA) where the origin of the PCA is from the ICA rather

than the BA (17-25%), hypoplasia of one or both posterior communicating arteries (PCOM) (25-34%), infundibular dilation of the PCOM (5-15%) and a missing or hypoplastic A1 segment of the anterior cerebral artery (15%) (Zampakis et al., 2015). Variations of the large intracranial arteries that feed the Circle of Willis are less reported; however, they may be more important in terms of long term hypoperfusion leading to increased risk for cognitive decline. For example, in prospective study of 1741 subjects with a 5 year follow up, carotid and vertebral artery tortuosity, kinking and coiling was assessed using computed tomography angiography (CTA). Of the 134 participants that developed AD, kinking and coiling of both the ICA (hazard ratio [HR]=1.93) and the VA (HR=1.73) were significantly associated with the development of AD (Zhou et al., 2015). In addition, vertebral artery hypoplasia (VAH) is an anatomical variation where the intracranial portion of one of the vertebral arteries is narrowed and accompanied with reduced blood flow (Figure 9). VAH has a prevalence rate of 15-35% (Kulyk et al., 2018; Ogeng'o et al., 2014; Park et al., 2007; Peterson et al., 2010; Thierfelder et al., 2014). Thus, although variations of the Circle of Willis have been well documented, further research on anatomical variations of the feeding arteries is warranted. Furthermore, variations of the large intracranial arteries may be more important to consider in situations of chronic hypoperfusion, as opposed to acute reductions in blood flow.

Determination of Vertebral Artery Hypoplasia

As described above, VAH is an anatomical variation associated with a narrowed vessel and reduced blood flow in one of the vertebral arteries. In many cases, blood flow in the contralateral vertebral artery is over twice the hypoplastic artery and the hypoplastic vessel is commonly on the right side (Hong et al., 2009; Schöning et al., 1994). The reported prevalence rate of VAH is varied

and ranges from 15-35% (Kulyk et al., 2018; Ogeng'o et al., 2014; Park et al., 2007; Peterson et al., 2010; Thierfelder et al., 2014). The large range in the prevalence may be because of differences in the technique used to image VAH (Doppler ultrasound, time of flight angiogram, phase contrast MRI, post-mortem evaluation) and the criteria used for VAH diagnosis. Many studies consider VAH to be defined as a vessel diameter less than 2.0 mm (Chuang et al., 2006; Hu et al., 2013; Park et al., 2007) and some also include criteria that includes blood flow levels less than 30-40 ml/min (Acar et al., 2005; Sato et al., 2015; Schöning et al., 1994; Seidel et al., 1999). Thus, though there is no exact consensus on VAH diagnosis, it requires imaging of the vessel in order to observe the structural components. Other studies also include blood flow measurements as a criterion. Importantly, many of the previous studies did not directly observe both angiographic and flow data to diagnose VAH. For example, time of flight angiograms and post-mortem evaluations do not provide flow information. Although ultrasound can provide both structural and flow data, it is restricted to extracranial measurements. Thus, phase contrast MRI can provide both structural and flow information to adequately diagnose VAH.

Consequences of Vertebral Artery Hypoplasia

Kulyk et. al described VAH as "an innocent lamb or a disguise" (Kulyk et al., 2018) and indeed, there are many cerebrovascular complications that have been reported in individuals with VAH. For example, differences in the diameters of the right and left VAs was the only independent predictor of moderate to severe BA curvature, which is associated with perivertebrobasilar junctional infarcts (Hong et al., 2009). This suggests that asymmetry of the VAs may contribute to hemodynamic dysfunction in the vertebrobasilar junction. In a study of ischemic stroke patients, those with VAH demonstrated reduced lower net VA flow volume compared to those without

VAH. In addition, the prevalence of VAH was over 72% of patients with a history of brainstem / cerebellar ischemia (n=18/33) suggesting that VAH is associated with acute posterior ischemic stroke (Chuang et al., 2006). When Kulyk, et al. examined first-ever ischemic stroke patients, VAH was more prevalent in those with a history of a posterior circulation infarction (34%) compared with an anterior infarction (14%) (Kulyk et al., 2018). In addition, patients with a history of posterior stroke and VAH demonstrated higher frequency of basilar artery stenosis and contralateral vertebral artery stenosis (Kulyk et al., 2018). Higher prevalence of VAH was also seen in another cohort of adults with a history of posterior stroke (44%) compared with anterior stroke (25%) and was an independent factor to VA occlusion (Mitsumura et al., 2016). VAH was a significant independent risk factor for posterior circulation infarction in patients with isolated vertigo (Zhang et al., 2017) and in patients with suspect stroke (Zhang et al., 2016). VAH is also associated with lower posterior cerebral territory blood flow (Park et al., 2007). Taken together, these findings suggest that VAH is associated with hypoperfusion of the brain, particularly in the posterior circulation. In addition, VAH may causally contribute to increased risk of ischemic stroke in the posterior circulation.

Despite the relatively high prevalence of VAH and its known increase in risk of posterior stroke, little is known on its effects on blood flow regulation in non-stroke populations. Even in the absence of stroke, VAH may contribute to long term cerebral hypoperfusion. In a study that evaluated global CBF in people with and without VAH, those with VAH demonstrated reduced global CBF and increase cerebrovascular resistance compared to those without VAH (Warnert et al., 2016). In addition, in patients with both VAH and hypertension, the contralateral vessel did not compensate for reduced flow velocities in the hypoplastic vessel. VAH was also associated with hypertension prevalence (Warnert et al., 2016). According to the selfish brain hypothesis,

posterior circulation blood flow is preserved in any expense, and lower blood flow to the brainstem may contribute to the development of hypertension to maintain adequate cerebral perfusion (Cates et al., 2012). Thus, it is possible that VAH may reduce blood flow in posterior areas such as the brain stem, as well as contribute to long-term cerebral hypoperfusion.

The influence of VAH on age-related changes in global CBF, as well as its impact on the pathogenesis of dementia, are unknown. To date, no studies have evaluated how VAH influences the trajectory of age-related decline in CBF. It is possible that the presence or absence of VAH may be contribute to the variability in the literature regarding age-related changes in cerebral blood flow. Furthermore, if the presence of VAH is associated with chronic hypoperfusion of the brain, the combination of age-related changes in CBF with VAH may be detrimental to cognitive health. Therefore, more research is needed regarding the impact of VAH on CBF regulation, especially in non-stroke populations.

Summary of Anatomical Variations and Vertebral Artery Hypoplasia

There are many common cerebral anatomical variations, with 50% of people displaying one or more variation. Cerebral anatomical variations that feed into the Circle of Willis are less commonly reported but may be more important regarding chronic cerebral hypoperfusion. VAH is an example of such a variation, where one of the vertebral arteries is narrowed with low flow. VAH has a relatively high prevalence (15-35%). There is no consensus regarding the determination of VAH, though many studies use both vessel structural and flow criteria. Common techniques to determine VAH either measure the vertebral arteries extracranially, or do not measure both vessel structure and flow. VAH has been implicated in posterior stroke, as well as reduced global CBF and increased incidence of hypertension. The impact of VAH on age-related changes in CBF, as well

as the cognitive consequences is unknown. Thus, further studies that evaluate the impact of VAH on CBF, specifically in non-stroke populations, are warranted.

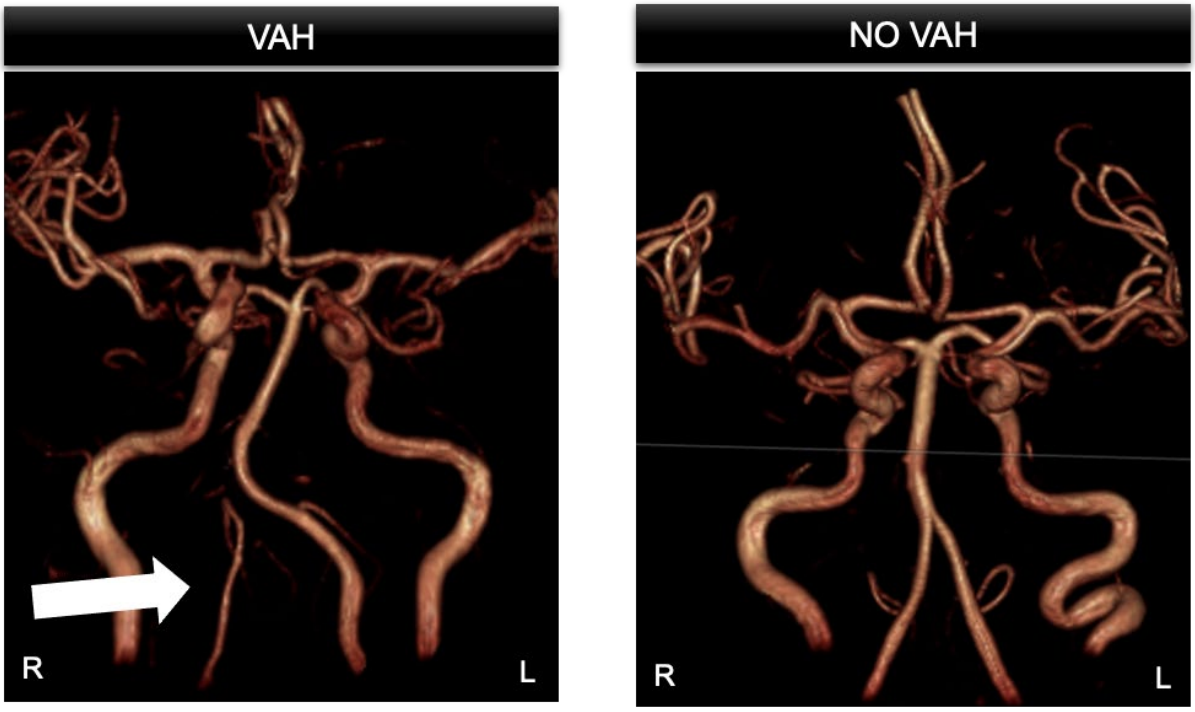

Figure 9. Example of vertebral artery hypoplasia.

The image on the left shows an example of a participant who has VAH. The arrow is pointing to the hypoplastic vessel, which is present on the right side. The image on the right shows an example of a participant who does not have VAH. R, right, L, left, VAH, vertebral artery hypoplasia.

Figure information:

Figure created using unpublished data from our laboratory.

1.5 GAPS IN LITERATURE & SIGNIFICANCE OF AIMS

The study of cerebral blood flow regulation is complex. There are multiple experimental design factors that need to be considered. Figure 10 shows a summary of studies that evaluate cerebrovascular reactivity to hypercapnia in young and older adults using the transcranial Doppler ultrasound method. There is a large variability regarding the effect of aging on cerebrovascular reactivity, with some studies showing a positive effect of aging, others showing no effect of aging and some suggesting a negative effect of aging on cerebrovascular reactivity. It is possible that experimental considerations contribute to this variability in the effect of aging on cerebrovascular reactivity. CBF results may be confounded by acute perturbations in blood pressure (Claassen et al., 2007; Coverdale et al., 2017; Galvin et al., 2010), posture (Ng et al., 2004), or blood gases (Ainslie and Ogoh, 2010; Hoiland et al., 2015, 2019). To address these factors, the studies in this dissertation are in the supine position in a quiet, temperature-controlled room. Perturbations in blood pressure are considered for all analyses. There also may be differences in how the carbon dioxide stimulus was administered and if it was accompanied with reductions in O_2 which may confound results. In this dissertation, CO_2 stimuli are accompanied with 21% oxygen. Demographic information on the participant sample is also important as there is evidence to suggest that vascular risk (Davis et al., 1983; Galvin et al., 2010; Silvestrini et al., 2006), sex (Kastrup et al., 1997; Miller et al., 2013), and menstrual cycle hormones (Krejza et al., 2013; Usselman et al., 2015) may influence CBF. In the studies in this dissertation, participants with low-vascular risk are recruited. In study 1 and 2, both men and women are recruited. Young women are studied during days 2-6 of their menstrual cycle. In addition, participants in study 1 and 2 are habitual exercisers who performed at least 150 minutes of aerobic exercise per week for at least 1 year prior to study enrollment. In study 3, participants with low to moderate vascular risk were

included and vascular risk is considered in the analysis. In addition to study conditions and participants, the technique to measure CBF is important to consider (Fierstra et al., 2013). The collection of studies in this dissertation utilizes a novel technology, 4D Flow MRI, to simultaneously measure blood flow and vascular anatomy in a single scan acquisition (Schrauben et al., 2015). This technique has multiple advantages. The first is that blood flow can be calculated, rather than using blood velocity as a surrogate for blood flow. Thus, assumptions regarding the vasoactive nature of the large intracranial vasculature can be mitigated (Brothers and Zhang, 2016; Hoiland and Ainslie, 2016). Secondly, because the major arteries of the entire cerebral circulation can be visualized, identification of cerebral anatomical variations that may impact blood flow, such as vertebral artery hypoplasia, can be done using both structural and flow criteria. This is important as many studies of CBF do not consider analysis of anatomical variations which may impact CBF regulation (Zarrinkoob et al., 2015). These studies include both healthy adults and an existing cohort of adults who are cognitively unimpaired but at an elevated risk for AD. By studying these groups before they demonstrate cognitive decline, this aids in understanding how CBF contributes to age-related disease progression. In addition, this may be an optimal timeframe for developing interventions to slow vascular dysfunction and attenuate disease progression. As the world population continues to age, the prevalence of neurodegenerative diseases is also increasing in a parallel manner. Furthermore, there is evidence of an overlap between neuropathology and vascular pathology in the etiology of dementia (Iadecola, 2010; Kisler et al., 2017). Thus, studies on the cerebral circulation are imperative to understand diseases that increase in prevalence with advancing age. This work contributes necessary insights into a building body of evidence highlighting the importance of brain blood flow regulation in the progression of cognitive decline (Berman et al., 2015, 2017; Wolters et al., 2017). It also identifies the potential

usefulness of VAH as a model of cerebral hypoperfusion and sets up rationale for longitudinal studies that evaluate the influence of VAH on cognitive function and dementia risk.

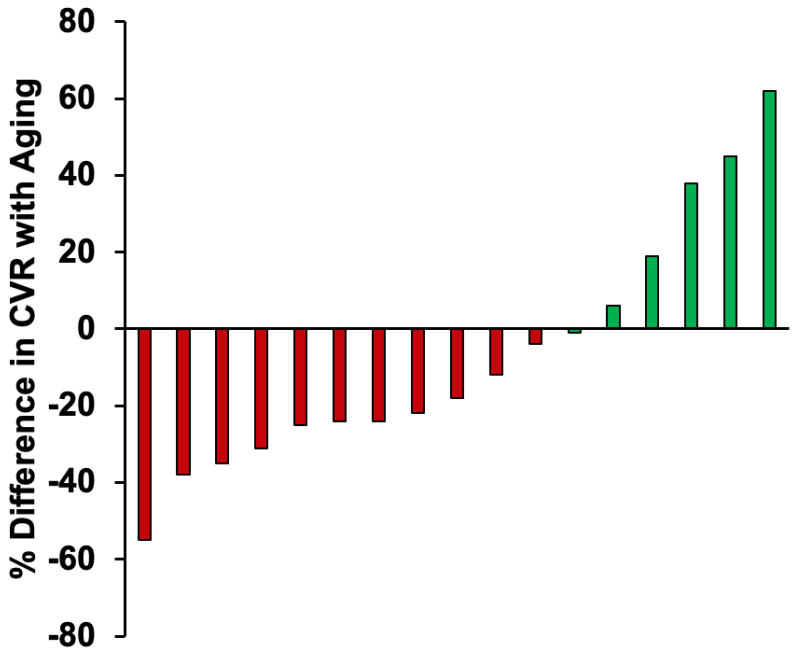

Figure 10. Summary of cerebrovascular reactivity and aging literature

This figure displays a summary of results from studies in the literature that describe cerebrovascular reactivity and cross-sectional aging. Each study included measured the middle cerebral artery blood velocity response to carbon dioxide. Each bar represents a different study and shows the reported percent difference in cerebrovascular reactivity to hypercapnia (CVR) between age groups. Red bars represent a study that reported an age-related decline in CVR and green bars represent a study that reported an age-related increase in CVR.

Figure information:

Figure adapted from Hoiland, R. L., Fisher, J. A., & Ainslie, P. N. (2019). Regulation of the Cerebral Circulation by Arterial Carbon Dioxide. Comprehensive Physiology, 9(3), 1101–1154.

CHAPTER 2

2. STUDY 1: IMPACT OF AGING ON CEREBROVASCULAR REACTIVITY TO HYPERCAPNIA

A selection of the data presented was published previously:

Miller, K.B., Howery, A.J., Rivera-Rivera, L.A., Johnson, S.C., Rowley, H.A., Wieben, O., and Barnes, J.N. (2019). Age-Related Reductions in Cerebrovascular Reactivity Using 4D Flow MRI. Front. Aging Neurosci. 11.

2.1 INTRODUCTION

The cerebral blood flow response to a vasoactive stimulus, such as hypercapnia, is termed cerebrovascular reactivity and is an important indicator of cerebrovascular health (Gupta et al., 2012; Portegies et al., 2014; Shim et al., 2015). There have been numerous studies evaluating the effect of aging on cerebrovascular reactivity to hypercapnia in large intracranial vessels; however, whether or not aging impacts cerebrovascular reactivity to hypercapnia remains controversial [see Table 3 from the review by (Hoiland et al., 2019)]. Most studies suggest that there are age-related differences in cerebrovascular reactivity. Differences in the subject population studied (individuals with high or low vascular risk), methods used to quantify cerebral blood flow or cerebral blood velocity, and methods used to administer CO_2 may account for discrepancies in the literature. For example, in our previous cross-sectional study, it was found that cerebrovascular reactivity was not different between young and older adults who habitually exercise, suggesting that lifestyle factors may be important contributors to cerebrovascular health (Miller et al., 2018). Furthermore, many studies do not address sex-related differences due to unequal distributions of men and women or do not control the menstrual cycle during study procedures. Because sex hormones influence the blood vessels in the cerebral circulation, the effect of aging on hypercapnic cerebrovascular reactivity may be sex-specific (Deer and Stallone, 2016; Miller et al., 2013).

Importantly, the majority of the existing work relies on using non-invasive imaging techniques to measure cerebral blood velocity, including transcranial Doppler ultrasound (Aaslid et al., 1982). Transcranial Doppler ultrasound measures blood velocity of the large intracranial vessels. To assume that changes in blood velocity are reflective of changes in blood flow, the vessel diameter must not change during the measurement period. Recent MRI studies have challenged this assumption by suggesting that the MCA is vasoactive during hypercapnia (Al-

Khazraji et al., 2019; Coverdale et al., 2015; Verbree et al., 2014) and vasoactive nature of the vessel may vary with age (Coverdale et al., 2017). This is an active area of debate (Brothers and Zhang, 2016; Hoiland and Ainslie, 2016).

Therefore, the objective of this study is to systematically evaluate age-related differences in cerebrovascular reactivity to hypercapnia in young and older healthy adults using two-techniques: transcranial Doppler ultrasound and 4D flow phase contrast MRI. 4D flow phase contrast MRI allows for simultaneous angiographic and quantitative blood flow measurements in the large intracranial arteries without the use of a contrast agent. It has been validated at rest (Clark et al., 2017; Rivera-Rivera et al., 2017; Schrauben et al., 2015; Wen et al., 2019; Wu et al., 2016) and during a hypercapnic challenge (Mikhail Kellawan et al., 2016). However, this approach has not been utilized to address the effect of primary aging on cerebrovascular reactivity to hypercapnia.

To address limitations of previous research, this study evaluates **Specific Aim 1** of this dissertation: to determine the impact of aging on cerebrovascular reactivity to hypercapnia. The first hypothesis is that similar to our previous study in healthy, habitually exercising adults (Miller et al., 2018), age related differences in cerebrovascular reactivity to hypercapnia when evaluating cerebral blood velocity with TCD will not be observed. However, since TCD may be underestimating blood flow responses due to the vasodilation of the middle cerebral artery, the second hypothesis is that older adults will have reduced cerebrovascular reactivity to hypercapnia compared with young adults when cerebral blood flow using 4D flow MRI is evaluated. The third hypothesis is that the middle cerebral artery will increase in diameter in response to hypercapnia in young adults, but not older adults.

2.2 MATERIALS AND METHODS

Participant Recruitment

Participants were recruited from the Madison, WI and surrounding areas with recruitment flyers and word of mouth. Young (age = 18-35) and older (age = 50-69) men and women were recruited. Exclusion criteria included current smoker, history or evidence of hepatic, renal, or hematological disease, peripheral vascular disease, stroke or neurovascular disease, cardiovascular disease, hypertension, diabetes, or other chronic pathologies as determined by a health-history questionnaire. Premenopausal women were not pregnant, and all older women were postmenopausal and not taking hormone replacement therapy. Participants were also excluded if they had any counterindication for participating in an MRI study such as an implanted metallic device, as determined by an MRI screening form. All MRI scans were reviewed by a neuroradiologist (HAR) for incidental findings.

All participants were habitual exercisers (>150 min/week of moderate intensity aerobic exercise) for at least one year prior to enrollment. Recruitment flyers specifically stated this, and exercise participation was verified during the phone screening. Participants also completed a weekly exercise log and the GODIN leisure-time exercise questionnaire (Godin, 2011; Godin and Shephard, 1985) during the screening visit. If the participant did not reach the habitual exercise requirements, they were excluded from participating in the study. All study procedures were approved by the Institutional Review Board of the University of Wisconsin–Madison (IRB: 2016-0430) and performed according to the Declaration of Helsinki, including obtaining written informed consent from each participant.

Screening

Preliminary screening for study eligibility was assessed using a phone screening. If eligible, participants were scheduled for an in-person screening and consent visit. During this visit, optimal placement of the TCD to measure MCA velocity was measured. Participants also practiced breathing CO_2 through a facemask. During the screening visit, the randomized study visits were scheduled. Participants were asked to maintain the same diet and exercise regimen three days prior to each study visit and were given a diet and exercise log to track their activities. It is important to note that the day before each study visit, participants were asked to fast for 4 hours and to abstain from caffeine, alcohol, and exercise for 24 hours. This was noted to them in a reminder email two days prior to the study visit, as well as confirmed by the diet and exercise logs.

Study Procedures

Participants attended two separate study visits (Experimental Study Day A and Experimental Study Day B) conducted in a randomized order. Before each visit, participants were asked to fast for 4 hours and to abstain from caffeine, alcohol, and exercise for 24 hours as well as non-steroidal anti-inflammatory drugs for 5 days. In addition, participants were asked to withhold any over-the-counter medications, vitamins, or supplements on the day of the study visits. Young women were not pregnant and were studied on day 2-6 of the menstrual cycle or during the non-active pill phase of oral contraceptive pills.

Experimental Study Day A

Experimental Study Day A consisted of measurements of cardiovascular health and assessing cerebrovascular reactivity to hypercapnia using a transcranial Doppler ultrasound. This visit took

place in the Bruno Balke Biodynamics Laboratory at the University of Wisconsin Madison. Laboratory tests were conducted in controlled ambient temperature between 22 and 24°C. Upon arrival, height and weight was measured using a standard scale. After 10 minutes of supine rest, baseline mean arterial blood pressure was taken in triplicate using a non-invasive brachial blood pressure cuff (Datex Ohmeda, GE Healthcare, Fairfield, CT, United States). Participants were instrumented with a three-lead electrocardiogram to continually monitor HR and a pulse oximeter to monitor oxygen saturation (SpO_2) (Datex Ohmeda, GE Healthcare, Fairfield, CT, United States). Breath-by-breath end-tidal carbon dioxide ($ETCO_2$) was continually measured and recorded using a nasal cannula (Datex Ohmeda, GE Healthcare, Fairfield, CT, United States). A non-invasive finger blood pressure cuff placed around the middle finger continually measured and recorded beat-by-beat MAP (Finapres Medical Systems, Amsterdam, Netherlands). A height-correcting unit was used in order to account for any differences between the height of the finger and the height of the heart.

To determine vascular health, carotid–femoral pulse wave velocity (PWV) and aortic augmentation index (AIx) measurements were completed utilizing arterial tonometry. High-fidelity pressure waveforms were recorded for at least 10 heart beats non-invasively using a pencil-type Millar Micro-tip pressure transducer from the radial, femoral and carotid arteries (Sphygmocor, AtcorMedical, Sydney, NSW, Australia). An average of 3–5 trials of each PWV and AIx were obtained in succession. Tonometry transit distance from the carotid pulse site, the supra-sternal notch, and the femoral pulse site were measured with a tape measure. PWV was calculated using the intersection tangent foot-to-foot algorithm. An aortic pressure waveform was derived from the radial pulse using the application of a generalized transfer function to measure AIx. AIx was then corrected at a heart rate (HR) of 75 beats per minute.

Carotid ultrasound was performed using an 11 L probe with a transmission frequency of 4.5–12 MHz on a GE LOGIQ S8 machine (GE Healthcare, Waukesha, WI, United States). The left carotid artery was imaged in the longitudinal plane in B-mode 1–2 cm below the bifurcation. The carotid intima-media thickness (IMT) was measured using a semi-automated tracking software offline (Carotid Analyzer for Research, Medical Imaging Applications, Coralville, IA, United States). The average of the far wall IMT over approximately six cardiac cycles was reported. All carotid imaging and analysis were done by the same observer.

The left middle cerebral artery velocity (MCAv) was imaged using a 2 MHz Transcranial Doppler (TCD) probe (Spencer Technologies, Redmond, WA, United States). The 2 MHz probe was placed over the temporal bone of the skull just above the zygomatic arch between the frontal process and front of the ear. The probe was secured with a headband to maintain optimal insonation position and angle throughout the study protocol.

The stepped hypercapnia trials to measure cerebrovascular reactivity to hypercapnia were identical between study visits A and B. Participants were fitted with a facemask that covers their nose and mouth with a one-way valve to prevent re-breathing (Hans Rudolph, Inc., Shawnee, KS, United States). All compressed gas was medical grade. Participants breathed normocapnic air for approximately 10 min. Following normocapnia, participants breathed two stepwise elevations of 4% and 6% inspired CO_2 administered with oxygen maintained at 21% and balanced nitrogen for approximately 9 min at each level of CO_2. Participants were instructed to breathe normally and breathing rate was not controlled.

Experimental Study Day B

Experimental Study Day B consisted of measuring brain volumes and cerebral blood flow at rest as well as assessing cerebrovascular reactivity to hypercapnia. MR imaging was performed with a 3T clinical MRI scanner (MR750, GE Healthcare, Waukesha, WI, United States) at the Wisconsin Institutes for Medical Research in Madison, WI. Participants were supine and imaged with a 32-channel head coil (Nova Medical Head Coil, Nova Medical, Wilmington, MA, United States) with a gradient strength of 50 mT/m, and a gradient slew rate of 200 mT/m/ms. Throughout the MRI session, HR, and oxygen saturation (SPO_2) were acquired continuously using a pulse oximeter, and $ETCO_2$ was acquired continuously (breath-by-breath) using a nasal cannula. The pulse oximeter and nasal cannula was connected to an MRI compatible monitor (Medrad Veris MR Vital Signs Patient Monitor, Bayer Healthcare, Whippany, NJ, United States).

To determine brain volumes, a T1-weighted structural brain volume (BRAVO) scan was acquired with the following scan parameters: fast spoiled gradient echo sequence, inversion time = 450 ms, repetition time (TR) = 8.1 ms, echo time (TE) = 3.2 ms, flip angle = 12°, acquisition matrix = 256 × 256, field of view (FOV) = 256 mm, slice thickness = 1.0 mm, and scan time ∼8 min. A 3D time of flight (TOF) MRA of the Circle of Willis was acquired for visualization of the large intracranial vessels with the following scan parameters: TE = 2.5 ms, TR: 23 ms, flip angle = 20°, acquisition matrix = 448 x 224, FOV = 512 mm, slice thickness = 1.0 mm, pixel bandwidth = 162.78 kHz, spacing between slices = 0.5 mm, and scan time ~ 4 min 30 sec.

4D flow MRI data was acquired using a 3D radially under sampled sequence to provide high spatial and temporal resolution. No contrast agent was administered. The scan parameters were as follows: velocity encoding (Venc) = 80 cm/s, FOV = 220 mm, acquired isotropic spatial resolution = 0.7 mm × 0.7 mm × 0.7 mm, TR = 7.8 ms, TE = 2.7 ms, flip angle = 8°, bandwidth =

83.3 kHz, 14,000 projection angles and scan time ~7 min. The imaging volume covered the right and left MCA, right and left internal carotid arteries (ICA), and basilar artery (BA). Data was acquired continuously, such that a HR of 60 beats/min would provide a sampling of approximately 128 times per heartbeat. Time-resolved velocity and magnitude data was reconstructed offline by retrospectively gating into 20 cardiac phases using temporal interpolation.

Stepped hypercapnia trials were identical to Experimental Study Visit A. MRI acquisition started after participants' $ETCO_2$ reached steady state (approximately 1.5 mins). Mean arterial pressure was evaluated every 2 minutes with an oscillometric non-invasive brachial blood pressure cuff on the left arm (Medrad Veris MR Vital Signs Patient Monitor, Bayer Healthcare, Whippany, NJ, United States).

Data Analysis

During Experimental Study Visit A, data was collected at 250 Hz and analyzed offline using a signal processing software (WinDaq, DATAQ Instruments, Akron, OH, United States). Beat-by-beat hemodynamic measurements were averaged over minute four of the normocapnic condition and at each level of hypercapnia. To account for changes in perfusion pressure that may affect flow, cerebrovascular conductance index (CVCi) was calculated as MCAv/MAP. Cerebrovascular reactivity was quantified as the linear relationship between MCAv, CVCi and $ETCO_2$ during stepped hypercapnia.

For Experimental Study Visit B, cardiorespiratory variables ($ETCO_2$, HR, SPO_2 and MAP) were averaged over the length of each scan. Using the T1-weighted scans, brain volumes were segmented in Statistical Parametric Mapping version 12 (SMP12) into gray matter (GM), white matter (WM), and cerebral spinal fluid (CSF). For the 4D flow MRI scans, automatic phase

unwrapping was performed in all data sets to minimize potential for velocity aliasing (Loecher et al., 2016). Eddy current correction was also applied as previously described (Schrauben et al., 2015). A time average segmentation mask was generated using both phase and magnitude information. This was done for each subject and for each scan separately (normocapnia, 4% CO_2 and 6% CO_2) (Schrauben et al., 2015). Background phase offset corrections were performed in Matlab (The Mathworks, Natick, MA, United States). Individual vessel segmentation of the right and left MCA, right and left ICA, and BA was also done in Matlab using an in-house tool for semi-automated cerebrovascular flow analysis. All vessel segmentation was processed retrospectively. Blood flow was averaged along the length of each vessel. The MCAs were measured along the M1 segment. The ICAs were measured along the cervical and petrous portions below the carotid siphon. The BA was measured below the superior cerebellar artery and above the bifurcation of the vertebral arteries. Global flow was calculated as the sum of the right and left ICAs and the BA. To account for changes in perfusion pressure that may affect flow, cerebrovascular conductance index (CVC) was calculated as blood flow/ MAP. Cerebrovascular reactivity was quantified as the linear relationship between blood flow, CVC and $ETCO_2$. Pulsatility index was calculated as (maximum flow – minimum flow) / mean flow. Global pulsatility index was the average pulsatility of the ICAs and BA. Right and left MCA cross sectional area (CSA) was averaged across the M1 segment of the vessel. All analyses were conducted blind to the subject group (young or older, men or women) and experimental condition (normocapnia, 4% CO_2 or 6% CO_2).

Statistical Analysis

Estimates for a required sample size was calculated using G*Power 3.1.9.4 (Faul et al., 2007). In a previous study by Barnes et al., 2012, it was found that cerebrovascular reactivity to hypercapnia

was statistically different between young (n = 12) and older (n = 10) adults (1.0 ± 0.2 cm/s/mmHg^2 vs. 0.6 ± 0.1 cm/s/mmHg^2, respectively, $p < 0.05$) (Barnes et al., 2012). A post-hoc analysis of this effect size was $f = 1.3278$, with alpha = 0.05, and power (1-beta) = 0.99. The current study recruited two groups to test the age effects but sought to include equal numbers of men and women to determine the effects of age, sex, and the age x sex interaction as an exploratory analysis. To achieve a power of 0.80 or 80% with two groups at an effect size of $f = 1.3278$ and alpha = 0.05, G*Power estimated that the necessary sample size was 17 per group (Appendix 1). Thus, 20 subjects per group (n=40) were recruited to account for motion artifact issues with the MRI scan and potential covariates.

All statistical testing, aside from the sample size estimates, was done in Sigma Plot for Windows version 13.0 (Systat Software, San Jose, CA, United States). For all variables, normality was assessed using the Shapiro–Wilk test and equal variance was assessed using the Brown–Forsythe test prior to analysis. Participant demographics and baseline characteristics were compared between young and older adults using a one-way ANOVA. A two-way repeated measures ANOVA compared the cardiorespiratory variables between the two groups of interest (young and older adults) during each stage of the hypercapnic protocol (normocapnia, 4% CO_2 and 6% CO_2) followed by the Holm-Sidak method to test pairwise comparisons. This analysis method was chosen over a linear mixed model because there was no missing data as each subject completed each condition and the conditions were fixed. For the primary analysis comparing cerebrovascular reactivity between young and older adults, a one-way ANOVA was used. This analysis addressed hypothesis 1: there will be no age-related differences in cerebrovascular reactivity to hypercapnia in healthy, physically-active adults when evaluating cerebral blood velocity with TCD and hypothesis 2: older adults will have reduced cerebrovascular reactivity to hypercapnia compared

with young adults when evaluating cerebral blood flow using 4D flow MRI. Determining if any age-related differences in cerebrovascular reactivity were sex-specific was also of interest. As an exploratory analysis, cerebrovascular reactivity measures were compared by age group (young or old) and sex (male or female) by a two-way ANOVA followed by the Holm-Sidak method to test pairwise multiple comparisons. To assess if the MCA changed in cross-sectional area during hypercapnia, a paired t-test between conditions (normocapnia and 6% CO_2) within each subject group (young adults and older adults) was used. This analysis addressed hypothesis 3: the middle cerebral artery will increase in cross-sectional area in response to hypercapnia in young adults, but not older adults. If either the Shapiro–Wilk test of normality or the Brown–Forsythe of equal variance was significant ($p<0.05$), demonstrating non-normality or unequal variance, the parametric test execution was ended. Non-parametric statistical tests were used as appropriate including the Kruskal-Wallis ANOVA on Ranks followed by the Dunn's Method to test pairwise multiple comparisons. Effect sizes of the main outcome variables were calculated as Hedges' g. An exploratory analysis was also conducted to determine the correlation between central arterial stiffness (carotid-femoral PWV) and cerebral pulsatility index using a Pearson product-moment correlation. Statistical significance was set *a priori* at $p < 0.05$.

2.3 RESULTS

Participant Characteristics

Participant characteristics are shown in Table 3. Young and older adults had similar height, weight, BMI, and heart rate at rest. There was no significant difference between age groups in systolic and mean arterial pressure, though older adults had lower diastolic blood pressure compared with young adults. Central arterial stiffness data are shown in Table 4. Older adults also had greater carotid-femoral PWV, aortic augmentation index, and carotid IMT compared with young adults. Brain volumes are shown in Table 5. Older adults demonstrated lower grey matter volume, total brain volume, and brain volume indexed to intracranial volume. There were no age group differences in white matter volume and intracranial volume.

Study Day A Hemodynamics

Hemodynamic and cardiorespiratory measurements from study day A are shown in Table 6. As expected, $ETCO_2$ increased from baseline to 4% CO_2 and 6% CO_2 in both young and older adults. $ETCO_2$ was not different between young and older adults at any stage of the protocol, indicating the stimulus was similar between groups. Delta $ETCO_2$ from baseline to 6% CO_2 was not different between groups (Young adults: Δ 9 $\pm$ 2 mmHg vs. Older adults: Δ 8 $\pm$ 2 mmHg, p=0.35). There were no significant differences in respiratory rate between conditions or age groups. Mean arterial pressure also increased from baseline to 4% CO_2 and 6% CO_2 in both young and older adults. There were no differences between age groups in mean arterial pressure at baseline and 4% CO_2. However, older adults demonstrated greater mean arterial pressure during 6% CO_2 compared with young adults. Heart rate also increased from baseline to 4% CO_2 in older adults, and from baseline

to 6% CO_2 in young and older adults. There were no age group differences in heart rate at any stage of the protocol.

Study Day A Blood Velocity Characteristics

Left MCA blood velocity characteristics measured using transcranial Doppler ultrasound are shown in Table 7. Left MCAv increased from baseline to 4% CO_2 and 6% CO_2 in both young and older adults. Differences in MCAv between age groups at each condition (baseline, 4% CO_2 and 6% CO_2) did not reach the threshold for statistical significance. CVCi also increased from baseline to 4% CO_2 and 6% CO_2 in both age groups. Age related differences in CVCi at baseline and 4% CO_2 did not reach the threshold for statistical significance. However, older adults demonstrated lower CVCi compared with young adults during the 6% CO_2 condition. Pulsatility index decreased from baseline to 4% CO_2 and 6% CO_2 in young adults. In older adults, pulsatility index decreased from baseline to 6% CO_2, there was no change from baseline to 4% CO_2. There were no differences between age groups in pulsatility index at each condition (baseline, 4% CO_2 and 6% CO_2).

Study Day A Cerebrovascular Reactivity

Left MCA reactivity is shown in Figure 11. There were no significant differences between age groups in MCAv reactivity ($p=0.92$, ANOVA on ranks, hedges' $g=0.02$) or CVCi reactivity ($p=0.50$, hedges' $g=0.22$). Mean arterial blood pressure reactivity is shown in Figure 12. The difference between age groups did not reach the threshold for significance ($p=0.07$, ANOVA on ranks, hedges' $g=0.42$).

There were no age, sex, or interaction effects in MCAv or CVCi reactivity (Figure 13) or MAP reactivity (Figure 14).

Table 3. Characteristics of participants in Study 1

Variable	*Young Adults N = 20*	*Older Adults N = 20*	*P-value*
Female Subjects	N = 10	N = 10	
Age (years)	25 ± 3	62 ± 5	<0.001
Height (cm)	173 ± 8	172 ± 9	0.61
Weight (kg)	71 ± 10	69 ± 15	0.71
Body Mass Index (kg/m^2)	23 ± 2	23 ± 3	0.75
Heart Rate at Rest (beats per minute)	53 ± 8	54 ± 8	0.72
GODIN Questionnaire Score	62 ± 31	61 ± 17	0.92
Systolic Blood Pressure (mmHg)	120 ± 10	122 ± 12	0.57
Diastolic Blood Pressure (mmHg)	69 ± 6	74 ± 7	0.02
Mean Arterial Pressure (mmHg)	86 ± 7	91 ± 9	0.09

Characteristics of young and older adults. Data are mean ± standard deviation. GODIN, Godin-Shephard leisure time physical activity questionnaire. *P-value* in the column reflects the comparison between age groups.

Table 4. Central arterial stiffness of participants in Study 1

Variable	*Young Adults N = 20*	*Older Adults N = 20*	*P-value*
Carotid-Femoral PWV (m/s)	6.2 ± 1.0	7.8 ± 1.8	<0.001
Aortic Augmentation Index (%)	-2.4 ± 9.6	16.1 ± 9.6	<0.001
Carotid IMT (mm)	0.50 ± 0.08	0.71 ± 0.10	<0.001

Central arterial stiffness of young and older adults. Data are mean ± standard deviation. *P-value* in the column reflects the comparison between age groups. IMT, intima-media thickness. PWV, pulse wave velocity. For PWV and aortic augmentation index measurements, n = 37. Aortic augmentation index was corrected for a heart rate of 75 beats per minute.

Table 5. Brain volumes of participants in Study 1

Variable	*Young Adults N = 20*	*Older Adults N = 20*	*P-value*
Grey Matter Volume (L)	0.75 ± 0.07	0.65 ± 0.08	<0.001
White Matter Volume (L)	0.45 ± 0.05	0.45 ± 0.06	0.95
Brain Volume (L)	1.20 ± 0.12	1.10 ± 0.13	0.01
Intracranial Volume (L)	1.44 ± 0.14	1.45 ± 0.15	0.89
Brain Volume / Intracranial Volume (L)	0.83 ± 0.03	0.76 ± 0.03	<0.001

Brain volumes of young and older adults. Data are mean ± standard deviation. *P-value* in the column reflects the comparison between age groups.

Table 6. Study day A hemodynamics

Variable	*Young Adults N = 20*	*Older Adults N = 20*	*P-value*
$ETCO_2$ (mmHg)			
Baseline	40 ± 3	40 ± 3	0.62
4% CO_2	47 ± 3*	46 ± 3*	0.32
6% CO_2	49 ± 2*	48 ± 4*	0.23
Respiratory Rate (breaths per minute)			
Baseline	12 ± 4	11 ± 3	0.14
4% CO_2	13 ± 3	12 ± 3	0.55
6% CO_2	13 ± 3	12 ± 4	0.31
Mean Arterial Pressure (mmHg)			
Baseline	84 ± 7	86 ± 8	0.33
4% CO_2	87 ± 9*	90 ± 10*	0.29
6% CO_2	89 ± 10*	96 ± 10*	0.03
Heart Rate (bpm)			
Baseline	51 ± 7	51 ± 7	0.95
4% CO_2	53 ± 8	52 ± 7*	0.87
6% CO_2	58 ± 10*	55 ± 7*	0.27

Hemodynamic and cardiorespiratory variables on study day A, the laboratory visit, during the stepped hypercapnia protocol. Data are mean ± standard deviation. $ETCO_2$, end-tidal carbon dioxide. *P-value* in the column reflects the comparison between age groups. *$p<0.05$ compared with baseline.

Table 7. Study day A blood velocity characteristics

Variable	*Young Adults N = 20*	*Older Adults N = 20*	*P-value*
MCAv (cm/s)			
Baseline	57 ± 11	50 ± 11	0.10
4% CO_2	63 ± 14*	56 ± 14*	0.09
6% CO_2	68 ± 14*	59 ± 14*	0.06
CVCi (cm/s/mmHg)			
Baseline	0.68 ± 0.14	0.58 ± 0.17	0.09
4% CO_2	0.73 ± 0.17*	0.63 ± 0.19*	0.08
6% CO_2	0.76 ± 0.19*	0.63 ± 0.17*	0.01
Pulsatility Index			
Baseline	0.80 ± 0.14	0.77 ± 0.13	0.41
4% CO_2	0.73 ± 0.09*	0.74 ± 0.11	0.73
6% CO_2	0.69 ± 0.09*	0.73 ± 0.11*	0.32

Left middle cerebral artery measurements during study day A, the laboratory visit, measured using transcranial Doppler ultrasound. Data are mean ± standard deviation. CVCi, cerebrovascular conductance index, MCAv, middle cerebral artery velocity. *P-value* in the column reflects the comparison between age groups. *$p<0.05$ compared with baseline.

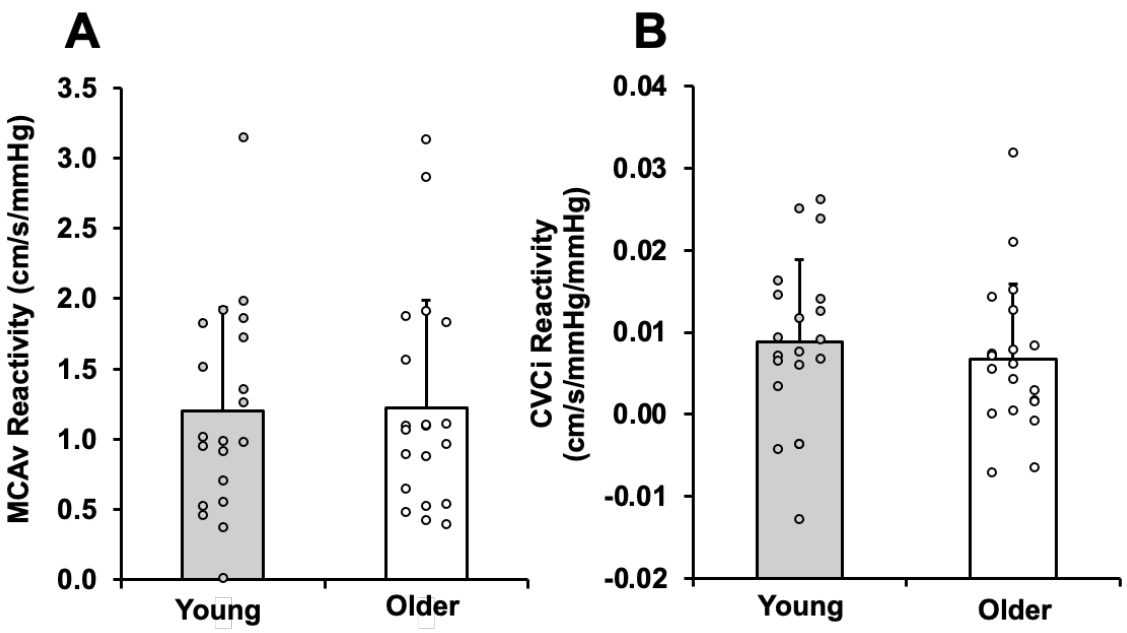

Figure 11. Cerebrovascular reactivity of the MCA from study day A.

Data are mean ± standard deviation and individual data points. Reactivity to hypercapnia of the left MCA measured using transcranial Doppler ultrasound. A) MCA velocity (MCAv) reactivity B) Cerebrovascular conductance index (CVCi) reactivity.

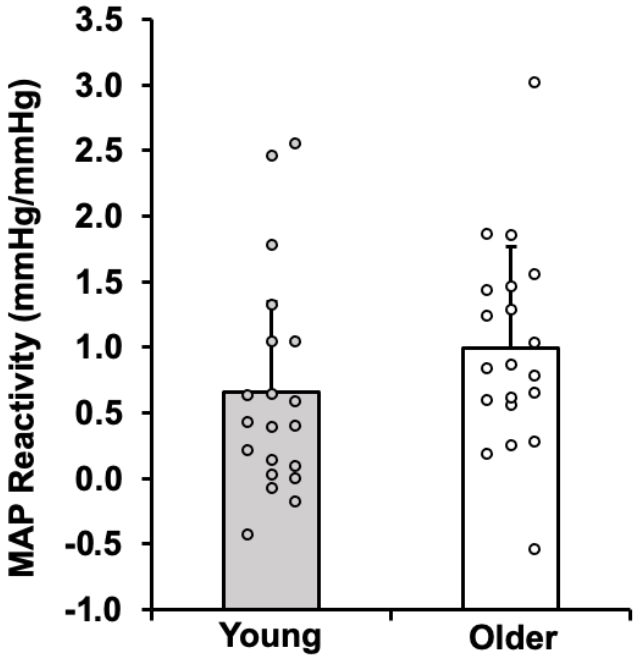

Figure 12. Mean arterial pressure reactivity from study day A.

Data are mean ± standard deviation and individual data points. Mean arterial blood pressure (MAP) reactivity to stepped hypercapnia measured during study day A, the laboratory visit.

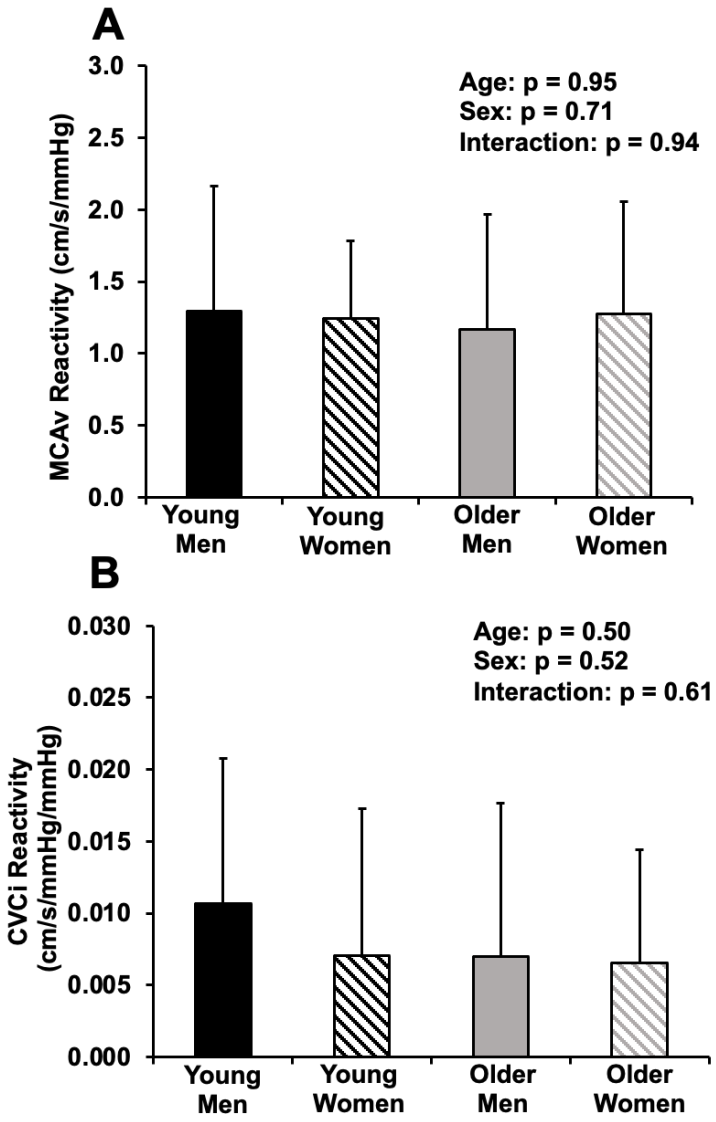

Figure 13. Cerebrovascular reactivity in men and women from study day A

Data are mean ± standard deviation. This figure shows reactivity of the middle cerebral artery (MCA) to hypercapnia in young and older men and women measured using transcranial Doppler ultrasound on study day A. A) MCA velocity (MCAv) reactivity B) Cerebrovascular conductance index (CVCi) reactivity. Young adults are shown in black, young women in black stripes, older men in gray and older women in gray stripes.

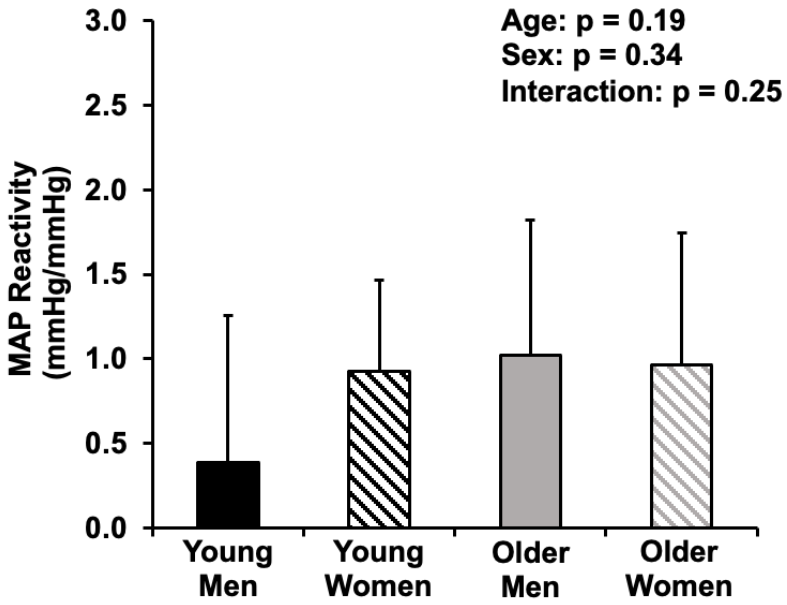

Figure 14. Mean arterial pressure reactivity in men and women from study day A.

Data are mean ± standard deviation. This figure shows mean arterial pressure (MAP) reactivity to hypercapnia in young and older men and women measured during study day A, the laboratory visit. Young adults are shown in black, young women in black stripes, older men in gray and older women in gray stripes.

Study Day B Hemodynamics

Hemodynamic and cardiorespiratory measurements from study day B are shown in Table 8. As expected, $ETCO_2$ increased from baseline to 4% CO_2 and 6% CO_2 in both young and older adults. Although older adults demonstrated lower $ETCO_2$ at baseline compared with young adults, this did not reach statistical significance during the 4% and 6% CO_2 conditions. In addition, delta $ETCO_2$ from baseline to 6% CO_2 was not different between groups (Young adults: Δ 6 ± 3 mmHg vs. Older adults: Δ 6 ± 4 mmHg, p=0.52) indicating the stimulus was similar between groups. There were no significant differences in respiratory rate between age groups or conditions. In young adults, there was no difference in mean arterial pressure from baseline to 4% CO_2 or 6% CO_2. However, mean arterial pressure increased from baseline to 4% CO_2 and 6% CO_2 in older adults. Older adults also demonstrated greater mean arterial pressure compared with young adults during each condition (baseline, 4% CO_2 and 6% CO_2). Heart rate increased from baseline to 4% CO_2 and 6% CO_2 in young adults and from baseline to 6% CO_2 in older adults. There were no age group differences in heart rate at any condition (baseline, 4% CO_2 and 6% CO_2).

Study Day B Individual Vessel Characteristics - ICA

An example 4D flow MRI scan of the large intracranial vessels is shown in Figure 15. Data from one older female was not usable due to motion artifact during the MRI scan.

Data from the left ICA is shown in Table 9. Left ICA diameter increased from baseline to 4% CO_2 and 6% CO_2 in both young and older adults. There were no differences in left ICA diameter between age groups at any condition. Left ICA mean velocity increased from baseline to 6% CO_2 in young adults, and from baseline to 4% CO_2 and 6% CO_2 in older adults. Older adults demonstrated lower mean velocity at each condition (baseline, 4% CO_2 and 6% CO_2) compared

with young adults. Max velocity increased from baseline to both 4% CO_2 and 6% CO_2 in both young and older adults. Older adults demonstrated lower max velocity at baseline compared with young adults. There were no significant differences in max velocity between age groups at 4% CO_2 and 6% CO_2. Blood flow expressed in mL/beat increased from baseline to 6% CO_2 in young adults and increased from baseline to both 4% CO_2 and 6% CO_2 in older adults. There were no significant age group differences in flow in mL/beat at any condition. Blood flow expressed in mL/min increased from baseline to 4% CO_2 and 6% CO_2 in both young and older adults. There were no significant age group differences in flow in mL/min at any condition. Cerebrovascular conductance of the left ICA increased from baseline to both 4% CO_2 and 6% CO_2 in young adults, and from baseline to 6% CO_2 in older adults. The age group difference in left ICA cerebrovascular conductance did not reach statistical significance at baseline; however, older adults demonstrated lower cerebrovascular conductance at both 4% CO_2 and 6% CO_2 compared with young adults. Left ICA pulsatility index decreased from baseline to 6% CO_2 in young adults. There was no change in pulsatility index from baseline to both 4% CO_2 and 6% CO_2 in older adults. The age group difference in left ICA pulsatility index did not reach statistical significance at baseline; however, older adults demonstrated higher left ICA pulsatility index at both 4% CO_2 and 6% CO_2 compared with young adults.

Measurements of the right ICA are shown in Table 10. Similar to the left ICA, the right ICA diameter increased from baseline to both 4% CO_2 and 6% CO_2 in young adults; however, there was no change in right ICA diameter from baseline to 4% CO_2 or 6% CO_2 in older adults. There were no differences in right ICA diameter between age groups at any condition. Right ICA mean velocity increased from baseline to 6% CO_2 in young adults, and from baseline to both 4% CO_2 and 6% CO_2 in older adults. Older adults demonstrated lower right ICA mean velocity at

baseline compared with young adults. There were no differences in right ICA mean velocity between age groups at both 4% CO_2 and 6% CO_2. Max velocity increased from baseline to 4% CO_2 in young adults, and from baseline to both 4% CO_2 and 6% CO_2 in older adults. There were no significant differences in right ICA max velocity between age groups at any condition. Blood flow expressed in mL/beat increased from baseline to 6% CO_2 in young adults and increased from baseline to both 4% CO_2 and 6% CO_2 in older adults. There were no significant age group differences in right ICA flow in mL/beat at any condition. Blood flow expressed in mL/min increased from baseline to both 4% CO_2 and 6% CO_2 in both young and older adults. There were no significant age group differences in flow in mL/min at any condition. Right ICA cerebrovascular conductance increased from baseline to 4% CO_2 and 6% CO_2 in young adults, and from baseline to 6% CO_2 in older adults. The age group difference in right ICA cerebrovascular conductance did not reach statistical significance at baseline; however, older adults demonstrated lower cerebrovascular conductance at both 4% CO_2 and 6% CO_2 compared with young adults. Right ICA pulsatility index decreased from baseline to 6% CO_2 in young adults. There was no change in pulsatility index from baseline to 4% CO_2 or 6% CO_2 in older adults. Older adults demonstrated higher pulsatility index at baseline and 6% CO_2 compared with young adults. There were no significant differences in pulsatility index between age groups at 4% CO_2.

Study Day B Individual Vessel Characteristics - MCA

Measurements of the left MCA are shown in Table 11. Left MCA diameter increased from baseline to 6% CO_2 in young adults. There was no change in diameter from baseline to 4% CO_2 or 6% CO_2 in older adults. There were no differences in left MCA diameter between age groups at any condition. There was no change in mean velocity from baseline to either 4% CO_2 or 6% CO_2 in young adults. Left MCA mean velocity increased from baseline to 6% CO_2 in older adults.

Older adults demonstrated lower mean velocity compared with young adults at each condition (baseline, 4% CO_2 and 6% CO_2). Left MCA max velocity increased from baseline to 6% CO_2 in both young and older adults. Older adults demonstrated lower max velocity compared with young adults at each condition (baseline, 4% CO_2 and 6% CO_2). Left MCA blood flow in mL/beat did not change from baseline to 4% CO_2 or 6% CO_2 in either young or older adults. Older adults had lower left MCA flow in mL/beat compared with young adults at each condition (baseline, 4% CO_2 and 6% CO_2). Blood flow expressed in mL/min increased from baseline to both 4% CO_2 and 6% CO_2 in young and from baseline to 6% CO_2 in older adults. Older adults had lower left MCA flow in mL/min compared with young adults at each condition (baseline, 4% CO_2 and 6% CO_2). Left MCA cerebrovascular conductance increased from baseline to both 4% CO_2 and 6% CO_2 in young adults. There was no change in left MCA cerebrovascular conductance from baseline to 4% CO_2 or 6% CO_2 in older adults. Older adults had lower left MCA cerebrovascular conductance compared with young adults at each condition (baseline, 4% CO_2 and 6% CO_2). There was no change in pulsatility index from baseline to either 4% CO_2 or 6% CO_2 in young or older adults. Older adults demonstrated higher pulsatility index at each condition compared with young adults (baseline, 4% CO_2 and 6% CO_2).

Measurements of the right MCA are shown in Table 12. Similar to the left MCA, the right MCA diameter increased from baseline to 6% CO_2 in young adults. There was no change in diameter from baseline to either 4% CO_2 or 6% CO_2 in older adults. There were no differences in right MCA diameter between age groups at any condition. There was no change in right MCA mean velocity from baseline to either 4% CO_2 or 6% CO_2 in young adults. Right MCA mean velocity increased from baseline to 6% CO_2 in older adults. Older adults demonstrated lower mean velocity compared with young adults at each condition (baseline, 4% CO_2 and 6% CO_2). There

was no change in max velocity from baseline to either 4% CO_2 or 6% CO_2 in young adults. Right MCA max velocity increased from baseline to 6% CO_2 in older adults. Older adults demonstrated lower max velocity compared with young adults at baseline and 4% CO_2. Age group differences in max velocity at 6% CO_2 did not reach the threshold for statistical significance. Blood flow expressed in mL/beat increased from baseline to 6% CO_2 in both young and older adults. Older adults had lower right MCA flow in mL/beat compared with young adults at each condition (baseline, 4% CO_2 and 6% CO_2). Blood flow expressed in mL/min increased from baseline to both 4% CO_2 and 6% CO_2 in young and older adults. Older adults had lower right MCA flow in mL/min compared with young adults at each condition (baseline, 4% CO_2 and 6% CO_2). Right MCA cerebrovascular conductance increased from baseline to both 4% CO_2 and 6% CO_2 in young adults and from baseline to 6% CO_2 in older adults. Older adults had lower right MCA cerebrovascular conductance compared with young adults at each condition (baseline, 4% CO_2 and 6% CO_2). There was no change in right MCA pulsatility index from baseline to 4% CO_2 or 6% CO_2 in young or older adults. Older adults demonstrated higher right MCA pulsatility index at each condition compared with young adults (baseline, 4% CO_2 and 6% CO_2).

Study Day B Individual Vessel Characteristics – Basilar Artery

Basilar artery measurements are shown in Table 13. Basilar artery diameter increased from baseline to 6% CO_2 in young adults. There was no change in diameter from baseline to either 4% CO_2 or 6% CO_2 in older adults. There were no differences in diameter between age groups at any condition. Basilar artery mean velocity increased from baseline to 6% CO_2 in young adults and from baseline to both 4% CO_2 and 6% CO_2 in older adults. Older adults demonstrated lower mean velocity compared with young adults at each condition (baseline, 4% CO_2 and 6% CO_2). Max

velocity increased from baseline to 6% CO_2 in both young and older adults. There were no significant differences in max velocity between young and older adults in any condition. Basilar artery flow expressed in mL/beat increased from baseline to 6% CO_2 in both young and older adults. Older adults had lower basilar artery flow in mL/beat compared with young adults at each condition (baseline, 4% CO_2 and 6% CO_2). Basilar artery flow expressed in mL/min increased from baseline to both 4% CO_2 and 6% CO_2 in both young and older adults. Older adults had lower flow in mL/min compared with young adults at each condition (baseline, 4% CO_2 and 6% CO_2), though the difference at baseline and 4% CO_2 did not reach the threshold for significance. Basilar artery cerebrovascular conductance increased from baseline to both 4% CO_2 and 6% CO_2 in young adults and from baseline to 6% CO_2 in older adults. Older adults had lower cerebrovascular conductance compared with young adults at each condition (baseline, 4% CO_2 and 6% CO_2). There was no change in pulsatility index from baseline to either 4% CO_2 or 6% CO_2 in young or older adults. Older adults demonstrated higher pulsatility index at each condition compared with young adults (baseline, 4% CO_2 and 6% CO_2).

Study Day B Global Cerebral Blood Flow Characteristics

Global cerebral blood flow measurements are shown in Table 14. Global cerebral blood flow increased from baseline to both 4% CO_2 and 6% CO_2 in both young and older adults. There were no differences in global cerebral blood flow between age groups at baseline or 4% CO_2; however, older adults demonstrated lower global cerebral blood flow compared with young adults at 6% CO_2. Global cerebral blood flow adjusted for brain volume / ICV also increased from baseline to 4% CO_2 and 6% CO_2 in both young and older adults. There were no differences in global cerebral blood flow adjusted for brain volume / ICV between age groups at any condition. Global

cerebrovascular conductance increased from baseline to both 4% CO_2 and 6% CO_2 in young adults and from baseline to 6% CO_2 in older adults. Older adults demonstrated lower global cerebrovascular conductance compared with young adults at each condition (baseline, 4% CO_2 and 6% CO_2). Global pulsatility index decreased from baseline to 6% CO_2 in young adults. There was no change in pulsatility index from baseline to 4% CO_2 or 6% CO_2 in older adults. Older adults demonstrated greater global pulsatility index compared with young adults at each condition (baseline, 4% CO_2 and 6% CO_2).

Study Day B Cerebrovascular Reactivity

Cerebrovascular reactivity of the internal carotid arteries to hypercapnia are shown in Figure 16. There were no significant differences between groups in the left ICA flow reactivity (p=0.14, p=0.25 no outlier, hedges' g=0.49) or right ICA (p=0.25 ANOVA on ranks, p=0.21 no outlier, hedges' g=0.34). Older adults demonstrated lower ICA conductance reactivity compared with young adults in both the left ICA (p=0.01, hedges' g=0.90) and the right ICA (p=0.02, p=0.04 no outlier, hedges' g=0.77).

Figure 17 shows cerebrovascular reactivity to hypercapnia in the MCAs. There were no significant differences between groups in left MCA flow reactivity (p=0.24, p=0.42 no outlier, hedges' g=0.39) or right MCA (p=0.20 ANOVA on ranks, hedges' g=0.37). Older adults demonstrated lower MCA conductance reactivity compared with young adults in both left MCA (p=0.02, p=0.04 no outlier, hedges' g=0.79) and right MCA (p=0.01, p=0.03 no outlier, hedges' g=0.82).

Basilar artery cerebrovascular reactivity to hypercapnia is shown in Figure 18. There were no significant differences between groups in basilar flow reactivity (p=0.09, p=0.17 no outlier,

hedges' g=0.56). Older adults demonstrated lower basilar conductance reactivity compared with young adults (p=0.01, p=0.01 no outlier, hedges' g=0.90).

Global cerebrovascular reactivity to hypercapnia is shown in Figure 19. There were no significant differences between groups in global flow reactivity (p=0.16 ANOVA on ranks, p=0.29 no outlier, hedges' g=0.46). Older adults demonstrated lower global cerebrovascular conductance reactivity compared with young adults (p=0.02 ANOVA on ranks, p=0.03 no outlier ANOVA on ranks, hedges' g=0.88).

Results from the exploratory analysis of age, sex, and interaction effects on global cerebrovascular reactivity to hypercapnia are shown in Figure 20. There was a significant age and sex interaction in both global flow and global cerebrovascular conductance reactivity. Young men demonstrated higher global flow and cerebrovascular conductance reactivity compared with older men. There were no differences in global flow or cerebrovascular conductance reactivity between young women and older women. Young men also demonstrated greater global flow and cerebrovascular conductance reactivity compared with young women; however, there were no sex-differences in global flow or cerebrovascular conductance reactivity in older adults. Results from the exploratory analysis of age, sex, and interaction effects on cerebrovascular reactivity of the large intracranial arteries to hypercapnia are shown in Figure 21. There was a significant age and sex interaction in the flow reactivity of the basilar artery, left ICA and left MCA such that young men demonstrated higher flow reactivity compared with young women and older men. There was also an age and sex interaction in the cerebrovascular conductance reactivity in all the large intracranial vessels of interest (basilar artery, left and right ICA, left and right MCA) such that young men demonstrated higher cerebrovascular conductance reactivity compared with young women and older men.

Table 8. Study day B hemodynamics

Variable	*Young Adults N = 20*	*Older Adults N = 19*	*P-value*
$ETCO_2$ (mmHg)			
Baseline	41 ± 4	38 ± 5	0.02
4% CO_2	44 ± 5*	41 ± 4*	0.06
6% CO_2	47 ± 6*	44 ± 5*	0.06
Respiratory Rate (breaths per minute)			
Baseline	15 ± 3	13 ± 4	0.07
4% CO_2	14 ± 2	13 ± 4	0.19
6% CO_2	14 ± 3	13 ± 4	0.23
Mean Arterial Pressure (mmHg)			
Baseline	94 ± 7	103 ± 13	0.01
4% CO_2	93 ± 5	106 ± 14*	<0.001
6% CO_2	96 ± 6	109 ± 13*	<0.001
Heart Rate (bpm)			
Baseline	53 ± 6	54 ± 7	0.62
4% CO_2	56 ± 7*	55 ± 7	0.89
6% CO_2	58 ± 6*	56 ± 7*	0.65

Hemodynamic and cardiorespiratory measurements from study day B, the MRI visit. Data are mean ± standard deviation. $ETCO_2$, end-tidal carbon dioxide. *P-value* in the column reflects the comparison between age groups. *$p<0.05$ compared with baseline.

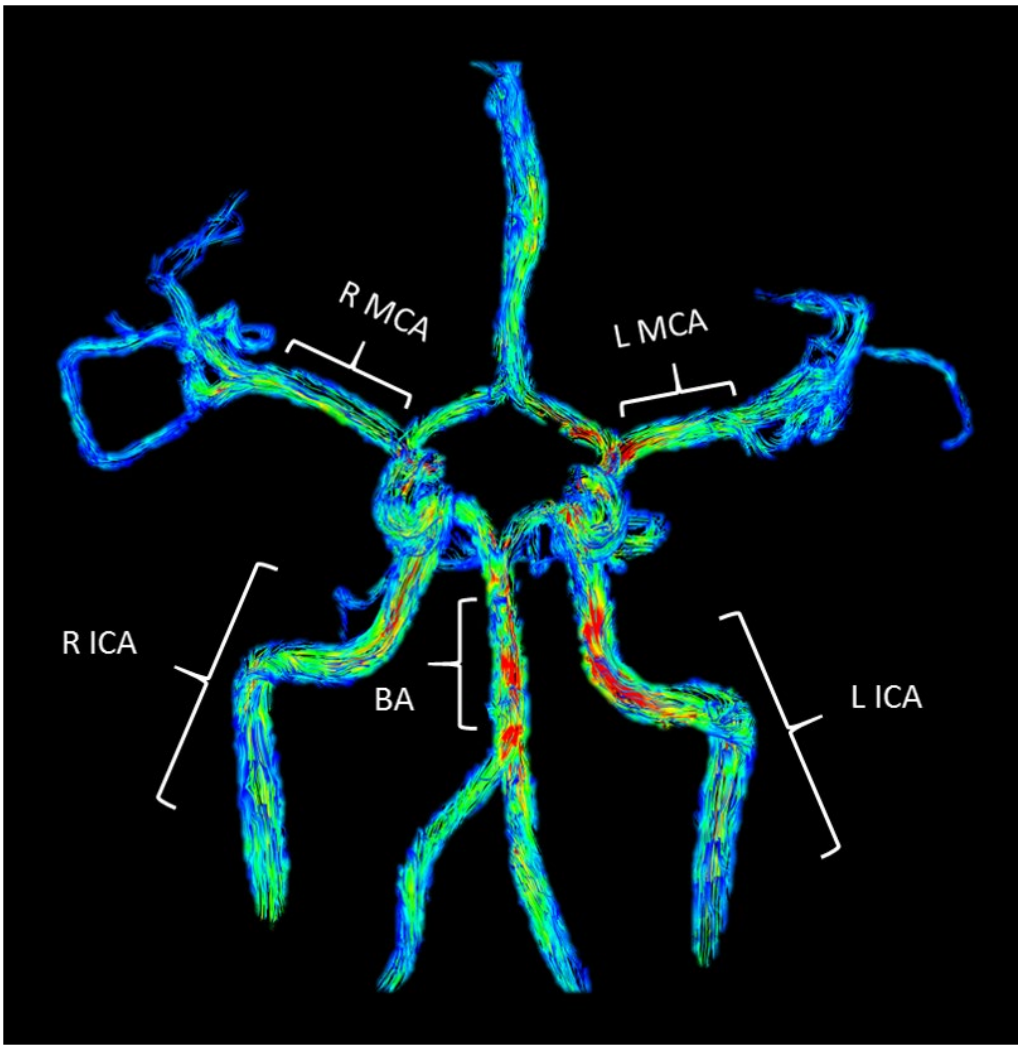

Figure 15. Example segmentation of the 4D flow MRI scan.

This image shows an example participant's 4D flow MRI scan during normocapnia. Warmer colors indicate higher blood velocity. The middle cerebral arteries (MCA) were measured along the M1 segment. The internal carotid arteries (ICA) were measured along the cervical and petrous portions below the carotid siphon. The basilar artery (BA) was measured below the superior cerebellar artery and above the bifurcation of the vertebral arteries. Global flow was calculated as the sum of the right and left ICA and the BA flows.

Table 9. Left internal carotid artery measurements at baseline and hypercapnia

Variable	*Young Adults N = 20*	*Older Adults N = 19*	*P-value*
Diameter (cm)			
Baseline	0.443 ± 0.038	0.445 ± 0.036	0.91
4% CO_2	0.447 ± 0.038*	0.450 ± 0.038*	0.86
6% CO_2	0.453 ± 0.042*	0.452 ± 0.036*	0.92
Mean Velocity (cm/s)			
Baseline	27 ± 4	23 ± 4	0.02
4% CO_2	27 ± 4	24 ± 4*	0.03
6% CO_2	28 ± 4*	25 ± 5*	0.03
Max Velocity (cm/s)			
Baseline	61 ± 7	56 ± 7	0.03
4% CO_2	62 ± 6*	57 ± 7*	0.07
6% CO_2	63 ± 7*	60 ± 7*	0.17
Flow (mL/beat)			
Baseline	4.1 ± 0.8	3.6 ± 1.0	0.16
4% CO_2	4.2 ± 0.9	3.8 ± 1.0*	0.19
6% CO_2	4.6 ± 1.1*	4.0 ± 1.0*	0.08
Flow (mL/min)			
Baseline	219 ± 56	199 ± 58	0.33
4% CO_2	237 ± 65*	212 ± 59*	0.23
6% CO_2	268 ± 82*	230 ± 65*	0.08
Cerebrovascular Conductance (mL/min/mmHg)			
Baseline	235 ± 60	197 ± 56	0.07
4% CO_2	255 ± 71*	205 ± 55	0.02
6% CO_2	281 ± 86*	214 ± 54*	0.003
Pulsatility Index			
Baseline	0.93 ± 0.11	0.99 ± 0.11	0.08
4% CO_2	0.92 ± 0.10	0.99 ± 0.10	0.04
6% CO_2	0.88 ± 0.10*	0.99 ± 0.09	0.002

Left internal carotid artery measurements from study day B using 4D flow MRI. Data are mean ± standard deviation. *P-value* in the column reflects the comparison between age groups. *$p<0.05$ compared with baseline.

Table 10. Right internal carotid artery measurements at baseline and hypercapnia

Variable	*Young Adults N = 20*	*Older Adults N = 19*	*P-value*
Diameter (cm)			
Baseline	0.443 ± 0.038	0.450 ± 0.037	0.54
4% CO_2	0.446 ± 0.037*	0.451 ± 0.038	0.70
6% CO_2	0.452 ± 0.040*	0.454 ± 0.037	0.86
Mean Velocity (cm/s)			
Baseline	26 ± 4	23 ± 4	0.03
4% CO_2	27 ± 4	24 ± 4*	0.13
6% CO_2	28 ± 4*	25 ± 5*	0.06
Max Velocity (cm/s)			
Baseline	60 ± 6	57 ± 7	0.17
4% CO_2	60 ± 7	58 ± 7*	0.33
6% CO_2	63 ± 6*	60 ± 7*	0.26
Flow (mL/beat)			
Baseline	4.0 ± 0.8	3.7 ± 0.9	0.25
4% CO_2	4.1 ± 0.8	3.9 ± 0.9*	0.39
6% CO_2	4.5 ± 1.0*	4.1 ± 0.9*	0.16
Flow (mL/min)			
Baseline	213 ± 49	199 ± 49	0.41
4% CO_2	229 ± 56*	213 ± 51*	0.35
6% CO_2	259 ± 64*	230 ± 54*	0.11
Cerebrovascular Conductance (mL/min/mmHg)			
Baseline	230 ± 59	196 ± 44	0.07
4% CO_2	247 ± 65*	206 ± 45	0.03
6% CO_2	272 ± 71*	214 ± 44*	0.002
Pulsatility Index			
Baseline	0.93 ± 0.11	1.01 ± 0.11	0.02
4% CO_2	0.93 ± 0.11	0.98 ± 0.09	0.15
6% CO_2	0.89 ± 0.07*	0.98 ± 0.11	0.006

Right internal carotid artery measurements from study day B, using 4D flow MRI. Data are mean ± standard deviation. *P-value* in the column reflects the comparison between age groups. *p<0.05 compared with baseline.

Table 11. Left middle cerebral artery measurements at baseline and hypercapnia

Variable	*Young Adults N = 20*	*Older Adults N = 19*	*P-value*
Diameter (cm)			
Baseline	0.296 ± 0.015	0.297 ± 0.026	0.88
4% CO_2	0.295 ± 0.015	0.298 ± 0.027	0.72
6% CO_2	0.300 ± 0.017*	0.299 ± 0.028	0.88
Mean Velocity (cm/s)			
Baseline	35 ± 6	28 ± 5	<0.001
4% CO_2	35 ± 6	29 ± 5	<0.001
6% CO_2	36 ± 7	30 ± 5*	0.001
Max Velocity (cm/s)			
Baseline	79 ± 13	69 ± 9	0.01
4% CO_2	79 ± 11	71 ± 10	0.02
6% CO_2	81 ± 12*	73 ± 10*	0.02
Flow (mL/beat)			
Baseline	2.4 ± 0.4	2.0 ± 0.5	0.004
4% CO_2	2.5 ± 0.4	2.0 ± 0.5	0.01
6% CO_2	2.6 ± 0.5	2.1 ± 0.5	0.003
Flow (mL/min)			
Baseline	129 ± 31	106 ± 28	0.02
4% CO_2	137 ± 31*	112 ± 27	0.01
6% CO_2	152 ± 39*	121 ± 28*	0.003
Cerebrovascular Conductance (mL/min/mmHg)			
Baseline	139 ± 35	105 ± 28	0.002
4% CO_2	147 ± 34*	108 ± 26	<0.001
6% CO_2	160 ± 42*	113 ± 25	<0.001
Pulsatility Index			
Baseline	1.01 ± 0.19	1.13 ± 0.21	0.03
4% CO_2	0.94 ± 0.15	1.12 ± 0.15	0.002
6% CO_2	0.93 ± 0.16	1.07 ± 0.16	0.01

Left middle cerebral artery measurements from study day B, using 4D flow MRI. Data are mean ± standard deviation. *P-value* in the column reflects the comparison between age groups. *p<0.05 compared with baseline.

Table 12. Right middle cerebral artery measurements at baseline and hypercapnia

Variable	*Young Adults N = 20*	*Older Adults N = 19*	*P-value*
Diameter (cm)			
Baseline	0.295 ± 0.016	0.291 ± 0.024	0.48
4% CO_2	0.298 ± 0.018	0.292 ± 0.026	0.38
6% CO_2	0.302 ± 0.018*	0.294 ± 0.025	0.22
Mean Velocity (cm/s)			
Baseline	36 ± 7	29 ± 5	<0.001
4% CO_2	36 ± 7	30 ± 6	0.003
6% CO_2	37 ± 6	31 ± 6*	0.003
Max Velocity (cm/s)			
Baseline	80 ± 13	70 ± 9	0.007
4% CO_2	80 ± 12	72 ± 11	0.03
6% CO_2	82 ± 12	75 ± 9*	0.06
Flow (mL/beat)			
Baseline	2.4 ± 0.4	1.9 ± 0.5	<0.001
4% CO_2	2.5 ± 0.4	2.0 ± 0.5	0.001
6% CO_2	2.7 ± 0.4*	2.1 ± 0.5*	<0.001
Flow (mL/min)			
Baseline	131 ± 29	104 ± 28	0.008
4% CO_2	141 ± 29*	111 ± 30*	0.003
6% CO_2	154 ± 35*	119 ± 28*	<0.001
Cerebrovascular Conductance (mL/min/mmHg)			
Baseline	140 ± 34	102 ± 25	<0.001
4% CO_2	151 ± 35*	107 ± 28	<0.001
6% CO_2	162 ± 38*	110 ± 23*	<0.001
Pulsatility Index			
Baseline	0.92 ± 0.10	1.10 ± 0.18	0.001
4% CO_2	0.92 ± 0.12	1.11 ± 0.18	<0.001
6% CO_2	0.94 ± 0.12	1.10 ± 0.25	0.01

Right middle cerebral artery measurements from study day B, using 4D flow MRI. Data are mean ± standard deviation. *P-value* in the column reflects the comparison between age groups. *p<0.05 compared with baseline.

Table 13. Basilar artery measurements at baseline and hypercapnia

Variable	*Young Adults N = 20*	*Older Adults N = 19*	*P-value*
Diameter (cm)			
Baseline	0.323 ± 0.028	0.312 ± 0.032	0.28
4% CO_2	0.324 ± 0.027	0.312 ± 0.031	0.22
6% CO_2	0.327 ± 0.030*	0.315 ± 0.031	0.20
Mean Velocity (cm/s)			
Baseline	31 ± 6	26 ± 4	0.01
4% CO_2	32 ± 6	27 ± 4*	0.03
6% CO_2	33 ± 7*	28 ± 5*	0.01
Max Velocity (cm/s)			
Baseline	67 ± 10	61 ± 8	0.08
4% CO_2	67 ± 10	63 ± 8	0.19
6% CO_2	70 ± 11*	66 ± 9*	0.13
Flow (mL/beat)			
Baseline	2.5 ± 0.5	2.0 ± 0.6	0.02
4% CO_2	2.6 ± 0.5	2.1 ± 0.6	0.02
6% CO_2	2.8 ± 0.7*	2.2 ± 0.7*	0.01
Flow (mL/min)			
Baseline	134 ± 36	109 ± 34	0.05
4% CO_2	145 ± 41*	117 ± 34*	0.05
6% CO_2	163 ± 48*	126 ± 36*	0.01
Cerebrovascular Conductance (mL/min/mmHg)			
Baseline	145 ± 44	109 ± 35	0.01
4% CO_2	156 ± 47*	114 ± 35	0.003
6% CO_2	172 ± 54*	119 ± 35*	<0.001
Pulsatility Index			
Baseline	0.96 ± 0.11	1.09 ± 0.16	0.002
4% CO_2	0.95 ± 0.11	1.07 ± 0.11	0.002
6% CO_2	0.92 ± 0.10	1.05 ± 0.11	<0.001

Basilar artery measurements from study day B, using 4D flow MRI. Data are mean ± standard deviation. *P-value* in the column reflects the comparison between age groups. *p<0.05 compared with baseline.

Table 14. Global cerebral blood flow measurements at baseline and hypercapnia

Variable	*Young Adults N = 20*	*Older Adults N = 19*	*P-value*
Global Flow (mL/min)			
Baseline	567 ± 113	482 ± 162	0.16
4% CO_2	612 ± 135*	542 ± 120*	0.10
6% CO_2	690 ± 166*	587 ± 120*	0.02
Global Flow / Brain Volume (mL/min/L)			
Baseline	679 ± 132	667 ± 148	0.81
4% CO_2	734 ± 160*	714 ± 146*	0.69
6% CO_2	827 ± 196*	773 ± 146*	0.29
Global Cerebrovascular Conductance (mL/min/mmHg)			
Baseline	610 ± 136	502 ± 113	0.02
4% CO_2	658 ± 157*	525 ± 111	0.004
6% CO_2	725 ± 182*	547 ± 105*	<0.001
Global Pulsatility Index			
Baseline	0.94 ± 0.09	1.03 ± 0.11	0.01
4% CO_2	0.93 ± 0.09	1.01 ± 0.09	0.01
6% CO_2	0.90 ± 0.07*	1.01 ± 0.09	<0.001

Global cerebral blood flow measurements from study day B, using 4D flow MRI. Global flow = internal carotid artery + basilar artery flow. Data are mean ± standard deviation. *P-value* in the column reflects the comparison between age groups. *p<0.05 compared with baseline.

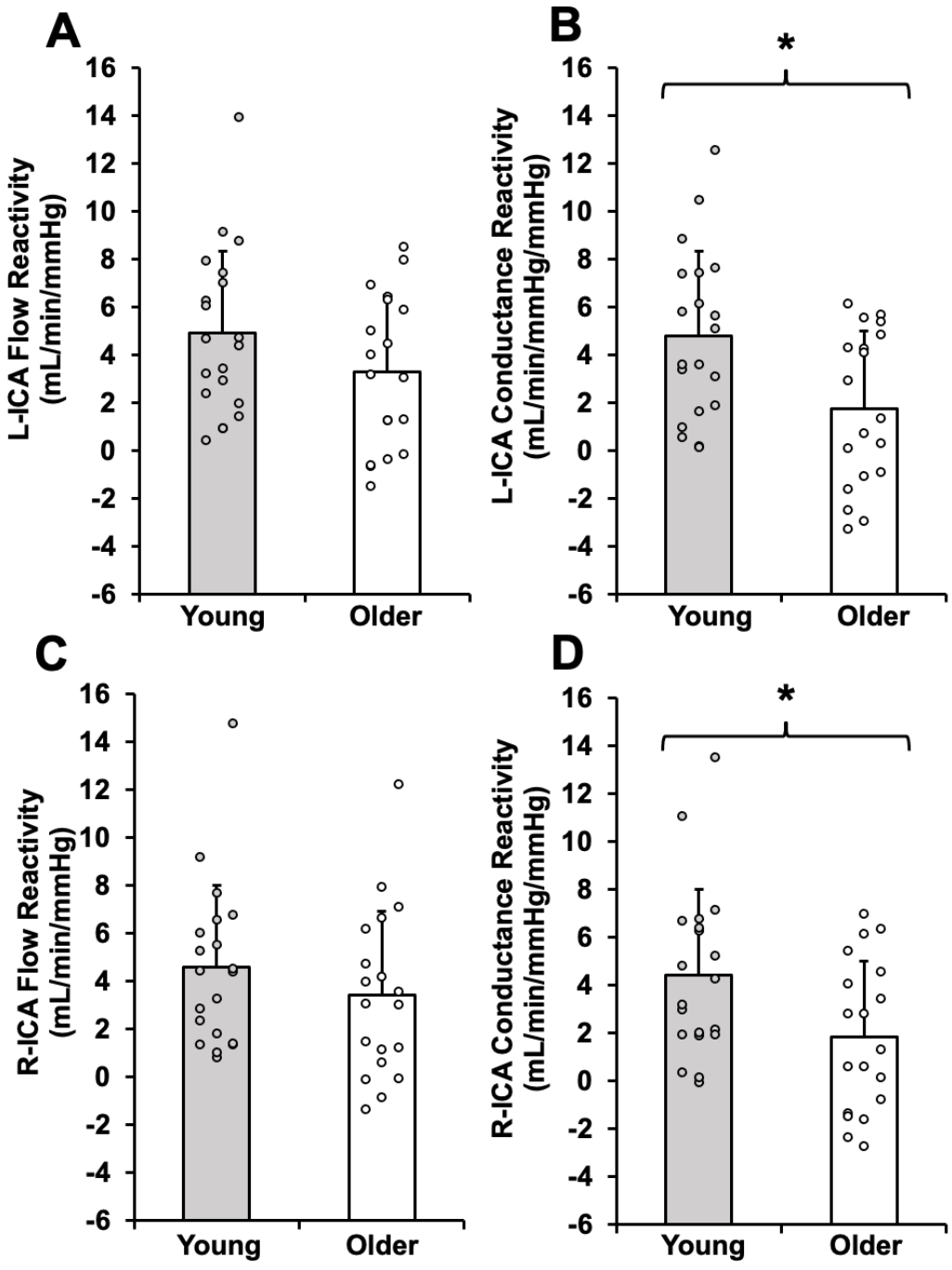

Figure 16. Internal carotid artery cerebrovascular reactivity from study day B

Data are mean ± standard deviation and individual data points. Right (R) and left (L) internal carotid artery (ICA) cerebrovascular reactivity to hypercapnia from study day B, using 4D flow MRI. A) Left ICA flow reactivity B) Left ICA conductance reactivity C) Right ICA flow reactivity D) Right ICA conductance reactivity. *$p<0.05$.

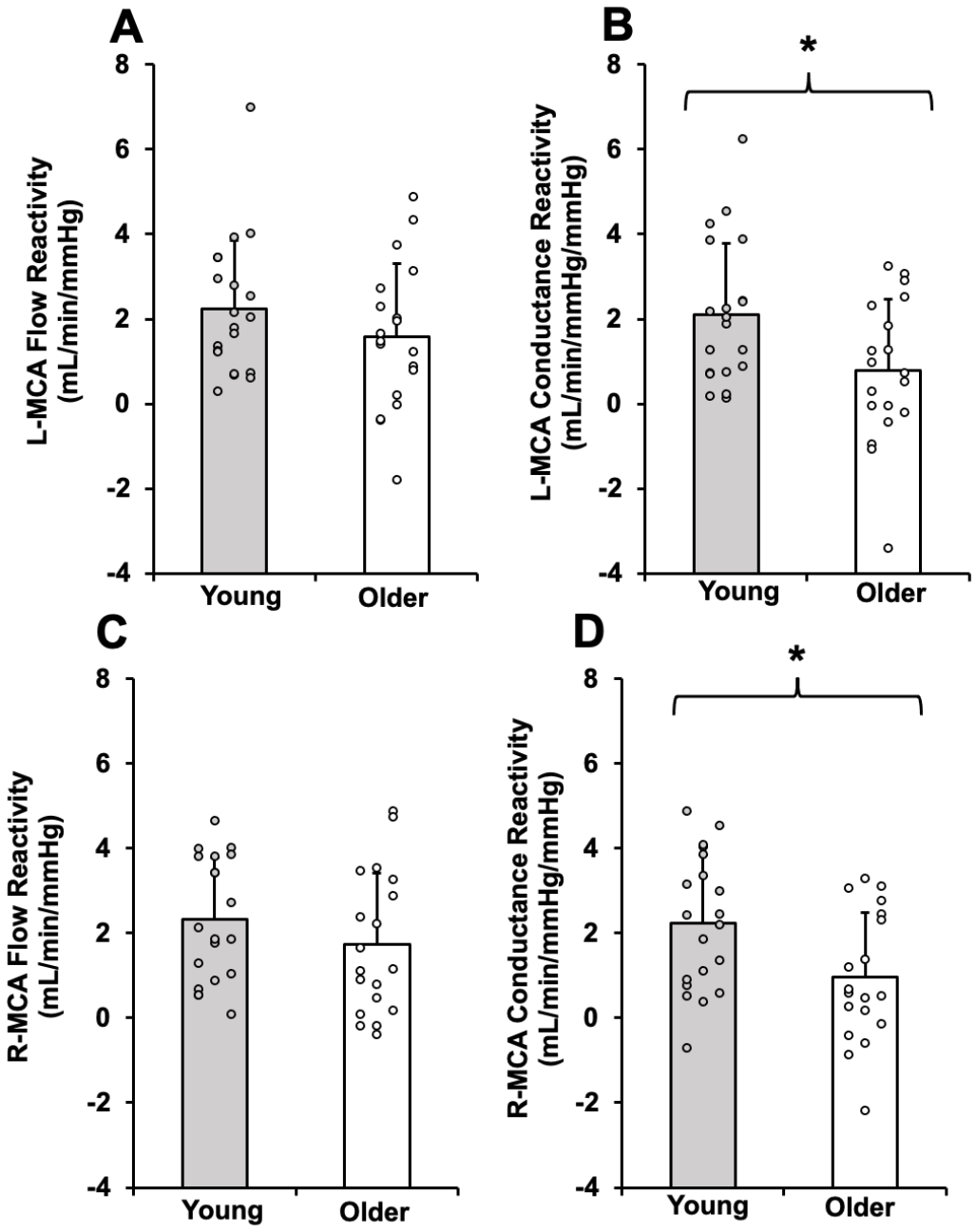

Figure 17. Middle cerebral artery cerebrovascular reactivity from study day B.

Data are mean ± standard deviation and individual data points. Right (R) and left (L) middle cerebral artery (MCA) cerebrovascular reactivity to hypercapnia from study day B using 4D flow MRI. A) Left MCA flow reactivity B) Left MCA conductance reactivity C) Right MCA flow reactivity D) Right MCA conductance reactivity. *$p<0.05$.

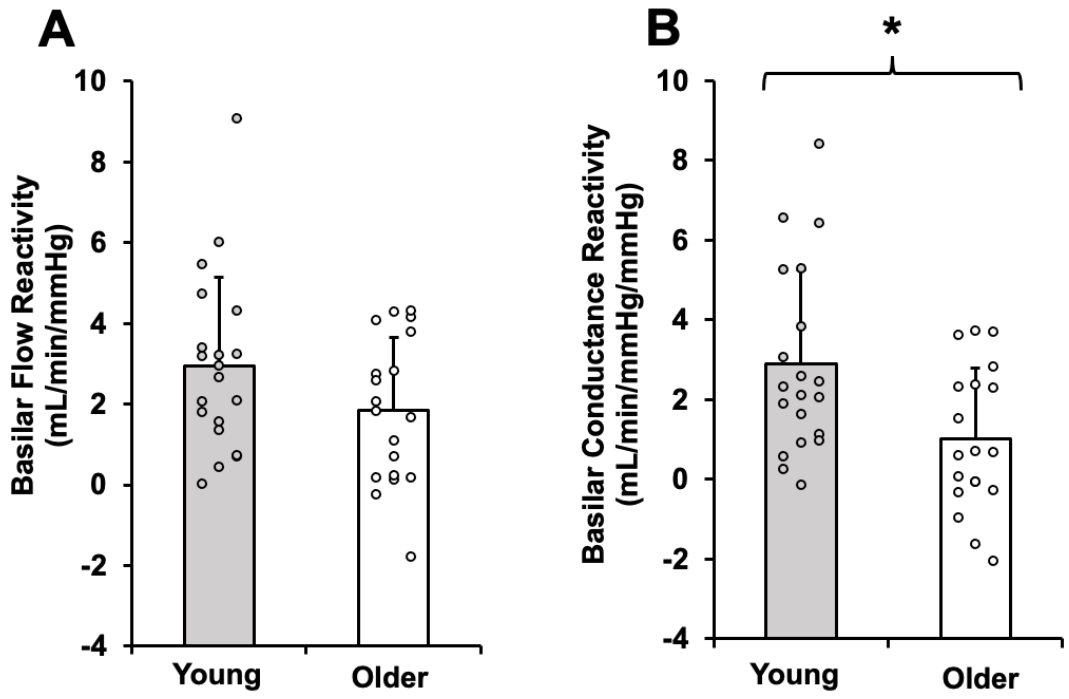

Figure 18. Basilar artery cerebrovascular reactivity from study day B.

Data are mean ± standard deviation and individual data points. Basilar artery cerebrovascular reactivity to hypercapnia from study day B using 4D flow MRI. A) Basilar artery flow reactivity B) Basilar artery cerebrovascular conductance reactivity. *$p<0.05$.

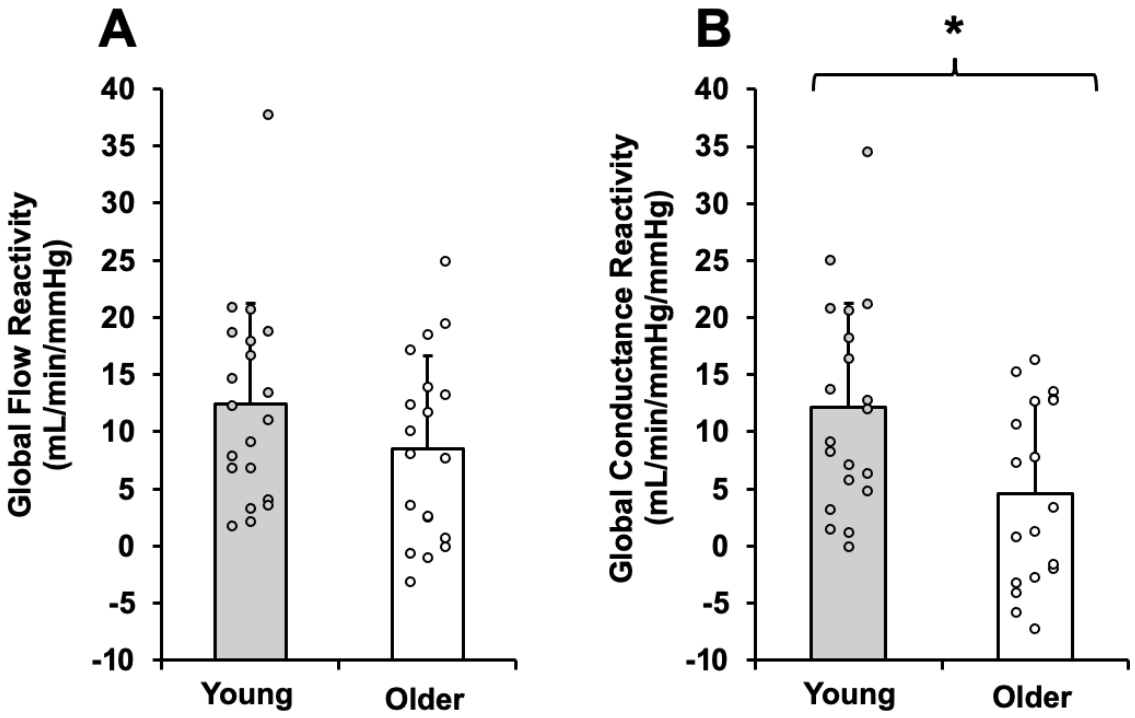

Figure 19. Global cerebrovascular reactivity from study day B.

Data are mean ± standard deviation and individual data points. Global cerebrovascular reactivity to hypercapnia from study day B using 4D flow MRI. A) global flow reactivity to hypercapnia and B) global cerebrovascular conductance reactivity to hypercapnia. Global flow = internal carotid artery flow + basilar artery flow. *$p<0.05$.

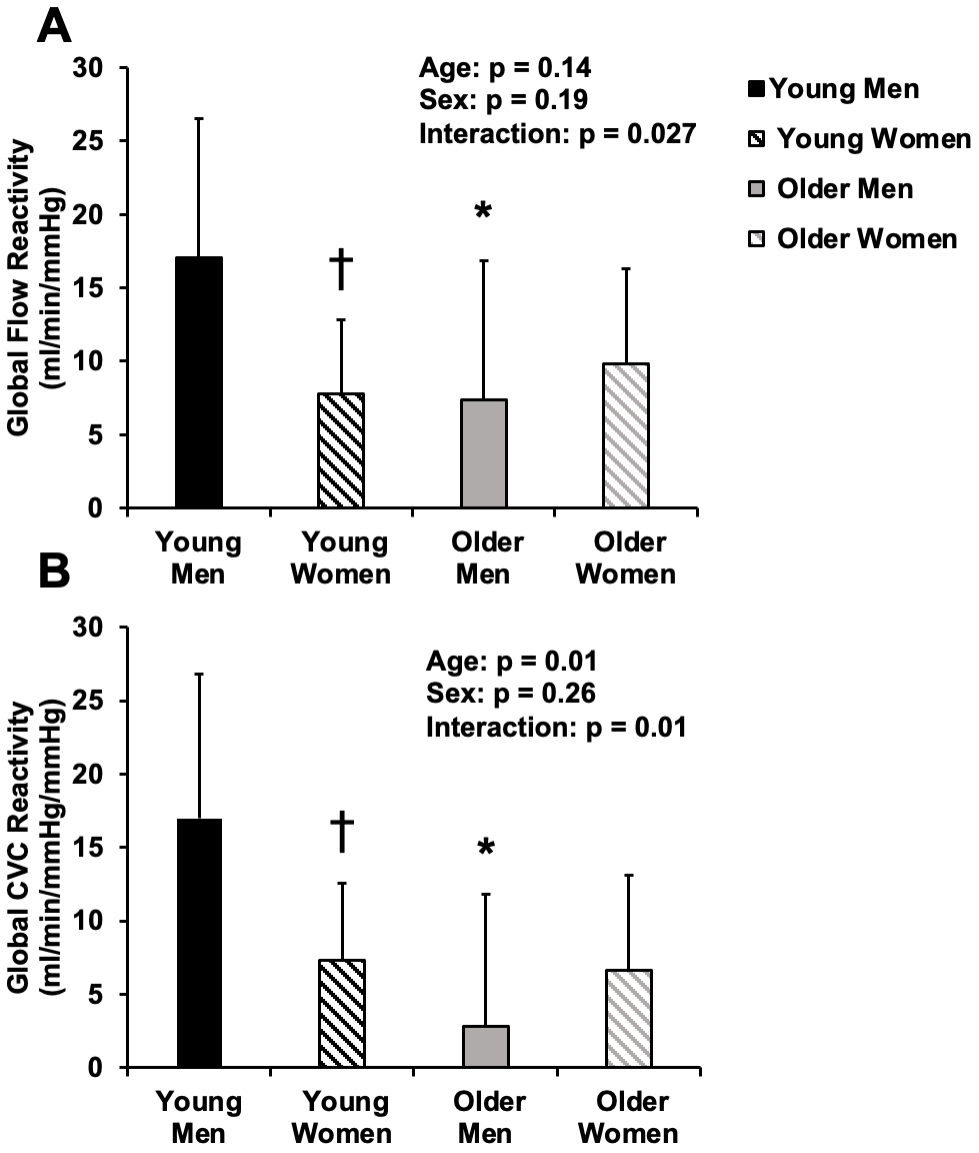

Figure 20. Global cerebrovascular reactivity in men and women from study day B

Data are mean ± standard deviation. Global cerebrovascular reactivity to hypercapnia from study day B using 4D flow MRI. A) global flow reactivity to hypercapnia and B) global cerebrovascular conductance (CVC) reactivity to hypercapnia. Young men are shown in black, young women in black stripes, older men in gray and older women in gray stripes. *$p<0.05$ vs. age within sex group, †$p<0.05$ vs. sex within age groups.

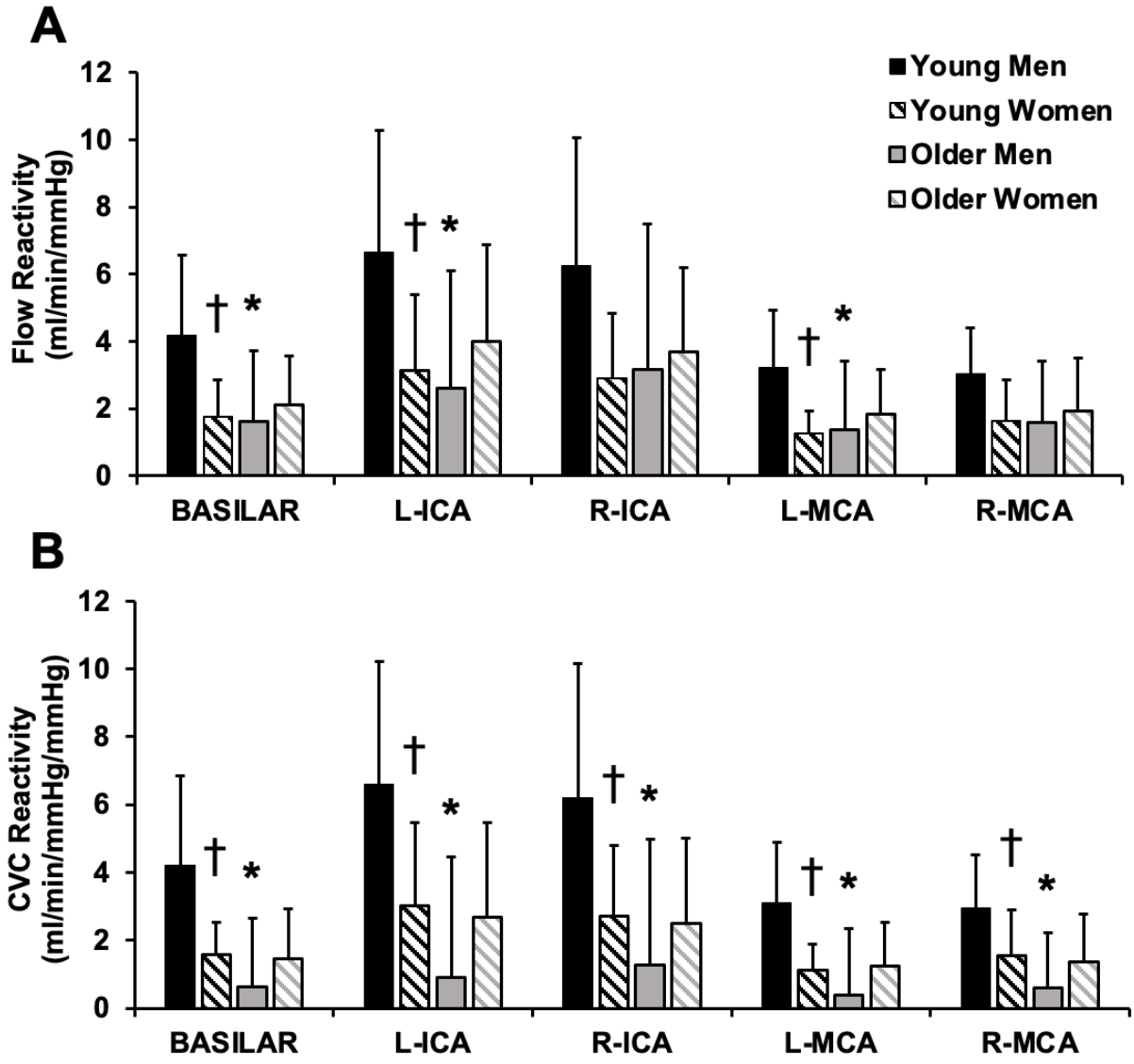

Figure 21. Cerebrovascular reactivity in the large intracranial vessels of men and women from study day B

Data are mean ± standard deviation. Cerebrovascular reactivity to hypercapnia in the large intracranial vessels of young and older adults measured during study day B using 4D flow MRI. A) Flow reactivity in the basilar artery, left internal carotid artery (L-ICA), right ICA (R-ICA), left middle cerebral artery (L-MCA) and right MCA (R-MCA). B) Cerebrovascular conductance (CVC) reactivity in the basilar artery, L-ICA, R-ICA, L-MCA, R-MCA. Young men are shown in black, young women in black stripes, older men in gray and older women in gray stripes. *$p<0.05$ vs. age within sex group, †$p<0.05$ vs. sex within age groups.

Study Day B Middle Cerebral Artery Cross-Sectional Area

The cross-sectional area of the right and left MCA during baseline and 6% CO_2 is shown in Figure 22. Young adults demonstrated a significant change in left (p=0.004, hedges' g=0.28) and right (p=0.002, hedges' g=0.40) MCA CSA from baseline to 6% CO_2. There was no significant change from baseline to 6% CO_2 in the right (p=0.08, hedges' g=0.09) or left (p=0.19, hedges' g=0.13) MCA CSA in older adults.

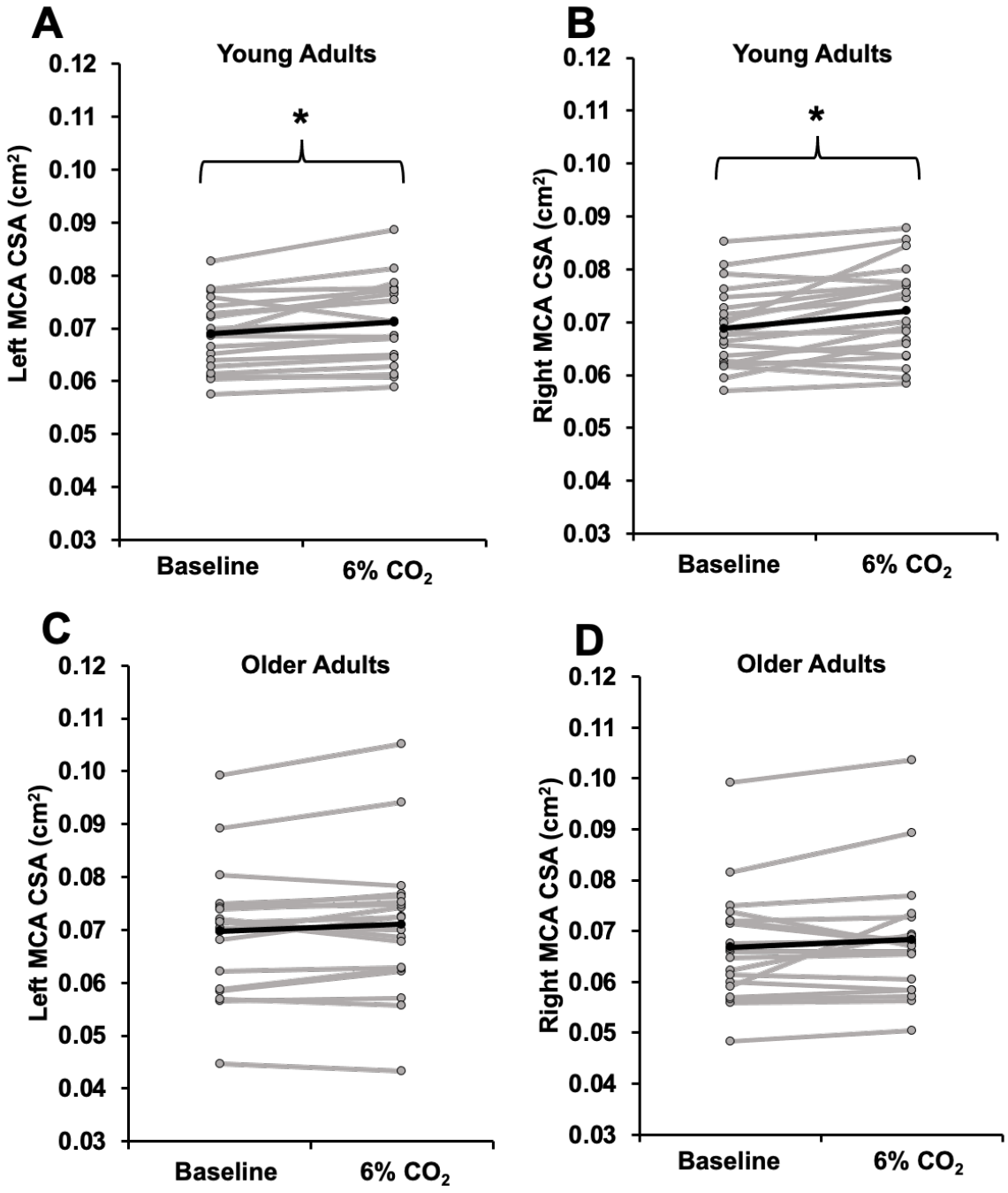

Figure 22. Middle cerebral artery cross sectional area during baseline and hypercapnia

Middle cerebral artery (MCA) cross-sectional area (CSA) at baseline and during 6% CO_2. Data collected during study visit B using 4D flow MRI. A) Left MCA CSA in young adults. B) right MCA CSA in young adults. C) Left MCA CSA in older adults D) Right MCA CSA older adults. Individual data is shown in gray and group averages are shown in black. *$p<0.05$ compared with baseline.

Central Arterial Stiffness and Cerebral Pulsatility Index

An exploratory analysis of the association between central arterial stiffness (carotid-femoral PWV) and cerebral pulsatility index is shown in Figure 23. In young adults, there were no significant correlations between carotid-femoral PWV and cerebral pulsatility index in either the anterior (ICAs) or posterior circulation (basilar artery). However, in older adults, there was a significant positive association between carotid-femoral PWV and ICA pulsatility index such that individuals with higher central arterial stiffness demonstrated greater pulsatility index in the ICAs. In older adults, the association between carotid-femoral PWV and basilar artery pulsatility did not reach significance.

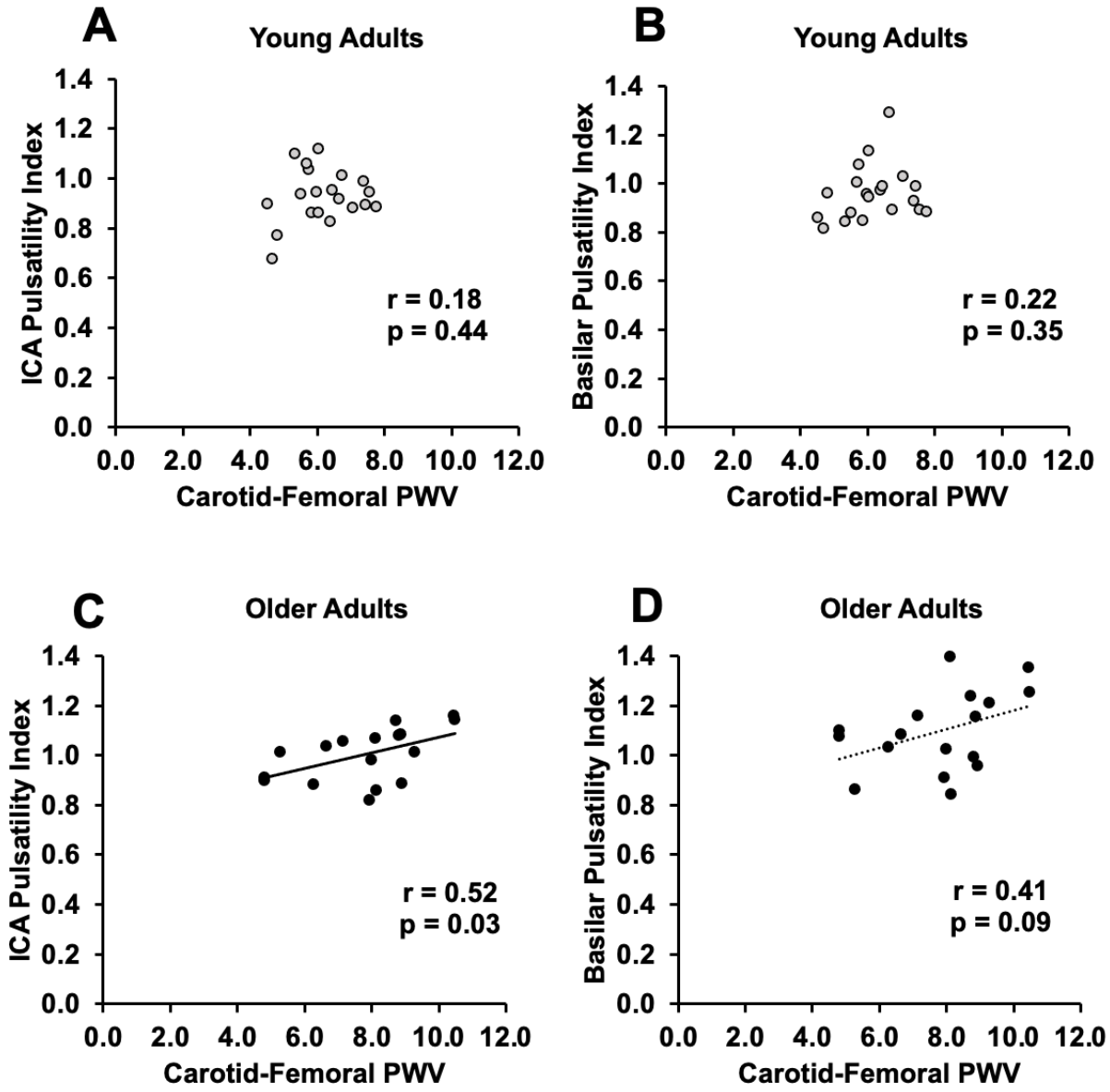

Figure 23. Association between central arterial stiffness and cerebral pulsatility index

Associations between central arterial stiffness and cerebral pulsatility index in young and older adults. Pulsatility index was measured during study visit B from 4D flow MRI. A) Carotid-femoral pulse wave velocity (PWV) and internal carotid artery (ICA) pulsatility index in young adults. B) Carotid-femoral PWV and basilar artery pulsatility index in young adults C) Carotid-femoral PWV and ICA pulsatility index in older adults. D) Carotid-femoral PWV and basilar pulsatility index in older adults. Solid line indicates a significant correlation. Dashed line indicates a correlation that did not reach the threshold for significance.

Summary of Study 1 Results

This study addressed **Specific Aim 1**: to evaluate the impact of aging on cerebrovascular reactivity to hypercapnia using two imaging techniques. The first hypothesis of Specific Aim 1 was: There will be no age-related differences in cerebrovascular reactivity to hypercapnia in healthy, habitually exercising adults when evaluating cerebral blood velocity with TCD. The results from study 1 support this hypothesis as the TCD did not detect any age, sex, or interaction effects on cerebrovascular reactivity to hypercapnia. The second hypothesis of Specific Aim 1 was: Older adults will have lower cerebrovascular reactivity to hypercapnia compared with young adults when evaluating cerebral blood flow using 4D flow MRI. The results from study 1 support this hypothesis as there were age-related differences in the cerebrovascular conductance reactivity response to hypercapnia, with older adults demonstrating lower cerebrovascular conductance reactivity compared with young adults. Older adults had lower cerebrovascular conductance reactivity globally, as well as in each blood vessel of interest (Right and left MCA, right and left ICA and basilar artery) compared with young adults. In addition, there was an age and sex interaction such that young men had greater cerebrovascular conductance reactivity globally and in each intracranial vessel compared with young women and older men. The third hypothesis of Specific Aim 1 was: The middle cerebral artery will increase in cross-sectional area in response to hypercapnia in young adults, but not older adults. The results from study 1 support this hypothesis, as the MCA dilated significantly during hypercapnia in young adults but not in older adults. An exploratory analysis found that despite having low vascular risk, there was a positive association between central arterial stiffness and cerebral pulsatility index in the anterior circulation of older adults. In summary, aging is associated with a reduction in cerebrovascular conductance reactivity to hypercapnia. Furthermore, the left and right MCA vasodilated in response to hypercapnia in

young adults, but not in older adults. These findings suggest that simultaneous angiographic, blood flow, and arterial blood pressure measures to quantify cerebrovascular responses may be necessary to appropriately investigate age-related differences in the cerebral circulation.

CHAPTER 3

3. STUDY 2: AGE-RELATED CHANGES IN CEREBRAL BLOOD FLOW IN ADULTS WITH VERTEBRAL ARTERY HYPOPLASIA

A selection of the data presented was published previously:

Miller, K.B., Gallo, S.J., Rivera-Rivera, L.A., Corkery, A. T., Howery, A.J., Johnson, S.C., Rowley, H.A., Wieben, O., and Barnes, J.N. Vertebral Artery Hypoplasia Influences Age-Related Differences in Blood Flow of the Large Intracranial Arteries. Aging Brain, 1, 100019.

3.1 INTRODUCTION

Cerebral blood flow (CBF) is critical for maintaining optimal brain function and lower global CBF is associated with higher risk of all-cause mortality (Sabayan et al., 2013). Previous studies have shown age-related differences in global CBF across the lifespan (Albayrak et al., 2007; Bakker et al., 2004; Hagstadius and Risberg, 1989; Kety, 1956; Leenders et al., 1990; Liu et al., 2012b; Lu et al., 2011; Martin et al., 1991; Melamed et al., 1980; Scheel et al., 2000; Zarrinkoob et al., 2015) which are independent of regional grey matter atrophy (Chen et al., 2011). Despite the lower age-related CBF reported, there is substantial variability in the time course and magnitude of this difference. Furthermore, it is possible the impact of aging may affect blood flow to certain brain regions more than others. Studies have reported larger age-related differences in blood flow in brain areas supplied by the anterior circulation (Lu et al., 2011; Matsuda et al., 1984; Melamed et al., 1980; Pagani et al., 2002). However, others have suggested the magnitude of age-related differences in posterior cerebral circulation is relatively larger than the age-related differences in the anterior cerebral circulation blood flow using ultrasonography (Albayrak et al., 2007; Dörfler et al., 2000; Olesen et al., 2019) or 2D phase contrast magnetic resonance angiography (MRA) (Zhao et al., 2007). Importantly, many of these studies (1) only evaluated the extracranial portion of the large cerebral arteries, (2) only measured one internal carotid artery (ICA) or vertebral artery (VA) which may demonstrate flow asymmetry between the right and left sides and (3) were restricted to capturing blood flow under resting conditions. It is possible that regional differences in CBF may become more prominent when a vasoactive stimulus is present. In addition, higher pulsatility index in the large intracranial vessels may reflect increased distal vascular resistance in the cerebral microvessels (Giller et al., 1990).

Vertebral artery hypoplasia (VAH) is a congenital anatomical variation common in healthy asymptomatic individuals where one VA diameter is smaller than the other. The hypoplastic vessel is usually less than 2 mm accompanied with reduced blood flow in the posterior cerebral circulation. Thus, VAH will likely affect regional blood flow distribution in the brain and increasing the risk of posterior stroke (Chuang et al., 2006; Kulyk et al., 2018; Mitsumura et al., 2016; Park et al., 2007; Zhang et al., 2016). Recent studies suggest the prevalence of VAH is 15 - 35% (Kulyk et al., 2018; Ogeng'o et al., 2014; Park et al., 2007; Peterson et al., 2010; Thierfelder et al., 2014). It has also been reported that individuals with VAH have lower global cerebral blood flow compared with their age-matched peers (Warnert et al., 2016). Yet, the impact of VAH on the age-related differences in CBF are unknown.

Recent advances in MRI technology allow for the comprehensive assessment of cerebrovascular macroscopic flow. 4D flow phase contrast MRI allows for in-vivo acquisition of both volumetric flow and vascular area data of multiple vessels. This scan has high spatial resolution and no contrast agent. 4D flow MRI is an ideal candidate to measure the effects of VAH on cerebral blood flow because it can be used to detect VAH with both structural and flow criteria. With this in mind, the purpose of this study is to retrospectively determine the prevalence of VAH and determine how VAH may impact age-related changes in CBF.

This study evaluates **Specific Aim 2** of this dissertation: to determine the impact of VAH on the age-related differences in regional blood flow in the large intracranial arteries. The first hypothesis is that in healthy adults without VAH, age-related differences in CBF will be greater in posterior vessels compared with anterior vessels both at rest and during hypercapnia. Because individuals with VAH already demonstrate reduced blood flow in the hypoplastic vessel, the second hypothesis is that in healthy adults with VAH, age-related differences in CBF will be

greater in anterior vessels compared with posterior vessels both at rest and during hypercapnia. The exploratory hypothesis is that older adults will demonstrate higher pulsatility index in the large intracranial vessels compared with young adults in both groups with and without VAH.

3.2 MATERIALS AND METHODS

Participant Recruitment

4D flow phase contrast MRI scans were used to retrospectively identify VAH from individuals that participated in Study 1 of this dissertation (Appendix 2). All study procedures were approved by the Institutional Review Board of the University of Wisconsin–Madison (IRB: 2016-0430) and were performed according to the Declaration of Helsinki, including obtaining written informed consent from each participant.

Cardiovascular Measurements

On a separate study visit, carotid–femoral pulse wave velocity (PWV) and aortic augmentation index (AIx) measurements were completed utilizing arterial tonometry. High-fidelity pressure waveforms were recorded for at least 10 heart beats non-invasively using a pencil-type Millar Micro-tip pressure transducer from the radial, femoral and carotid arteries (Sphygmocor, AtcorMedical, Sydney, NSW, Australia). An average of 3–5 trials of each PWV and AIx were obtained in succession. Tonometry transit distance from the carotid pulse site, the supra-sternal notch, and the femoral pulse site were measured with a tape measure. PWV was calculated using the intersection tangent foot-to-foot algorithm. An aortic pressure waveform was derived from the radial pulse using the application of a generalized transfer function to measure AIx. AIx was then corrected at a heart rate (HR) of 75 beats per minute.

Carotid ultrasound was performed using an 11 L probe with a transmission frequency of 4.5–12 MHz on a GE LOGIQ S8 machine (GE Healthcare, Waukesha, WI, United States). The left carotid artery was imaged in the longitudinal plane in B-mode 1–2 cm below the bifurcation. The carotid intima-media thickness (IMT) was measured using a semi-automated tracking

software offline (Carotid Analyzer for Research, Medical Imaging Applications, Coralville, IA, United States). The average of the far wall IMT over approximately six cardiac cycles was reported. All carotid imaging and analysis were done by the same observer.

MRI Imaging

MRI imaging consisted of brain volume measurements, and measurements of cerebral blood flow at rest and during hypercapnia. MR imaging was performed with a 3T clinical MRI scanner (MR750, GE Healthcare, Waukesha, WI, United States) at the Wisconsin Institutes for Medical Research in Madison, WI. Participants were supine and imaged with a 32-channel head coil (Nova Medical Head Coil, Nova Medical, Wilmington, MA, United States) with a gradient strength of 50 mT/m, and a gradient slew rate of 200 mT/m/ms. Throughout the MRI session, HR, and oxygen saturation (SPO_2) were acquired continuously using a pulse oximeter, and $ETCO_2$ was acquired continuously (breath-by-breath) using a nasal cannula. The pulse oximeter and nasal cannula was connected to an MRI compatible monitor (Medrad Veris MR Vital Signs Patient Monitor, Bayer Healthcare, Whippany, NJ, United States).

To determine brain volumes, a T1-weighted structural brain volume (BRAVO) scan was acquired with the following scan parameters: fast spoiled gradient echo sequence, inversion time = 450 ms, repetition time (TR) = 8.1 ms, echo time (TE) = 3.2 ms, flip angle = 12°, acquisition matrix = 256 × 256, field of view (FOV) = 256 mm, slice thickness = 1.0 mm, and scan time ∼8 min. A 3D time of flight (TOF) MRA of the Circle of Willis was acquired for visualization of the large intracranial vessels with the following scan parameters: TE = 2.5 ms, TR: 23 ms, flip angle = 20°, acquisition matrix = 448 x 224, FOV = 512 mm, slice thickness = 1.0 mm, pixel bandwidth = 162.78 kHz, spacing between slices = 0.5 mm, and scan time ~ 4 min 30 sec.

4D flow MRI data was acquired using a 3D radially under sampled sequence to provide high spatial and temporal resolution. No contrast agent was administered. The scan parameters were as follows: velocity encoding (Venc) = 80 cm/s, FOV = 220 mm, acquired isotropic spatial resolution = 0.7 mm × 0.7 mm × 0.7 mm, TR = 7.8 ms, TE = 2.7 ms, flip angle = 8°, bandwidth = 83.3 kHz, 14,000 projection angles and scan time ~7 min. The imaging volume covered the right and left ICAs, VAs and BA. Data was acquired continuously, such that a HR of 60 beats/min would provide a sampling of approximately 128 times per heartbeat. Time-resolved velocity and magnitude data was reconstructed offline by retrospectively gating into 20 cardiac phases using temporal interpolation.

For the hypercapnic stimulus, participants were fitted with a facemask that covers their nose and mouth with a one-way valve to prevent re-breathing (Hans Rudolph, Inc., Shawnee, KS, United States). All compressed gas was medical grade. Participants breathed normocapnic air for approximately 10 min. Following normocapnia, participants breathed two stepwise elevations of 4% and 6% inspired CO_2 administered with oxygen maintained at 21% and balanced nitrogen for approximately 9 min at each level of CO_2. Participants were instructed to breathe normally and breathing rate was not controlled. The data of interest for this study was from the baseline and the 6% CO_2 conditions.

Determination of VAH

Determination of VAH were retrospectively defined using both structural and flow criteria independently by two investigators. The VA segments were measured approximately 2 mm below the junction with the BA. Although there is no consensus for unilateral VAH diagnosis, conservative standard criteria was followed including vessel diameter less than or equal to 2.0 mm

(Chuang et al., 2006) and flow less than or equal to 50 mL/min. VAH diameter measures were assessed with both a time-of-flight angiogram and the 4D flow MRI scan. Several studies have suggested using flow criteria < 30-40 ml/min to define VAH; (Acar et al., 2005; Sato et al., 2015; Schöning et al., 1994; Seidel et al., 1999) however, most studies relied on ultrasound which may underestimate flow values. In addition, many of these studies included adults with confounding vascular risk factors that are associated with reduced CBF. All participants with VAH in this study also had a flow asymmetry ratio of 2.0 or greater between the right and left VA; thus, none of the participants in this study had bilateral VAH. All MRI scans were overviewed by a neuroradiologist.

Data Analysis

Total brain volume was derived from the T1-weighted scans. Scans were segmented in Statistical Parametric Mapping version 12 (SMP12) into gray matter (GM), white matter (WM), and cerebral spinal fluid (CSF). Total brain volume was calculated as the sum of GM and WM volume. Intracranial volume was calculated as the sum of GM, WM and CSF. Brain volume was also reported as brain volume divided by intracranial volume. 4D flow MRI scans were analyzed as described in Study 1. Blood flow was averaged along the length of each vessel. Pulsatility index was calculated as (maximum flow – minimum flow) / mean flow. Global pulsatility index was the average pulsatility of the ICAs and BA. Conductance was calculated as blood flow / MAP. Global blood flow was calculated as the sum of the right and left ICAs and the BA. Global cerebral blood flow was also reported as global cerebral blood flow divided by intracranial volume.

Statistical Analysis

Estimates for a required sample size was calculated using G*Power 3.1.9.4 (Faul et al., 2007). In a previous study by Olesen et al., 2019 blood flow through the vertebral arteries was statistically different between young (n = 22) and older (n = 11) adults without VAH (219 ± 50 ml/min vs. 138 ± 48 ml/min, respectively, $p<0.001$) (Olesen et al., 2019). A post-hoc analysis of this effect size was f =0.78 with alpha = 0.05 and power (1-beta) = 0.99. To achieve a power of 0.80 or 80% at an effect size of f = 0.78 and alpha = 0.05, G*Power estimated that the necessary total sample size was 16 individuals per group (Appendix 1). This was a retrospective study of 40 subjects. It is estimated that prevalence of VAH is 15-35%; thus, the range of the number of participants with VAH is 3 – 7 per age group, for a total of 6 – 14 participants. Because this study is retrospective in nature, the sample size of subjects with VAH was predetermined. The estimated number of participants without VAH is 13 – 17 per age group, for a total of 26 – 34 participants. Because of the potential of an under-powered sample of young and older participants with VAH, both parametric and non-parametric statistics were performed.

Statistical testing, except for the sample size estimate, was completed using Sigma Plot for Windows version 13.0 (Systat Software, San Jose, CA, United States). Prior to all analyses, normality and equal variance was assessed using the Shapiro-Wilk test and Brown-Forsythe test respectively. Prevalence of VAH was calculated as the number of subjects with VAH divided by the number of total subjects. The primary outcome measures were blood flow in the large intracranial arteries (ICA and BA) at baseline and during 6% CO_2. The pulsatility index of the large intracranial arteries (ICA and BA) at baseline and during 6% CO_2 was also evaluated. One participant's data was not included due to motion artifact on the MRI scan (older female). In adults without VAH, participant demographics were compared between age groups (Young and Older

adults) using unpaired, two-tailed t-tests. A two-way repeated measures ANOVA compared the hemodynamic, flow characteristics and vessel characteristics between the two groups of interest (young and older adults without VAH) during each stage of the protocol (normocapnia and 6% CO_2) followed by the Holm-Sidak method to test pairwise comparisons. Effect sizes of the primary outcome measures were calculated as Hedges' g. This analysis addressed hypothesis 1: in healthy adults without VAH, age-related difference in CBF will be greater in posterior vessels compared with anterior vessels at rest and during hypercapnia. It also addresses the exploratory hypothesis: older adults will demonstrate higher pulsatility index in the large intracranial vessels compared with young adults.

In adults with VAH, participant demographics and blood flow characteristics were compared between age groups using unpaired, two-tailed t-tests. A two-way repeated measures ANOVA compared the hemodynamic, flow characteristics and vessel characteristics between the two groups of interest (young and older adults with VAH) during each stage of the protocol (normocapnia and 6% CO_2) followed by the Holm-Sidak method to test pairwise comparisons. Primary outcome measures were also assessed using non-parametric statistics including a Mann-Whitney Rank Sum Test or Kruskal-Wallis ANOVA on Ranks followed by the Dunn's Method to test pairwise multiple comparisons as appropriate. Effect sizes of the primary outcome measures were calculated as Hedges' g. This analysis will address hypothesis 2: in healthy adults with VAH, age-related difference in CBF will be greater in anterior vessels compared with posterior vessels at rest and during hypercapnia. It will also address the exploratory hypothesis: older adults will demonstrate higher pulsatility index in the large intracranial vessels compared with young adults. Statistical significance was set *a priori* at $p < 0.05$.

3.3 RESULTS

Identification of Vertebral Artery Hypoplasia

The characteristics of the vertebral arteries are displayed in Table 15. Data from one older female was not usable due to motion artifact during the MRI scan. Out of the 39 total participants, VAH was identified in 10 participants (5 young and 5 older; 26% prevalence). An example is shown in Figure 24. The hypoplastic artery was most common on the right side (n=8). As expected, the hypoplastic VA in the VAH+ group was smaller, had lower flow and lower conductance compared with the ipsilateral (right) VA in the No VAH group. The hypoplastic VA in the VAH+ group also had a greater pulsatility index compared with the ipsilateral (right) VA in the No VAH group. The contralateral VA in the VAH+ group was larger, as measured by the time-of-flight scan, and it had greater flow and greater conductance compared with the contralateral (left) VA in the No VAH group. The contralateral VA in the No VAH group also had lower pulsatility index compared with the contralateral (left) VA in the No VAH group.

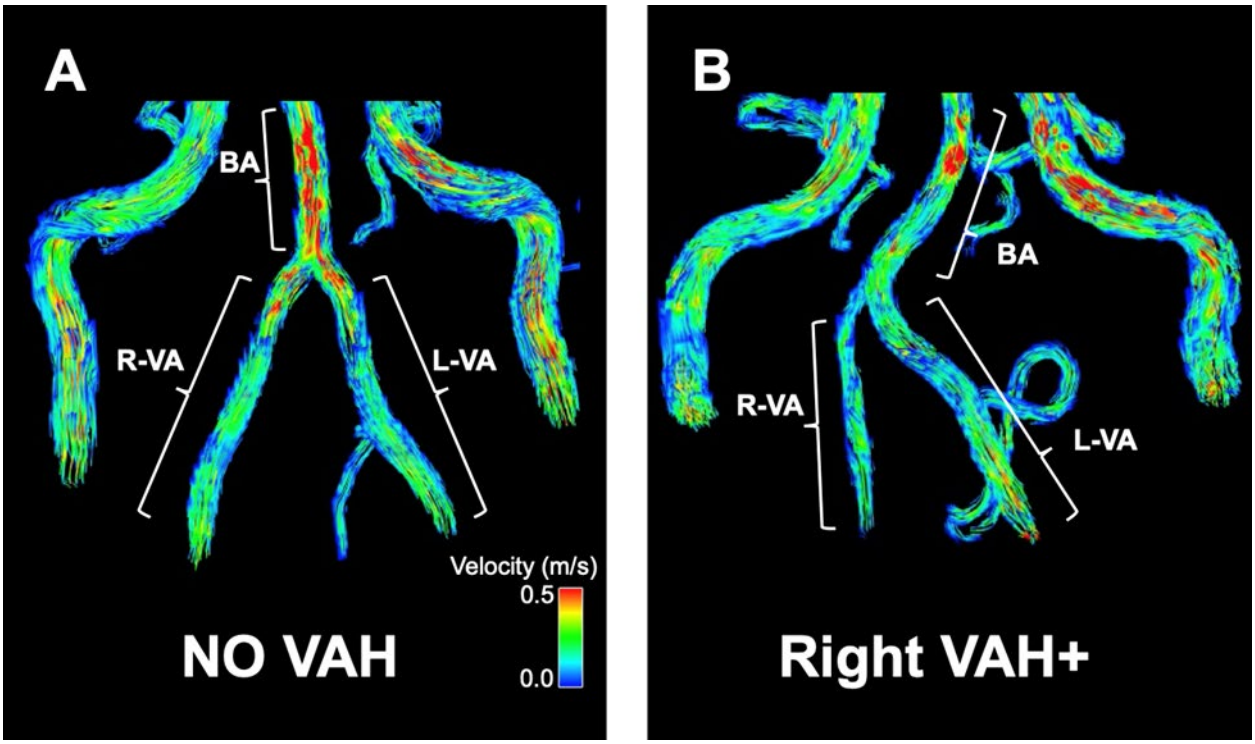

Figure 24. Example 4D flow MRI scan with and without vertebral artery hypoplasia

This figure displays example images of the large intracranial arteries from the 4D flow MRI scan. A) example of a participant without vertebral artery hypoplasia (No VAH). B) example of a participant with VAH on the right side (VAH+). Warmer colors reflect higher blood velocity. BA, basilar artery, L, left, R, right, VA, vertebral artery, VAH, vertebral artery hypoplasia.

Table 15. Vertebral artery characteristics

Variable	*No VAH N = 29*	*VAH+ N = 10*	*P-value*
Ipsilateral VA Diameter TOF (mm)	3.22 ± 0.46	1.93 ± 0.10	<0.001
Contralateral VA Diameter TOF (mm)	3.12 ± 0.25	3.47 ± 0.49	0.009
Ipsilateral VA Diameter 4D flow PC (mm)	3.11 ± 0.40	2.56 ± 0.15	<0.001
Contralateral VA Diameter 4D flow PC (mm)	3.23 ± 0.47	3.37 ± 0.40	0.403
Ipsilateral VA flow (mL/beat)	1.41 ± 0.52	0.60 ± 0.19	<0.001
Contralateral VA flow (mL/beat)	1.51 ± 0.51	2.02 ± 0.58	0.012
Ipsilateral VA flow (mL/min)	76 ± 28	32 ± 11	<0.001
Contralateral VA flow (mL/min)	82 ± 30	104 ± 25	0.04
Ipsilateral VA Conductance (mL/min/mmHg)	79 ± 30	35 ± 12	<0.001
Contralateral VA Conductance (mL/min/mmHg)	85 ± 35	113 ± 31	0.031
Ipsilateral VA Pulsatility Index	1.11 ± 0.17	1.42 ± 0.35	0.001
Contralateral VA Pulsatility Index	1.09 ± 0.16	0.98 ± 0.13	0.041

Data are mean ± standard deviation. Vertebral artery (VA) measurements in adults without vertebral artery hypoplasia (No VAH) and with vertebral artery hypoplasia (VAH+). Ipsilateral measurements refer to the hypoplastic vessel, which was commonly on the right side (n=8). In the No VAH group, ipsilateral VA measurements are from the right VA and contralateral measurements are from the left VA. *P-value* in the column reflects the comparison between groups. 4D flow PC, 4D flow phase contrast, TOF, time of flight.

Participant Characteristics – No VAH

Table 16 describes the characteristics of participants without VAH. In the No VAH group, there were no differences between young and older adults for BMI, heart rate at rest, and systolic blood pressure. However, older adults in the No VAH group demonstrated higher diastolic blood pressure and mean arterial pressure compared with young adults in the No VAH group. Table 17 shows the central arterial stiffness in the No VAH group. Older adults had a higher carotid-femoral PWV, aortic augmentation index and carotid IMT compared with young adults. Brain volumes in the No VAH group are shown in Table 18. Older adults had a smaller grey matter volume and total brain volume compared with young adults. This finding remained when total brain volume was normalized to intracranial volume. There were no age group differences in white matter volume or intracranial volume.

Hemodynamic Measurements – No VAH

Hemodynamic and cardiorespiratory measurements from the No VAH group are shown in Table 19. $ETCO_2$ increased from baseline to 6% CO_2 in both young and older adults. Age group differences in $ETCO_2$ at baseline did not reach statistical significance. Older adults demonstrated lower $ETCO_2$ at 6% CO_2 compared with young adults. However, delta $ETCO_2$ from baseline to 6% CO_2 was not different between age groups (Young adults: Δ 7 $\pm$ 3 mmHg vs. Older adults: Δ 6 $\pm$ 4 mmHg, p=0.68). Respiratory rate did not change between conditions in either group. Young adults had greater respiratory rates at baseline compared with older adults but there was no difference between age groups at 6% CO_2. There was no change in mean arterial pressure from baseline to 6% CO_2 in young adults. However, mean arterial pressure increased from baseline to 6% CO_2 in older adults. Older adults demonstrated higher mean arterial pressure at baseline and

at 6% CO_2 compared with young adults. Heart rate increased from baseline to 6% CO_2 in both young and older adults. There were no differences between the age groups in heart rate at either condition (baseline or 6% CO_2).

Individual Vessel Characteristics – No VAH

Measurements of the basilar artery in the No VAH group are shown in Table 20. Basilar artery diameter increased from baseline to 6% CO_2 in both young and older adults. There were no differences in basilar artery diameter between age groups at either condition. Basilar artery mean velocity increased from baseline to 6% CO_2 in young and older adults. The age group difference in mean velocity at baseline did not reach significance. However, older adults demonstrated lower basilar artery mean velocity at 6% CO_2 compared with young adults. Basilar artery max velocity increased from baseline to 6% CO_2 in both young and older adults. There were no significant differences in max velocity between young and older adults in either condition. Blood flow expressed in mL/beat increased from baseline to 6% CO_2 in both young and older adults. Older adults had lower flow in mL/beat compared with young adults at both conditions (baseline and 6% CO_2). Basilar artery blood flow expressed in mL/min increased from baseline to 6% CO_2 in both young and older adults. Older adults had lower flow in mL/min compared with young adults at both conditions (baseline and 6% CO_2), though the difference at baseline did not reach the threshold for significance. Basilar artery cerebrovascular conductance increased from baseline to 6% CO_2 in young adults. There were no differences in basilar artery cerebrovascular conductance from baseline to 6% CO_2 in older adults. Older adults had lower cerebrovascular conductance compared with young adults at both conditions (baseline and 6% CO_2). Basilar artery pulsatility index decreased from baseline to 6% CO_2 in young adults. Pulsatility index did not change from

baseline to 6% CO_2 in older adults. Older adults demonstrated higher basilar artery pulsatility index at both conditions compared with young adults (baseline and 6% CO_2).

Data from the right ICA in the No VAH group is shown in Table 21. Right ICA diameter increased from baseline to 6% CO_2 in young adults. There was no change in diameter from baseline to 6% CO_2 in older adults. There were no differences in diameter between age groups at either condition. Right ICA mean velocity increased from baseline to 6% CO_2 in young and older adults. There were no age group differences in mean velocity at either condition. Right ICA max velocity increased from baseline to 6% CO_2 in both young and older adults. There were no significant differences in max velocity between young and older adults in either condition (baseline or 6% CO_2). Blood flow expressed in mL/beat increased from baseline to 6% CO_2 in both young and older adults. There were no significant differences in right ICA flow in mL/beat between young and older adults in either condition (baseline or 6% CO_2). Blood flow expressed in mL/min increased from baseline to 6% CO_2 in both young and older adults. There were no significant differences in right ICA flow in mL/min between young and older adults in either condition (baseline or 6% CO_2). Right ICA cerebrovascular conductance increased from baseline to 6% CO_2 in young and older adults. There were no age group differences in right ICA cerebrovascular conductance at baseline. However, older adults had lower right ICA cerebrovascular conductance compared with young adults at 6% CO_2. Right ICA pulsatility index decreased from baseline to 6% CO_2 in young adults. Pulsatility index did not change from baseline to 6% CO_2 in older adults. Age group differences in right ICA pulsatility index at baseline did not reach statistical significance. However, older adults demonstrated higher pulsatility index at 6% CO_2 compared with young adults.

Data from the left ICA in the No VAH group is shown in Table 22. Left ICA diameter increased from baseline to 6% CO_2 in young and older adults. There were no differences in left ICA diameter between age groups at either condition. Mean velocity increased from baseline to 6% CO_2 in young and older adults. There were no age group differences in mean velocity at either condition. There was no change in left ICA max velocity from baseline to 6% CO_2 in young or older adults. There were also no significant differences in max velocity between young and older adults in either condition. Blood flow expressed in mL/beat increased from baseline to 6% CO_2 in both young and older adults. There were no significant differences in left ICA flow in mL/beat between young and older adults in either condition. Blood flow expressed in mL/min increased from baseline to 6% CO_2 in both young and older adults. There were no significant differences in left ICA flow in mL/min between young and older adults in either condition. Left ICA cerebrovascular conductance increased from baseline to 6% CO_2 in young adults. There was no change in left ICA cerebrovascular conductance from baseline to 6% CO_2 in older adults. There were no age group differences in left ICA cerebrovascular conductance at baseline. However, older adults had lower left ICA cerebrovascular conductance compared with young adults at 6% CO_2. Left ICA pulsatility index decreased from baseline to 6% CO_2 in young adults. Left ICA pulsatility index did not change from baseline to 6% CO_2 in older adults. There were no age group differences in pulsatility index at baseline. However, older adults demonstrated higher left ICA pulsatility index at 6% CO_2 compared with young adults.

Global Cerebral Blood Flow Characteristics - No VAH

Global cerebral blood flow measurements in the No VAH group are shown in Table 23. Global cerebral blood flow increased from baseline to 6% CO_2 in both young and older adults. There were

no age group differences in global cerebral blood flow at either condition (baseline or 6% CO_2). Global cerebral blood flow adjusted for brain volume increased from baseline to 6% CO_2 in both young and older adults. However, there were no age group differences in global cerebral blood flow adjusted for brain volume at either condition (baseline or 6% CO_2). Global cerebrovascular conductance increased from baseline to 6% CO_2 in both young and older adults. There were no age group differences in global cerebrovascular conductance at baseline. However, older adults demonstrated lower global cerebrovascular conductance during 6% CO_2 compared with young adults. Global pulsatility index decreased from baseline to 6% CO_2 in young adults. There was no change in global pulsatility index from baseline to 6% CO_2 in older adults. Older adults demonstrated higher global pulsatility index at baseline and 6% CO_2 compared with young adults.

Summary of Anterior, Posterior and Global Flow Characteristics – No VAH

Anterior, posterior, and global cerebral blood flow data in the large intracranial arteries from the No VAH group are in Figure 25. Basilar flow was lower in older adults compared with young adults at baseline (p=0.02, hedges' g=0.92) and during hypercapnia (p=0.02, hedges' g=0.97). There were no age group differences in ICA flow at baseline (p=0.82, hedges' g=0.09) or during hypercapnia (p=0.31, hedges' g=0.39). There were also no age group differences in global flow at baseline (p=0.43, hedges' g=0.30) or during hypercapnia (p=0.12, hedges' g=0.59).

Cerebrovascular conductance of the large intracranial arteries in the No VAH group are shown in Figure 26. Basilar artery conductance was lower in older adults compared with young adults at baseline (p=0.01, p=0.02 no outlier, hedges' g=1.00) and during hypercapnia (p=0.001, hedges' g=1.33). There were no age group differences in ICA conductance at baseline (p=0.17, hedges' g=0.53). Older adults demonstrated lower ICA conductance during hypercapnia compared

with young adults (p=0.02, hedges' g=0.94). There were no age-related differences in global conductance at baseline (p=0.07, p=0.13 no outlier, hedges' g=0.70). However, older adults demonstrated lower global conductance during hypercapnia compared with young adults (p=0.01, hedges' g=1.11).

Pulsatility index of the large intracranial arteries from the No VAH group are shown in Figure 27. Older adults had greater pulsatility index in the basilar arteries at baseline (p=0.002, hedges' g=1.25) and during hypercapnia (p<0.001 ANOVA on ranks, hedges' g=1.60) compared with young adults. There were no age-related differences in ICA pulsatility index at baseline (p=0.13, hedges' g=0.58). During hypercapnia, older adults demonstrated greater ICA pulsatility index compared with young adults (p=0.006, hedges' g=1.11). Older adults also demonstrated greater global pulsatility index at baseline (p=0.007, hedges' g=1.10) and during hypercapnia (p<0.001, hedges' g=1.50).

Table 16. Characteristics of participants in No VAH

Variable	***Young No VAH N = 15***	***Older No VAH N = 14***	***P-value***
Men / Women	10 / 5	9 / 5	
Age (years)	24 ± 3	62 ± 5	<0.001
Height (cm)	176 ± 6	173 ± 8	0.25
Weight (kg)	74 ± 9	72 ± 13	0.65
Body Mass Index (kg/m^2)	24 ± 2	24 ± 3	0.90
Heart Rate at Rest (beats per minute)	54 ± 8	54 ± 7	0.82
Systolic Blood Pressure (mmHg)	123 ± 10	124 ± 9	0.77
Diastolic Blood Pressure (mmHg)	70 ± 5	76 ± 5	<0.01
Mean Arterial Pressure (mmHg)	87 ± 6	93 ± 7	0.04

Characteristics of participants without vertebral artery hypoplasia (No VAH). Data are mean ± standard deviation. VAH, vertebral artery hypoplasia. *P-value* in the column reflects the comparison between age groups.

Table 17. Central arterial stiffness in No VAH

Variable	*Young No VAH N = 15*	*Older No VAH N = 14*	*P-value*
Carotid-Femoral PWV (m/s)	6.2 ± 1.0	7.8 ± 1.7	<0.01
Aortic Augmentation Index (%)	-5.0 ± 8.0	16.0 ± 9.5	<0.001
Carotid IMT (mm)	0.50 ± 0.09	0.74 ± 0.10	<0.001

Central arterial stiffness of participants in the No VAH group. Data are mean ± standard deviation. *P-value* in the column reflects the comparison between age groups. IMT, intima-media thickness. PWV, pulse wave velocity. For aortic augmentation index, n = 18. Aortic augmentation index was corrected for a heart rate of 75 beats per minute.

Table 18. Brain volumes in No VAH

Variable	*Young No VAH N = 15*	*Older No VAH N = 14*	*P-value*
Grey Matter Volume (L)	0.77 ± 0.07	0.67 ± 0.07	<0.001
White Matter Volume	0.46 ± 0.05	0.46 ± 0.05	0.99
Brain Volume (L)	1.23 ± 0.11	1.13 ± 0.10	0.02
Intracranial Volume (L)	1.48 ± 0.13	1.48 ± 0.14	0.95
Brain Volume / Intracranial Volume (L)	0.83 ± 0.02	0.76 ± 0.03	<0.001

Brain volumes of participants in the No VAH group. Data are mean ± standard deviation. *P-value* in the column reflects the comparison between age groups.

Table 19. Hemodynamic measurements in No VAH

Variable	*Young No VAH N = 15*	*Older No VAH N = 14*	*P-value*
$ETCO_2$ (mmHg)			
Baseline	42 ± 4	39 ± 5	0.06
6% CO_2	49 ± 5*	45 ± 5*	0.03
Respiratory Rate (breaths per minute)			
Baseline	14 ± 3	12 ± 3	0.04
6% CO_2	14 ± 3	12 ± 3	0.18
Mean Arterial Pressure (mmHg)			
Baseline	93 ± 6	104 ± 7	<0.001
6% CO_2	96 ± 6	111 ± 8*	<0.001
Heart Rate (bpm)			
Baseline	54 ± 7	55 ± 7	0.71
6% CO_2	58 ± 6*	58 ± 7*	0.88

Hemodynamic and cardiorespiratory measurements in adults without vertebral artery hypoplasia (No VAH). Data are mean ± standard deviation. $ETCO_2$, end-tidal carbon dioxide. *P-value* in the column reflects the comparison between age groups. *p<0.05 compared with baseline.

Table 20. Basilar artery measurements in No VAH

Variable	*Young No VAH N = 15*	*Older No VAH N = 14*	*P-value*
Diameter (cm)			
Baseline	0.328 ± 0.028	0.311 ± 0.035	0.16
6% CO_2	0.333 ± 0.031*	0.316 ± 0.036*	0.16
Mean Velocity (cm/s)			
Baseline	31 ± 7	26 ± 4	0.06
6% CO_2	34 ± 8*	29 ± 5*	0.02
Max Velocity (cm/s)			
Baseline	67 ± 11	63 ± 7	0.24
6% CO_2	72 ± 13*	66 ± 8*	0.13
Flow (mL/beat)			
Baseline	2.6 ± 0.5	2.0 ± 0.6	0.03
6% CO_2	3.0 ± 0.7*	2.3 ± 0.7*	0.01
Flow (mL/min)			
Baseline	140 ± 38	111 ± 38	0.02
6% CO_2	174 ± 49*	131 ± 39*	0.02
Cerebrovascular Conductance (mL/min/mmHg)			
Baseline	151 ± 46	108 ± 40	0.02
6% CO_2	183 ± 55*	119 ± 39	<0.001
Pulsatility Index			
Baseline	0.96 ± 0.13	1.12 ± 0.14	<0.001
6% CO_2	0.90 ± 0.10*	1.07 ± 0.12	<0.001

Basilar artery measurements in adults without vertebral artery hypoplasia (No VAH). Data are mean ± standard deviation. *P-value* in the column reflects the comparison between age groups. *p<0.05 compared with baseline.

Table 21. Right internal carotid artery measurements in No VAH

Variable	*Young No VAH N = 15*	*Older No VAH N = 14*	*P-value*
Diameter (cm)			
Baseline	0.447 ± 0.034	0.457 ± 0.033	0.42
6% CO_2	0.458 ± 0.036*	0.461 ± 0.033	0.82
Mean Velocity (cm/s)			
Baseline	26 ± 4	24 ± 4	0.23
6% CO_2	28 ± 4*	26 ± 4*	0.19
Max Velocity (cm/s)			
Baseline	59 ± 7	58 ± 5	0.61
6% CO_2	63 ± 6*	62 ± 5*	0.49
Flow (mL/beat)			
Baseline	4.0 ± 0.7	3.9 ± 0.7	0.73
6% CO_2	4.6 ± 1.0*	4.3 ± 0.7*	0.35
Flow (mL/min)			
Baseline	214 ± 48	212 ± 43	0.90
6% CO_2	267 ± 65*	248 ± 43*	0.32
Cerebrovascular Conductance (mL/min/mmHg)			
Baseline	231 ± 58	205 ± 42	0.22
6% CO_2	280 ± 73*	225 ± 41*	0.01
Pulsatility Index			
Baseline	0.94 ± 0.12	1.01 ± 0.11	0.07
6% CO_2	0.89 ± 0.07*	0.99 ± 0.12	0.02

Right internal carotid artery measurements in adults without vertebral artery hypoplasia (No VAH). Data are mean ± standard deviation. *P-value* in the column reflects the comparison between age groups. *$p<0.05$ compared with baseline.

Table 22. Left internal carotid artery measurements in No VAH

Variable	*Young No VAH N = 15*	*Older No VAH N = 14*	*P-value*
Diameter (cm)			
Baseline	0.447 ± 0.042	0.456 ± 0.034	0.53
6% CO_2	0.459 ± 0.044*	0.464 ± 0.034*	0.73
Mean Velocity (cm/s)			
Baseline	26 ± 4	24 ± 4	0.20
6% CO_2	28 ± 5*	26 ± 4*	0.16
Max Velocity (cm/s)			
Baseline	61 ± 7	58 ± 7	0.22
6% CO_2	64 ± 8	62 ± 6	0.41
Flow (mL/beat)			
Baseline	4.1 ± 0.8	3.9 ± 0.9	0.71
6% CO_2	4.7 ± 1.2*	4.4 ± 0.8*	0.35
Flow (mL/min)			
Baseline	222 ± 63	216 ± 57	0.82
6% CO_2	277 ± 91*	252 ± 52*	0.32
Cerebrovascular Conductance (mL/min/mmHg)			
Baseline	238 ± 68	209 ± 60	0.28
6% CO_2	290 ± 95*	229 ± 52	0.03
Pulsatility Index			
Baseline	0.95 ± 0.10	1.00 ± 0.11	0.20
6% CO_2	0.89 ± 0.10*	1.00 ± 0.10	0.01

Left internal carotid artery measurements in adults without vertebral artery hypoplasia (No VAH). Data are mean ± standard deviation. *P-value* in the column reflects the comparison between age groups. *$p<0.05$ compared with baseline.

Table 23. Global cerebral blood flow measurements in No VAH

Variable	*Young No VAH N = 15*	*Older No VAH N = 14*	*P-value*
Global Flow (mL/min)			
Baseline	576 ± 129	539 ± 111	0.47
6% CO_2	719 ± 181*	631 ± 101*	0.09
Global Flow / Brain Volume (mL/min/L)			
Baseline	693 ± 151	706 ± 149	0.83
6% CO_2	864 ± 212*	827 ± 122*	0.54
Global Cerebrovascular Conductance (mL/min/mmHg)			
Baseline	620 ± 152	522 ± 125	0.09
6% CO_2	752 ± 200*	573 ± 107*	0.003
Global Pulsatility Index			
Baseline	0.95 ± 0.09	1.04 ± 0.11	0.01
6% CO_2	0.89 ± 0.08*	1.02 ± 0.10	0.001

Global cerebral blood flow measurements in adults without vertebral artery hypoplasia (No VAH). Data are mean ± standard deviation. Global flow = internal carotid artery + basilar artery flow. *P-value* in the column reflects the comparison between age groups. *p<0.05 compared with baseline.

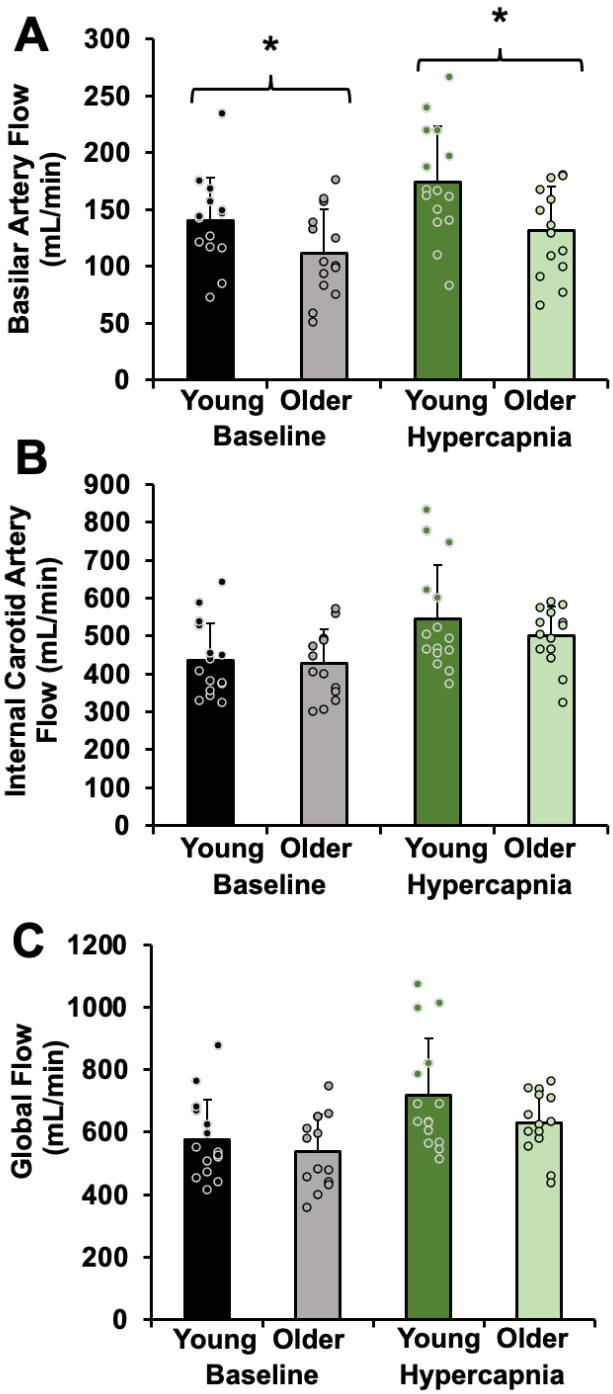

Figure 25. Flow measurements in No VAH

Data are mean ± standard deviation and individual data points. This figure shows flow in the large intracranial arteries at baseline (black & grey) and during hypercapnia (green) in adults without vertebral artery hypoplasia (No VAH). A) Basilar artery (BA) flow, B) Internal carotid artery (ICA) flow C) global flow (sum of ICAs and BA). *$p<0.05$ compared with young.

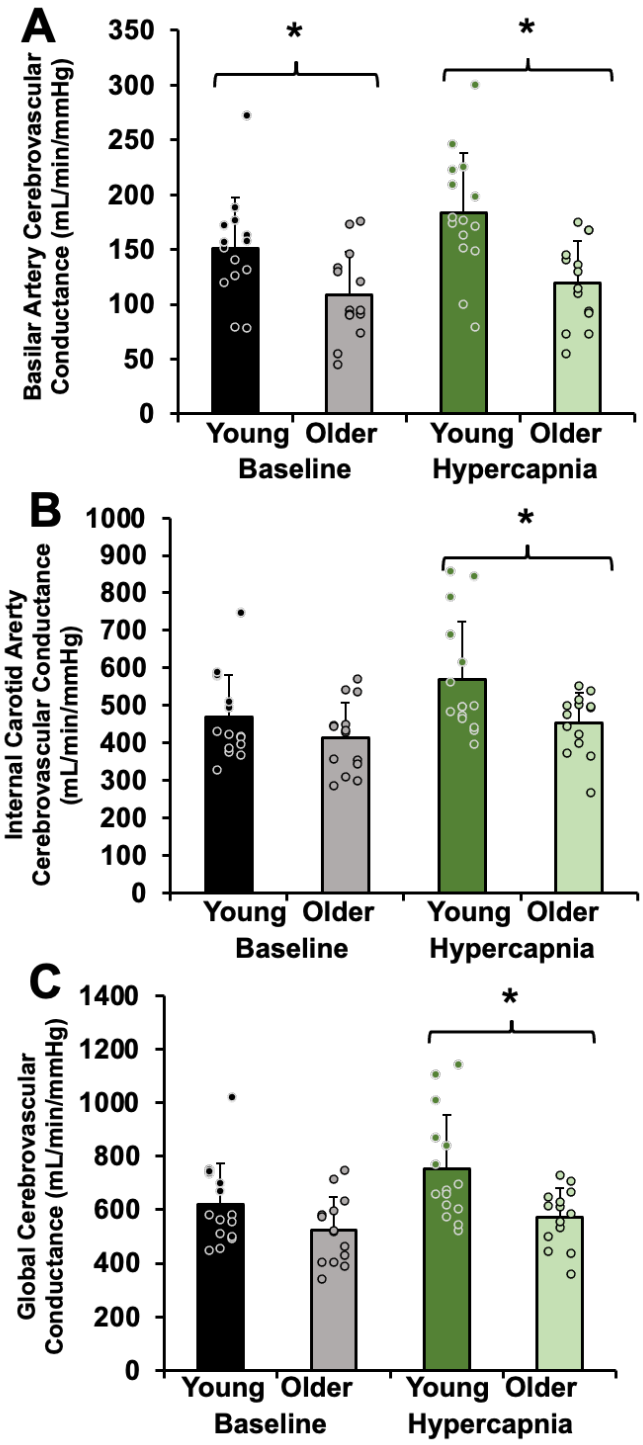

Figure 26. Conductance measurements in No VAH

Data are mean ± standard deviation and individual data points. This figure shows cerebrovascular conductance in the large intracranial arteries at baseline (black & grey) and during hypercapnia (green) in adults without vertebral artery hypoplasia (No VAH). A) Basilar artery (BA) conductance, B) Internal carotid artery (ICA) conductance C) global conductance (sum of ICAs and BA). *$p<0.05$ compared with young.

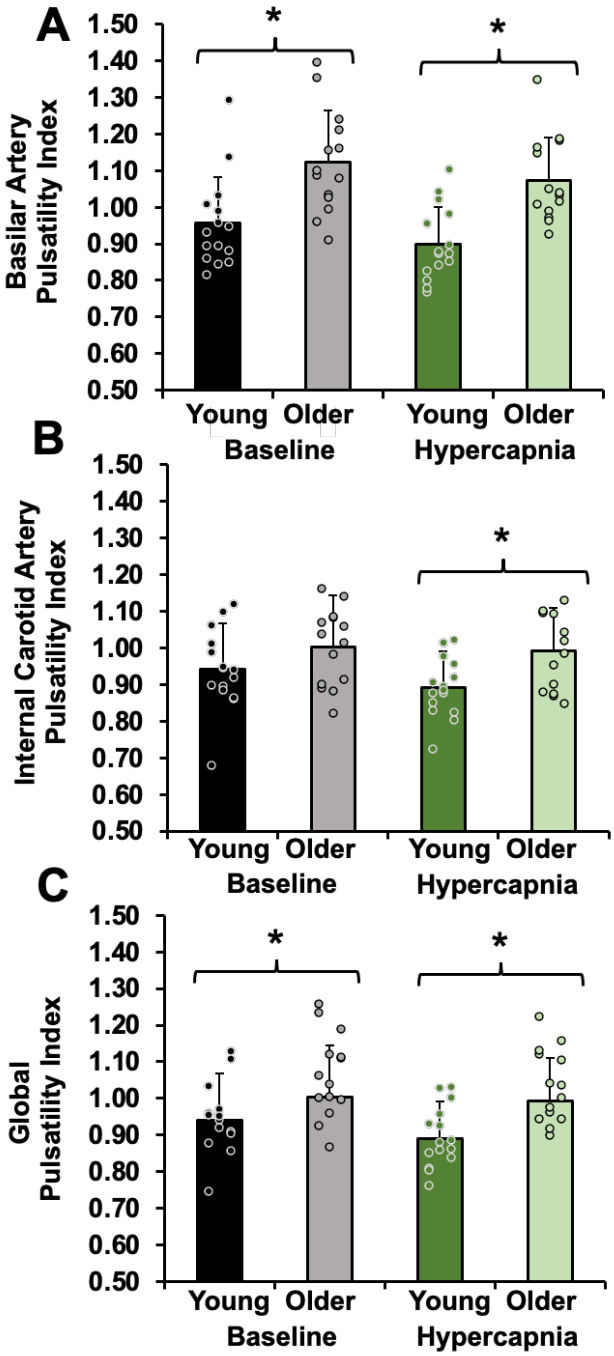

Figure 27. Pulsatility index measures in No VAH

Data are mean ± standard deviation and individual data points. This figure shows pulsatility index in the large intracranial arteries at baseline (black & grey) and during hypercapnia (green) in adults without vertebral artery hypoplasia (No VAH). A) Basilar artery (BA) pulsatility index, B) Internal carotid artery (ICA) pulsatility index C) global pulsatility index (average of ICAs and BA). *$p<0.05$ compared with young.

Participant Characteristics –VAH+

Participant characteristics of adults with VAH are shown in Table 24. In the VAH+ group, there were no age group differences in height, weight, body mass index or heart rate at rest. There were also no age group differences in systolic, diastolic, and mean arterial blood pressure. Table 25 shows the central arterial stiffness measures in the VAH+ group. There were no differences between age groups in carotid-femoral PWV or aortic augmentation index. However, older adults had a greater carotid IMT compared with young adults. Table 26 shows brain volumes in the VAH+ group. There were no age group differences in grey matter, white matter, or total brain volume. There were also no age group differences in intracranial volume. However, older adults had smaller brain volumes adjusted for intracranial volumes compared with young adults.

Hemodynamic Measurements –VAH+

Hemodynamic and cardiorespiratory measurements from the VAH+ group are shown in Table 27. $ETCO_2$ increased from baseline to 6% CO_2 in both young and older adults. Although older adults had lower $ETCO_2$ at baseline compared with young adults, there were no significant differences between age groups in $ETCO_2$ at 6% CO_2. Delta $ETCO_2$ from baseline to 6% CO_2 was not statistically different between age groups (Young adults: Δ 3 $\pm$ 1 mmHg vs. Older adults: Δ 6 $\pm$ 5 mmHg, p=0.21). There were no differences between age groups or conditions in respiratory rate. Mean arterial pressure did not significantly change from baseline to 6% CO_2 in young adults. However, in older adults, mean arterial pressure increased from baseline to 6% CO_2. There were no differences in mean arterial pressure between age groups. Heart rate increased from baseline to 6% CO_2 in young adults. There was no change in heart rate from baseline to 6% CO_2 in older

adults. There were no differences between age groups in heart rate at either condition (baseline or 6% CO_2).

Individual Vessel Characteristics –VAH+

The characteristics of the basilar artery in the VAH+ group are shown in Table 28. There was no change in basilar artery diameter from baseline to 6% CO_2 in young or older adults. There were also no differences in basilar artery diameter between age groups at either condition. There was no change in basilar artery mean velocity from baseline to 6% CO_2 in young adults. However, mean velocity increased from baseline to 6% CO_2 in older adults. There were no age group differences in basilar artery mean velocity at either condition. There was no change in basilar artery max velocity from baseline to 6% CO_2 in young adults. However, max velocity increased from baseline to 6% CO_2 in older adults. There were no significant differences in basilar artery max velocity between young and older adults in either condition. Basilar artery blood flow expressed in mL/beat did not change from baseline to 6% CO_2 in either young or older adults. There were also no significant differences in basilar artery flow in mL/beat between young and older adults in either condition. Blood flow expressed in mL/min also did not change from baseline to 6% CO_2 in either young or older adults. There were also no significant differences in basilar artery flow in mL/min between young and older adults in either condition. Basilar artery cerebrovascular conductance increased from baseline to 6% CO_2 in young adults. There was no change in basilar artery cerebrovascular conductance from baseline to 6% CO_2 in older adults. There were no age group differences in basilar artery cerebrovascular conductance at baseline or 6% CO_2. Basilar artery pulsatility index did not change from baseline to 6% CO_2 in young or older adults. There were also no age group differences in basilar artery pulsatility index at either condition.

Ipsilateral ICA measurements are shown in Table 29. The ipsilateral side refers to the same side as the hypoplastic VA. There was no change in ipsilateral ICA diameter from baseline to 6% CO_2 in young or older adults. There were also no differences in ipsilateral ICA diameter between age groups at either condition. There was no change in ipsilateral ICA mean velocity from baseline to 6% CO_2 in young or older adults. Ipsilateral ICA mean velocity was lower in older adults compared with young adults at baseline. However, there were no age group differences in mean velocity at 6% CO_2. There was no change in ipsilateral ICA max velocity from baseline to 6% CO_2 in young or older adults. There were no significant differences in max velocity between young and older adults in either condition. Ipsilateral ICA blood flow expressed in mL/beat did not change from baseline to 6% CO_2 in young adults. However, ipsilateral ICA flow in mL/beat increased from baseline to 6% CO_2 in older adults. There were no significant differences in ipsilateral ICA flow in mL/beat between young and older adults in either condition. Ipsilateral ICA flow in mL/min increased from baseline to 6% CO_2 in young adults. There was no change in ipsilateral ICA flow in mL/min from baseline to 6% CO_2 in older adults. Age group differences at baseline and 6% CO_2 did not meet the threshold for significance. Ipsilateral ICA cerebrovascular conductance increased from baseline to 6% CO_2 in young adults. There was no change in ipsilateral ICA cerebrovascular conductance from baseline to 6% CO_2 in older adults. There were no age group differences in ipsilateral ICA cerebrovascular conductance at baseline. However, older adults demonstrated lower cerebrovascular conductance at 6% CO_2 compared with young adults. Ipsilateral ICA pulsatility index did not change from baseline to 6% CO_2 in young or older adults. There were also no age group differences in ipsilateral ICA pulsatility index at either condition (baseline or 6% CO_2).

Contralateral ICA measurements are shown in Table 30. The contralateral side refers to the opposite side as the hypoplastic VA. There was no change in contralateral ICA diameter from baseline to 6% CO_2 in young or older adults. There were also no differences in contralateral ICA diameter between age groups at either condition. There was no change in contralateral ICA mean velocity from baseline to 6% CO_2 in young or older adults. Age group differences in mean velocity at baseline did not reach significance. There were no age group differences in contralateral ICA mean velocity at 6% CO_2. There was no change in contralateral ICA max velocity from baseline to 6% CO_2 in young adults. Max velocity increased from baseline to 6% CO_2 in older adults. There were no significant differences in contralateral ICA max velocity between young and older adults in either condition. Contralateral ICA blood flow expressed in mL/beat did not change from baseline to 6% CO_2 in young or older adults. There were also no significant differences in contralateral ICA flow in mL/beat between young and older adults in either condition. Contralateral ICA blood flow expressed in mL/min increased from baseline to 6% CO_2 in young adults. There was no change in flow in mL/min from baseline to 6% CO_2 in older adults. Age group differences in contralateral ICA flow in mL/min at baseline and 6% CO_2 did not meet the threshold for significance. Contralateral ICA cerebrovascular conductance increased from baseline to 6% CO_2 in young adults. There was no change in contralateral ICA cerebrovascular conductance from baseline to 6% CO_2 in older adults. Age group differences in cerebrovascular conductance at baseline did not reach significance. However, older adults demonstrated lower contralateral ICA cerebrovascular conductance at 6% CO_2 compared with young adults. Contralateral ICA pulsatility index did not change from baseline to 6% CO_2 in young or older adults. There were also no age group differences in contralateral ICA pulsatility index at either condition (baseline or 6% CO_2).

Global Cerebral Blood Flow Characteristics – VAH+

Global cerebral blood flow measurements in adults with VAH are shown in Table 31. Global cerebral blood flow increased from baseline to 6% CO_2 in young adults. There was no change in global cerebral blood flow from baseline to 6% CO_2 in older adults. Older adults demonstrated lower global cerebral blood flow at baseline and 6% CO_2. When adjusted for brain volume, global cerebral blood flow increased from baseline to 6% CO_2 in young adults but not in older adults. Age group differences in global cerebral blood flow adjusted for brain volume did not reach significance at both conditions. Global cerebrovascular conductance increased from baseline to 6% CO_2 in young adults. There was no significant change in global cerebrovascular conductance from baseline to 6% CO_2 in older adults. Older adults demonstrated lower cerebrovascular conductance at both conditions (baseline and 6% CO_2). Global pulsatility index did not change from baseline to 6% CO_2 in young or older adults. There were also no age group differences in pulsatility index at either condition.

Summary of Anterior, Posterior and Global Flow Characteristics –VAH+

Global blood flow and blood flow through the large intracranial arteries are shown in Figure 28. There were no significant differences between age groups in basilar flow at baseline (p=0.32, ANOVA on ranks p=0.55, hedges' g=0.67) or during hypercapnia (p=0.32, ANOVA on ranks p=0.42, hedges' g=0.67). Internal carotid artery flow was lower in older adults with VAH compared with young adults with VAH both at baseline (p=0.01, ANOVA on ranks p=0.03, hedges' g=2.10) and during hypercapnia (p=0.01, ANOVA on ranks p=0.01, hedges' g=2.04). Global cerebral blood flow was also lower in older adults with VAH compared with young adults

with VAH at baseline (p=0.01, ANOVA on ranks p=0.02, hedges' g=2.23) and during hypercapnia (p=0.02, ANOVA on ranks p=0.01, hedges' g=1.96).

Cerebrovascular conductance of the large intracranial arteries is shown in Figure 29. There were no age-related differences in basilar artery conductance at baseline (p=0.38, ANOVA on ranks p=0.42, hedges' g=0.59) or during hypercapnia (p=0.28, ANOVA on ranks p=0.31, hedges' g=0.74). ICA conductance was lower in older adults with VAH compared with young adults with VAH at baseline (p=0.01, ANOVA on ranks p=0.02, hedge's g=2.37) and during hypercapnia (p=0.003, ANOVA on ranks p=0.01, hedges' g=2.69). Global cerebrovascular conductance was also lower in older adults with VAH compared with young adults with VAH at baseline (p=0.01, ANOVA on ranks p=0.03, hedges' g=2.25) and during hypercapnia (p=0.01, ANOVA on ranks p=0.03, hedges' g=2.33).

Pulsatility index of the large intracranial arteries is shown in Figure 30. There were no age-related differences in the pulsatility index of the basilar artery at baseline (p=0.93, ANOVA on ranks p=0.69, hedges' g=0.06) or during hypercapnia (p=0.47, ANOVA on ranks p=0.55, hedges' g=0.49). There were no age group differences in the ICA pulsatility at baseline (p=0.21, ANOVA on ranks p=0.31, hedges' g=0.86). However, during hypercapnia, older adults had higher ICA pulsatility index compared with young adults (p=0.04, ANOVA on ranks p=0.03, hedges' g=1.55). There were no significant differences between age groups in global pulsatility at baseline (p=0.49, ANOVA on ranks p=0.69, hedges' g=0.46) or during hypercapnia (p=0.07, ANOVA on ranks p=0.10, hedges' g=1.32).

Table 24. Characteristics of participants in VAH+

Variable	*Young VAH+ N = 5*	*Older VAH+ N = 5*	*P-value*
Men / Women	0 / 5	1 / 4	
Age (years)	24 ± 4	61 ± 6	<0.001
Height (cm)	166 ± 9	170 ± 12	0.50
Weight (kg)	62 ± 7	65 ± 19	0.76
Body Mass Index (kg/m^2)	23 ± 1	22 ± 4	0.73
Heart Rate at Rest (beats per minute)	51 ± 7	56 ± 8	0.37
Systolic Blood Pressure (mmHg)	113 ± 9	116 ± 16	0.76
Diastolic Blood Pressure (mmHg)	68 ± 7	69 ± 11	0.90
Mean Arterial Pressure (mmHg)	83 ± 7	84 ± 13	0.89

Characteristics of participants with vertebral artery hypoplasia (VAH+). Data are mean ± standard deviation. VAH, vertebral artery hypoplasia. *P-value* in the column reflects the comparison between age groups.

Table 25. Central arterial stiffness in VAH+

Variable	*Young VAH+ N = 5*	*Older VAH+ N = 5*	*P-value*
Carotid-Femoral PWV (m/s)	6.2 ± 1.1	8.0 ± 2.6	0.22
Aortic Augmentation Index (%)	6.6 ± 10.4	16.6 ± 11.4	0.24
Carotid IMT (mm)	0.48 ± 0.06	0.63 ± 0.06	0.01

Central arterial stiffness of participants in the VAH+ group. Data are mean ± standard deviation. *P-value* in the column reflects the comparison between age groups. IMT, intima-media thickness. PWV, pulse wave velocity. For aortic augmentation index and PWV, n = 8. Aortic augmentation index was corrected for a heart rate of 75 beats per minute.

Table 26. Brain volumes in VAH+

Variable	*Young VAH+ N = 5*	*Older VAH+ N = 5*	*P-value*
Grey Matter Volume (L)	0.70 ± 0.06	0.61 ± 0.08	0.09
White Matter Volume (L)	0.42 ± 0.05	0.43 ± 0.07	0.75
Brain Volume (L)	1.12 ± 0.11	1.04 ± 0.15	0.38
Intracranial Volume (L)	1.33 ± 0.10	1.40 ± 0.15	0.40
Brain Volume / Intracranial Volume (L)	0.84 ± 0.04	0.74 ± 0.03	0.003

Brain volumes of participants in the VAH+ group. Data are mean ± standard deviation. *P-value* in the column reflects the comparison between age groups.

Table 27. Hemodynamic measurements in VAH+

Variable	*Young VAH+ N = 5*	*Older VAH+ N = 5*	*P-value*
$ETCO_2$ (mmHg)			
Baseline	39 ± 3	35 ± 3	0.01
6% CO_2	41 ± 4	41 ± 5*	0.99
Respiratory Rate (breaths per minute)			
Baseline	15 ± 5	13 ± 6	0.30
6% CO_2	15 ± 5	14 ± 5	0.50
Mean Arterial Pressure (mmHg)			
Baseline	94 ± 9	94 ± 15	0.97
6% CO_2	94 ± 7	98 ± 16*	0.60
Heart Rate (bpm)			
Baseline	52 ± 4	53 ± 7	0.71
6% CO_2	57 ± 7*	54 ± 6	0.54

Hemodynamic and cardiorespiratory measurements in adults with vertebral artery hypoplasia (VAH+). Data are mean ± standard deviation. $ETCO_2$, end-tidal carbon dioxide. *P-value* in the column reflects the comparison between age groups. *$p<0.05$ compared with baseline.

Table 28. Basilar artery measurements in VAH+

Variable	*Young VAH+ N = 5*	*Older VAH+ N = 5*	*P-value*
Diameter (cm)			
Baseline	0.307 ± 0.022	0.317 ± 0.024	0.49
6% CO_2	0.310 ± 0.024	0.312 ± 0.015	0.91
Mean Velocity (cm/s)			
Baseline	30 ± 3	25 ± 5	0.09
6% CO_2	30 ± 3	28 ± 6*	0.42
Max Velocity (cm/s)			
Baseline	66 ± 4	57 ± 10	0.14
6% CO_2	65 ± 3	64 ± 11*	0.80
Flow (mL/beat)			
Baseline	2.2 ± 0.4	2.0 ± 0.6	0.47
6% CO_2	2.3 ± 0.4	2.1 ± 0.6	0.62
Flow (mL/min)			
Baseline	117 ± 23	104 ± 16	0.39
6% CO_2	131 ± 30	113 ± 22	0.26
Cerebrovascular Conductance (mL/min/mmHg)			
Baseline	126 ± 32	112 ± 16	0.43
6% CO_2	140 ± 36*	117 ± 27	0.23
Pulsatility Index			
Baseline	0.98 ± 0.07	0.99 ± 0.17	0.93
6% CO_2	0.96 ± 0.11	1.00 ± 0.06	0.55

Basilar artery measurements in adults with vertebral artery hypoplasia (VAH+). Data are mean ± standard deviation. *P-value* in the column reflects the comparison between age groups. *p<0.05 compared with baseline.

Table 29. Ipsilateral internal carotid artery measurements in VAH+

Variable	*Young VAH+ N = 5*	*Older VAH+ N = 5*	*P-value*
Diameter (cm)			
Baseline	0.437 ± 0.025	0.430 ± 0.046	0.77
6% CO_2	0.444 ± 0.026	0.434 ± 0.043	0.67
Mean Velocity (cm/s)			
Baseline	28 ± 2	21 ± 6	0.04
6% CO_2	28 ± 1	23 ± 7	0.12
Max Velocity (cm/s)			
Baseline	62 ± 4	52 ± 11	0.09
6% CO_2	61 ± 3	56 ± 11	0.29
Flow (mL/beat)			
Baseline	4.2 ± 0.5	3.1 ± 1.1	0.07
6% CO_2	4.4 ± 0.5	3.4 ± 1.2*	0.12
Flow (mL/min)			
Baseline	221 ± 38	162 ± 52	0.08
6% CO_2	248 ± 45*	181 ± 52	0.05
Cerebrovascular Conductance (mL/min/mmHg)			
Baseline	239 ± 56	172 ± 44	0.07
6% CO_2	267 ± 60*	183 ± 42	0.03
Pulsatility Index			
Baseline	0.89 ± 0.09	0.99 ± 0.11	0.11
6% CO_2	0.87 ± 0.06	0.97 ± 0.09	0.14

Ipsilateral internal carotid artery measurements in adults with vertebral artery hypoplasia (VAH+). The vessel is on the ipsilateral side as the hypoplastic vertebral artery. Data are mean ± standard deviation. *P-value* in the column reflects the comparison between age groups. *$p<0.05$ compared with baseline.

Table 30. Contralateral internal carotid artery measurements in VAH+

Variable	*Young VAH+ N =5*	*Older VAH+ N = 5*	*P-value*
Diameter (cm)			
Baseline	0.424 ± 0.047	0.412 ± 0.019	0.61
6% CO_2	0.426 ± 0.049	0.419 ± 0.015	0.78
Mean Velocity (cm/s)			
Baseline	27 ± 4	22 ± 4	0.05
6% CO_2	28 ± 3	23 ± 5	0.11
Max Velocity (cm/s)			
Baseline	60 ± 6	52 ± 8	0.10
6% CO_2	61 ± 5	55 ± 9*	0.29
Flow (mL/beat)			
Baseline	3.9 ± 1.2	2.8 ± 0.4	0.10
6% CO_2	4.0 ± 1.2	3.2 ± 0.7	0.18
Flow (mL/min)			
Baseline	200 ± 46	150 ± 24	0.09
6% CO_2	224 ± 55*	170 ± 37	0.07
Cerebrovascular Conductance (mL/min/mmHg)			
Baseline	213 ± 42	161 ± 21	0.07
6% CO_2	237 ± 48*	175 ± 40	0.03
Pulsatility Index			
Baseline	0.89 ± 0.13	0.98 ± 0.10	0.23
6% CO_2	0.87 ± 0.11	0.98 ± 0.04	0.11

Contralateral internal carotid artery measurements in adults with vertebral artery hypoplasia (VAH+). The vessel is on the contralateral side from the hypoplastic vertebral artery. Data are mean ± standard deviation. *P-value* in the column reflects the comparison between age groups. *$p<0.05$ compared with baseline.

Table 31. Global cerebral blood flow measurements in VAH+

Variable	*Young VAH+ N = 5*	*Older VAH+ N = 5*	*P-value*
Global Flow (mL/min)			
Baseline	538 ± 35	416 ± 69	0.01
6% CO_2	603 ± 65*	464 ± 76	0.005
Global Flow / Brain Volume (mL/min/L)			
Baseline	638 ± 23	557 ± 76	0.10
6% CO_2	715 ± 63*	624 ± 101	0.07
Global Cerebrovascular Conductance (mL/min/mmHg)			
Baseline	578 ± 74	445 ± 40	0.01
6% CO_2	644 ± 81*	474 ± 64	0.002
Global Pulsatility Index			
Baseline	0.92 ± 0.09	0.99 ± 0.12	0.25
6% CO_2	0.90 ± 0.06	0.98 ± 0.05	0.15

Global cerebral blood flow measurements in adults with vertebral artery hypoplasia (VAH+). Data are mean ± standard deviation. *P-value* in the column reflects the comparison between age groups. *$p<0.05$ compared with baseline.

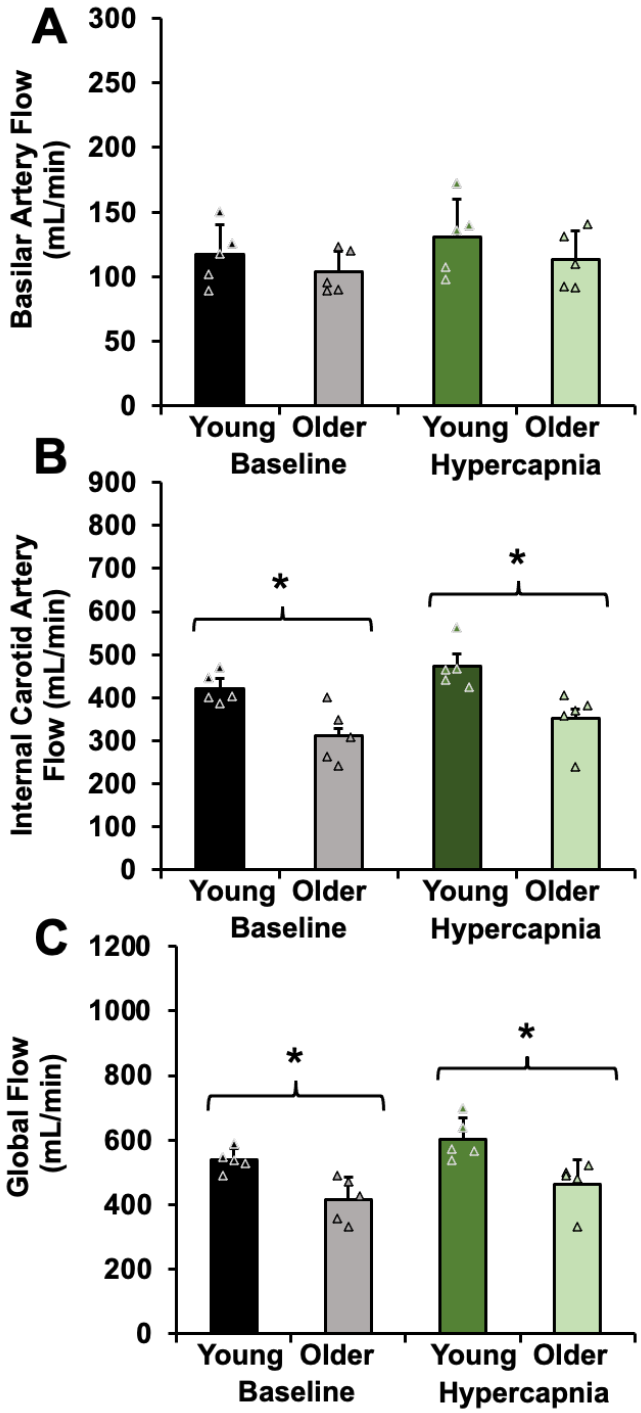

Figure 28. Flow measurements in VAH+

Data are mean ± standard deviation and individual data points. This figure shows flow in the large intracranial arteries at baseline (black & grey) and during hypercapnia (green) in adults with vertebral artery hypoplasia (VAH+). A) Basilar artery (BA) flow, B) Internal carotid artery (ICA) flow C) global flow (sum of ICAs and BA). *$p<0.05$ compared with young.

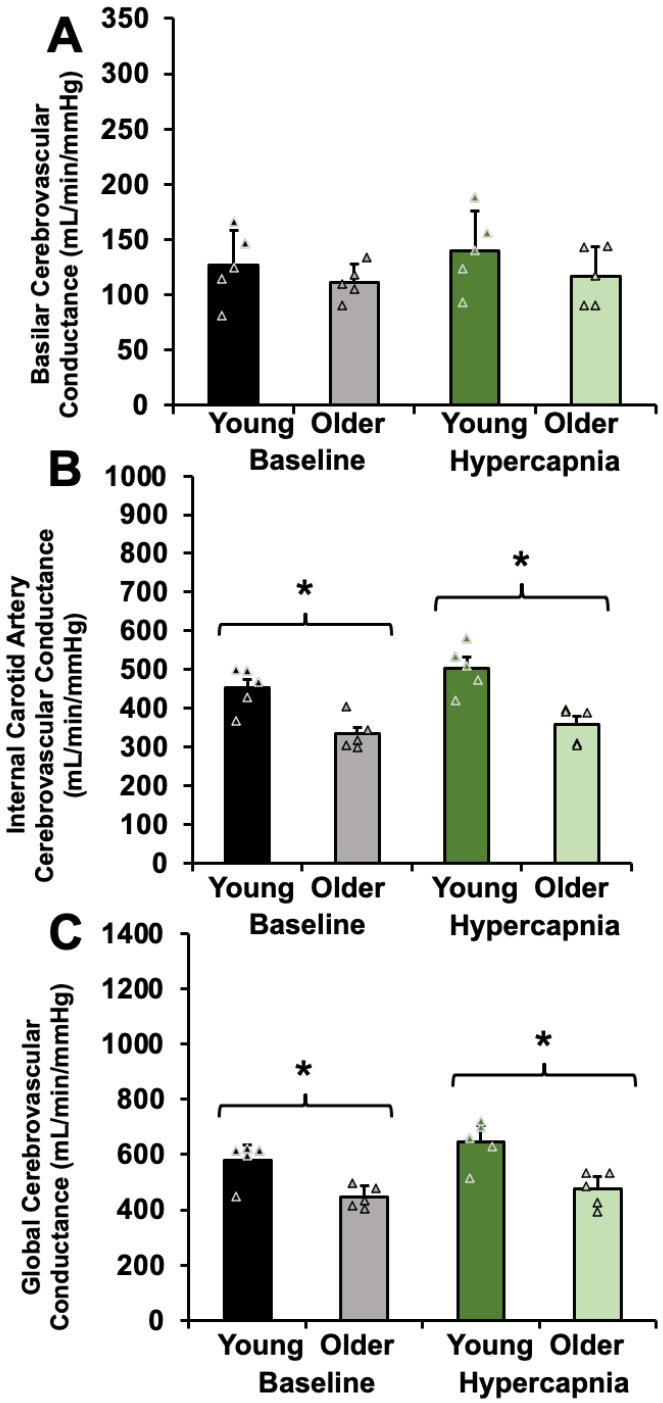

Figure 29. Conductance measurements in VAH+

Data are mean ± standard deviation and individual data points. This figure shows conductance in the large intracranial arteries at baseline (black & grey) and during hypercapnia (green) in adults with vertebral artery hypoplasia (VAH+). A) Basilar artery (BA) conductance, B) Internal carotid artery (ICA) conductance C) global conductance (sum of ICAs and BA). *$p<0.05$ compared with young.

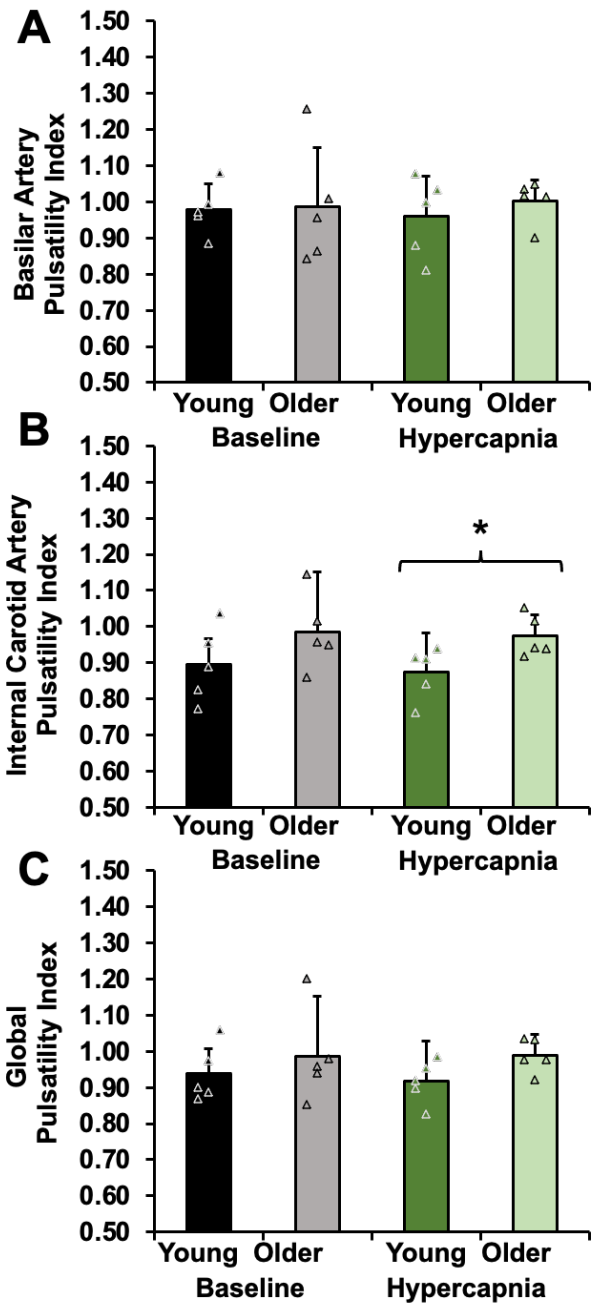

Figure 30. Pulsatility index measurements in VAH+

Data are mean ± standard deviation and individual data points. This figure shows pulsatility index in the large intracranial arteries at baseline (black & grey) and during hypercapnia (green) in adults with vertebral artery hypoplasia (VAH+). A) Basilar artery (BA) pulsatility index, B) Internal carotid artery (ICA) pulsatility index C) global pulsatility index (average of ICAs and BA). *$p<0.05$ compared with young.

Summary of Study 2 Results

This study addressed **Specific Aim 2**: to determine the impact of VAH on the age-related differences in regional blood flow in the large intracranial arteries. In the retrospective analysis of 39 adults, there were 10 who met criteria for vertebral artery hypoplasia (26% prevalence). This was similar to previous reported values of 15-35%. The first hypothesis of Specific Aim 2 was: In healthy adults without VAH, age-related differences in CBF will be greater in posterior vessels compared with anterior vessels at rest and during hypercapnia. The results from Study 2 support this hypothesis. The older adults without VAH demonstrated approximately 20% lower BA blood flow at rest and 25% lower BA blood flow during hypercapnia compared with young adults with VAH, which was not apparent in the ICAs. The second hypothesis of Specific Aim 2 was: In healthy adults with VAH, age-related differences in CBF will be greater in anterior vessels compared with posterior vessels at rest and during hypercapnia. The results from Study 2 support this hypothesis. Older adults with VAH demonstrated approximately 26% lower ICA blood flow at baseline and 29% lower ICA blood flow during hypercapnia but similar BA blood flow values compared with young adults with VAH. The exploratory hypothesis of Specific Aim 2 was: Older adults will demonstrate higher cerebral pulsatility index in the large intracranial anterior and posterior vessels compared with young adults in both groups with and without VAH. This hypothesis was partially supported, as there were some age-related differences in pulsatility index, but these were regionally specific and depended on the presence or absence of hypercapnia. In summary, participants with VAH show age-related differences in blood flow in the anterior circulation and in the whole brain. Therefore, the presence of VAH impacts the pattern of regional age-related differences in cerebral blood flow.

CHAPTER 4

4. STUDY 3: IMPACT OF VERTEBRAL ARTERY HYPOPLASIA ON CEREBRAL HEMODYNAMICS IN COGNITIVELY UNIMPAIRED ADULTS WITH ENRICHED RISK FOR ALZHEIMER'S DISEASE

4.1 INTRODUCTION

Cerebral anatomical variations are common, with over 50% of the population demonstrating a variation of the Circle of Willis (Alpers et al., 1959). Vertebral artery hypoplasia (VAH) is an anatomical variation in the posterior circulation where one of the vertebral arteries is narrowed and accompanied with reduced blood flow. VAH has a prevalence of 15-35% (Kulyk et al., 2018; Ogeng'o et al., 2014; Park et al., 2007; Peterson et al., 2010; Thierfelder et al., 2014) . Despite the relatively high prevalence of VAH and its known increase in risk of posterior stroke (Chuang et al., 2006; Kulyk et al., 2018; Mitsumura et al., 2016; Park et al., 2007; Zhang et al., 2016) little is known on its effects on blood flow regulation in non-stroke populations. In addition, the impact of VAH on cognitive function is unknown.

A recent study of adults with VAH reported they had reduced global cerebral blood flow compared with adults with normal posterior cerebral anatomy (Warnert et al., 2016). This suggests that individuals with VAH may experience chronic cerebral hypoperfusion. Importantly, reduced cerebral blood flow has been implicated in the context of cognitive decline (Wolters et al., 2017). Reductions in cerebral blood flow may precede the onset of cognitive impairment, and interact in a synergistic manner with existing neurogenic pathology (Iadecola, 2004; Kisler et al., 2017; Santisteban and Iadecola, 2018). Furthermore, increased pulsatility index in the large intracranial vessels have been associated with worsening progression through the Alzheimer's disease continuum (Rivera-Rivera et al., 2016) and may reflect increased distal vascular resistance (Giller et al., 1990).

The purpose of this study is twofold. The first objective is to determine the prevalence of VAH in a large, non-stroke cohort. This is important for future studies to examine the impact of VAH, independent of stroke, on blood flow characteristics and cognitive function. The second

objective is to determine the impact of VAH on cerebral blood flow and cerebral pulsatility index in the large intracranial arteries. This study addresses **Specific Aim 3** of this dissertation: to determine the impact of VAH on resting cerebral hemodynamics in a cohort of cognitively unimpaired adults with enriched risk for Alzheimer's disease. It is hypothesized that the prevalence of VAH will be similar to previously reported values (15-35%). The second hypothesis is that adults with VAH will have lower global CBF and lower blood flow in the large intracranial arteries compared with controls without VAH. The third hypothesis is that adults with VAH will have higher global cerebral pulsatility index and higher pulsatility in the major intracranial arteries compared with controls without VAH.

4.2 MATERIALS AND METHODS

Participant Recruitment

Participants in this study were recruited from existing cohorts of cognitively healthy adults enrolled in the Alzheimer's Disease Research Center (ADRC) Clinical Core who participated in an ancillary study in our laboratory: Brain Blood Flow in Middle-Aged Adults at Risk of Alzheimer's Disease. Exclusion for the ADRC Clinical Core included any significant neurologic disease (other than AD dementia), history of alcohol/substance dependence, major psychiatric disorders (including untreated major depression), or other significant medical illness, severe untreated obstructive sleep apnea, history of HIV/AIDs, severe kidney dysfunction requiring hemodialysis, severe congestive heart failure, and history of clinically significant ischemic or hemorrhagic stroke or significant cerebrovascular disease at discretion of investigators (Johnson et al., 2017). Additional exclusion criteria for the Brain Blood Flow in Middle-Aged Adults at Risk of Alzheimer's Disease study included age <55 or >69 years, diagnosis of mild cognitive impairment or AD (as determined by a consensus a panel of physicians and neuropsychologists at the Wisconsin ADRC), uncontrolled hypertension, uncontrolled diabetes, history or evidence of hepatic, renal, hematological, or peripheral vascular disease, significant surgical history and any counterindication to doing an MRI scan such as a metallic implanted device.

For the present study, participants were 1) previously enrolled in the Brain Blood Flow in Middle-Aged Adults at Risk of Alzheimer's Disease study and 2) had completed a 4D flow MRI scan. All participants included in this study were cognitively unimpaired at the time of study. Therefore, this study consisted of a retrospective analysis of approximately 95 participants aged 55 to 69 years old. Study procedures of the Wisconsin Alzheimer's Disease Research Center Clinical Core were approved by the Institutional Review Board of the University of Wisconsin–

Madison (IRB: 2015-0030) and were performed according to the Declaration of Helsinki, including obtaining written informed consent from each participant. All study procedures of the ancillary study Brain Blood Flow in Middle-Aged Adults at Risk of Alzheimer's Disease were approved by the Institutional Review Board of the University of Wisconsin-Madison (IRB: 2017-0441) and were performed according to the Declaration of Helsinki, including obtaining written informed consent from each participant. The retrospective analysis of the MRI scans in the present study was determined exempt from full IRB review (IRB: 2020-0108) due to the nature of the project being secondary research for which additional consent is not required.

Participant Characteristics

Participant characteristics including cognitive status, years of education, health history, parental history of AD and APOE genotype were collected as part of assessments by the Wisconsin Alzheimer's Disease Research Center (ADRC) Clinical Core. Parental history of AD was considered positive if a biological parent had probable or definite AD. Parental history of AD was considered negative if the biological mother lived to at least 75 years and father at least 70 years without symptoms of dementia. APOE ε4 genotyping was done as previously described (Johnson et al., 2011). In the covariate analysis, participants were categorized as ε4 non-carriers (zero ε4 alleles) or ε4 carriers (one or two ε4 alleles, APOE4+).

Cardiovascular Measurements

On a separate study visit from the MRI scan, carotid–femoral pulse wave velocity (PWV) and aortic augmentation index (AIx) measurements were completed utilizing arterial tonometry. After 10 minutes of supine rest, high-fidelity pressure waveforms were recorded for at least 10 heart beats non-invasively using a pencil-type Millar Micro-tip pressure transducer from the radial,

femoral and carotid arteries (Sphygmocor, AtcorMedical, Sydney, NSW, Australia). An average of 3–5 trials of each PWV and AIx were obtained in succession. Tonometry transit distance from the carotid pulse site, the supra-sternal notch, and the femoral pulse site were measured with a tape measure. PWV was calculated using the intersection tangent foot-to-foot algorithm. An aortic pressure waveform was derived from the radial pulse using the application of a generalized transfer function to measure AIx. AIx was then corrected at a heart rate (HR) of 75 beats per minute.

MRI Imaging

MRI imaging consisted of brain volume measurements and measurements of cerebral blood flow at rest. MR imaging was performed with a 3T clinical MRI scanner (MR750, GE Healthcare, Waukesha, WI, United States) at the Wisconsin Institutes for Medical Research in Madison, WI. Participants were supine and imaged with a 32-channel head coil (Nova Medical Head Coil, Nova Medical, Wilmington, MA, United States) with a gradient strength of 50 mT/m, and a gradient slew rate of 200 mT/m/ms. Throughout the MRI session, HR, and oxygen saturation (SPO_2) were acquired continuously using a pulse oximeter. The pulse oximeter was connected to an MRI compatible monitor (Medrad Veris MR Vital Signs Patient Monitor, Bayer Healthcare, Whippany, NJ, United States).

To determine brain volumes, a T1-weighted structural brain volume (BRAVO) scan was acquired with the following scan parameters: fast spoiled gradient echo sequence, inversion time = 450 ms, repetition time (TR) = 8.1 ms, echo time (TE) = 3.2 ms, flip angle = 12°, acquisition matrix = 256 × 256, field of view (FOV) = 256 mm, slice thickness = 1.0 mm, and scan time ∼8 min.

4D flow MRI data was acquired using a 3D radially under sampled sequence to provide high spatial and temporal resolution. No contrast agent was administered. The scan parameters were as follows: velocity encoding (Venc) = 80 cm/s, FOV = 220 mm, acquired isotropic spatial resolution = 0.7 mm × 0.7 mm × 0.7 mm, TR = 7.8 ms, TE = 2.7 ms, flip angle = 8°, bandwidth = 83.3 kHz, 14,000 projection angles and scan time ∼7 min. The imaging volume covered the right and left ICA, VAs, and BA. Data was acquired continuously, such that a HR of 60 beats/min would provide a sampling of approximately 128 times per heartbeat. Time-resolved velocity and magnitude data was reconstructed offline by retrospectively gating into 20 cardiac phases using temporal interpolation.

Data Analysis

MRI scans were analyzed similar to Study 1 and Study 2. Total brain volume was derived from the T1-weighted scans. Scans were segmented in Statistical Parametric Mapping version 12 (SMP12) into gray matter (GM), white matter (WM), and cerebral spinal fluid (CSF). Total brain volume was calculated as the sum of GM and WM volume. Intracranial volume was calculated as the sum of GM, WM, and CSF. Brain volume was also reported as brain volume divided by intracranial volume (ICV). 4D flow MRI scans were also analyzed as described in Study 1 & 2. Briefly, scans underwent automatic phase unwrapping, eddy current correction and background phase offset corrections. Segmentation was performed offline using an inhouse tool in Matlab and the large intracranial vessels including the ICAs, BAs and VAs were segmented. Blood flow was averaged along the length of each vessel. Global blood flow was calculated as the sum of the right and left ICAs and the BA. Global cerebral blood flow was also reported as global cerebral blood flow divided by intracranial volume. Pulsatility index was calculated as (maximum flow –

minimum flow) / mean flow. Global pulsatility index was the average pulsatility index of the ICAs and BA.

Determination of VAH

VAH was retrospectively identified from a 4D flow phase contrast MRI scans using both structural and flow criteria, as described in Study 2. Briefly, VAH was considered a vessel diameter less than or equal to 3.0 mm. This is greater than the cut off from the study in chapter 3 (2.0 mm) because there was no time-of-flight scan to measure vessel diameter and the 4D flow MRI scans have slightly greater vessel diameter measurements. Flow in the hypoplastic vessel was less than or equal to 50 mL/min, and there was a flow asymmetry ratio of 2.0. VAH was unilateral, i.e., only one vessel is hypoplastic. There were two exceptions to the asymmetry ratio, where the participants met the vessel size and flow criteria, and their flow asymmetry ratio was 1.8.

Statistical Analysis

Estimates for a required sample size was calculated using G*Power 3.1.9.4. (Faul et al., 2007). In a previous study by Warnert et al., 2016 blood flow through the basilar artery was statistically different between individuals with VAH (n=39) and individuals without VAH (n=36) (10.4 ± 0.9 ml/100g/min vs. 13.4 ± 0.9 ml/100g/min, respectively, p=0.002) (Warnert et al., 2016). A post-hoc analysis of this effect size was f =1.665 with alpha = 0.05 and power (1-beta) = 0.99. To achieve a power of 0.80 or 80% at an effect size of f = 1.665 and alpha = 0.05, G*Power estimated that the necessary total sample size was 6 individuals per group (Appendix 1). Based on previous studies suggesting that the prevalence of VAH is between 15-35%, it is hypothesized a range of 14-33 participants with VAH will be identified. Statistical testing, except for the sample size

estimate, was completed using Sigma Plot for Windows version 13.0 (Systat Software, San Jose, CA, United States). Prior to all analyses, normality and equal variance was assessed using the Shapiro-Wilk test and Brown-Forsythe test respectively. Non-parametric statistical testing such as Kruskal-Wallis ANOVA on Ranks followed by the Dunn's Method to test pairwise multiple comparisons was employed if necessary. Prevalence of VAH was calculated as the number of subjects with VAH divided by the number of total subjects. This analysis addresses hypothesis 1: the prevalence of VAH in this cohort will be comparable to previously reported values (15-35%). Characteristics of subjects with and without VAH was compared using an unpaired, two-tailed t-test or a Chi-squared test. Blood flow characteristics including global cerebral blood flow, blood flow in the large intracranial vessels (ICAs, BA, VAs), and pulsatility index was compared between VAH and non-VAH groups using a one-way ANOVA or equivalent non-parametric test if necessary. Effect sizes comparing blood flow variables between adults with and without VAH were calculated using Hedges' g. This analysis addresses hypothesis 2: adults with VAH will have reduced global CBF and reduced blood flow in the major intracranial arteries compared with controls without VAH and hypothesis 3: adults with VAH will have higher global pulsatility index and higher cerebral pulsatility in the major intracranial arteries compared with controls without VAH. In order to control for confounding effects of vascular and Alzheimer's disease risk factors on global cerebral blood flow, multivariable linear regression analysis was employed. Categorical factors of presence of VAH, treatment for hypertension, treatment for hypercholesterolemia, presence of APOE4 genotype and parental history of Alzheimer's disease were coded as 1 = yes and 0 = no. Sex was coded as 1 = male and 0 = female. Age and brain volume / ICV were continuous variables. Four models were assessed including one model with age, sex, VAH, and brain volume / ICV, a second with age, sex, VAH, and Alzheimer's disease risk factors, a third

with age, sex, VAH, and vascular risk factors, and a fourth model with age, sex, VAH and both vascular and Alzheimer's disease risk factors. Statistical significance was set *a priori* at $p < 0.05$.

4.3 RESULTS

Identification of VAH

The characteristics of the vertebral arteries are displayed in Table 32. Data from seven participants was not usable due the inability to properly segment the vertebral arteries. Therefore, out of the 88 remaining data sets, VAH was identified in 24 participants (27% prevalence). Four different examples of participants with VAH are shown in Figure 31. The hypoplastic artery was most common on the right side (n=16). In the VAH+ group, the hypoplastic VA was smaller, had lower flow and lower conductance compared with the ipsilateral (right) VA in the No VAH group. The hypoplastic VA in the VAH+ group also had a greater pulsatility index compared with the ipsilateral (right) VA in the No VAH group. The contralateral VA in the VAH+ group was larger, had greater flow and greater conductance compared with the contralateral (left) VA in the No VAH group. Group differences in contralateral VA pulsatility index did not reach significance. The sum of the flow in the VAs was significantly lower in the VAH+ group compared with the No VAH group when flow was expressed in either mL/beat or mL/min. Furthermore, the cerebrovascular conductance in the sum of the VAs was lower in the VAH+ group compared with the No VAH group.

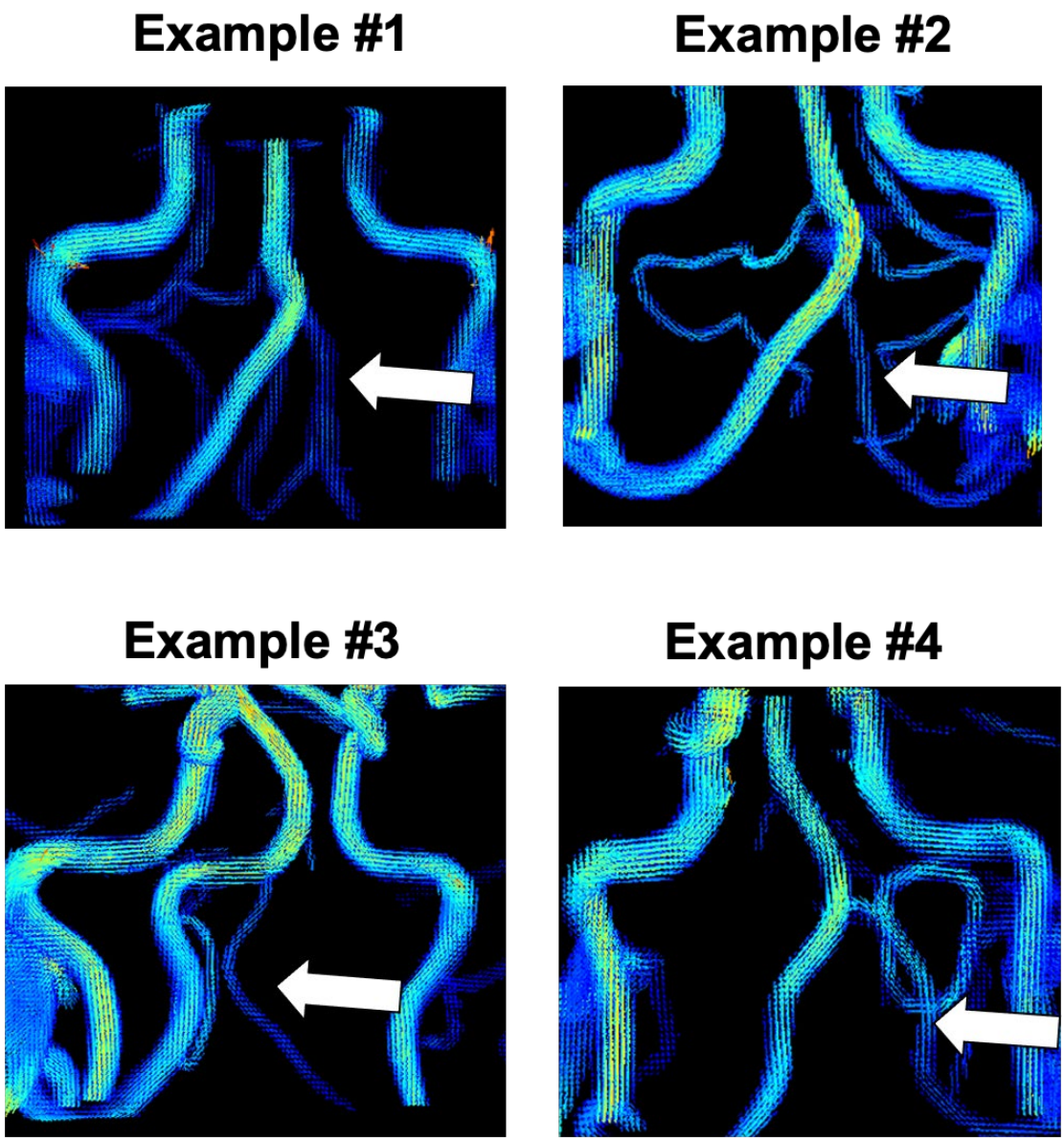

Figure 31. Examples of vertebral artery hypoplasia from 4D flow MRI

This figure shows four different examples of participants that had vertebral artery hypoplasia (VAH). The arrow is pointing at the hypoplastic vessel, which is on the right side in each of these cases. Warmer colors indicate higher blood velocity.

Table 32. Vertebral artery measurements from Study 3

Variable	*No VAH N = 64*	*VAH+ N = 24*	*P-value*
Ipsilateral VA Diameter (cm)	0.314 ± 0.030	0.259 ± 0.026	<0.001
Contralateral VA Diameter (cm)	0.326 ± 0.041	0.354 ± 0.040	0.007
Ipsilateral VA flow (mL/beat)	1.22 ± 0.34	0.54 ± 0.17	<0.001
Contralateral VA flow (mL/beat)	1.33 ± 0.47	1.64 ± 0.44	0.007
Sum of VAs flow (mL/beat)	2.5 ± 0.7	2.2 ± 0.5	0.02
Ipsilateral VA flow (mL/min)	77 ± 29	33 ± 11	<0.001
Contralateral VA flow (mL/min)	84 ± 38	99 ± 27	0.02
Sum of VAs flow (mL/min)	160 ± 60	131 ± 33	0.03
Ipsilateral VA Conductance (mL/min/mmHg)	85 ± 32	37 ± 12	<0.001
Contralateral VA Conductance (mL/min/mmHg)	93 ± 43	113 ± 33	0.01
Sum of VAs Conductance (mL/min/mmHg)	178 ± 67	150 ± 38	0.05
Ipsilateral VA Pulsatility Index	1.32 ± 0.20	1.75 ± 0.42	<0.001
Contralateral VA Pulsatility Index	1.34 ± 0.21	1.24 ± 0.15	0.052

Data are mean ± standard deviation. Vertebral artery (VA) measurements in adults without vertebral artery hypoplasia (No VAH) and with vertebral artery hypoplasia (VAH+). Ipsilateral measurements refer to the hypoplastic vessel, which was commonly on the right side (n=16). In the No VAH group, ipsilateral VA measurements are from the right VA and contralateral measurements are from the left VA. *P-value* in the column reflects the comparison between groups. 4D flow PC, 4D flow phase contrast MRI.

Participant Characteristics

Characteristics of participants are shown in Table 33. No VAH and VAH+ groups had similar ages, education years, height, weight, and BMI. There were no significant differences between groups in heart rate at rest, systolic, diastolic, or mean arterial blood pressure. There were also no significant differences in the prevalence of vascular risk factors including having diabetes or being treated for hypertension or hypercholesterolemia. There were no significant group differences in the prevalence of AD risk factors including parental history of Alzheimer's disease and APOE 3/4 or APOE 4/4 genotype. Table 34 shows the central arterial stiffness measurements. There were no differences between No VAH and VAH+ groups in carotid femoral PWV or aortic augmentation index. Brain volumes are shown in Table 35. Adults with VAH had lower grey matter volume, brain volume, and brain volume adjusted for intracranial volume compared with adults without VAH. Group differences in white matter volume did not reach significance. There were no differences in intracranial volume between groups.

Individual Vessel Characteristics

Characteristics of the basilar artery are shown in Table 36. There were no differences in basilar artery diameter, mean velocity or max velocity between No VAH and VAH+ groups. Group differences in flow measured as mL/beat or mL/min did not reach significance. There were also no differences in cerebrovascular conductance or pulsatility index.

Characteristics of the ipsilateral ICA are shown in Table 37. Ipsilateral ICA refers to the ICA on the same side as the hypoplastic VA. In the No VAH group, this is the right ICA. There were no group differences in ipsilateral ICA diameter. Group differences in mean velocity did not reach the threshold for significance. There were also no differences in max velocity, flow in

mL/beat, flow in mL/min, cerebrovascular conductance or pulsatility index between No VAH and VAH+ groups.

Characteristics of the contralateral ICA are shown in Table 38. Contralateral ICA refers to the ICA on the opposite side as the hypoplastic VA. In the No VAH group, this is the left ICA. There were no group differences in contralateral ICA diameter. The VAH+ group had slower mean velocity and max velocity compared with the No VAH group. The VAH+ also had lower flow in mL/beat and mL/min, as well as lower cerebrovascular conductance compared with the No VAH group. There were no group differences in pulsatility index.

Anterior, Posterior and Global Flow Characteristics

Anterior, poster and global cerebral blood flow in the large intracranial arteries are shown in Figure 32. There were no group differences in basilar flow (p=0.10 ANOVA on ranks, p=0.11 no outlier, hedges' g=0.42). However, VAH+ had lower ICA flow compared with No VAH (p=0.04 ANOVA on ranks, hedges' g=0.55). VAH+ also had lower global flow compared with No VAH (p=0.04 ANOVA on ranks, hedges' g=0.56).

Cerebrovascular conductance in the large intracranial arteries is shown in Figure 33. There was no significant difference in basilar conductance between groups (p=0.27, p=0.17 no outlier, hedges' g=0.37). Group differences in ICA conductance did not reach significance (p=0.07, hedges' g=0.43). Group differences in global conductance also did not reach significance (p=0.11, hedges' g=0.45).

Pulsatility index in the large intracranial arteries is shown in Figure 34. There were no group differences in basilar artery (p=0.47, hedges' g=0.16), ICA (p=0.98, hedges' g=0.08) or global (p=0.72, hedges' g=0.08) pulsatility index.

Table 33. Characteristics of participants from Study 3

Variable	*No VAH N = 64*	*VAH+ N = 24*	*P-value*
Men / Women	22 / 42	6 / 18	0.39
Age (years)	62 ± 4	63 ± 4	0.33
Education Years	17 ± 3	17 ± 2	0.82
Height (cm)	169 ± 9	168 ± 8	0.52
Weight (kg)	76 ± 15	77 ± 16	0.80
Body Mass Index (kg/m^2)	26 ± 4	27 ± 4	0.49
Heart Rate at Rest (beats per minute)	65 ± 9	63 ± 8	0.35
Systolic Blood Pressure (mmHg)	120 ± 14	115 ± 12	0.16
Diastolic Blood Pressure (mmHg)	76 ± 8	74 ± 7	0.43
Mean Arterial Pressure (mmHg)	91 ± 10	88 ± 8	0.25
Treatment for Hypertension	16%	21%	0.58
Menopausal Hormone Therapy †	17%	28%	0.21
Diabetes (Type I or Type II)	3%	0%	0.31
Treatment for Hypercholesterolemia	28%	33%	0.65
Parental History of AD	75%	66%	0.35
APOE 3/4	27%	29%	0.64
APOE 4/4	6%	0%	0.31

Characteristics of participants without (No VAH) and with (VAH+) vertebral artery hypoplasia. Data are mean ± standard deviation or percentage of participants. APOE 3/4, apolipoprotein E-3/4 genotype, APOE 4/4, apolipoprotein E-4/4 genotype, VAH, vertebral artery hypoplasia. For APOE results, n=80. *P-value* in the column reflects the comparison between groups. †percentage of women

Table 34. Central arterial stiffness of participants from Study 3

Variable	***No VAH N = 64***	***VAH+ N = 24***	***P-value***
Carotid-Femoral PWV (m/s)	8.5 ± 1.6	8.0 ± 1.5	0.16
Aortic Augmentation Index (%)	25.4 ± 8.7	24.8 ± 7.0	0.79

Central arterial stiffness of participants without (No VAH) and with (VAH+) vertebral artery hypoplasia. Data are mean ± standard deviation. *P-value* in the column reflects the comparison between age groups. PWV, pulse wave velocity. For PWV, n = 75. For aortic augmentation index, n = 84. Aortic augmentation index was corrected for a heart rate of 75 beats per minute.

Table 35. Brain volumes of participants from Study 3

Variable	*No VAH N = 64*	*VAH+ N = 24*	*P-value*
Grey Matter Volume (L)	0.68 ± 0.06	0.65 ± 0.06	0.03
White Matter Volume (L)	0.45 ± 0.05	0.43 ± 0.06	0.08
Brain Volume (L)	1.13 ± 0.10	1.08 ± 0.11	0.03
Intracranial Volume (L)	1.45 ± 0.13	1.41 ± 0.14	0.22
Brain Volume / Intracranial Volume (L)	0.78 ± 0.04	0.76 ± 0.04	0.04

Brain volumes of participants without (No VAH) and with (VAH+) vertebral artery hypoplasia. Data are mean ± standard deviation. *P-value* in the column reflects the comparison between groups.

Table 36. Basilar artery measurements

Variable	*No VAH N = 64*	*VAH+ N = 24*	*P-value*
Diameter (cm)	0.318 ± 0.029	0.309 ± 0.028	0.21
Mean Velocity (cm/s)	26 ± 6	25 ± 6	0.17
Max Velocity (cm/s)	66 ± 9	64 ± 9	0.54
Flow (mL/beat)	2.1 ± 0.6	1.9 ± 0.6	0.09
Flow (mL/min)	134 ± 55	113 ± 39	0.10
Cerebrovascular Conductance (mL/min/mmHg)	149 ± 61	129 ± 42	0.27
Pulsatility Index	1.17 ± 0.17	1.20 ± 0.17	0.47

Basilar artery measurements in adults without (No VAH) and with vertebral artery hypoplasia (VAH+). Data are mean ± standard deviation. *P-value* in the column reflects the comparison between groups.

Table 37. Ipsilateral or right internal carotid artery measurements

Variable	*No VAH N = 64*	*VAH+ N = 24*	*P-value*
Diameter (cm)	0.446 ± 0.033	0.444 ± 0.030	0.84
Mean Velocity (cm/s)	25 ± 4	23 ± 3	0.05
Max Velocity (cm/s)	63 ± 7	61 ± 6	0.17
Flow (mL/beat)	3.9 ± 0.8	3.6 ± 0.6	0.10
Flow (mL/min)	241 ± 60	219 ± 54	0.14
Cerebrovascular Conductance (mL/min/mmHg)	270 ± 75	249 ± 60	0.34
Pulsatility Index	1.07 ± 0.11	1.07 ± 0.11	0.75

Ipsilateral internal carotid artery measurements in adults without (No VAH) and with vertebral artery hypoplasia (VAH+). Data are mean ± standard deviation. The ipsilateral side refers to the same side as the hypoplastic vertebral artery. For the No VAH group, this is the right internal carotid artery. *P-value* in the column reflects the comparison between groups.

Table 38. Contralateral or left internal carotid artery measurements

Variable	*No VAH N = 64*	*VAH+ N = 24*	*P-value*
Diameter (cm)	0.447 ± 0.036	0.435 ± 0.034	0.18
Mean Velocity (cm/s)	25 ± 4	23 ± 4	0.03
Max Velocity (cm/s)	63 ± 7	59 ± 7	0.03
Flow (mL/beat)	3.9 ± 0.7	3.4 ± 0.8	0.007
Flow (mL/min)	240 ± 55	206 ± 55	0.01
Cerebrovascular Conductance (mL/min/mmHg)	268 ± 67	235 ± 62	0.04
Pulsatility Index	1.08 ± 0.11	1.06 ± 0.10	0.57

Contralateral internal carotid artery measurements in adults without (No VAH) and with vertebral artery hypoplasia (VAH+). Data are mean ± standard deviation. The contralateral side refers to the opposite side as the hypoplastic vertebral artery. For the No VAH group, this is the left internal carotid artery. *P-value* in the column reflects the comparison between groups.

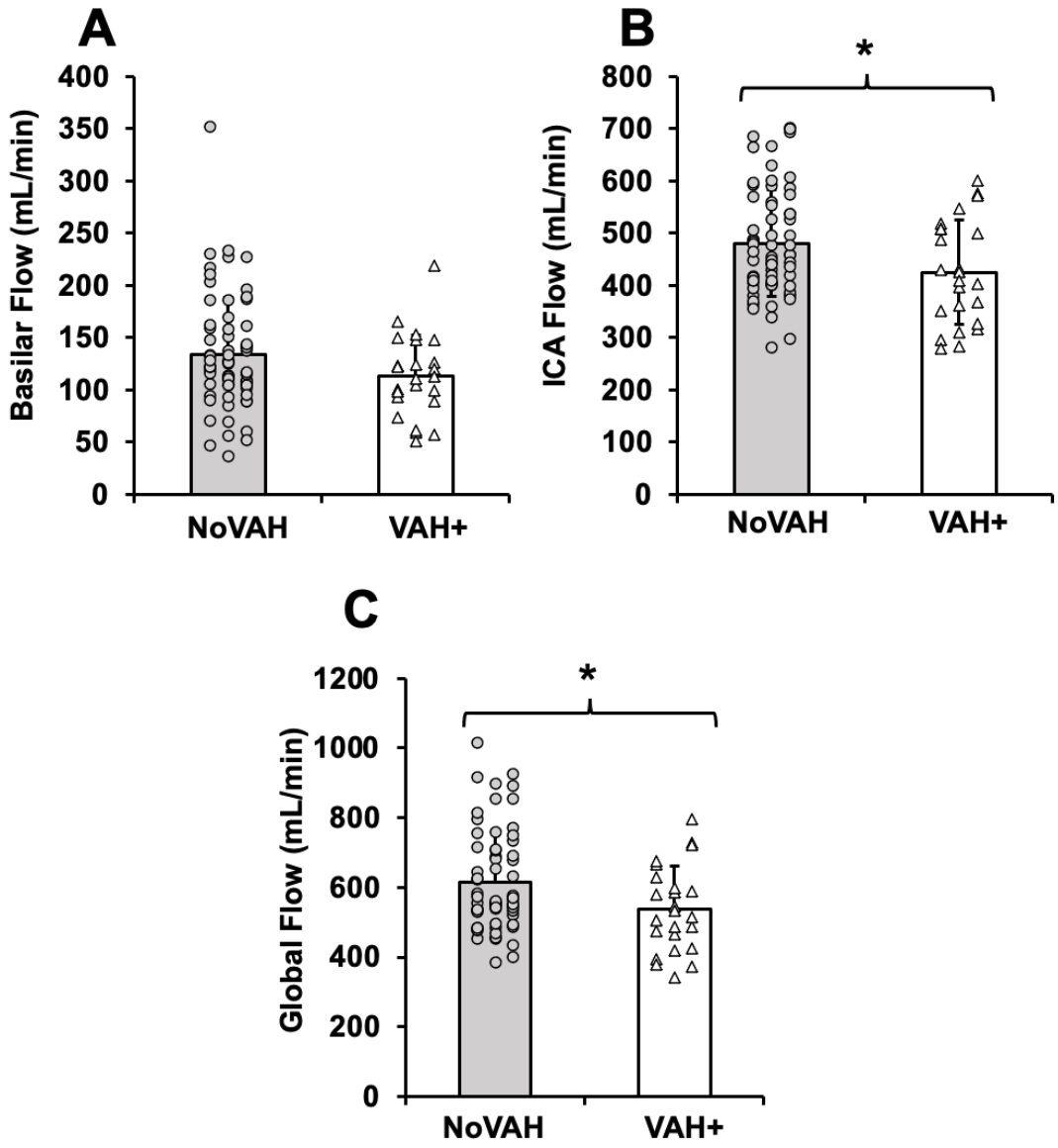

Figure 32. Intracranial artery blood flow in adults with and without VAH

Data are mean ± standard deviation and individual data points. This figure shows flow in the large intracranial arteries in adults without (NoVAH) and with (VAH+) vertebral artery hypoplasia. A) Basilar artery (BA) flow, B) internal carotid artery (ICA) flow C) global flow (sum of ICAs and BA). *$p<0.05$ compared with NoVAH.

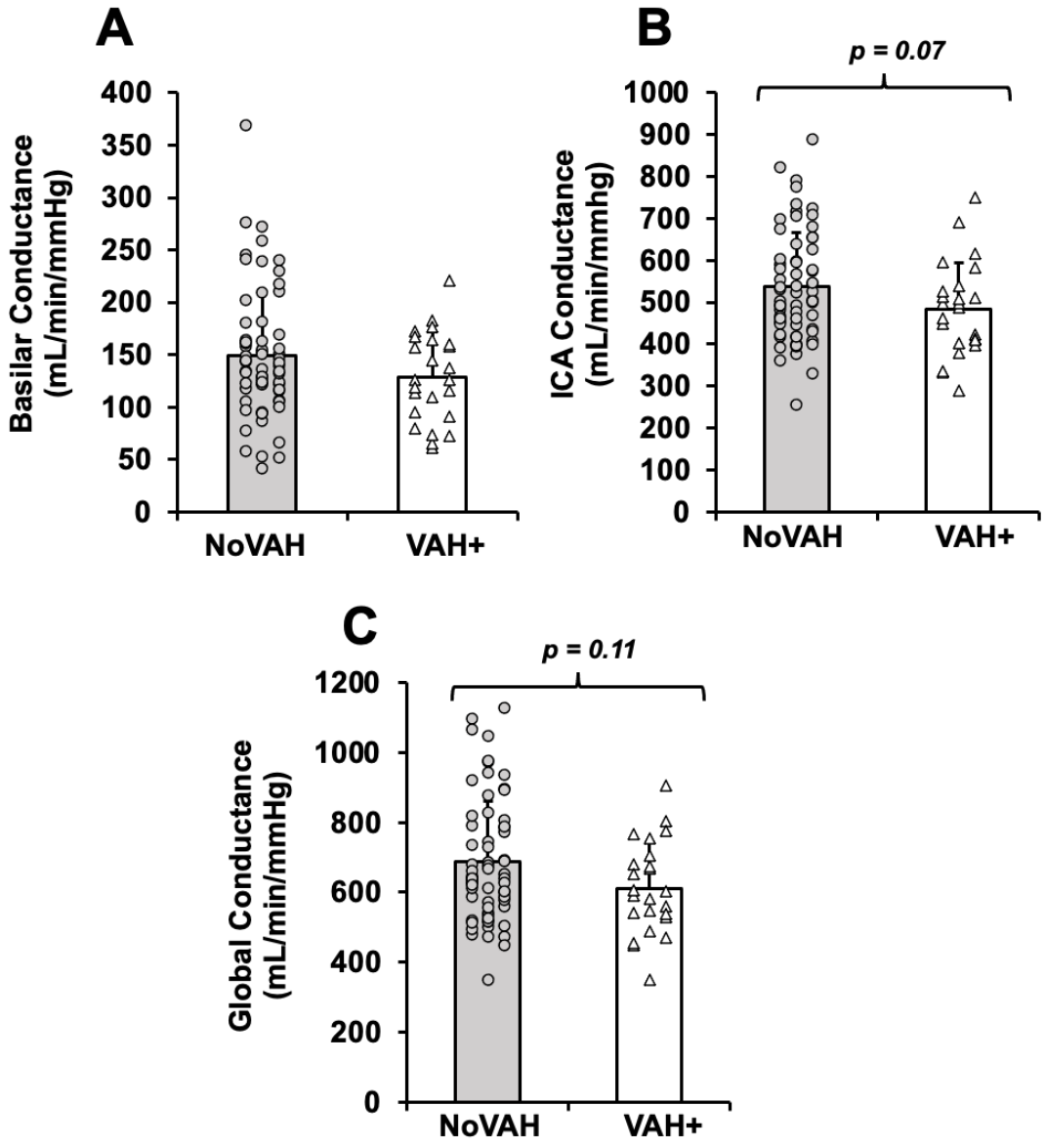

Figure 33. Intracranial artery conductance in adults with and without VAH

Data are mean ± standard deviation and individual data points. This figure shows cerebrovascular conductance in the large intracranial arteries in adults without (NoVAH) and with (VAH+) vertebral artery hypoplasia. A) Basilar artery (BA) conductance, B) internal carotid artery (ICA) conductance C) global conductance (sum of ICAs and BA).

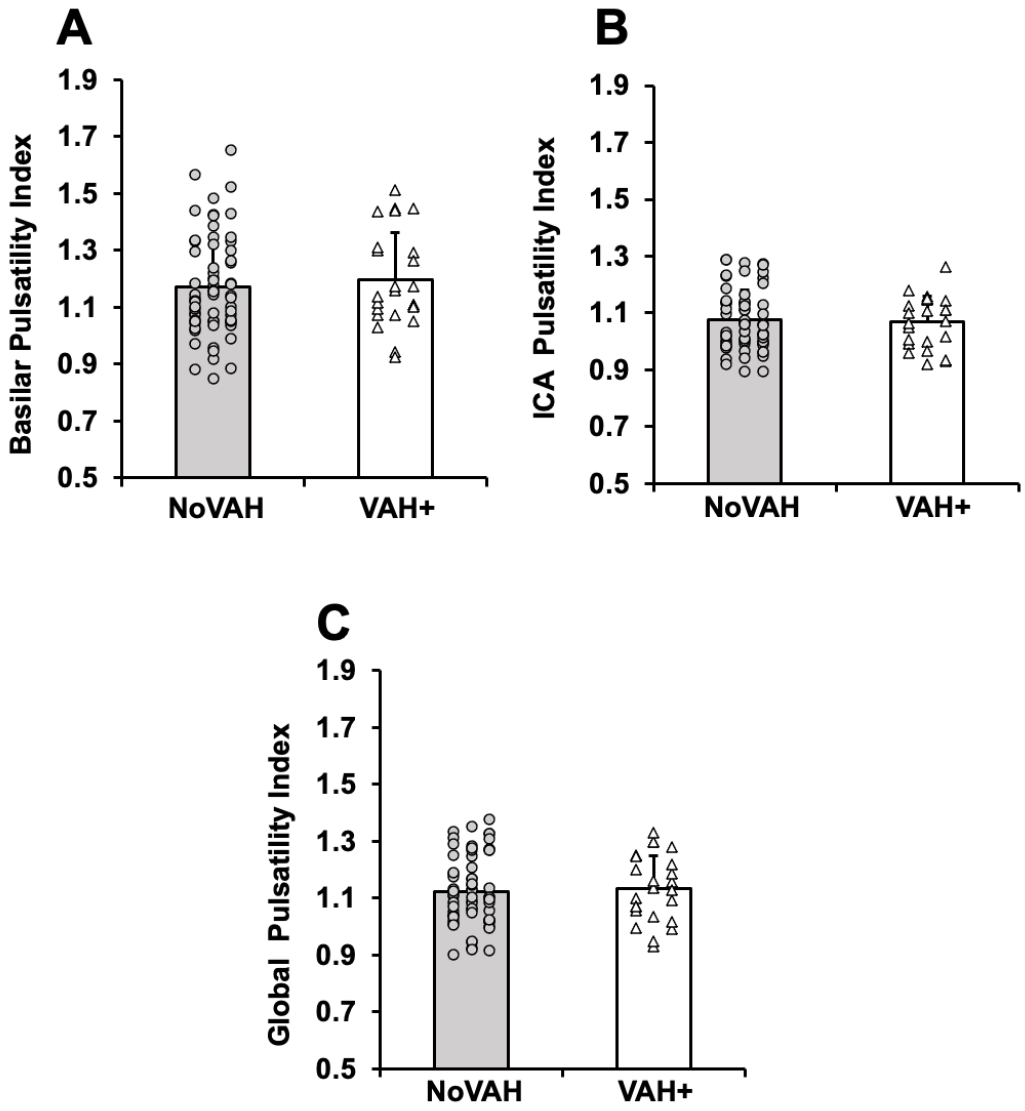

Figure 34. Cerebral pulsatility index in adults with and without VAH

Data are mean ± standard deviation and individual data points. This figure shows cerebral pulsatility index in the large intracranial arteries in adults without (NoVAH) and with (VAH+) vertebral artery hypoplasia. A) Basilar artery (BA) pulsatility index, B) internal carotid artery (ICA) pulsatility index C) global pulsatility index (average of ICAs and BA).

Covariate Analysis

Multivariable linear regression was employed to assess the effect of VAH on global cerebral blood flow while considering other variables that may influence global cerebral blood flow. Model 1 included age, sex, VAH, and brain volume / ICV (Table 39). The overall model did not reach the threshold for significance. Model 2 contained age, sex, VAH, and Alzheimer's disease risk factors (brain volume / ICV, APOE4+ and parental history of Alzheimer's disease) (Table 40). This overall model also did not reach the threshold for significance. Model 3 contained age, sex, VAH, and vascular risk factors (treatment for hypertension, treatment for hypercholesterolemia, and diabetes) (Table 41). VAH was the only significant contributor to the model and the overall model was significant. Model 4 contained age, sex, VAH and both vascular and Alzheimer's disease risk factors (Table 42). The overall model did not reach the threshold for significance.

Table 39. Global Cerebral Blood Flow Model 1: VAH, Age, Sex and Brain Volume

Parameter	*Coefficient*	*SE*	*t*	*P*	*Standardized Coefficient*	*VIF*
Intercept	786.477	440.850	1.784	0.078		
Age	-1.227	3.869	-0.317	0.752	-0.0343	1.043
Sex	-28.870	33.724	-0.856	0.394	-0.0953	1.104
VAH+	-80.516	35.008	-2.300	0.024	-0.254	1.088
Brain Volume	-109.394	437.136	-0.250	0.803	-0.0285	1.157

Multivariable linear regression model of global cerebral blood flow. Sex is coded as 1 = male and 0 = female. VAH+ is coded as 1 = yes and 0 = no. Brain volume and age are continuous variables. Brain volume was adjusted for intracranial volume. VAH+, presence of vertebral artery hypoplasia, SE, standard error, VIF, variance inflation factor.

Table 40. Global Cerebral Blood Flow Model 2: VAH, Age, Sex, and Alzheimer's Disease Risk Factors

Parameter	*Coefficient*	*SE*	*t*	*P*	*Standardized Coefficient*	*VIF*
Intercept	795.355	440.126	1.807	0.075		
Age	0.357	3.999	0.0894	0.929	0.0100	1.067
Sex	-36.064	34.544	-1.044	0.300	-0.120	1.116
VAH+	-75.981	35.522	-2.139	0.036	-0.244	1.102
Brain Volume	-309.273	440.058	-0.703	0.484	-0.0827	1.171
APOE4+	74.437	32.891	2.263	0.027	0.252	1.049
Parental History of AD	24.052	34.387	0.699	0.486	0.0773	1.032

Multivariable linear regression model of global cerebral blood flow. Sex is coded as 1 = male and 0 = female. VAH+, APOE4+ and parental history of AD are coded as 1 = yes and 0 = no. Brain volume and age are continuous variables. Brain volume was adjusted for intracranial volume. AD, Alzheimer's disease, APOE4+, apolipoprotein E-3/4 or 4/4 genotype, SE, standard error, VAH+, presence of vertebral artery hypoplasia, VIF, variance inflation factor.

Table 41. Global Cerebral Blood Flow Model 3: VAH, Age, Sex, and Vascular Risk Factors

Parameter	*Coefficient*	*SE*	*t*	*P*	*Standardized Coefficient*	*VIF*
Intercept	729.290	234.590	3.109	0.003		
Age	-1.785	3.801	-0.470	0.640	-0.0499	1.044
Sex	-46.304	33.343	-1.389	0.169	-0.153	1.119
VAH+	-74.710	33.672	-2.219	0.029	-0.236	1.044
Treatment of Hypertension	-27.111	39.903	-0.679	0.499	-0.0722	1.045
Treatment of Hypercholesterolemia	39.653	34.506	1.149	0.254	0.128	1.150
Diabetes	176.075	103.860	1.695	0.094	0.186	1.112

Multivariable linear regression model of global cerebral blood flow. Sex is coded as 1 = male and 0 = female. VAH+, treatment of hypertension, treatment of hypercholesterolemia, and diabetes are coded as 1 = yes and 0 = no. Age is a continuous variable. SE, standard error, VAH+, presence of vertebral artery hypoplasia, VIF, variance inflation factor.

Table 42. Global Cerebral blood flow Model 4: VAH, Age, Sex, Alzheimer's Disease Risk Factors and Vascular Risk Factors

Parameter	*Coefficient*	*SE*	*t*	*P*	*Standardized Coefficient*	*VIF*
Intercept	827.072	444.367	1.861	0.067		
Age	-0.489	3.967	-0.123	0.902	-0.0137	1.081
Sex	-53.670	35.020	-1.533	0.130	-0.179	1.180
VAH+	-72.621	35.586	-2.041	0.045	-0.233	1.137
Treatment of Hypertension	-22.822	45.835	-0.498	0.620	-0.0579	1.174
Treatment of Hypercholesterolemia	50.423	35.907	1.404	0.165	0.164	1.187
Diabetes	146.567	106.031	1.382	0.171	0.163	1.202
Brain Volume	-294.396	446.287	-0.660	0.512	-0.0787	1.239
APOE4+	72.835	32.477	2.243	0.028	0.247	1.052
Parental History of AD	23.520	36.127	0.651	0.517	0.0756	1.172

Multivariable linear regression model of global cerebral blood flow. Sex is coded as 1 = male and 0 = female. VAH+, treatment of hypertension, treatment of hypercholesterolemia, diabetes, APOE4+, and parental history of AD are coded as 1 = yes and 0 = no. Age and brain volume are continuous variables. Brain volume was adjusted for intracranial volume. AD, Alzheimer's disease, APOE4+, apolipoprotein E-3/4 or 4/4 genotype, SE, standard error, VAH+, presence of vertebral artery hypoplasia, VIF, variance inflation factor.

Summary of Study 3 Results

This study addressed **Specific Aim 3**: to evaluate the impact of VAH on resting cerebral hemodynamics in a cohort of cognitively unimpaired adults with enriched risk for Alzheimer's disease. The first hypothesis of Specific Aim 3 was: The prevalence of VAH in this cohort will be comparable to previously reported values (15-35%). The results from this study support this hypothesis. In this retrospective analysis of 88 adults, 24 of them met criteria for VAH (27% prevalence). The second hypothesis of Specific Aim 3 was: Adults with VAH will have lower global CBF and lower blood flow in the major intracranial arteries compared with controls without VAH. The results from study 3 partially support this hypothesis. Using 4D flow MRI to evaluate blood flow in the large intercranial arteries, adults with VAH had lower ICA blood flow and global blood flow compared with adults without VAH. In addition, the flow in the sum of the VAs was lower in the VAH+ group compared with the no VAH group. However, contrary to our hypothesis, there were no significant differences in BA blood flow between adults with VAH and adults without VAH. The impact of VAH on global cerebral blood flow remained significant when controlling for multiple covariates including a separate model with vascular risk factors. The third hypothesis of Specific Aim 3 was: Adults with VAH will have higher global cerebral pulsatility index and higher pulsatility in the major intracranial arteries compared with controls without VAH. This hypothesis was not supported. There were no differences in pulsatility index of the ICAs, BA or globally when comparing adults with and without VAH. In summary, VAH prevalence was 27% in a cohort of cognitively unimpaired adults with enriched risk for Alzheimer's disease and was associated with lower global cerebral blood flow.

CHAPTER 5

5. DISCUSSION

Overview

The central aim of this thesis was to evaluate cerebral blood flow (CBF) regulation in the large intracranial vessels in aging humans. The overarching hypothesis was that there are age-related differences in CBF regulation and a regional cerebral anatomical variation, vertebral artery hypoplasia (VAH), would influence CBF regulation. The results from the series of three studies supported the overarching hypothesis. In Study 1, age-related differences in cerebrovascular function were observed when accounting for blood pressure and blood vessel diameter. In the second study, the anatomical variation VAH influenced the regional distribution of age-related changes in CBF. In the third study, adults with VAH had lower global CBF compared with adults without VAH even when accounting for multiple vascular covariates. Taken together, these findings suggest that age-related differences in cerebral blood flow regulation may be influenced by VAH. Furthermore, these findings in healthy, cognitively unimpaired adults may aid in the understanding of how CBF contributes to age-related cerebrovascular diseases including dementia.

Study 1: the impact of aging on cerebrovascular reactivity to hypercapnia using two imaging techniques

Study 1 addressed **Specific Aim 1**: To evaluate the impact of aging on cerebrovascular reactivity to hypercapnia using two imaging techniques. The main findings from this study were that in healthy adults with low vascular risk, there were no age-related differences detected in the middle cerebral blood velocity response to hypercapnia measured with TCD. However, older adults had lower cerebrovascular conductance reactivity globally as well as in each intracranial vessel of

interest (basilar, left and right MCA, left and right ICA) compared with young adults when cerebral blood flow was measured using 4D flow MRI. In addition, young adults demonstrated a significant change in both the right and left MCA cross-sectional area from baseline to hypercapnia. However, there was no significant change in MCA cross-sectional area from baseline to hypercapnia in older adults. These findings suggest that simultaneous angiographic, blood flow, and arterial blood pressure measures to quantify cerebrovascular responses may be necessary to appropriately investigate age-related differences in the cerebrovascular function.

No age-related differences in cerebrovascular reactivity with TCD

The first hypothesis of **Specific Aim 1** was: There will be no age-related differences in cerebrovascular reactivity to hypercapnia in healthy, habitually exercising adults when evaluating cerebral blood velocity with TCD. The results from study 1 support this hypothesis as the TCD did not detect any age, sex, or interaction effects on cerebrovascular reactivity to hypercapnia. This has been observed previously in our study of healthy, habitually exercising adults using a similar CO_2 stimulus and the same MCA velocity measurement technique (Miller et al., 2018). The older adults in this study had exceptionally good vascular health as they had vascular stiffness measures in the low ends of normative ages (Niiranen et al., 2017), and they did not have history or evidence of underlying vascular disease. Although there were no age-related differences in the reactivity measurements, which are quantified as the slope of the relationship between end-tidal CO_2 and cerebral blood velocity, older adults demonstrated approximately 17% lower absolute cerebrovascular conductance index measures during the 6% CO_2 condition compared to young adults. This indicates that the absolute value of cerebrovascular conductance index of the MCA is lower in older adults compared with young adults during a vasodilatory stimulus, which could still

have implications for brain perfusion. Despite the low vascular risk in these participants, it is possible that the age-effects were not detected using this methodology because of the issue of the MCA vasodilating during the CO_2 stimulus in young adults, which would only be detectable with MRI. This could suggest that blood velocity measurements alone may not be accurate for quantifying changes in blood flow. Ultimately, though TCD has the potential to evaluate brain blood velocity in a variety of settings without the limitations of an MRI scanner, studies evaluating cerebrovascular reactivity in the intracranial vessels should consider that cerebrovascular reactivity could be under-estimated if vessel diameter is not quantified.

Age-related differences in cerebrovascular reactivity with 4D flow MRI

The second hypothesis of **Specific Aim 1** was: Older adults will have lower cerebrovascular reactivity to hypercapnia compared with young adults when evaluating cerebral blood flow using 4D flow MRI. The results from study 1 support this hypothesis as there were age-related differences in the cerebrovascular conductance reactivity response to hypercapnia, with older adults demonstrating lower cerebrovascular reactivity compared with young adults. Older adults had lower cerebrovascular conductance reactivity globally, as well as in each blood vessel of interest (Right and left MCA, right and left ICA and basilar artery) compared with young adults. It was also observed the MCA increased in diameter during the CO_2 stimulus in young adults, but not in older adults. There were many advantages of using the 4D flow MRI technique to assess age-related differences in cerebrovascular function. The existing literature regarding cerebrovascular function and aging is fraught with methodological limitations including: (1) the study population (e.g., confounding vascular risk factors, medication use, unequal distribution of men and women, and habitual exercise status); (2) limiting the assessment to one artery; or (3)

failure to consider the hypercapnia-induced changes in arterial blood pressure. To address these experimental and technical limitations, this study included simultaneous angiographic and blood flow measurements of multiple intracranial arteries, assessed blood pressure responses during hypercapnia, as well as determining the diameter of the MCA during hypercapnia. It is important to note that the older adults in this study were in the middle-aged range (average age of 61 years). It is likely that inclusion of an older population would demonstrate larger age-associated differences in cerebrovascular reactivity compared with a group of young adults. Regarding the individual vessels, the responses were consistent between the right and left sides as well as in the different intracranial vessels. In the internal carotid arteries and the basilar artery, the older adults increased velocity during the 4% CO_2 condition where there was no increase in velocity in young adults, despite an increase in flow in both groups. This indicates that compared with older adults, young adults may be experiencing greater downstream vasodilation resulting in larger increases in flow that is not necessarily reflected by changes in velocity. The idea that young adults may be experiencing greater downstream vasodilation compared with older adults may also explain why there were no age-related differences in the MCA velocity reactivity observed using the TCD in study A. Future studies can evaluate the sensitivity of the cerebral blood flow and cerebral blood velocity response to differing levels of carbon dioxide at various timepoints. Taken together, these results suggest that simultaneous velocity, angiographic and blood pressure measures may be necessary to appropriately investigate age-related differences in cerebrovascular function, which may be un-detected if angiographic information is omitted.

Increase in MCA cross-sectional area during hypercapnia

The third hypothesis of **Specific Aim 1** was: The middle cerebral artery will increase in cross-sectional area in response to hypercapnia in young adults, but not older adults. The results from study 1 support this hypothesis, as the MCA dilated significantly during hypercapnia in young adults but not in older adults. Hypercapnia had a significant effect on the MCA cross-sectional area in young adults, and this was a small to medium effect size. The change in cross-sectional area from baseline to hypercapnia was approximately 4%. These cross-sectional area changes were modest but consistent with studies utilizing different neuroimaging techniques to address this issue (Al-Khazraji et al., 2019; Coverdale et al., 2015; Verbree et al., 2014). These results suggests that vasodilation to hypercapnia within the intracranial vessels may be age-dependent. Furthermore, the fact that the MCA may vasodilate during hypercapnia makes TCD and MRI studies difficult to directly compare and may contribute to discrepancies in the literature. For example, using blood velocity as a surrogate measure of blood flow may not accurately quantify blood flow (Burley et al., 2021). Importantly, this highlights the need for other techniques to address the effect of age on cerebrovascular reactivity. Future studies should address the impact of aging, as well as sex, and vascular risk factors on the changes in cross-sectional area of the large intracranial vessels during hypercapnia or other potentially vasoactive stimuli. In addition, it would be useful to verify the change in MCA cross-sectional area during hypercapnia with multiple MRI techniques including both dark blood and bright blood magnetic resonance angiography.

Sex-specific decline in cerebrovascular function

The results of the exploratory analysis of the 4D flow MRI data show that the age-related differences in cerebrovascular reactivity were only apparent in men, and not women. Furthermore,

with 4D flow MRI, it was observed that sex-differences were present in cerebrovascular reactivity young adults, such that young men had greater cerebrovascular reactivity compared with young women. This is the first known study to show sex differences in cerebrovascular reactivity to hypercapnia using 4D flow MRI. Future studies should assess how vessel size and potential changes in vessel diameter during a vasodilatory stimulus may influence sex differences in cerebrovascular reactivity. Men and women exhibit distinctive features of cerebrovascular disease etiology and clinical outcomes (Carter et al., 2012; Haast et al., 2012); therefore, it is possible that sex differences also exist in cerebrovascular function. There were no sex-differences detected in the middle cerebral artery velocity response to hypercapnia measured using TCD, which is consistent with multiple other studies that have used TCD (Madureira et al., 2017; Oláh et al., 2000; Peltonen et al., 2015). However, sex differences in cerebrovascular reactivity have been observed with other MRI studies including one that utilized blood-oxygen-level-dependent (BOLD) MRI (Kassner et al., 2010). It is possible that the MCA cross-sectional area change during hypercapnia varies by sex. The present study was underpowered to test sex differences in the MCA cross-sectional area change during hypercapnia; however, this would be an important future direction of the work. A possible explanation for sex-differences in cerebrovascular reactivity in young adults may be due to differences in vasodilatory reserve. Because previous studies have shown that baseline cerebral perfusion in young women is greater than men (Alwatban et al., 2021; Ghisleni et al., 2015; Liu et al., 2016, 2012b) they may require a greater hypercapnic stimulus to initiate vasodilation of the cerebral microvasculature compared with men. In addition, the mechanisms for increasing cerebral blood flow during a vasodilatory stimulus may differ by sex. For example, in a small sample of post-menopausal women, cyclooxygenase inhibition had a greater effect on cerebral vasodilatory capacity, measured by the cerebral blood velocity response

to hypercapnia with TCD, compared with age-matched men, suggesting a greater reliance on vasodilatory prostaglandins (Miller et al., 2013). Furthermore, chemoreceptor sensitivity and the subsequent sympathetic nervous system response to hypercapnia may be sex-specific (Usselman et al., 2015). As this analysis of the age, sex and interaction effects in this study was exploratory, it was not designed to provide mechanistic insight into why sex differences in cerebrovascular function are apparent. Therefore, interpretations are speculative and subject for future studies.

Mean arterial blood pressure responses during hypercapnia

During the cerebrovascular reactivity testing of study day A, continuous beat-by-beat blood pressure, beat-by-beat heart rate, and breath-by-breath end-tidal carbon dioxide responses were measured. Young and older adults had similar heart rate and end-tidal CO_2 responses to the hypercapnic stimulus. However, older adults had a greater mean arterial pressure (MAP) during the 6% CO_2 condition compared with young adults despite no age-related differences at baseline. There was also a moderate effect of aging on MAP reactivity measured during study visit A though this finding did not reach statistical significance. This suggests that older adults require an augmentation of MAP during hypercapnia to elevate cerebrovascular conductance to a level similar to young adults. This result is in accordance with recent studies reporting an elevated MAP response to hypercapnia in older adults compared to young adults (Claassen et al., 2007; Coverdale et al., 2017) and our previous work (Miller et al., 2018). It is possible that older adults had a more pronounced sympathoexcitation during hypercapnia contributing to the higher blood pressure response. Thus, future studies can evaluate the role of the sympathetic nervous system and its relationship with mean arterial pressure and cerebral blood flow during a vasodilatory stimulus.

Central vascular stiffness and cerebral pulsatility

Measurements of central arterial stiffness were evaluated in this study as part of the assessment of vascular health of the participants. Healthy older adults demonstrated higher central arterial stiffness compared with young adults. As mentioned previously, despite these age-associated differences, the central arterial stiffness values in older adults are considerably lower than many other reports in the literature (Niiranen et al., 2017) indicating the overall health of the older adults included in this study. Importantly, it has been suggested that stiffening of the central arteries could be a mechanism of primary aging resulting in decreased cerebrovascular function. The central arteries are responsible for dampening the pulsatile forces that occur with each cardiac contraction and when the vessels stiffen, excess pulsatile energy could be transmitted into the cerebral microcirculation leading to microvascular damage (Cermakova et al.; Mitchell et al., 2011; Watson et al., 2011). Although this was not part of the primary hypothesis for study 1, an exploratory analysis was conducted to evaluate the relationship between central arterial stiffness and cerebral pulsatility index. The results from study 1 show that there is a positive association between carotid-femoral PWV and cerebral pulsatility index in the anterior circulation measured with 4D flow MRI in older adults. This association was not apparent in young adults. This suggest that older adults that have stiffer central arteries also have greater pulsatility in the blood vessels supplying the brain. In addition, aging may enhance the relationship between central vascular stiffness and cerebral pulsatility. This finding is in agreement with a study by Tarumi et al., 2014 that found age and sex related differences in cerebral blood pulsatility were independently associated with carotid pulse pressure, and that higher pulsatility of CBF was associated with greater volume of white matter hyperintensities in older adults (Tarumi et al., 2014). Another finding from the present study is that in the internal carotid arteries, the pulsatility index significantly declined in young adults

during the 6% CO_2 stimulus compared with baseline levels. This was not apparent in older adults. This suggests that in young adults, the vasoactive stimulus results in a reduction in distal vascular resistance that does not occur in older adults. Future studies should further explore the influence of central arterial stiffness on cerebrovascular function, especially in conditions where central arterial stiffness is augmented.

Contrasting Measures: TCD and MRI techniques

In study 1, whether age-related differences in cerebrovascular reactivity to hypercapnia in the MCA were detected depended on the technique used to quantify cerebral blood velocity or flow. In study day A, measuring blood velocity responses of the MCA during hypercapnia using TCD in adults with low vascular risk did not reveal age-related differences in cerebrovascular reactivity. However, in study day B, older adults demonstrated lower cerebrovascular reactivity to hypercapnia when blood flow responses of the MCA were quantified using 4D flow MRI. This suggests that blood velocity responses, at least in the MCA of adults with low vascular risk, may not accurately quantify blood flow. The results from study 1 agree with a recent study by Burley et al., 2021. In 10 young and 10 older adults with low vascular risk, cerebrovascular reactivity to hypercapnia (5% CO_2) was measured using 3 techniques, TCD, BOLD MRI and PC-MRI. Their results suggested that age-related differences were present when they quantified blood flow, rather than blood velocity responses. BOLD cerebrovascular reactivity did not reach the threshold for age-related differences. Furthermore, cerebrovascular reactivity metrics were not correlated between PC-MRI, BOLD and TCD measurements (Burley et al., 2021). In addition, many studies rely on measuring the MCA as a surrogate of the entire cerebral circulation. This approach, while useful to determine MCA responses, does not consider regional differences in cerebral blood flow

between the anterior and posterior circulations (Zarrinkoob et al., 2015). Furthermore, these studies do not consider anatomical variations that may be present in the anterior or the posterior circulations. Taken together, the results from the present study, in accordance with the study by Burley et al., 2021, highlight the complexity of evaluating the age-related differences in cerebrovascular reactivity using different modalities and cautions the direct comparison between techniques. It is important to be considerate of the technique used, as well as the part of the vascular tree that is assessed, including the anterior circulation and or the posterior circulation. As cerebral anatomical variations are relatively common, the influence of cerebral anatomical variations on the age-related changes in cerebral blood flow regulation warrants further investigation, as was part of the rationale for doing study 2 and study 3 of this dissertation.

Study 2: impact of vertebral artery hypoplasia on age-related changes in regional cerebral blood flow

Study 2 addressed **Specific Aim 2:** To determine the impact of VAH on the age-related differences in regional blood flow in the large intracranial arteries. The prevalence of VAH in this study was 26%. The main findings were that in adults without VAH, aging is associated with a lower blood flow in the posterior circulation (basilar artery) and higher pulsatility index in the basilar artery. There were no age-associated differences in anterior (ICA) flow. Conversely, in adults with VAH, aging is associated with lower blood flow in the anterior circulation (ICAs) and globally. There were no age-associated differences in posterior flow (basilar artery). These findings were consistent at baseline and during a vasodilatory stimulus, hypercapnia. This suggest that VAH impacts the regional distribution of age-related differences in cerebral blood flow. Identification and further evaluation of this anatomical variation is warranted in larger cohorts.

Regional cerebral blood flow in adults without VAH

The first hypothesis of **Specific Aim 2** was: In healthy adults without VAH, age-related differences in CBF will be greater in posterior vessels compared with anterior vessels at rest and during hypercapnia. This hypothesis was based on previous findings from studies that utilized ultrasound or phase-contrast MRI techniques to evaluate blood flow in the large intracranial vessels and observed greater age-related differences in posterior vessels compared with anterior vessels (Albayrak et al., 2007; Dörfler et al., 2000; Olesen et al., 2019; Zhao et al., 2007). The results from Study 2 support this hypothesis. The older adults without VAH demonstrated approximately 20% lower BA blood flow at rest and 25% lower BA blood flow during hypercapnia compared with young adults with VAH, which was not apparent in the ICAs. This suggests that in healthy adults, early age-related declines in relative blood flow may be localized to the posterior circulation and not in the anterior circulation. The consequences of this may be that posterior brain areas and the brain stem may be more vulnerable to age-related hypoperfusion, at least in the context of healthy, adults without VAH. These findings are consistent with previous cross-sectional studies of adults with normal cerebral anatomy that reported the age-related difference in VA flow is larger than ICA flow (Albayrak et al., 2006; Dörfler et al., 2000; Olesen et al., 2019). In fact, Olesen et al., reported the magnitude of the age-associated difference in VA flow was four times greater than ICA flow when they cross-sectionally compared young adults (age = 24 ± 3 years) with older adults (age = 70 ± 5 years). In the study by Albayrak et al., 2007, the relationship between ICA flow and age was stronger than VA flow and age; however, the relative difference in flow between the youngest (20-39 years) and oldest (60-79 years) age groups were approximately 16% in the ICAs and approximately 25% in the VAs. Our findings are in contrast with Scheel et al., 2000 who

reported significant age-related differences in ICA flow with no observed relationship between VA flow and age in adults aged 20-85 years (Scheel et al., 2000). There have also been reports of age-related differences in middle cerebral artery velocity in adults with various vascular risk factors (Ainslie et al., 2008; Barnes et al., 2012; Demirkaya et al., 2008). However, these studies are difficult to compare with our findings because: 1) they do not report cerebral anatomical variants such as VAH; 2) one middle cerebral artery only contributes to about 21% of total CBF as opposed to the sum of the ICAs contributing to 72% of total CBF (Zarrinkoob et al., 2015). It is also possible that the regional pattern of age-related declines in CBF may change beyond the 6th decade of life, as the older participants in our study averaged ~61 years of age. In addition, there may be an impact of vascular risk factors on age-related decline in regional cerebral blood flow that was not observed because the participants in this study had low vascular risk. Taken together, these findings suggest that in healthy adults without VAH, lower relative cerebral blood flow is observed in the posterior circulation when measuring blood flow in the large intracranial vessels. These findings highlight the importance of measuring both the anterior and posterior circulations when evaluating age-related differences in cerebral blood flow.

Regional cerebral blood flow in adults with VAH

The second hypothesis of **Specific Aim 2** was: In healthy adults with VAH, age-related differences in CBF will be greater in anterior vessels compared with posterior vessels at rest and during hypercapnia. This hypothesis was based on the idea that individuals with VAH already have low blood flow in the posterior circulation due to the hypoplastic vertebral artery. The results from Study 2 support this hypothesis. Older adults with VAH demonstrated approximately 26% lower ICA blood flow at baseline and 29% lower ICA blood flow during hypercapnia but similar BA

blood flow values compared with young adults with VAH. Because blood flow in the posterior circulation is already lower due to the anatomical variation, this could be interpreted as a preservation of BA blood flow with age, at the expense of blood flow of the anterior cerebral circulation. In this context, preserving BA blood flow could be a way of protecting vulnerable posterior areas such as the brainstem from hypoperfusion. However, this may put aging individuals with VAH at risk for global cerebral hypoperfusion, as the ICAs are responsible for supplying over 70% of the global cerebral blood flow. This idea is speculative, and complex when put into the context that individuals with VAH are at a greater risk for posterior territory stroke (Szárazová et al., 2012) , which may alter CBF hemodynamics in the posterior circulation. Taken together, the combination of aging and VAH may place individuals with VAH at high risk for age-related cerebrovascular diseases, even outside of the context of stroke.

A recent study of adults with VAH reported they had reduced global cerebral blood flow compared with adults with normal posterior cerebral anatomy. In addition, in adults with both VAH and hypertension, blood flow the contralateral vessel was not able to compensate for flow in the hypoplastic vessel (Warnert et al., 2016). This suggests that the combination of the presence of VAH, along with additional vascular risk, could augment age-related differences in cerebral blood flow. In the present study, adults with hypertension were excluded and all participants had low vascular risk. Therefore, additional vascular risk was unable to be considered in the analysis. Consideration of the impact of VAH on cerebral blood flow with additional risk factors was part of the rationale for study 3. In addition, because there were no age-related differences in BA blood flow observed in study 2, part of the rationale for study 3 was to assess the impact of VAH on blood flow in the large intracranial vessels independent of age. Ultimately, the interaction of aging and VAH on CBF remains understudied, especially in non-stroke populations. Future work should

longitudinally assess how VAH impacts CBF in the anterior circulation, posterior circulation and globally. In addition, it would be important to assess how the interaction of aging and VAH, contribute to risk for development of age-related cerebrovascular diseases.

Age-related differences in pulsatility index

The exploratory hypothesis of **Specific Aim 2** was: Older adults will demonstrate higher cerebral pulsatility index in the large intracranial anterior and posterior vessels compared with young adults in both groups with and without VAH. This hypothesis was partially supported, as there were some age-related differences in pulsatility index, but these were regionally specific and depended on the presence or absence of hypercapnia. For example, older adults without VAH demonstrated a greater pulsatility index in the basilar artery both at rest and during hypercapnia compared with young adults. This was not the case for adults with VAH. Although pulsatility does not directly measure cerebrovascular resistance, the higher pulsatility in the BA could suggest an age-associated alteration of blood flow hemodynamics in the BA, possibly because of elevated vascular stiffness. Thus, the combination of higher pulsatility index and lower BA blood flow may augment risk of hypoperfusion in posterior brain areas of older adults without VAH. Studies that evaluate differences in pulsatility index the anterior compared with the posterior circulation are limited. In a post-mortem study, posterior cerebral arteries had a higher prevalence of elastin loss, concentric intima thickening, wall thickening and nonatherosclerotic stenosis compared to anterior cerebral arteries (Roth et al., 2017), which suggests that posterior vessels may be more vulnerable to age-related stiffening.

Age-related differences in pulsatility index of the anterior circulation were not observed at rest. However, during hypercapnia, older adults demonstrated higher pulsatility index compared

with young adults. This was independent of the presence of VAH. This finding suggests that older adults may experience elevated distal vascular resistance during a vasodilatory stimulus compared with young adults. This finding is in support of a study by Heffernan et al., 2018 where pulsatility index of the MCA was greater in older adults compared with young adults during a cognitive challenge, despite no differences at baseline (Heffernan et al., 2018). High distal vascular resistance could be indicative of arterial stiffening, elevated cerebral perfusion pressure or a reduced vasodilatory function. However, these ideas are speculative and future studies could address the mechanisms that are responsible for age-related differences in regional cerebral pulsatility both at rest and during a vasodilatory stimulus. Furthermore, there have been no studies that have assessed the impact of VAH on pulsatility index in the large intracranial vessels independent of age, which was part of the rationale for study 3.

Study 3: impact of VAH on resting cerebral hemodynamics in a cohort of cognitively unimpaired adults with enriched risk for Alzheimer's disease.

Study 3 addressed **Specific Aim 3**: To evaluate the impact of VAH on resting cerebral hemodynamics in a cohort of cognitively unimpaired adults with enriched risk for Alzheimer's disease. The main findings of this study were that in this cohort, the prevalence of VAH was 27%. VAH was associated with a lower blood flow in the ICAs as well as a lower global blood flow even after controlling for multiple vascular covariates compared with adults without VAH. In addition, the sum of the flow in the VAs was lower in the VAH+ group compared with the no VAH group. Group differences in BA flow did not reach statistical significance. There were no significant differences in cerebral pulsatility index between adults with and without VAH. In

summary, VAH is associated with lower global cerebral blood flow and could be important to consider as a risk factor for cerebral hypoperfusion.

Prevalence of VAH in cohort of cognitively unimpaired adults

The first hypothesis of **Specific Aim 3** was: The prevalence of VAH in this cohort will be comparable to previously reported values (15-35%). The results from this study support this hypothesis. Out of the 88 participants, 24 of them met the criteria for VAH, resulting in a 27% prevalence. This is also very similar to the results from study 2 where the prevalence of VAH was 26%. As many studies have reported the prevalence of VAH in stroke cohorts (Park et al., 2007; Szárazová et al., 2012; Thierfelder et al., 2014), future studies could continue to evaluate the impact of VAH on cerebral blood flow regulation in healthy, asymptomatic individuals.

Impact of VAH on cerebral blood flow

The second hypothesis of **Specific Aim 3** was: Adults with VAH will have lower global CBF and lower blood flow in the major intracranial arteries compared with controls without VAH. The results from study 3 partially support this hypothesis. Using 4D flow MRI to evaluate blood flow in the large intracranial arteries, adults with VAH had lower ICA blood flow and global blood flow compared with adults without VAH. They also had lower flow in the sum of the VAs. However, contrary to our hypothesis, there were no significant differences in BA blood flow between adults with VAH and adults without VAH. There was a small to medium effect of VAH on BA blood flow, but this finding did not reach statistical significance. It is possible that sum of the VAs is including flow to the cerebellum that the BA is not capturing. Ultimately, VAH is associated with an approximately 12% lower blood flow in the anterior circulation (ICAs) and 13% lower blood

flow globally compared to age matched participants without VAH. For context, the age-related differences in ICA flow between older adults with VAH and young adults approximately 37 years younger was 26%. Global cerebral blood flow was lower in adults with VAH compared with adults without VAH even after adjusting for multiple covariates including vascular factors (treatment for hypertension, treatment for hypocholesterolemia, and diabetes). Taken together, this suggests that the collateral circulation in the brain may not make up for the hypoplastic vertebral artery. The finding that VAH is associated with lower global cerebral blood flow has important implications for cerebral hypoperfusion. Because the participants in this study were in their 60's, (mean age = 63 years), it is possible that the combination of aging and VAH could negatively impact cerebral perfusion. This may be particularly important in women, as a recent collaborative study with pooled data from multiple institutions including our laboratory suggested that the age-related decline in cerebral blood flow in women is most prevalent between age 61 and 70 (Alwatban et al., 2021). In addition, future studies could evaluate the relationship between cerebral perfusion in adults with VAH and AD biomarkers. For example, in a study by Berman et al., 2015 at the Wisconsin Alzheimer's Disease Research Center, intracranial blood flow measured with 4D flow MRI was associated with cerebrospinal fluid markers of amyloid pathology (Berman et al., 2015). Therefore, future studies could identify individuals with VAH and assess their cerebral blood flow, vascular risk, and Alzheimer's disease risk longitudinally.

Impact of VAH on cerebral pulsatility index

The third hypothesis of **Specific Aim 3** was: Adults with VAH will have higher global cerebral pulsatility index and higher pulsatility in the major intracranial arteries compared with controls without VAH. This hypothesis was not supported. There were no differences in pulsatility index

of the ICAs, BA or globally at rest when comparing adults with and without VAH. This indicates that although VAH is associated with lower global cerebral blood flow, it is not associated with higher cerebral pulsatility compared with age-matched adults without VAH at rest. This suggests that the presence of VAH may not be associated with higher resting distal vascular resistance. In this context, a 4D flow MRI study of individuals who had Alzheimer's disease, mild cognitive impairment, or were cognitively healthy suggested that resting cerebral pulsatility index increased with disease progression. However, Circle of Willis variations were not attributed to differences in cerebral hemodynamics between groups (Rivera-Rivera et al., 2016). It is important to note that VAH was not considered in that study. In the current study 1 and study 2, cerebral blood flow and pulsatility index were evaluated both at rest and during a hypercapnic stimulus. Although the findings from study 3 suggest that VAH did not impact cerebral pulsatility index at rest, it is possible that differences in cerebral pulsatility between adults with and without VAH may be unveiled during a vasodilatory stimulus. This is what occurred when evaluating the age-related differences in cerebral pulsatility in the ICAs in study 1 and 2. Future studies could assess the impact of VAH not only cerebral blood flow and cerebral pulsatility index at rest but also during a vasodilatory or vasoconstrictor stimulus, which may provide more information regarding the health of the cerebral blood vessels.

Feasibility of 4D flow MRI to determine VAH

Study 2 and study 3 established feasibility of determining VAH in large cohorts using both structural and flow criteria with 4D flow MRI. 4D flow MRI is also a useful method to use to evaluate the effect of VAH on cerebral blood flow regulation. It allows for in-vivo acquisition of both volumetric flow and vascular area of multiple intracranial vessels from a single acquisition.

Using this technique addresses some of the limitations of previous techniques used to determine VAH. For example, 2D PC MRI relies on user-dependent placement of measurement planes which may be difficult to reproduce, B-mode ultrasound assessment relies on user-dependent insonation of the vessels extracranially (Gaigalaite et al., 2016), and manual inspection of the cerebral anatomy requires post-mortem evaluation (Ogeng'o et al., 2014). There is no consensus for the criteria for establishing VAH. Many studies use structural criteria, flow criteria and/or a ratio of flow or size between the two sides of the vertebral artery. A diameter of less than or equal to 2.0 mm was the structural criteria set by Park et al., 2007 where VAH was determined in a group of 529 stroke patients using magnetic resonance angiography and considered conservative (Park et al., 2007). Study 2 utilized this conservative criterion and added flow criterion for the determination of VAH (vessel diameter less than or equal to 2.0 mm and flow less than or equal to 50 mL/min). Study 2 utilized both 4D flow and time-of-flight angiography imaging for the structural measurements. It was noted that the vessel diameters from the 4D flow scan were slightly larger than the diameters acquired from time-of-flight measurements. Importantly, the diameter measurements from the time-of-flight scans required manual delineation of the vessel wall whereas the 4D flow vessels were segmented using a semi-automated protocol and included multiple cut points along the vessel. In study 3, no time-of-flight scans were acquired; therefore, VAH criteria were determined solely from the 4D flow MRI scans. The structural criteria were changed to a vessel diameter less than or equal to 3 mm, while the flow criteria remained the same (flow less than or equal to 50 mL/min with a flow asymmetry ratio of 2.0). These criteria were similar to a more recent study by Gaigalanite et al., 2016 who used a cut off of a vessel diameter less than or equal to 3 mm measured with MRA or computed tomography angiography to determine prevalence of VAH in asymptomatic individuals (Gaigalaite et al., 2016). Ultimately, the exact cut

points for determining VAH may need to be specific to the study population (i.e. older adults who may have large vessels in general (Xu et al., 2017) or adults with high vascular risk and the tools used to measure structural and flow data in the large intracranial vessels. 4D flow MRI provides both the structural and flow data, which is beneficial in the investigation of the impact of VAH on cerebral blood flow. Therefore, because of its high prevalence and impact on cerebral blood flow, determination of VAH in multiple cohorts using 4D flow MRI could be useful for future investigation.

Limitations of the work

Although the studies presented here utilized novel techniques and addressed many of the gaps in the literature, there are several limitations of the work. In study 1, the purpose of the study was to evaluate the impact of aging on cerebrovascular reactivity to hypercapnia using two imaging techniques. Aging was assessed cross-sectionally, therefore no conclusions can be made regarding observations outside of the age-ranges that were studied. The conclusions may not reflect the timing and trajectory of changes in cerebral blood flow parameters with aging that would require longitudinal follow-up over years or decades. This is also relevant to study 2, as study 2 was a retrospective analysis that included the participants in study 1. A strength of both study 1 and study 2 was that the older adults studied had low vascular risk and were habitual exercisers. This was to minimize any cofounding effects of vascular risk and inactivity on age-related differences in cerebral blood flow regulation. In addition, a criteria of 150 minutes per week of habitual aerobic exercise was used for inclusion into the study. This was based on self-report information from a phone screening interview and exercise training logs. However, there was no type of stratification regarding individuals that reported more than 150 minutes of habitual aerobic exercise per week,

and habitual exercise status was not accessed via an accelerometer. The effect of habitual exercise (mode, frequency, and duration) on cerebral blood flow regulation is an active area of research and was not assessed in the current study; however, future research should evaluate the interaction between aging and habitual exercise on cerebral blood flow regulation, as was the subject of a recent metanalysis (Smith et al., 2021). In both study 1 and study 2, some of the young women in were taking oral contraceptives. To date, there is no evidence that oral contraceptives affect cerebral blood flow regulation using TCD or 4D flow MRI techniques, but that does not exclude the possibility that oral contraceptives affect the ability of the intracranial vessels to dilate in response to hypercapnia. In study 1, 4D flow MRI was used to determine vessel cross-sectional area. 4D flow MRI has the advantage of measuring the cross-sectional across the entire vessel without having to manually delineate the lumen; however, since the cross-sectional area is determined by the functional outer boundaries of the blood flow velocity profiles, heterogeneous blood flow responses, or partial volume effects could impact the cross-sectional area measurements. This methodology has been validated using 2D phase contrast using phantom experiments for given flow rates (Schrauben et al., 2015) but, it is important that future experiments evaluating intracranial vessel dilation also utilize high-resolution MRI, include both black-blood and bright-blood sequences, and validate this technique using changing flow conditions. In both study 2 and study 3, 4D flow MRI was used to determine VAH. Because these studies were retrospective, there are inherent limitations to the approach. In order to conduct a prospective study on the impact of VAH on age-related differences in cerebral blood flow or cerebral hypoperfusion, an MRI scan would be required to identify VAH prior to study enrollment. There is no way to determine the cause of VAH based on a retrospective analysis. Study 2 had a relatively low sample size of individuals with VAH which increases the risk for Type II errors.

While the sample size of adults with VAH was greater in study 3, there are still biases in the sampling that may be a product of the retrospective cohorts. Nevertheless, studies 2 and 3 provide rationale to further investigate the impact of VAH on cerebral blood flow regulation. In addition, in both studies 2 and 3 the impact of VAH on cerebral blood flow was characterized using 4D flow MRI. Other perfusion imaging such as arterial spin labeling (ASL) or blood-oxygen-level-dependent imaging (BOLD) may unveil additional regional blood flow differences that were unable to be captured by limiting the analysis to large major arteries. The calculation of global cerebral blood flow was based off the contributions of the large intracranial arteries (BA and ICAs); therefore, it did not include the contribution of cerebellar arteries. Importantly, because the interest was in how VAH may affect blood flow in the large major arteries, the effect of other anatomical variations of the Circle of Willis such as fetal origin posterior cerebral arteries (PCA) or hypoplastic anterior cerebral arteries was not evaluated. Determining the impact of other cerebral anatomical variations, in addition to or independent from VAH, will be critical in future studies. Finally, although the participants in studies 1, 2 and 3 were deemed to have low to moderate vascular risk, it is possible that they had amyloid pathology in their brains. Determining the levels of amyloid pathology, in combination with cerebral blood flow parameters, will be important for future research that evaluates the impact of cerebral hypoperfusion on dementia risk.

Summary and Overall Discussion

The central aim of this thesis was to evaluate cerebral blood flow (CBF) regulation in the large intracranial vessels in aging humans. The overarching hypothesis was that there are age-related differences in CBF regulation and a regional cerebral anatomical variation, vertebral artery hypoplasia (VAH), would influence CBF regulation. The significance of this central aim is that as

our global population continues to age, it is important to understand the impact of cerebral blood flow regulation on age-related cerebrovascular diseases and determine physiology from pathology. CBF regulation is complex and difficult to study. The encapsulation of the brain in the skull makes the brain's vasculature challenging to image. Therefore, many studies make assumptions regarding the cerebral blood velocity and location of measurement as an index of global cerebral blood flow. The results from study 1 suggest that age-related differences in cerebrovascular function in adults with low vascular risk are unveiled when quantifying cerebral blood flow, rather than cerebral blood velocity responses. Furthermore, the middle cerebral artery, which is commonly used to assess cerebrovascular function, vasodilated in response to hypercapnia in young adults, not in older adults. These results highlight the complexity of evaluating the age-related differences in cerebrovascular reactivity and suggest that simultaneous velocity, angiographic and blood pressure measures may be necessary to appropriately investigate age-related differences in cerebrovascular function. This was the first study of its kind to evaluate the effects of aging on cerebrovascular function using 4D flow MRI. One of the main advantages of using 4D flow MRI, besides the simultaneous assessment of velocity and angiographic data, is that multiple of the large intracranial vessels can be observed. In many previous studies evaluating the effect of aging on cerebrovascular function, only the middle cerebral artery is considered as a surrogate of the entire cerebral circulation, which does not consider differences in regulation of the anterior and posterior circulations. Furthermore, 26% of the participants in study 1 had an anatomical variation of the posterior circulation, where one of the vertebral arteries, the main vessel that supplies the posterior circulation, was hypoplastic, termed vertebral artery hypoplasia (VAH). Therefore, in study 2, the impact of VAH on age-related differences in cerebral blood flow was assessed. In adults with VAH, there were greater age-related differences in blood flow of the anterior circulation (internal

carotid arteries) despite no age-related differences in blood flow of the posterior circulation (basilar artery). The blood flow pattern of distribution was opposite in adults without VAH, who had greater age-related differences in blood flow of the basilar artery than the internal carotid arteries. These findings suggest that VAH impacts age-related differences in the regional distribution of cerebral blood flow. The results from study 2 have important implications for the impact of VAH on age-related cerebral hypoperfusion. This study was also the first to use 4D flow MRI to determine VAH using both structural and flow criteria and measure its impact on the age-related differences in cerebral blood flow. Although the participant numbers of individuals with VAH in this study were relatively low, this study was still important in generating interest in further evaluating the impact of VAH on cerebral hemodynamics. Thus, study 3 evaluated the impact of VAH on cerebral blood flow in a larger cohort of cognitively unimpaired adults between age 55-69 with enriched risk for Alzheimer's disease. This study combined data obtained in our laboratory regarding vascular health and leveraged existing 4D flow MRI scans to evaluate the impact of VAH on cerebral blood flow and cerebral pulsatility index in the large intracranial blood vessels. In study 3, the prevalence of VAH was 27%, which was very similar to what we observed in the smaller participant group in study 2 (26%). VAH was associated with lower blood flow in the anterior circulation (internal carotid arteries), the sum of the VAs, and globally compared with adults without VAH. This finding remained even after adjustment for multiple factors that may increase vascular risk. These findings suggest that the presence of VAH may put individuals at risk for cerebral hypoperfusion and could impact future risk for age-related cerebrovascular diseases. Because of its high prevalence in cognitively healthy adults, future studies evaluating VAH, and it impact on age-related changes in cerebral blood flow are imperative.

In summary, evaluating the age-related changes in cerebral blood flow and cerebrovascular function is complex and results from this dissertation suggest that simultaneous velocity, angiographic, and blood pressure data may be necessary to accurately quantify age-related differences in cerebrovascular function. 4D flow MRI is a useful tool to quantify cerebral blood flow, and it has many advantages including the ability to determine the structure of the intracranial arteries and their variations. A common variation in the posterior circulation, vertebral artery hypoplasia, was associated with age-related reductions in the anterior circulation and globally. Furthermore, adults with vertebral artery hypoplasia had lower anterior cerebral blood flow, flow in the sum of the VAs, and global cerebral blood flow even after adjustments for vascular risk factors compared to adults without vertebral artery hypoplasia. These findings suggest that vertebral artery hypoplasia may impact cerebral blood flow regulation and VAH could be a risk factor for cerebral hypoperfusion. Future studies can evaluate the impact of both aging and anatomical variations on cerebral blood flow regulation, as well as risk for cerebrovascular diseases including dementia.

REFERENCES

Aaslid, R., Markwalder, T.-M., and Nornes, H. (1982). Noninvasive transcranial Doppler ultrasound recording of flow velocity in basal cerebral arteries. J. Neurosurg. *57*, 769–774.

Acar, M., Degirmenci, B., Yucel, A., Albayrak, R., Haktanir, A., and Yaman, M. (2005). Comparison of vertebral artery velocity and flow volume measurements for diagnosis of vertebrobasilar insufficiency using color duplex sonography. Eur. J. Radiol. *54*, 221–224.

Adachi, K., Takahashi, S., Melzer, P., Campos, K.L., Nelson, T., Kennedy, C., and Sokoloff, L. (1994). Increases in local cerebral blood flow associated with somatosensory activation are not mediated by NO. Am. J. Physiol. *267*, H2155-2162.

Ainslie, P.N., and Duffin, J. (2009). Integration of cerebrovascular CO2 reactivity and chemoreflex control of breathing: mechanisms of regulation, measurement, and interpretation. Am. J. Physiol. Regul. Integr. Comp. Physiol. *296*, R1473-1495.

Ainslie, P.N., and Ogoh, S. (2010). Regulation of cerebral blood flow in mammals during chronic hypoxia: a matter of balance. Exp. Physiol. *95*, 251–262.

Ainslie, P.N., and Subudhi, A.W. (2014). Cerebral blood flow at high altitude. High Alt. Med. Biol. *15*, 133–140.

Ainslie, P.N., Cotter, J.D., George, K.P., Lucas, S., Murrell, C., Shave, R., Thomas, K.N., Williams, M.J.A., and Atkinson, G. (2008). Elevation in cerebral blood flow velocity with aerobic fitness throughout healthy human ageing. J. Physiol. *586*, 4005–4010.

Albayrak, R., Fidan, F., Unlu, M., Sezer, M., Degirmenci, B., Acar, M., Haktanir, A., and Yaman, M. (2006). Extracranial carotid Doppler ultrasound evaluation of cerebral blood flow volume in COPD patients. Respir. Med. *100*, 1826–1833.

Albayrak, R., Degirmenci, B., Acar, M., Haktanir, A., Colbay, M., and Yaman, M. (2007). Doppler sonography evaluation of flow velocity and volume of the extracranial internal carotid and vertebral arteries in healthy adults. J. Clin. Ultrasound JCU *35*, 27–33.

Al-Khazraji, B.K., Shoemaker, L.N., Gati, J.S., Szekeres, T., and Shoemaker, J.K. (2019). Reactivity of larger intracranial arteries using 7 T MRI in young adults. J. Cereb. Blood Flow Metab. *39*, 1204–1214.

Alonso, A., Mosley, T.H., Gottesman, R.F., Catellier, D., Sharrett, A.R., and Coresh, J. (2009). Risk of dementia hospitalisation associated with cardiovascular risk factors in midlife and older age: the Atherosclerosis Risk in Communities (ARIC) study. J. Neurol. Neurosurg. Psychiatry *80*, 1194–1201.

Alpers, B.J., Berry, R.G., and Paddison, R.M. (1959). Anatomical Studies of the Circle of Willis in Normal Brain. AMA Arch. Neurol. Psychiatry *81*, 409–418.

Alwatban, M.R., Aaron, S.E., Kaufman, C.S., Barnes, J.N., Brassard, P., Ward, J.L., Miller, K.B., Howery, A.J., Labrecque, L., and Billinger, S.A. (2021). Effects of Age and Sex on Middle Cerebral Artery Blood Velocity and Flow Pulsatility Index Across the Adult Lifespan. J. Appl. Physiol.

Amyot, F., Kenney, K., Moore, C., Haber, M., Turtzo, L.C., Shenouda, C., Silverman, E., Gong, Y., Qu, B.-X., Harburg, L., et al. (2018). Imaging of Cerebrovascular Function in Chronic Traumatic Brain Injury. J. Neurotrauma *35*, 1116–1123.

Attinger, E.O. (1965). The physics of pulsatile blood flow with particular reference to small vessels. Invest. Ophthalmol. *4*, 973–987.

Azarpazhooh, M.R., Avan, A., Cipriano, L.E., Munoz, D.G., Sposato, L.A., and Hachinski, V. (2018). Concomitant vascular and neurodegenerative pathologies double the risk of dementia. Alzheimers Dement. J. Alzheimers Assoc. *14*, 148–156.

Bailey, D.M., Marley, C.J., Brugniaux, J.V., Hodson, D., New, K.J., Ogoh, S., and Ainslie, P.N. (2013). Elevated aerobic fitness sustained throughout the adult lifespan is associated with improved cerebral hemodynamics. Stroke *44*, 3235–3238.

Bain, C. a. L., Walters, M.R., Lees, K.R., and Lumsden, M.A. (2004). The effect of HRT on cerebral haemodynamics and cerebral vasomotor reactivity in post-menopausal women. Hum. Reprod. Oxf. Engl. *19*, 2411–2414.

Bakker, S.L.M., de Leeuw, F.-E., den Heijer, T., Koudstaal, P.J., Hofman, A., and Breteler, M.M.B. (2004). Cerebral Haemodynamics in the Elderly: The Rotterdam Study. Neuroepidemiology *23*, 178–184.

Barnes, J.N., Schmidt, J.E., Nicholson, W.T., and Joyner, M.J. (2012). Cyclooxygenase inhibition abolishes age-related differences in cerebral vasodilator responses to hypercapnia. J. Appl. Physiol. *112*, 1884–1890.

Barnes, J.N., Taylor, J.L., Kluck, B.N., Johnson, C.P., and Joyner, M.J. (2013). Cerebrovascular reactivity is associated with maximal aerobic capacity in healthy older adults. J. Appl. Physiol. *114*, 1383–1387.

Barnes, J.N., Harvey, R.E., Eisenmann, N.A., Miller, K.B., Johnson, M.C., Kruse, S.M., Lahr, B.D., Joyner, M.J., and Miller, V.M. (2019). Cerebrovascular reactivity after cessation of menopausal hormone treatment. Climacteric J. Int. Menopause Soc. 1–8.

Battisti-Charbonney, A., Fisher, J., and Duffin, J. (2011). The cerebrovascular response to carbon dioxide in humans. J. Physiol. *589*, 3039–3048.

Beason-Held, L.L., Kraut, M.A., and Resnick, S.M. (2009). Stability Of Default-Mode Network Activity In The Aging Brain. Brain Imaging Behav. *3*, 123–131.

van Beek, A.H.E.A., de Wit, H.M., Olde Rikkert, M.G.M., and Claassen, J.A.H.R. (2011). Incorrect performance of the breath hold method in the old underestimates cerebrovascular

reactivity and goes unnoticed without concomitant blood pressure and end-tidal CO(2) registration. J. Neuroimaging Off. J. Am. Soc. Neuroimaging *21*, 340–347.

Begley, D.J., and Brightman, M.W. (2003). Structural and functional aspects of the blood-brain barrier. Prog. Drug Res. Fortschritte Arzneimittelforschung Progres Rech. Pharm. *61*, 39–78.

Bellner, J., Romner, B., Reinstrup, P., Kristiansson, K.-A., Ryding, E., and Brandt, L. (2004). Transcranial Doppler sonography pulsatility index (PI) reflects intracranial pressure (ICP). Surg. Neurol. *62*, 45–51; discussion 51.

Bergfeld, G.R., and Forrester, T. (1992). Release of ATP from human erythrocytes in response to a brief period of hypoxia and hypercapnia. Cardiovasc. Res. *26*, 40–47.

Berkenbosch, A., Bovill, J.G., Dahan, A., DeGoede, J., and Olievier, I.C. (1989). The ventilatory CO2 sensitivities from Read's rebreathing method and the steady-state method are not equal in man. J. Physiol. *411*, 367–377.

Berman, S.E., Rivera-Rivera, L.A., Clark, L.R., Racine, A.M., Keevil, J.G., Bratzke, L.C., Carlsson, C.M., Bendlin, B.B., Rowley, H.A., Blennow, K., et al. (2015). Intracranial arterial four-dimensional flow is associated with metrics of brain health and Alzheimer's disease. Alzheimers Dement. Diagn. Assess. Dis. Monit. *1*, 420–428.

Berman, S.E., Clark, L.R., Rivera-Rivera, L.A., Norton, D., Racine, A.M., Rowley, H.A., Bendlin, B.B., Blennow, K., Zetterberg, H., Carlsson, C.M., et al. (2017). Intracranial Arterial 4D Flow in Individuals with Mild Cognitive Impairment is Associated with Cognitive Performance and Amyloid Positivity. J. Alzheimers Dis. JAD *60*, 243–252.

Bill, O., Lambrou, D., Sotomayor, G.T., Meyer, I., Michel, P., Moreira, T., Niederhauser, J., and Hirt, L. (2020). Predictors of the pulsatility index in the middle cerebral artery of acute stroke patients. Sci. Rep. *10*, 17110.

Bleys, R.L., Cowen, T., Groen, G.J., Hillen, B., and Ibrahim, N.B. (1996). Perivascular nerves of the human basal cerebral arteries: I. Topographical distribution. J. Cereb. Blood Flow Metab. Off. J. Int. Soc. Cereb. Blood Flow Metab. *16*, 1034–1047.

Bogousslavsky, J., and Regli, F. (1990). Anterior cerebral artery territory infarction in the Lausanne Stroke Registry. Clinical and etiologic patterns. Arch. Neurol. *47*, 144–150.

Bowler, J.V. (2007). Modern concept of vascular cognitive impairment. Br. Med. Bull. *83*, 291–305.

Brassard, P., Tymko, M.M., and Ainslie, P.N. (2017). Sympathetic control of the brain circulation: Appreciating the complexities to better understand the controversy. Auton. Neurosci. Basic Clin. *207*, 37–47.

Braz, I.D., and Fisher, J.P. (2016). The impact of age on cerebral perfusion, oxygenation and metabolism during exercise in humans. J. Physiol. *594*, 4471–4483.

Braz, I.D., Flück, D., Lip, G.Y.H., Lundby, C., and Fisher, J.P. (2017). Impact of aerobic fitness on cerebral blood flow and cerebral vascular responsiveness to CO2 in young and older men. Scand. J. Med. Sci. Sports *27*, 634–642.

Breteler, M.M., van Swieten, J.C., Bots, M.L., Grobbee, D.E., Claus, J.J., van den Hout, J.H., van Harskamp, F., Tanghe, H.L., de Jong, P.T., and van Gijn, J. (1994). Cerebral white matter lesions, vascular risk factors, and cognitive function in a population-based study: the Rotterdam Study. Neurology *44*, 1246–1252.

Brian, J.E., Faraci, F.M., and Heistad, D.D. (1996). Recent insights into the regulation of cerebral circulation. Clin. Exp. Pharmacol. Physiol. *23*, 449–457.

Brothers, R.M., and Zhang, R. (2016). CrossTalk opposing view: The middle cerebral artery diameter does not change during alterations in arterial blood gases and blood pressure. J. Physiol. *594*, 4077–4079.

Brown, C.M., Dütsch, M., Hecht, M.J., Neundörfer, B., and Hilz, M.J. (2003). Assessment of cerebrovascular and cardiovascular responses to lower body negative pressure as a test of cerebral autoregulation. J. Neurol. Sci. *208*, 71–78.

Buijs, P.C., Krabbe-Hartkamp, M.J., Bakker, C.J., de Lange, E.E., Ramos, L.M., Breteler, M.M., and Mali, W.P. (1998). Effect of age on cerebral blood flow: measurement with ungated two-dimensional phase-contrast MR angiography in 250 adults. Radiology *209*, 667–674.

Burley, C.V., Francis, S.T., Thomas, K.N., Whittaker, A.C., Lucas, S.J.E., and Mullinger, K.J. (2021). Contrasting Measures of Cerebrovascular Reactivity Between MRI and Doppler: A Cross-Sectional Study of Younger and Older Healthy Individuals. Front. Physiol. *12*.

Buterbaugh, J., Wynstra, C., Provencio, N., Combs, D., Gilbert, M., and Parthasarathy, S. (2015). Cerebrovascular reactivity in young subjects with sleep apnea. Sleep *38*, 241–250.

Carter, C.L., Resnick, E.M., Mallampalli, M., and Kalbarczyk, A. (2012). Sex and gender differences in Alzheimer's disease: recommendations for future research. J. Womens Health 2002 *21*, 1018–1023.

Cates, M.J., Dickinson, C.J., Hart, E.C.J., and Paton, J.F.R. (2012). Neurogenic hypertension and elevated vertebrobasilar arterial resistance: is there a causative link? Curr. Hypertens. Rep. *14*, 261–269.

Cavuşoğlu, M., Pfeuffer, J., Uğurbil, K., and Uludağ, K. (2009). Comparison of pulsed arterial spin labeling encoding schemes and absolute perfusion quantification. Magn. Reson. Imaging *27*, 1039–1045.

Cermakova, P., Ding, J., Meirelles, O., Reis, J., Religa, D., Schreiner, P.J., Jacobs, D.R., Bryan, R.N., and Launer, L.J. Carotid Intima–Media Thickness and Markers of Brain Health in a Biracial Middle-Aged Cohort: CARDIA Brain MRI Sub-study. J. Gerontol. Ser. A.

Chapman, S.B., Aslan, S., Spence, J.S., Defina, L.F., Keebler, M.W., Didehbani, N., and Lu, H. (2013). Shorter term aerobic exercise improves brain, cognition, and cardiovascular fitness in aging. Front. Aging Neurosci. *5*, 75.

Chen, J.J., Rosas, H.D., and Salat, D.H. (2011). Age-Associated Reductions in Cerebral Blood Flow Are Independent from Regional Atrophy. NeuroImage *55*, 468–478.

Chuang, Y.-M., Huang, Y.-C., Hu, H.-H., and Yang, C.-Y. (2006). Toward a Further Elucidation: Role of Vertebral Artery Hypoplasia in Acute Ischemic Stroke. Eur. Neurol. *55*, 193–197.

Churchill, N.W., Hutchison, M.G., Graham, S.J., and Schweizer, T.A. (2019). Evaluating Cerebrovascular Reactivity during the Early Symptomatic Phase of Sport Concussion. J. Neurotrauma *36*, 1518–1525.

Claassen, J.A.H.R., Zhang, R., Fu, Q., Witkowski, S., and Levine, B.D. (2007). Transcranial Doppler estimation of cerebral blood flow and cerebrovascular conductance during modified rebreathing. J. Appl. Physiol. Bethesda Md 1985 *102*, 870–877.

Clark, L.R., Berman, S.E., Rivera-Rivera, L.A., Hoscheidt, S.M., Darst, B.F., Engelman, C.D., Rowley, H.A., Carlsson, C.M., Asthana, S., Turski, P., et al. (2017). Macrovascular and microvascular cerebral blood flow in adults at risk for Alzheimer's disease. Alzheimers Dement. *7*, 48–55.

Cohen, P.J., Alexander, S.C., Smith, T.C., Reivich, M., and Wollman, H. (1967). Effects of hypoxia and normocarbia on cerebral blood flow and metabolism in conscious man. J. Appl. Physiol. *23*, 183–189.

Coverdale, N.S., Lalande, S., Perrotta, A., and Shoemaker, J.K. (2015). Heterogeneous patterns of vasoreactivity in the middle cerebral and internal carotid arteries. Am. J. Physiol. Heart Circ. Physiol. *308*, H1030-1038.

Coverdale, N.S., Badrov, M.B., and Shoemaker, J.K. (2017). Impact of age on cerebrovascular dilation versus reactivity to hypercapnia. J. Cereb. Blood Flow Metab. *37*, 344–355.

Cox, S.B., Woolsey, T.A., and Rovainen, C.M. (1993). Localized Dynamic Changes in Cortical Blood Flow with Whisker Stimulation Corresponds to Matched Vascular and Neuronal Architecture of Rat Barrels. J. Cereb. Blood Flow Metab. *13*, 899–913.

Crompton, M.R. (1962). The pathology of ruptured middle-cerebral aneurysms with special reference to the differences between the sexes. Lancet Lond. Engl. *2*, 421–425.

Dahl, A., Russell, D., Rootwelt, K., Nyberg-Hansen, R., and Kerty, E. (1995). Cerebral vasoreactivity assessed with transcranial Doppler and regional cerebral blood flow measurements. Dose, serum concentration, and time course of the response to acetazolamide. Stroke *26*, 2302–2306.

Dalbak, L.G., Straand, J., and Melbye, H. (2015). Should pulse oximetry be included in GPs' assessment of patients with obstructive lung disease? Scand. J. Prim. Health Care *33*, 305–310.

Dandona, P., James, I.M., Newbury, P.A., Woollard, M.L., and Beckett, A.G. (1978). Cerebral blood flow in diabetes mellitus: evidence of abnormal cerebrovascular reactivity. Br. Med. J. *2*, 325–326.

Davis, S.M., Ackerman, R.H., Correia, J.A., Alpert, N.M., Chang, J., Buonanno, F., Kelley, R.E., Rosner, B., and Taveras, J.M. (1983). Cerebral blood flow and cerebrovascular CO2 reactivity in stroke-age normal controls. Neurology *33*, 391–399.

Deegan, Sorond, Galica, Lipsitz, O'Laighin, and Serrador (2011). Elderly Women Regulate Brain Blood Flow Better Than Men Do. Stroke *42*, 1988–1993.

Deer, R.R., and Stallone, J.N. (2016). Effects of estrogen on cerebrovascular function: age-dependent shifts from beneficial to detrimental in small cerebral arteries of the rat. Am. J. Physiol. - Heart Circ. Physiol. *310*, H1285–H1294.

Demirkaya, S., Uluc, K., Bek, S., and Vural, O. (2008). Normal blood flow velocities of basal cerebral arteries decrease with advancing age: a transcranial Doppler sonography study. Tohoku J. Exp. Med. *214*, 145–149.

Diomedi, M., Cupini, L.M., Rizzato, B., Ferrante, F., Giacomini, P., and Silvestrini, M. (2001). Influence of physiologic oscillation of estrogens on cerebral hemodynamics. J. Neurol. Sci. *185*, 49–53.

Donahue, M.J., Dethrage, L.M., Faraco, C.C., Jordan, L.C., Clemmons, P., Singer, R., Mocco, J., Shyr, Y., Desai, A., O'Duffy, A., et al. (2014). Routine clinical evaluation of cerebrovascular reserve capacity using carbogen in patients with intracranial stenosis. Stroke *45*, 2335–2341.

Dörfler, P., Puls, I., Schliesser, M., Mäurer, M., and Becker, G. (2000). Measurement of cerebral blood flow volume by extracranial sonography. J. Cereb. Blood Flow Metab. Off. J. Int. Soc. Cereb. Blood Flow Metab. *20*, 269–271.

Easton, P.A., Slykerman, L.J., and Anthonisen, N.R. (1986). Ventilatory response to sustained hypoxia in normal adults. J. Appl. Physiol. Bethesda Md 1985 *61*, 906–911.

Ellsworth, M.L., Forrester, T., Ellis, C.G., and Dietrich, H.H. (1995). The erythrocyte as a regulator of vascular tone. Am. J. Physiol. *269*, H2155-2161.

Eriksson, S., Hagenfeldt, L., Law, D., Patrono, C., Pinca, E., and Wennmalm, A. (1983). Effect of prostaglandin synthesis inhibitors on basal and carbon dioxide stimulated cerebral blood flow in man. Acta Physiol. Scand. *117*, 203–211.

Evans, D.H. (1985). On the measurement of the mean velocity of blood flow over the cardiac cycle using Doppler ultrasound. Ultrasound Med. Biol. *11*, 735–741.

Fan, A.P., Jahanian, H., Holdsworth, S.J., and Zaharchuk, G. (2016). Comparison of cerebral blood flow measurement with [15O]-water positron emission tomography and arterial spin labeling magnetic resonance imaging: A systematic review. J. Cereb. Blood Flow Metab. *36*, 842–861.

Fantini, S., Sassaroli, A., Tgavalekos, K.T., and Kornbluth, J. (2016). Cerebral blood flow and autoregulation: current measurement techniques and prospects for noninvasive optical methods. Neurophotonics *3*.

Faul, F., Erdfelder, E., Lang, A.-G., and Buchner, A. (2007). G*Power 3: a flexible statistical power analysis program for the social, behavioral, and biomedical sciences. Behav. Res. Methods *39*, 175–191.

Fierstra, J., Sobczyk, O., Battisti-Charbonney, A., Mandell, D.M., Poublanc, J., Crawley, A.P., Mikulis, D.J., Duffin, J., and Fisher, J.A. (2013). Measuring cerebrovascular reactivity: what stimulus to use? J. Physiol. *591*, 5809–5821.

Fisher, J.A. (2016). The CO2 stimulus for cerebrovascular reactivity: Fixing inspired concentrations vs. targeting end-tidal partial pressures. J. Cereb. Blood Flow Metab. *36*, 1004–1011.

Flodin, P., Jonasson, L.S., Riklund, K., Nyberg, L., and Boraxbekk, C.J. (2017). Does Aerobic Exercise Influence Intrinsic Brain Activity? An Aerobic Exercise Intervention among Healthy Old Adults. Front. Aging Neurosci. *9*.

Floyd, T.F., Clark, J.M., Gelfand, R., Detre, J.A., Ratcliffe, S., Guvakov, D., Lambertsen, C.J., and Eckenhoff, R.G. (2003). Independent cerebral vasoconstrictive effects of hyperoxia and accompanying arterial hypocapnia at 1 ATA. J. Appl. Physiol. Bethesda Md 1985 *95*, 2453–2461.

Flück, D., Beaudin, A.E., Steinback, C.D., Kumarpillai, G., Shobha, N., McCreary, C.R., Peca, S., Smith, E.E., and Poulin, M.J. (2014). Effects of aging on the association between cerebrovascular responses to visual stimulation, hypercapnia and arterial stiffness. Front. Physiol. *5*.

Foerstl, H., Biedert, S., and Hewer, W. (1989). Multiinfarct and Alzheimer-type dementia investigated by transcranial Doppler sonography. Biol. Psychiatry *26*, 590–594.

Fog, M. (1938). THE RELATIONSHIP BETWEEN THE BLOOD PRESSURE AND THE TONIC REGULATION OF THE PIAL ARTERIES. J. Neurol. Psychiatry *1*, 187–197.

Forster, B.B., MacKay, A.L., Whittall, K.P., Kiehl, K.A., Smith, A.M., Hare, R.D., and Liddle, P.F. (1998). Functional magnetic resonance imaging: the basics of blood-oxygen-level dependent (BOLD) imaging. Can. Assoc. Radiol. J. J. Assoc. Can. Radiol. *49*, 320–329.

Freitag, M.H., Peila, R., Masaki, K., Petrovitch, H., Ross, G.W., White, L.R., and Launer, L.J. (2006). Midlife pulse pressure and incidence of dementia: the Honolulu-Asia Aging Study. Stroke *37*, 33–37.

Furuhata, H., Suzuki, N., Yoshimura, S., Kodaira, K., Aoyagi, T., Obara, K., Fujishiro, K., Shimizu, H., and Mikawa, H. (1983). Non-invasive and quantitative measurement of volume flow-rate at internal and external carotid and vertebral arteries. Ultrasound Med. Biol. *Suppl 2*, 239–242.

Gadda, G., Majka, M., Zieliński, P., Gambaccini, M., and Taibi, A. (2018). A multiscale model for the simulation of cerebral and extracerebral blood flows and pressures in humans. Eur. J. Appl. Physiol. *118*, 2443–2454.

Gaigalaite, V., Vilimas, A., Ozeraitiene, V., Dementaviciene, J., Janilionis, R., Kalibatiene, D., and Rocka, S. (2016). Association between vertebral artery hypoplasia and posterior circulation stroke. BMC Neurol. *16*, 118.

Galvin, S.D., Celi, L.A., Thomas, K.N., Clendon, T.R., Galvin, I.F., Bunton, R.W., and Ainslie, P.N. (2010). Effects of age and coronary artery disease on cerebrovascular reactivity to carbon dioxide in humans. Anaesth. Intensive Care *38*, 710–717.

Ghisleni, C., Bollmann, S., Biason-Lauber, A., Poil, S.-S., Brandeis, D., Martin, E., Michels, L., Hersberger, M., Suckling, J., Klaver, P., et al. (2015). Effects of Steroid Hormones on Sex Differences in Cerebral Perfusion. PLoS ONE *10*.

Gibbs, F.A., Gibbs, E.L., and Lennox, W.G. (1935). Changes in human cerebral blood flow consequent on alterations in blood gases. Am. J. Physiol.-Leg. Content *111*, 557–563.

Giller, C.A., Hodges, K., and Batjer, H.H. (1990). Transcranial Doppler pulsatility in vasodilation and stenosis. J. Neurosurg. *72*, 901–906.

Girouard, H., and Iadecola, C. (2006). Neurovascular coupling in the normal brain and in hypertension, stroke, and Alzheimer disease. J. Appl. Physiol. *100*, 328–335.

Glenner, G.G., and Wong, C.W. (1984). Alzheimer's disease: initial report of the purification and characterization of a novel cerebrovascular amyloid protein. Biochem. Biophys. Res. Commun. *120*, 885–890.

Godin, G. (2011). The Godin-Shephard Leisure-Time Physical Activity Questionnaire. Health Fit. J. Can. *4*, 18–22.

Godin, G., and Shephard, R.J. (1985). A simple method to assess exercise behavior in the community. Can. J. Appl. Sport Sci. J. Can. Sci. Appl. Au Sport *10*, 141–146.

Gorelick, P.B., Scuteri, A., Black, S.E., Decarli, C., Greenberg, S.M., Iadecola, C., Launer, L.J., Laurent, S., Lopez, O.L., Nyenhuis, D., et al. (2011). Vascular contributions to cognitive impairment and dementia: a statement for healthcare professionals from the american heart association/american stroke association. Stroke *42*, 2672–2713.

Gosling, R.G., and King, D.H. (1974). Arterial assessment by Doppler-shift ultrasound. Proc. R. Soc. Med. *67*, 447–449.

Gottesman, R.F., Schneider, A.L.C., Zhou, Y., Coresh, J., Green, E., Gupta, N., Knopman, D.S., Mintz, A., Rahmim, A., Sharrett, A.R., et al. (2017). Association Between Midlife Vascular Risk Factors and Estimated Brain Amyloid Deposition. JAMA *317*, 1443–1450.

Guo, S., and Lo, E.H. (2009). Dysfunctional cell-cell signaling in the neurovascular unit as a paradigm for central nervous system disease. Stroke *40*, S4-7.

Guo, H., Tierney, N., Schaller, F., Raven, P.B., Smith, S.A., and Shi, X. (2006). Cerebral autoregulation is preserved during orthostatic stress superimposed with systemic hypotension. J. Appl. Physiol. Bethesda Md 1985 *100*, 1785–1792.

Gupta, A., Chazen, J.L., Hartman, M., Delgado, D., Anumula, N., Shao, H., Mazumdar, M., Segal, A.Z., Kamel, H., Leifer, D., et al. (2012). Cerebrovascular reserve and stroke risk in patients with carotid stenosis or occlusion: a systematic review and meta-analysis. Stroke *43*, 2884–2891.

Haast, R.A.M., Gustafson, D.R., and Kiliaan, A.J. (2012). Sex differences in stroke. J. Cereb. Blood Flow Metab. *32*, 2100–2107.

Häggendal, E., and Johansson, B. (1965). Effects of arterial carbon dioxide tension and oxygen saturation on cerebral blood flow autoregulation in dogs. Acta Physiol. Scand. Suppl. *258*, 27–53.

Hagstadius, S., and Risberg, J. (1989). Regional cerebral blood flow characteristics and variations with age in resting normal subjects. Brain Cogn. *10*, 28–43.

Haight, T.J., Bryan, R.N., Erus, G., Davatzikos, C., Jacobs, D.R., D'Esposito, M., Lewis, C.E., and Launer, L.J. (2015). Vascular risk factors, cerebrovascular reactivity, and the default-mode brain network. NeuroImage *115*, 7–16.

Hall, C.N., Reynell, C., Gesslein, B., Hamilton, N.B., Mishra, A., Sutherland, B.A., O'Farrell, F.M., Buchan, A.M., Lauritzen, M., and Attwell, D. (2014). Capillary pericytes regulate cerebral blood flow in health and disease. Nature *508*, 55–60.

Hamel, E. (2006). Perivascular nerves and the regulation of cerebrovascular tone. J. Appl. Physiol. *100*, 1059–1064.

Hamner, J.W., and Tan, C.O. (2014). Relative contributions of sympathetic, cholinergic, and myogenic mechanisms to cerebral autoregulation. Stroke *45*, 1771–1777.

Harmel, M.H., and Hafkenschiel, J.H. (1949). The effect of bilateral stellate ganglion block on the cerebral circulation in normotensive and hypertensive patients. J. Clin. Invest. *28*, 415–418.

Harper, A.M., and Bell, R.A. (1963). THE EFFECT OF METABOLIC ACIDOSIS AND ALKALOSIS ON THE BLOOD FLOW THROUGH THE CEREBRAL CORTEX. J. Neurol. Neurosurg. Psychiatry *26*, 341–344.

Harper, A.M., and Glass, H.I. (1965). Effect of alterations in the arterial carbon dioxide tension on the blood flow through the cerebral cortex at normal and low arterial blood pressures. J. Neurol. Neurosurg. Psychiatry *28*, 449–452.

Hays, C.C., Zlatar, Z.Z., and Wierenga, C.E. (2016). The Utility of Cerebral Blood Flow as a Biomarker of Preclinical Alzheimer's Disease. Cell. Mol. Neurobiol. *36*, 167–179.

Heffernan, K.S., Augustine, J.A., Lefferts, W.K., Spartano, N.L., Hughes, W.E., Jorgensen, R.S., and Gump, B.B. (2018). Arterial stiffness and cerebral hemodynamic pulsatility during cognitive engagement in younger and older adults. Exp. Gerontol. *101*, 54–62.

Heistad, D.D., Marcus, M.L., and Abboud, F.M. (1978a). Role of Large Arteries in Regulation of Cerebral Blood Flow in Dogs. J. Clin. Invest. *62*, 761–768.

Heistad, D.D., Marcus, M.L., and Gross, P.M. (1978b). Effects of sympathetic nerves on cerebral vessels in dog, cat, and monkey. Am. J. Physiol. *235*, H544-552.

Henley, B.C., Shin, D.C., Zhang, R., and Marmarelis, V.Z. (2017). Compartmental and Data-Based Modeling of Cerebral Hemodynamics: Nonlinear Analysis. IEEE Trans. Biomed. Eng. *64*, 1078–1088.

Herscovitch, P., Markham, J., and Raichle, M.E. (1983). Brain blood flow measured with intravenous H2(15)O. I. Theory and error analysis. J. Nucl. Med. Off. Publ. Soc. Nucl. Med. *24*, 782–789.

Hoiland, R.L., and Ainslie, P.N. (2016). CrossTalk proposal: The middle cerebral artery diameter does change during alterations in arterial blood gases and blood pressure. J. Physiol. *594*, 4073–4075.

Hoiland, R.L., Bain, A.R., Rieger, M.G., Bailey, D.M., and Ainslie, P.N. (2015). Hypoxemia, oxygen content, and the regulation of cerebral blood flow. Am. J. Physiol.-Regul. Integr. Comp. Physiol. *310*, R398–R413.

Hoiland, R.L., Tymko, M.M., Bain, A.R., Wildfong, K.W., Monteleone, B., and Ainslie, P.N. (2016). Carbon dioxide-mediated vasomotion of extra-cranial cerebral arteries in humans: a role for prostaglandins? J. Physiol. *594*, 3463–3481.

Hoiland, R.L., Fisher, J.A., and Ainslie, P.N. (2019). Regulation of the Cerebral Circulation by Arterial Carbon Dioxide. Compr. Physiol. *9*, 1101–1154.

Hong, J.M., Chung, C.-S., Bang, O.Y., Yong, S.W., Joo, I.S., and Huh, K. (2009). Vertebral artery dominance contributes to basilar artery curvature and peri-vertebrobasilar junctional infarcts. J. Neurol. Neurosurg. Psychiatry *80*, 1087–1092.

Hori, D., Nomura, Y., Ono, M., Joshi, B., Mandal, K., Cameron, D., Kocherginsky, M., and Hogue, C.W. (2017). Optimal blood pressure during cardiopulmonary bypass defined by cerebral autoregulation monitoring. J. Thorac. Cardiovasc. Surg. *154*, 1590-1598.e2.

Hosford, P.S., and Gourine, A.V. (2019). What is the key mediator of the neurovascular coupling response? Neurosci. Biobehav. Rev. *96*, 174–181.

Hu, X.-Y., Li, Z.-X., Liu, H.-Q., Zhang, M., Wei, M.-L., Fang, S., Chen, W., Pan, H., Huang, J.-X., Zhu, Y.-M., et al. (2013). Relationship between vertebral artery hypoplasia and posterior circulation stroke in Chinese patients. Neuroradiology *55*, 291–295.

Iadecola, C. (2004). Neurovascular regulation in the normal brain and in Alzheimer's disease. Nat. Rev. Neurosci. *5*, 347–360.

Iadecola, C. (2010). The overlap between neurodegenerative and vascular factors in the pathogenesis of dementia. Acta Neuropathol. (Berl.) *120*, 287–296.

Iadecola, C. (2017). The Neurovascular Unit Coming of Age: A Journey through Neurovascular Coupling in Health and Disease. Neuron *96*, 17–42.

Ide, K., Boushel, R., Sørensen, H.M., Fernandes, A., Cai, Y., Pott, F., and Secher, N.H. (2000). Middle cerebral artery blood velocity during exercise with beta-1 adrenergic and unilateral stellate ganglion blockade in humans. Acta Physiol. Scand. *170*, 33–38.

Ide, K., Worthley, M., Anderson, T., and Poulin, M.J. (2007). Effects of the nitric oxide synthase inhibitor L-NMMA on cerebrovascular and cardiovascular responses to hypoxia and hypercapnia in humans. J. Physiol. *584*, 321–332.

Iliff, L.D., Zilkha, E., Boulay, G.H.D., Marshall, J., Russell, R.W.R., and Symon, L. (1974). Cerebrovascular CO2 Reactivity of the Fast and Slow Clearing Compartments. Stroke *5*, 607–611.

Iooss, B., Lhuillier, C., and Jeanneau, H. (2002). Numerical simulation of transit-time ultrasonic flowmeters: uncertainties due to flow profile and fluid turbulence. Ultrasonics *40*, 1009–1015.

Iqbal, S. (2013). A Comprehensive Study of the Anatomical Variations of the Circle of Willis in Adult Human Brains. J. Clin. Diagn. Res. JCDR *7*, 2423–2427.

Iscoe, S., and Fisher, J.A. (2005). Hyperoxia-induced hypocapnia: an underappreciated risk. Chest *128*, 430–433.

Ito, H., Kanno, I., Kato, C., Sasaki, T., Ishii, K., Ouchi, Y., Iida, A., Okazawa, H., Hayashida, K., Tsuyuguchi, N., et al. (2004). Database of normal human cerebral blood flow, cerebral blood volume, cerebral oxygen extraction fraction and cerebral metabolic rate of oxygen measured by positron emission tomography with 15O-labelled carbon dioxide or water, carbon monoxide and oxygen: a multicentre study in Japan. Eur. J. Nucl. Med. Mol. Imaging *31*, 635–643.

Itoh, M., Hatazawa, J., Miyazawa, H., Matsui, H., Meguro, K., Yanai, K., Kubota, K., Watanuki, S., Ido, T., and Matsuzawa, T. (1990). Stability of cerebral blood flow and oxygen metabolism during normal aging. Gerontology *36*, 43–48.

Iturria-Medina, Y., Sotero, R.C., Toussaint, P.J., Mateos-Pérez, J.M., Evans, A.C., and Alzheimer's Disease Neuroimaging Initiative (2016). Early role of vascular dysregulation on late-onset Alzheimer's disease based on multifactorial data-driven analysis. Nat. Commun. *7*, 11934.

Jaruchart, T., Suwanwela, N.C., Tanaka, H., and Suksom, D. (2016). Arterial stiffness is associated with age-related differences in cerebrovascular conductance. Exp. Gerontol. *73*, 59–64.

Jellinger, K.A. (2006). Alzheimer 100--highlights in the history of Alzheimer research. J. Neural Transm. Vienna Austria 1996 *113*, 1603–1623.

Jeng, J.S., Yip, P.K., Huang, S.J., and Kao, M.C. (1999). Changes in hemodynamics of the carotid and middle cerebral arteries before and after endoscopic sympathectomy in patients with palmar hyperhidrosis: preliminary results. J. Neurosurg. *90*, 463–467.

Johnson, N.A., Jahng, G.-H., Weiner, M.W., Miller, B.L., Chui, H.C., Jagust, W.J., Gorno-Tempini, M.L., and Schuff, N. (2005). Pattern of Cerebral Hypoperfusion in Alzheimer Disease and Mild Cognitive Impairment Measured with Arterial Spin-labeling MR Imaging: Initial Experience. Radiology *234*, 851–859.

Johnson, S.C., La Rue, A., Hermann, B.P., Xu, G., Koscik, R.L., Jonaitis, E.M., Bendlin, B.B., Hogan, K.J., Roses, A.D., Saunders, A.M., et al. (2011). The effect of TOMM40 poly-T length on gray matter volume and cognition in middle-aged persons with APOE ε3/ε3 genotype. Alzheimers Dement. *7*, 456–465.

Johnson, S.C., Koscik, R.L., Jonaitis, E.M., Clark, L.R., Mueller, K.D., Berman, S.E., Bendlin, B.B., Engelman, C.D., Okonkwo, O.C., Hogan, K.J., et al. (2017). The Wisconsin Registry for Alzheimer's Prevention: A review of findings and current directions. Alzheimers Dement. Diagn. Assess. Dis. Monit. *10*, 130–142.

Jones, E.G. (1970). On the mode of entry of blood vessels into the cerebral cortex. J. Anat. *106*, 507–520.

Joyner, M.J., Barnes, J.N., Hart, E.C., Wallin, B.G., and Charkoudian, N. (2015). Neural Control of the Circulation: How Sex and Age Differences Interact in Humans. Compr. Physiol. *5*, 193–215.

Kang, J., Lemaire, H.G., Unterbeck, A., Salbaum, J.M., Masters, C.L., Grzeschik, K.H., Multhaup, G., Beyreuther, K., and Müller-Hill, B. (1987). The precursor of Alzheimer's disease amyloid A4 protein resembles a cell-surface receptor. Nature *325*, 733–736.

Karnik Ronald, Valentin Andreas, Winkler Walther-Benedikt, Khaffaf Nadja, Donath Peter, and Slany Jörg (1996). Sex-Related Differences in Acetazolamide-Induced Cerebral Vasomotor Reactivity. Stroke *27*, 56–58.

Kassner, A., Winter, J.D., Poublanc, J., Mikulis, D.J., and Crawley, A.P. (2010). Blood-oxygen level dependent MRI measures of cerebrovascular reactivity using a controlled respiratory challenge: reproducibility and gender differences. J. Magn. Reson. Imaging *31*, 298–304.

Kastrup, Dichgans, Niemeier, and Schabet Martin (1998). Changes of Cerebrovascular CO2 Reactivity During Normal Aging. Stroke *29*, 1311–1314.

Kastrup, A., Thomas, C., Hartmann, C., and Schabet, M. (1997). Sex dependency of cerebrovascular CO2 reactivity in normal subjects. Stroke *28*, 2353–2356.

Kastrup, A., Happe, V., Hartmann, C., and Schabet, M. (1999). Gender-related effects of indomethacin on cerebrovascular CO2 reactivity. J. Neurol. Sci. *162*, 127–132.

Kearney-Schwartz, A., Rossignol, P., Bracard, S., Felblinger, J., Fay, R., Boivin, J.-M., Lecompte, T., Lacolley, P., Benetos, A., and Zannad, F. (2009). Vascular structure and function is correlated to cognitive performance and white matter hyperintensities in older hypertensive patients with subjective memory complaints. Stroke *40*, 1229–1236.

Kelly, R., Hayward, C., Avolio, A., and O'Rourke, M. (1989). Noninvasive determination of age-related changes in the human arterial pulse. Circulation *80*, 1652–1659.

Kety, S.S. (1956). Human cerebral blood flow and oxygen consumption as related to aging. J. Chronic Dis. *3*, 478–486.

Kety, S.S., and Schmidt, C.F. (1945). The determination of cerebral blood flow in man by the use of nitrous oxide in low concentrations. Am. J. Physiol.-Leg. Content *143*, 53–66.

Kety, S.S., and Schmidt, C.F. (1946). Measurement of cerebral blood flow and cerebral oxygen consumption in man. Fed. Proc. *5*, 264.

Kety, S.S., and Schmidt, C.F. (1948a). The nitrous oxide method for the quantative determination of cerebral blood flow in man: theory, procedure, and normal values. J. Clin. Invest. *27*, 476–483.

Kety, S.S., and Schmidt, C.F. (1948b). The effects of altered arterial tensions of carbon dioxide and oxygen on cerebral blood flow and cerebral oxygen consumption of normal young men. J. Clin. Invest. *27*, 484–492.

Khan, M.A., Liu, J., Tarumi, T., Lawley, J.S., Liu, P., Zhu, D.C., Lu, H., and Zhang, R. (2017). Measurement of cerebral blood flow using phase contrast magnetic resonance imaging and duplex ultrasonography. J. Cereb. Blood Flow Metab. *37*, 541–549.

Kidwell, C.S., el-Saden, S., Livshits, Z., Martin, N.A., Glenn, T.C., and Saver, J.L. (2001). Transcranial Doppler pulsatility indices as a measure of diffuse small-vessel disease. J. Neuroimaging Off. J. Am. Soc. Neuroimaging *11*, 229–235.

Kiliç, T., and Akakin, A. (2008). Anatomy of cerebral veins and sinuses. Front. Neurol. Neurosci. *23*, 4–15.

Kilroy, Apostolova, Liu, Yan, Ringman, and Wang (2014). Reliability of two-dimensional and three-dimensional pseudo-continuous arterial spin labeling perfusion MRI in elderly populations: comparison with 15O-water positron emission tomography (J Magn Reson Imaging).

Kim, S.-G., and Ogawa, S. (2012). Biophysical and physiological origins of blood oxygenation level-dependent fMRI signals. J. Cereb. Blood Flow Metab. Off. J. Int. Soc. Cereb. Blood Flow Metab. *32*, 1188–1206.

Kinahan, P.E., and Noll, D.C. (1999). A direct comparison between whole-brain PET and BOLD fMRI measurements of single-subject activation response. NeuroImage *9*, 430–438.

Kisler, K., Nelson, A.R., Montagne, A., and Zlokovic, B.V. (2017). Cerebral blood flow regulation and neurovascular dysfunction in Alzheimer disease. Nat. Rev. Neurosci. *18*, 419–434.

Kitazono, T., Faraci, F.M., Taguchi, H., and Heistad, D.D. (1995). Role of Potassium Channels in Cerebral Blood Vessels. Stroke *26*, 1713–1723.

Kivipelto, M., Helkala, E.L., Laakso, M.P., Hänninen, T., Hallikainen, M., Alhainen, K., Soininen, H., Tuomilehto, J., and Nissinen, A. (2001). Midlife vascular risk factors and Alzheimer's disease in later life: longitudinal, population based study. BMJ *322*, 1447–1451.

Krejza, J., Rudzinski, W., Arkuszewski, M., Onuoha, O., and Melhem, E.R. (2013). Cerebrovascular reactivity across the menstrual cycle in young healthy women. Neuroradiol. J. *26*, 413–419.

Kulyk, C., Voltan, C., Simonetto, M., Palmieri, A., Farina, F., Vodret, F., Viaro, F., and Baracchini, C. (2018). Vertebral artery hypoplasia: an innocent lamb or a disguise? J. Neurol. *265*, 2346–2352.

Lambertsen, C.J., Semple, S.J., Smyth, M.G., and Gelfand, R. (1961). H and pCO2 as chemical factors in respiratory and cerebral circulatory control. J. Appl. Physiol. *16*, 473–484.

Lassen, N.A. (1959). Cerebral Blood Flow and Oxygen Consumption in Man. Physiol. Rev. *39*, 183–238.

Lautt, W.W. (1989). Resistance or conductance for expression of arterial vascular tone. Microvasc. Res. *37*, 230–236.

Lee, C., Lopez, O.L., Becker, J.T., Raji, C., Dai, W., Kuller, L.H., and Gach, H.M. (2009). Imaging cerebral blood flow in the cognitively normal aging brain with arterial spin labeling: implications for imaging of neurodegenerative disease. J. Neuroimaging Off. J. Am. Soc. Neuroimaging *19*, 344–352.

Leenders, K.L., Perani, D., Lammertsma, A.A., Heather, J.D., Buckingham, P., Healy, M.J., Gibbs, J.M., Wise, R.J., Hatazawa, J., and Herold, S. (1990). Cerebral blood flow, blood volume and oxygen utilization. Normal values and effect of age. Brain J. Neurol. *113 (Pt 1)*, 27–47.

Levine, B.D., Giller, C.A., Lane, L.D., Buckey, J.C., and Blomqvist, C.G. (1994). Cerebral versus systemic hemodynamics during graded orthostatic stress in humans. Circulation *90*, 298–306.

van Lieshout, J.J., Pott, F., Madsen, P.L., van Goudoever, J., and Secher, N.H. (2001). Muscle tensing during standing: effects on cerebral tissue oxygenation and cerebral artery blood velocity. Stroke *32*, 1546–1551.

Lim, E.-Y., Yang, D.-W., Cho, A.-H., and Shim, Y.S. (2018). Cerebrovascular Hemodynamics on Transcranial Doppler Ultrasonography and Cognitive Decline in Mild Cognitive Impairment. J. Alzheimers Dis. JAD *65*, 651–657.

Linden, L. (1955). The effect of stellate ganglion block on cerebral circulation in cerebrovascular accidents. Acta Med. Scand. Suppl. *301*, 1–110.

Lipsitz, L.A., Mukai, S., Hamner, J., Gagnon, M., and Babikian, V. (2000). Dynamic regulation of middle cerebral artery blood flow velocity in aging and hypertension. Stroke *31*, 1897–1903.

Lipton, P. (1999). Ischemic cell death in brain neurons. Physiol. Rev. *79*, 1431–1568.

Liu, W., Lou, X., and Ma, L. (2016). Use of 3D pseudo-continuous arterial spin labeling to characterize sex and age differences in cerebral blood flow. Neuroradiology *58*, 943–948.

Liu, X., Li, C., Falck, J.R., Harder, D.R., and Koehler, R.C. (2012a). Relative contribution of cyclooxygenases, epoxyeicosatrienoic acids, and pH to the cerebral blood flow response to vibrissal stimulation. Am. J. Physiol. - Heart Circ. Physiol. *302*, H1075–H1085.

Liu, Y., Zhu, X., Feinberg, D., Guenther, M., Gregori, J., Weiner, M.W., and Schuff, N. (2012b). Arterial spin labeling MRI study of age and gender effects on brain perfusion hemodynamics. Magn. Reson. Med. *68*, 912–922.

Loecher, M., Schrauben, E., Johnson, K.M., and Wieben, O. (2016). Phase unwrapping in 4D MR flow with a 4D single-step laplacian algorithm. J. Magn. Reson. Imaging *43*, 833–842.

Longden, T.A., Dabertrand, F., Koide, M., Gonzales, A.L., Tykocki, N.R., Brayden, J.E., Hill-Eubanks, D., and Nelson, M.T. (2017). Capillary K+-sensing initiates retrograde hyperpolarization to increase local cerebral blood flow. Nat. Neurosci. *20*, 717–726.

López-Otín, C., Blasco, M.A., Partridge, L., Serrano, M., and Kroemer, G. (2013). The Hallmarks of Aging. Cell *153*, 1194–1217.

Lu, H., Xu, F., Rodrigue, K.M., Kennedy, K.M., Cheng, Y., Flicker, B., Hebrank, A.C., Uh, J., and Park, D.C. (2011). Alterations in Cerebral Metabolic Rate and Blood Supply across the Adult Lifespan. Cereb. Cortex N. Y. NY *21*, 1426–1434.

Lucas, S.J.E., Tzeng, Y.C., Galvin, S.D., Thomas, K.N., Ogoh, S., and Ainslie, P.N. (2010). Influence of changes in blood pressure on cerebral perfusion and oxygenation. Hypertens. Dallas Tex 1979 *55*, 698–705.

Madureira, J., Castro, P., and Azevedo, E. (2017). Demographic and Systemic Hemodynamic Influences in Mechanisms of Cerebrovascular Regulation in Healthy Adults. J. Stroke Cerebrovasc. Dis. *26*, 500–508.

Maillard, P., Mitchell, G.F., Himali, J.J., Beiser, A., Fletcher, E., Tsao, C.W., Pase, M.P., Satizabal, C.L., Vasan, R.S., Seshadri, S., et al. (2017). Aortic Stiffness, Increased White Matter Free Water, and Altered Microstructural Integrity: A Continuum of Injury. Stroke *48*, 1567–1573.

Mandell, Han, Poublanc, Crawley, Stainsby, Fisher, and Mikulis (2008). Mapping cerebrovascular reactivity using blood oxygen level-dependent MRI in Patients with arterial steno-occlusive disease: comparison with arterial spin labeling MRI (Stroke).

Markus, H., and Cullinane, M. (2001). Severely impaired cerebrovascular reactivity predicts stroke and TIA risk in patients with carotid artery stenosis and occlusion. Brain J. Neurol. *124*, 457–467.

Markus, H., and Harrison, M. (1992). Estimation of cerebrovascular reactivity using transcranial Doppler, including the use of breath-holding as the vasodilatory stimulus. Stroke *23*, 668–673.

Markwalder, T.-M., Grolimund, P., Seiler, R.W., Roth, F., and Aaslid, R. (1984). Dependency of Blood Flow Velocity in the Middle Cerebral Artery on End-Tidal Carbon Dioxide Partial Pressure—A Transcranial Ultrasound Doppler Study. J. Cereb. Blood Flow Metab. *4*, 368–372.

Marmarelis, V.Z., Mitsis, G.D., Shin, D.C., and Zhang, R. (2016). Multiple-input nonlinear modelling of cerebral haemodynamics using spontaneous arterial blood pressure, end-tidal CO2 and heart rate measurements. Philos. Transact. A Math. Phys. Eng. Sci. *374*.

Martin, A.J., Friston, K.J., Colebatch, J.G., and Frackowiak, R.S.J. (1991). Decreases in Regional Cerebral Blood Flow with Normal Aging. J. Cereb. Blood Flow Metab. *11*, 684–689.

Martin, P.J., Evans, D.H., and Naylor, A.R. (1994). Transcranial color-coded sonography of the basal cerebral circulation. Reference data from 115 volunteers. Stroke *25*, 390–396.

Matsuda, Maeda, Yamada, Gui, Tonami, and Hisada (1984). Age-matched normal values and topographic maps for regional cerebral blood flow measurements by Xe-133 inhalation. Stroke *15*, 336–342.

Matteis, M., Troisi, E., Monaldo, B.C., Caltagirone, C., and Silvestrini, M. (1998). Age and sex differences in cerebral hemodynamics: a transcranial Doppler study. Stroke *29*, 963–967.

Melamed, E., Lavy, S., Bentin, S., Cooper, G., and Rinot, Y. (1980). Reduction in regional cerebral blood flow during normal aging in man. Stroke *11*, 31–35.

Meng, L., Hou, W., Chui, J., Han, R., and Gelb, A.W. (2015). Cardiac Output and Cerebral Blood Flow: The Integrated Regulation of Brain Perfusion in Adult Humans. Anesthesiology *123*, 1198–1208.

Mies, G., Ishimaru, S., Xie, Y., Seo, K., and Hossmann, K.A. (1991). Ischemic thresholds of cerebral protein synthesis and energy state following middle cerebral artery occlusion in rat. J. Cereb. Blood Flow Metab. Off. J. Int. Soc. Cereb. Blood Flow Metab. *11*, 753–761.

Mikhail Kellawan, J., Harrell, J.W., Schrauben, E.M., Hoffman, C.A., Roldan-Alzate, A., Schrage, W.G., and Wieben, O. (2016). Quantitative cerebrovascular 4D flow MRI at rest and during hypercapnia challenge. Magn. Reson. Imaging *34*, 422–428.

Mikulis, D.J., Krolczyk, G., Desal, H., Logan, W., Deveber, G., Dirks, P., Tymianski, M., Crawley, A., Vesely, A., Kassner, A., et al. (2005). Preoperative and postoperative mapping of cerebrovascular reactivity in moyamoya disease by using blood oxygen level-dependent magnetic resonance imaging. J. Neurosurg. *103*, 347–355.

Miller, K.B., Howery, A.J., Harvey, R.E., Eldridge, M.W., and Barnes, J.N. (2018). Cerebrovascular Reactivity and Central Arterial Stiffness in Habitually Exercising Healthy Adults. Front. Physiol. *9*.

Miller, V.M., Garovic, V.D., Kantarci, K., Barnes, J.N., Jayachandran, M., Mielke, M.M., Joyner, M.J., Shuster, L.T., and Rocca, W.A. (2013). Sex-specific risk of cardiovascular disease and cognitive decline: pregnancy and menopause. Biol. Sex Differ. *4*, 6.

Mitchell, G.F. (2008). Effects of central arterial aging on the structure and function of the peripheral vasculature: implications for end-organ damage. J. Appl. Physiol. *105*, 1652–1660.

Mitchell, G.F., van Buchem, M.A., Sigurdsson, S., Gotal, J.D., Jonsdottir, M.K., Kjartansson, Ó., Garcia, M., Aspelund, T., Harris, T.B., Gudnason, V., et al. (2011). Arterial stiffness, pressure and flow pulsatility and brain structure and function: the Age, Gene/Environment Susceptibility – Reykjavik Study. Brain *134*, 3398–3407.

Mitsumura, H., Miyagawa, S., Komatsu, T., Hirai, T., Kono, Y., and Iguchi, Y. (2016). Relationship between Vertebral Artery Hypoplasia and Posterior Circulation Ischemia. J. Stroke Cerebrovasc. Dis. *25*, 266–269.

Miyazaki, M., and Kato, K. (1965). Measurement of Cerebral Blood Flow by Ultrasonic Doppler Technique. Jpn. Circ. J. *29*, 383–386.

van Mook, W.N.K.A., Rennenberg, R.J.M.W., Schurink, G.W., van Oostenbrugge, R.J., Mess, W.H., Hofman, P.A.M., and de Leeuw, P.W. (2005). Cerebral hyperperfusion syndrome. Lancet Neurol. *4*, 877–888.

Mosso, A. (1880). Sulla circolazione del cervello dell'uomo. Att R Accad Lincei *5*, 237–358.

Müller, H.R., Brunhölzl, C., Radü, E.W., and Buser, M. (1991). Sex and side differences of cerebral arterial caliber. Neuroradiology *33*, 212–216.

Murrell, C.J., Cotter, J.D., Thomas, K.N., Lucas, S.J.E., Williams, M.J.A., and Ainslie, P.N. (2013). Cerebral blood flow and cerebrovascular reactivity at rest and during sub-maximal exercise: effect of age and 12-week exercise training. Age Dordr. Neth. *35*, 905–920.

Neuroradiology, A.S. of (2005). Gray's Anatomy, 39th Edition: The Anatomical Basis of Clinical Practice. Am. J. Neuroradiol. *26*, 2703–2704.

Ng, I., Lim, J., and Wong, H.B. (2004). Effects of head posture on cerebral hemodynamics: its influences on intracranial pressure, cerebral perfusion pressure, and cerebral oxygenation. Neurosurgery *54*, 593–597; discussion 598.

Niiranen, T.J., Lyass, A., Larson, M.G., Hamburg, N.M., Benjamin, E.J., Mitchell, G.F., and Vasan, R.S. (2017). Prevalence, Correlates, and Prognosis of Healthy Vascular Aging in a Western Community-Dwelling Cohort: The Framingham Heart Study. Hypertension *70*, 267–274.

Numan, T., Bain, A.R., Hoiland, R.L., Smirl, J.D., Lewis, N.C., and Ainslie, P.N. (2014). Static autoregulation in humans: a review and reanalysis. Med. Eng. Phys. *36*, 1487–1495.

O'Connor, J.P.B. (2003). Thomas Willis and the background to Cerebri Anatome. J. R. Soc. Med. *96*, 139–143.

Ogawa, Y., Iwasaki, K., Aoki, K., Shibata, S., Kato, J., and Ogawa, S. (2007). Central hypervolemia with hemodilution impairs dynamic cerebral autoregulation. Anesth. Analg. *105*, 1389–1396, table of contents.

Ogeng'o, J., Olabu, B., Sinkeet, R., Ogeng'o, N.M., and Elbusaid, H. (2014). Vertebral Artery Hypoplasia in a Black Kenyan Population. Int. Sch. Res. Not. *2014*, 934510.

Ogoh, S., Brothers, R.M., Barnes, Q., Eubank, W.L., Hawkins, M.N., Purkayastha, S., O-Yurvati, A., and Raven, P.B. (2005). The effect of changes in cardiac output on middle cerebral artery mean blood velocity at rest and during exercise. J. Physiol. *569*, 697–704.

Ohta, S., Hadeishi, H., and Suzuki, M. (1990). Effect of Stellate Ganglion Block on Cerebral Blood Flow in Normoxemic and Hyperoxemic States. J. Neurosurg. Anesthesiol. *2*, 272–279.

Oláh, L., Valikovics, A., Bereczki, D., Fülesdi, B., Munkácsy, C., and Csiba, L. (2000). Gender-related differences in acetazolamide-induced cerebral vasodilatory response: a transcranial Doppler study. J. Neuroimaging *10*, 151–156.

Olesen, N.D., Nielsen, H.B., Olsen, N.V., and Secher, N.H. (2019). The age-related reduction in cerebral blood flow affects vertebral artery more than internal carotid artery blood flow. Clin. Physiol. Funct. Imaging *39*, 255–260.

O'Rourke, M.F. (1976). Pulsatile arterial haemodynamics in hypertension. Aust. N. Z. J. Med. *6 suppl 2*, 40–48.

Oudegeest-Sander, M.H., van Beek, A.H.E.A., Abbink, K., Olde Rikkert, M.G.M., Hopman, M.T.E., and Claassen, J.A.H.R. (2014). Assessment of dynamic cerebral autoregulation and cerebrovascular CO2 reactivity in ageing by measurements of cerebral blood flow and cortical oxygenation. Exp. Physiol. *99*, 586–598.

Pagani, M., Salmaso, D., Jonsson, C., Hatherly, R., Jacobsson, H., Larsson, S.A., and Wägner, A. (2002). Regional cerebral blood flow as assessed by principal component analysis and (99m)Tc-HMPAO SPET in healthy subjects at rest: normal distribution and effect of age and gender. Eur. J. Nucl. Med. Mol. Imaging *29*, 67–75.

Palazzo, P., Maggio, P., Passarelli, F., Altavilla, R., Altamura, C., Pasqualetti, P., and Vernieri, F. (2013). Lack of correlation between cerebral vasomotor reactivity and flow-mediated dilation in subjects without vascular disease. Ultrasound Med. Biol. *39*, 10–15.

Pantano, P., Baron, J.C., Lebrun-Grandié, P., Duquesnoy, N., Bousser, M.G., and Comar, D. (1984). Regional cerebral blood flow and oxygen consumption in human aging. Stroke *15*, 635–641.

Park, J.-H., Kim, J.-M., and Roh, J.-K. (2007). Hypoplastic vertebral artery: frequency and associations with ischaemic stroke territory. J. Neurol. Neurosurg. Psychiatry *78*, 954–958.

Peltonen, G.L., Harrell, J.W., Rousseau, C.L., Ernst, B.S., Marino, M.L., Crain, M.K., and Schrage, W.G. (2015). Cerebrovascular regulation in men and women: stimulus-specific role of cyclooxygenase. Physiol. Rep. *3*.

Peltonen, G.L., Harrell, J.W., Aleckson, B.P., LaPlante, K.M., Crain, M.K., and Schrage, W.G. (2016). Cerebral blood flow regulation in women across menstrual phase: differential contribution of cyclooxygenase to basal, hypoxic, and hypercapnic vascular tone. Am. J. Physiol. - Regul. Integr. Comp. Physiol. *311*, R222–R231.

Peterson, C., Phillips, L., Linden, A., and Hsu, W. (2010). Vertebral artery hypoplasia: prevalence and reliability of identifying and grading its severity on magnetic resonance imaging scans. J. Manipulative Physiol. Ther. *33*, 207–211.

Petit-Taboué, M.C., Landeau, B., Desson, J.F., Desgranges, B., and Baron, J.C. (1998). Effects of healthy aging on the regional cerebral metabolic rate of glucose assessed with statistical parametric mapping. NeuroImage *7*, 176–184.

Portegies, M.L.P., Bruijn, R.F.A.G. de, Hofman, A., Koudstaal, P.J., and Ikram, M.A. (2014). Cerebral Vasomotor Reactivity and Risk of Mortality: The Rotterdam Study. Stroke *45*, 42–47.

Prilipko, O., Huynh, N., Thomason, M.E., Kushida, C.A., and Guilleminault, C. (2014). An fMRI study of cerebrovascular reactivity and perfusion in obstructive sleep apnea patients before and after CPAP treatment. Sleep Med. *15*, 892–898.

Querido, J.S., Ainslie, P.N., Foster, G.E., Henderson, W.R., Halliwill, J.R., Ayas, N.T., and Sheel, A.W. (2013). Dynamic cerebral autoregulation during and following acute hypoxia: role of carbon dioxide. J. Appl. Physiol. Bethesda Md 1985 *114*, 1183–1190.

Raichle, M.E., Martin, W.R., Herscovitch, P., Mintun, M.A., and Markham, J. (1983). Brain blood flow measured with intravenous H2(15)O. II. Implementation and validation. J. Nucl. Med. Off. Publ. Soc. Nucl. Med. *24*, 790–798.

Rangel-Castillo, L., and Robertson, C.S. (2006). Management of intracranial hypertension. Crit. Care Clin. *22*, 713–732; abstract ix.

Reckelhoff, J.F., and Fortepiani, L.A. (2004). Novel mechanisms responsible for postmenopausal hypertension. Hypertens. Dallas Tex 1979 *43*, 918–923.

Reichmuth, K.J., Dopp, J.M., Barczi, S.R., Skatrud, J.B., Wojdyla, P., Hayes, D., and Morgan, B.J. (2009). Impaired Vascular Regulation in Patients with Obstructive Sleep Apnea. Am. J. Respir. Crit. Care Med. *180*, 1143–1150.

Ribatti, D. (2009). William Harvey and the discovery of the circulation of the blood. J. Angiogenesis Res. *1*, 3.

Richiardi, J., Monsch, A.U., Haas, T., Barkhof, F., Van de Ville, D., Radü, E.W., Kressig, R.W., and Haller, S. (2015). Altered cerebrovascular reactivity velocity in mild cognitive impairment and Alzheimer's disease. Neurobiol. Aging *36*, 33–41.

Riggs, H.E., and Rupp, C. (1963). Variation in Form of Circle of Willis: The Relation of the Variations to Collateral Circulation: Anatomic Analysis. Arch. Neurol. *8*, 8–14.

Rivera-Rivera, L.A., Turski, P., Johnson, K.M., Hoffman, C., Berman, S.E., Kilgas, P., Rowley, H.A., Carlsson, C.M., Johnson, S.C., and Wieben, O. (2016). 4D flow MRI for intracranial hemodynamics assessment in Alzheimer's disease. J. Cereb. Blood Flow Metab. Off. J. Int. Soc. Cereb. Blood Flow Metab. *36*, 1718–1730.

Rivera-Rivera, L.A., Schubert, T., Turski, P., Johnson, K.M., Berman, S.E., Rowley, H.A., Carlsson, C.M., Johnson, S.C., and Wieben, O. (2017). Changes in intracranial venous blood flow and pulsatility in Alzheimer's disease: A 4D flow MRI study. J. Cereb. Blood Flow Metab. *37*, 2149–2158.

Rosengarten, B., Aldinger, C., Kaufmann, A., and Kaps, M. (2001). Comparison of visually evoked peak systolic and end diastolic blood flow velocity using a control system approach. Ultrasound Med. Biol. *27*, 1499–1503.

Rosengarten, B., Aldinger, C., Spiller, A., and Kaps, M. (2003). Neurovascular coupling remains unaffected during normal aging. J. Neuroimaging Off. J. Am. Soc. Neuroimaging *13*, 43–47.

Roth, W., Morgello, S., Goldman, J., Mohr, J.P., Elkind, M.S.V., Marshall, R.S., and Gutierrez, J. (2017). Histopathological Differences Between the Anterior and Posterior Brain Arteries as a Function of Aging. Stroke *48*, 638–644.

Roy, C.S., and Sherrington, C.S. (1890). On the Regulation of the Blood-supply of the Brain. J. Physiol. *11*, 85-158.17.

Sabayan, B., van der Grond, J., Westendorp, R.G., Jukema, J.W., Ford, I., Buckley, B.M., Sattar, N., van Osch, M.J.P., van Buchem, M.A., and de Craen, A.J.M. (2013). Total cerebral blood flow and mortality in old age: a 12-year follow-up study. Neurology *81*, 1922–1929.

Saito, Ogasawara, Suzuki, Kuroda, Kobayashi, Yoshida, Kubo Y, and Ogawa (2011). Adverse effects of intravenous acetazolamide administration for evaluation of cerebrovascular reactivity using brain perfusion single-photon emission computed tomography in patients with major cerebral artery steno-occlusive diseases (Neurol Med Chir (Tokyo)).

Sam, Poublanc, Sobczyk, Han, Battisti-Charbonney, Dm, M., M, T., Ap, C., Ja, F., and Dj, M. (2015). Assessing the effect of unilateral cerebral revascularisation on the vascular reactivity of the non-intervened hemisphere: a retrospective observational study (BMJ Open).

Santisteban, M.M., and Iadecola, C. (2018). Hypertension, dietary salt and cognitive impairment. J. Cereb. Blood Flow Metab. *38*, 2112–2128.

Sato, K., Yoneya, M., Otsuki, A., Sadamoto, T., and Ogoh, S. (2015). Anatomical vertebral artery hypoplasia and insufficiency impairs dynamic blood flow regulation. Clin. Physiol. Funct. Imaging *35*, 485–489.

Scahill, R.I., Frost, C., Jenkins, R., Whitwell, J.L., Rossor, M.N., and Fox, N.C. (2003). A Longitudinal Study of Brain Volume Changes in Normal Aging Using Serial Registered Magnetic Resonance Imaging. Arch. Neurol. *60*, 989–994.

Scheel, P., Ruge, C., Uwe, P., and Schöning, M. (2000). Color Duplex Measurement of Cerebral Blood Flow Volume in Healthy Adults. Stroke *31*, 147–150.

Scheinberg, P. (1950). Cerebral blood flow in vascular disease of the brain; with observations on the effects of stellate ganglion block. Am. J. Med. *8*, 139–147.

Schmetterer, L., Findl, O., Strenn, K., Graselli, U., Kastner, J., Eichler, H.G., and Wolzt, M. (1997). Role of NO in the O2 and CO2 responsiveness of cerebral and ocular circulation in humans. Am. J. Physiol. *273*, R2005-2012.

Schneider, J.A., Arvanitakis, Z., Leurgans, S.E., and Bennett, D.A. (2009). The neuropathology of probable Alzheimer disease and mild cognitive impairment. Ann. Neurol. *66*, 200–208.

Schöning, M., Walter, J., and Scheel, P. (1994). Estimation of cerebral blood flow through color duplex sonography of the carotid and vertebral arteries in healthy adults. Stroke *25*, 17–22.

Schrauben, E., Wåhlin, A., Ambarki, K., Spaak, E., Malm, J., Wieben, O., and Eklund, A. (2015). Fast 4D flow MRI intracranial segmentation and quantification in tortuous arteries. J. Magn. Reson. Imaging *42*, 1458–1464.

Schrauben, E.M., Johnson, K.M., Huston, J., Del Rio, A.M., Reeder, S.B., Field, A., and Wieben, O. (2014). Reproducibility of cerebrospinal venous blood flow and vessel anatomy with the use of phase contrast-vastly undersampled isotropic projection reconstruction and contrast-enhanced MRA. AJNR Am. J. Neuroradiol. *35*, 999–1006.

Secomb, T.W., and Pries, A.R. (2013). Blood viscosity in microvessels: experiment and theory. Comptes Rendus Phys. *14*, 470–478.

Seidel, E., Eicke, B.M., Tettenborn, B., and Krummenauer, F. (1999). Reference values for vertebral artery flow volume by duplex sonography in young and elderly adults. Stroke *30*, 2692–2696.

Sercombe, R., Hardebo, J.E., Kåhrström, J., and Seylaz, J. (1990). Amine-induced responses of pial and penetrating cerebral arteries: evidence for heterogeneous responses. J. Cereb. Blood Flow Metab. Off. J. Int. Soc. Cereb. Blood Flow Metab. *10*, 808–818.

Serrador, J.M., Picot, P.A., Rutt, B.K., Shoemaker, J.K., and Bondar, R.L. (2000). MRI measures of middle cerebral artery diameter in conscious humans during simulated orthostasis. Stroke *31*, 1672–1678.

Severinghaus, J.W., Chiodi, H., Eger, E.I., Brandstater, B., and Hornbein, T.F. (1966). Cerebral blood flow in man at high altitude. Role of cerebrospinal fluid pH in normalization of flow in chronic hypocapnia. Circ. Res. *19*, 274–282.

Shapiro, W., Wasserman, A.J., Baker, J.P., and Patterson, J.L. (1970). Cerebrovascular response to acute hypocapnic and eucapnic hypoxia in normal man. J. Clin. Invest. *49*, 2362–2368.

Shenkin, H.A. (1969). Cervical sympathectomy on patients with occlusive cerebrovascular disease. Arch. Surg. Chic. Ill 1960 *98*, 317–320.

Shim, Y., Yoon, B., Shim, D.S., Kim, W., An, J.-Y., and Yang, D.-W. (2015). Cognitive Correlates of Cerebral Vasoreactivity on Transcranial Doppler in Older Adults. J. Stroke Cerebrovasc. Dis. *24*, 1262–1269.

Sidney, S., Go, A.S., Jaffe, M.G., Solomon, M.D., Ambrosy, A.P., and Rana, J.S. (2019). Association Between Aging of the US Population and Heart Disease Mortality From 2011 to 2017. JAMA Cardiol. *4*, 1280–1286.

Silver, I.A., and Erecińska, M. (1990). Intracellular and extracellular changes of [Ca2+] in hypoxia and ischemia in rat brain in vivo. J. Gen. Physiol. *95*, 837–866.

Silvestrini, M., Pasqualetti, P., Baruffaldi, R., Bartolini, M., Handouk, Y., Matteis, M., Moffa, F., Provinciali, L., and Vernieri, F. (2006). Cerebrovascular Reactivity and Cognitive Decline in Patients With Alzheimer Disease. Stroke *37*, 1010–1015.

Smith, E.E., and Greenberg, S.M. (2009). Beta-amyloid, blood vessels, and brain function. Stroke *40*, 2601–2606.

Smith, B.A., Clayton, E.W., and Robertson, D. (2011). Experimental Arrest of Cerebral Blood Flow in Human Subjects. Perspect. Biol. Med. *54*.

Smith, E.C., Pizzey, F.K., Askew, C.D., Mielke, G.I., Ainslie, P.N., Coombes, J.S., and Bailey, T.G. (2021). Effects of cardiorespiratory fitness and exercise training on cerebrovascular blood flow and reactivity: a systematic review with meta-analyses. Am. J. Physiol. Heart Circ. Physiol.

St George-Hyslop, P.H., Tanzi, R.E., Polinsky, R.J., Haines, J.L., Nee, L., Watkins, P.C., Myers, R.H., Feldman, R.G., Pollen, D., and Drachman, D. (1987). The genetic defect causing familial Alzheimer's disease maps on chromosome 21. Science *235*, 885–890.

Stark, R.D. (1968). Conductance or Resistance? Nature *217*, 779–779.

Stone, J., Johnstone, D.M., Mitrofanis, J., and O'Rourke, M. (2015). The mechanical cause of age-related dementia (Alzheimer's disease): the brain is destroyed by the pulse. J. Alzheimers Dis. JAD *44*, 355–373.

Sträter, A., Huber, A., Rudolph, J., Berndt, M., Rasper, M., Rummeny, E.J., and Nadjiri, J. (2018). 4D-Flow MRI: Technique and Applications. ROFO. Fortschr. Geb. Rontgenstr. Nuklearmed. *190*, 1025–1035.

Suzuki, J., Iwabuchi, T., and Hori, S. (1975). Cervical sympathectomy for cerebral vasospasm after aneurysm rupture. Neurol. Med. Chir. (Tokyo) *15 pt 1*, 41–50.

Szárazová, A.S., Bartels, E., and Turčáni, P. (2012). Vertebral artery hypoplasia and the posterior circulation stroke. Perspect. Med. *1*, 198–202.

Tan, C.O. (2012). Defining the characteristic relationship between arterial pressure and cerebral flow. J. Appl. Physiol. Bethesda Md 1985 *113*, 1194–1200.

Tarumi, T., Ayaz Khan, M., Liu, J., Tseng, B.Y., Tseng, B.M., Parker, R., Riley, J., Tinajero, C., and Zhang, R. (2014). Cerebral hemodynamics in normal aging: central artery stiffness, wave reflection, and pressure pulsatility. J. Cereb. Blood Flow Metab. Off. J. Int. Soc. Cereb. Blood Flow Metab. *34*, 971–978.

Tchistiakova, E., Anderson, N.D., Greenwood, C.E., and MacIntosh, B.J. (2014). Combined effects of type 2 diabetes and hypertension associated with cortical thinning and impaired cerebrovascular reactivity relative to hypertension alone in older adults. NeuroImage Clin. *5*, 36–41.

Tegeler, C.H., Crutchfield, K., Katsnelson, M., Kim, J., Tang, R., Passmore Griffin, L., Rundek, T., and Evans, G. (2013). Transcranial Doppler velocities in a large, healthy population. J. Neuroimaging Off. J. Am. Soc. Neuroimaging *23*, 466–472.

Thierfelder, K.M., Baumann, A.B., Sommer, W.H., Armbruster, M., Opherk, C., Janssen, H., Reiser, M.F., Straube, A., and von Baumgarten, L. (2014). Vertebral artery hypoplasia: frequency and effect on cerebellar blood flow characteristics. Stroke *45*, 1363–1368.

Thomas, G.D., and Segal, S.S. (2004). Neural control of muscle blood flow during exercise. J. Appl. Physiol. *97*, 731–738.

Thomas, B.P., Yezhuvath, U.S., Tseng, B.Y., Liu, P., Levine, B.D., Zhang, R., and Lu, H. (2013). Life-long aerobic exercise preserved baseline cerebral blood flow but reduced vascular reactivity to CO2. J. Magn. Reson. Imaging JMRI *38*, 1177–1183.

Thomas, B.P., Liu, P., Park, D.C., van Osch, M.J.P., and Lu, H. (2014). Cerebrovascular reactivity in the brain white matter: magnitude, temporal characteristics, and age effects. J. Cereb. Blood Flow Metab. Off. J. Int. Soc. Cereb. Blood Flow Metab. *34*, 242–247.

Thomas, K.N., Lewis, N.C.S., Hill, B.G., and Ainslie, P.N. (2015a). Technical recommendations for the use of carotid duplex ultrasound for the assessment of extracranial blood flow. Am. J. Physiol.-Regul. Integr. Comp. Physiol. *309*, R707–R720.

Thomas, T., Miners, S., and Love, S. (2015b). Post-mortem assessment of hypoperfusion of cerebral cortex in Alzheimer's disease and vascular dementia. Brain J. Neurol. *138*, 1059–1069.

Tominaga, S., Strandgaard, S., Uemura, K., Ito, K., and Kutsuzawa, T. (1976). Cerebrovascular CO2 reactivity in normotensive and hypertensive man. Stroke J. Cereb. Circ. *7*, 507–510.

Traystman, R.J. (2004). The paper that completely altered our thinking about cerebral blood flow measurement. J. Appl. Physiol. Bethesda Md 1985 *97*, 1601–1602.

Treggiari, M.M., Romand, J.-A., Martin, J.-B., Reverdin, A., Rüfenacht, D.A., and de Tribolet, N. (2003). Cervical sympathetic block to reverse delayed ischemic neurological deficits after aneurysmal subarachnoid hemorrhage. Stroke *34*, 961–967.

Tschanz, J.T., Corcoran, C.D., Schwartz, S., Treiber, K., Green, R.C., Norton, M.C., Mielke, M.M., Piercy, K., Steinberg, M., Rabins, P.V., et al. (2011). Progression of Cognitive, Functional and Neuropsychiatric Symptom Domains in a Population Cohort with Alzheimer's Dementia The Cache County Dementia Progression Study. Am. J. Geriatr. Psychiatry Off. J. Am. Assoc. Geriatr. Psychiatry *19*, 532–542.

Umeyama, T., Kugimiya, T., Ogawa, T., Kandori, Y., Ishizuka, A., and Hanaoka, K. (1995). Changes in cerebral blood flow estimated after stellate ganglion block by single photon emission computed tomography. J. Auton. Nerv. Syst. *50*, 339–346.

Urbanova, B.S., Schwabova, J.P., Magerova, H., Jansky, P., Markova, H., Vyhnalek, M., Laczo, J., Hort, J., and Tomek, A. (2018). Reduced Cerebrovascular Reserve Capacity as a Biomarker of Microangiopathy in Alzheimer's Disease and Mild Cognitive Impairment. J. Alzheimers Dis. JAD *63*, 465–477.

Usselman, C.W., Gimon, T.I., Nielson, C.A., Luchyshyn, T.A., Coverdale, N.S., Van Uum, S.H.M., and Shoemaker, J.K. (2015). Menstrual cycle and sex effects on sympathetic responses to acute chemoreflex stress. Am. J. Physiol. Heart Circ. Physiol. *308*, H664-671.

Vaitkevicius, P.V., Fleg, J.L., Engel, J.H., O'Connor, F.C., Wright, J.G., Lakatta, L.E., Yin, F.C., and Lakatta, E.G. (1993). Effects of age and aerobic capacity on arterial stiffness in healthy adults. Circulation *88*, 1456–1462.

Verbree, J., Bronzwaer, A.-S.G.T., Ghariq, E., Versluis, M.J., Daemen, M.J.A.P., van Buchem, M.A., Dahan, A., van Lieshout, J.J., and van Osch, M.J.P. (2014). Assessment of middle cerebral artery diameter during hypocapnia and hypercapnia in humans using ultra-high-field MRI. J. Appl. Physiol. *117*, 1084–1089.

Viticchi, G., Falsetti, L., Buratti, L., Luzzi, S., Bartolini, M., Acciarri, M.C., Provinciali, L., and Silvestrini, M. (2015). Metabolic syndrome and cerebrovascular impairment in Alzheimer's disease. Int. J. Geriatr. Psychiatry *30*, 1164–1170.

Vorstrup, S., Brun, B., and Lassen, N.A. (1986). Evaluation of the cerebral vasodilatory capacity by the acetazolamide test before EC-IC bypass surgery in patients with occlusion of the internal carotid artery. Stroke *17*, 1291–1298.

Wahl, M., Deetjen, P., Thurau, K., Ingvar, D.H., and Lassen, N.A. (1970). Micropuncture evaluation of the importance of perivascular pH for the arteriolar diameter on the brain surface. Pflugers Arch. *316*, 152–163.

Wang, Q., Paulson, O.B., and Lassen, N.A. (1992). Effect of nitric oxide blockade by NG-nitro-L-arginine on cerebral blood flow response to changes in carbon dioxide tension. J. Cereb. Blood Flow Metab. Off. J. Int. Soc. Cereb. Blood Flow Metab. *12*, 947–953.

Warnert, E.A.H., Rodrigues, J.C.L., Burchell, A.E., Neumann, S., Ratcliffe, L.E.K., Manghat, N.E., Harris, A.D., Adams, Z., Nightingale, A.K., Wise, R.G., et al. (2016). Is High Blood Pressure Self-Protection for the Brain? Circ. Res. *119*, e140–e151.

Watson, N.L., Sutton-Tyrrell, K., Rosano, C., Boudreau, R.M., Hardy, S.E., Simonsick, E.M., Najjar, S.S., Launer, L.J., Yaffe, K., Atkinson, H.H., et al. (2011). Arterial Stiffness and Cognitive Decline in Well-Functioning Older Adults. J. Gerontol. Ser. A *66A*, 1336–1342.

Wen, B., Tian, S., Cheng, J., Li, Y., Zhang, H., Xue, K., Zhang, Z., Fan, Y., and Wu, B. (2019). Test–retest multisite reproducibility of neurovascular 4D flow MRI. J. Magn. Reson. Imaging *49*, 1543–1552.

White, R.P., Deane, C., Vallance, P., and Markus, H.S. (1998). Nitric oxide synthase inhibition in humans reduces cerebral blood flow but not the hyperemic response to hypercapnia. Stroke *29*, 467–472.

Wijman, C.A., Babikian, V.L., Matjucha, I.C., Koleini, B., Hyde, C., Winter, M.R., and Pochay, V.E. (1998). Cerebral microembolism in patients with retinal ischemia. Stroke *29*, 1139–1143.

Williams, L.R., and Leggett, R.W. (1989). Reference values for resting blood flow to organs of man. Clin. Phys. Physiol. Meas. *10*, 187.

Willie, C.K., Macleod, D.B., Shaw, A.D., Smith, K.J., Tzeng, Y.C., Eves, N.D., Ikeda, K., Graham, J., Lewis, N.C., Day, T.A., et al. (2012). Regional brain blood flow in man during acute changes in arterial blood gases. J. Physiol. *590*, 3261–3275.

Willie, C.K., Tzeng, Y.-C., Fisher, J.A., and Ainslie, P.N. (2014). Integrative regulation of human brain blood flow. J. Physiol. *592*, 841–859.

Wintermark, M., Sesay, M., Barbier, E., Borbély, K., Dillon, W.P., Eastwood, J.D., Glenn, T.C., Grandin, C.B., Pedraza, S., Soustiel, J.-F., et al. (2005). Comparative Overview of Brain Perfusion Imaging Techniques. Stroke *36*, e83–e99.

Wolff, H.G., Lennox, W.G., and Allen, M.B. (1930). CEREBRAL CIRCULATION: XII. THE EFFECT ON PIAL VESSELS OF VARIATIONS IN THE OXYGEN AND CARBON DIOXIDE CONTENT OF THE BLOOD. Arch. Neurol. Psychiatry *23*, 1097–1120.

Wolters, Zonneveld, Hofman, van der Lugt, Koudstaal, Vernooij, and Ikram (2017). Cerebral Perfusion and the Risk of Dementia. Circulation *136*, 719–728.

Wu, C., Honarmand, A.R., Schnell, S., Kuhn, R., Schoeneman, S.E., Ansari, S.A., Carr, J., Markl, M., and Shaibani, A. (2016). Age-Related Changes of Normal Cerebral and Cardiac Blood Flow in Children and Adults Aged 7 Months to 61 Years. J. Am. Heart Assoc. *5*.

Wu, Y.-T., Beiser, A.S., Breteler, M.M.B., Fratiglioni, L., Helmer, C., Hendrie, H.C., Honda, H., Ikram, M.A., Langa, K.M., Lobo, A., et al. (2017). The changing prevalence and incidence of dementia over time - current evidence. Nat. Rev. Neurol. *13*, 327–339.

Xie, A., Skatrud, J.B., Morgan, B., Chenuel, B., Khayat, R., Reichmuth, K., Lin, J., and Dempsey, J.A. (2006). Influence of cerebrovascular function on the hypercapnic ventilatory response in healthy humans. J. Physiol. *577*, 319–329.

Xu, X., Wang, B., Ren, C., Hu, J., Greenberg, D.A., Chen, T., Xie, L., and Jin, K. (2017). Age-related Impairment of Vascular Structure and Functions. Aging Dis. *8*, 590–610.

Zampakis, P., Panagiotopoulos, V., Petsas, T., and Kalogeropoulou, C. (2015). Common and uncommon intracranial arterial anatomic variations in multi-detector computed tomography angiography (MDCTA). What radiologists should be aware of. Insights Imaging *6*, 33–42.

Zarrinkoob, L., Ambarki, K., Wåhlin, A., Birgander, R., Eklund, A., and Malm, J. (2015). Blood flow distribution in cerebral arteries. J. Cereb. Blood Flow Metab. *35*, 648–654.

Zhang, D.P., Ma, Q.K., Zhang, J.W., Zhang, S.L., Lu, G.F., and Yin, S. (2016). Vertebral artery hypoplasia, posterior circulation infarction and relative hypoperfusion detected by perfusion magnetic resonance imaging semiquantitatively. J. Neurol. Sci. *368*, 41–46.

Zhang, D.P., Lu, G.F., Zhang, J.W., Zhang, S.L., Ma, Q.K., and Yin, S. (2017). Vertebral Artery Hypoplasia and Posterior Circulation Infarction in Patients with Isolated Vertigo with Stroke Risk Factors. J. Stroke Cerebrovasc. Dis. Off. J. Natl. Stroke Assoc. *26*, 295–300.

Zhang, K., Herzog, H., Mauler, J., Filss, C., Okell, T.W., Kops, E.R., Tellmann, L., Fischer, T., Brocke, B., Sturm, W., et al. (2014). Comparison of cerebral blood flow acquired by simultaneous [15O]water positron emission tomography and arterial spin labeling magnetic resonance imaging. J. Cereb. Blood Flow Metab. Off. J. Int. Soc. Cereb. Blood Flow Metab. *34*, 1373–1380.

Zhao, M., Amin-Hanjani, S., Ruland, S., Curcio, A.P., Ostergren, L., and Charbel, F.T. (2007). Regional cerebral blood flow using quantitative MR angiography. AJNR Am. J. Neuroradiol. *28*, 1470–1473.

Zhou, R., Liu, D., Yu, K., Chen, Y., Li, L., Xu, J., and Zhou, H. (2015). Carotid and vertebral arterial variations in Alzheimer's disease. Curr. Alzheimer Res. *12*, 368–376.

Zhu, Y.-S., Tarumi, T., Tseng, B.Y., Palmer, D.M., Levine, B.D., and Zhang, R. (2013). Cerebral vasomotor reactivity during hypo- and hypercapnia in sedentary elderly and Masters athletes. J. Cereb. Blood Flow Metab. *33*, 1190–1196.

van Zijl, P.C., Eleff, S.M., Ulatowski, J.A., Oja, J.M., Uluğ, A.M., Traystman, R.J., and Kauppinen, R.A. (1998). Quantitative assessment of blood flow, blood volume and blood oxygenation effects in functional magnetic resonance imaging. Nat. Med. *4*, 159–167.

Zimmerman, B., Sutton, B.P., Low, K.A., Fletcher, M.A., Tan, C.H., Schneider-Garces, N., Li, Y., Ouyang, C., Maclin, E.L., Gratton, G., et al. (2014). Cardiorespiratory fitness mediates the effects of aging on cerebral blood flow. Front. Aging Neurosci. *6*, 59.

Zou, Q., Wu, C.W., Stein, E.A., Zang, Y., and Yang, Y. (2009). Static and dynamic characteristics of cerebral blood flow during the resting state. NeuroImage *48*, 515–524.

Appendix 1: Output from G*Power Sample Size Estimate

Post-hoc analysis of effect size from Barnes, J. N., Schmidt, J. E., Nicholson, W. T., & Joyner, M. J. (2012). Cyclooxygenase inhibition abolishes age-related differences in cerebral vasodilator responses to hypercapnia. *Journal of Applied Physiology*, *112*(11), 1884–1890. https://doi.org/10.1152/japplphysiol.01270.2011

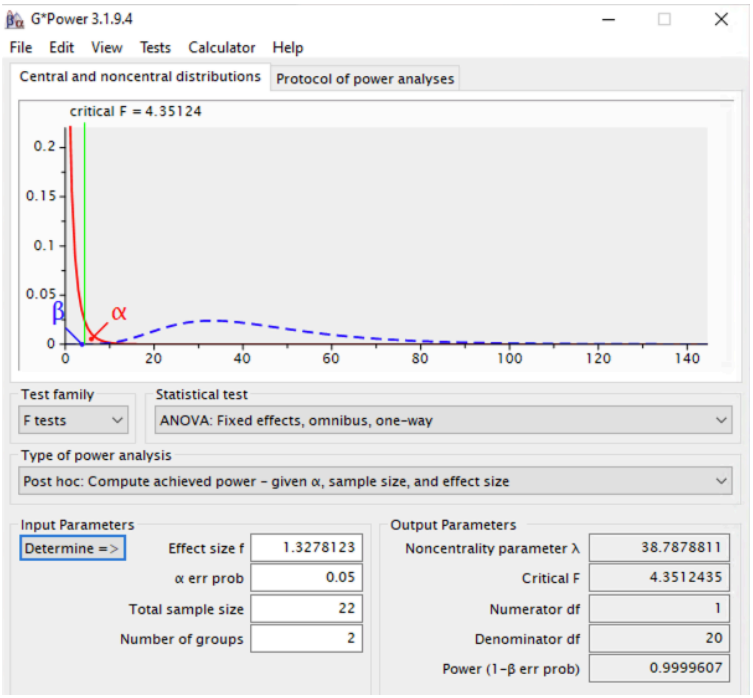

A priori analysis of sample size required for **Study 1** of the dissertation.

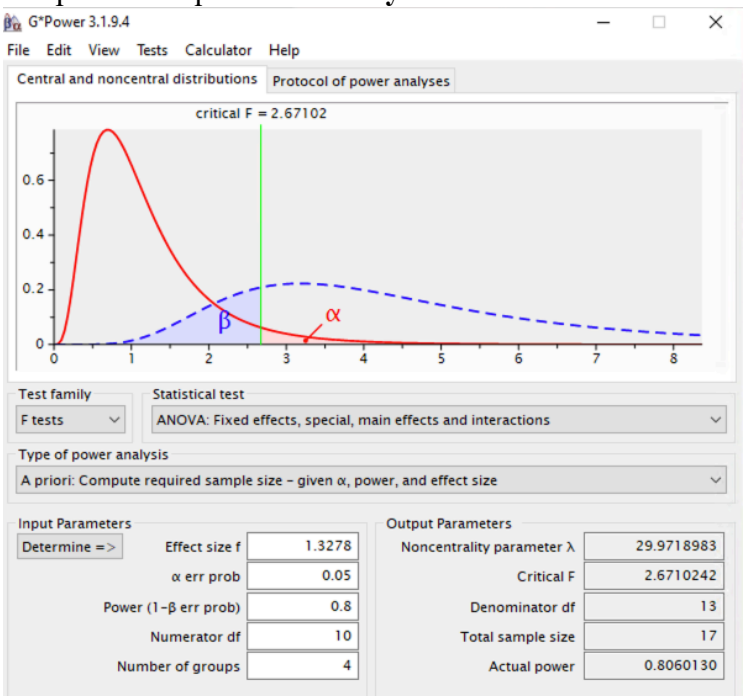

Post-hoc analysis of effect size from Olesen, N. D., Nielsen, H. B., Olsen, N. V., & Secher, N. H. (2019). The age-related reduction in cerebral blood flow affects vertebral artery more than internal carotid artery blood flow. *Clinical Physiology and Functional Imaging*, *39*(4), 255–260. https://doi.org/10.1111/cpf.12568

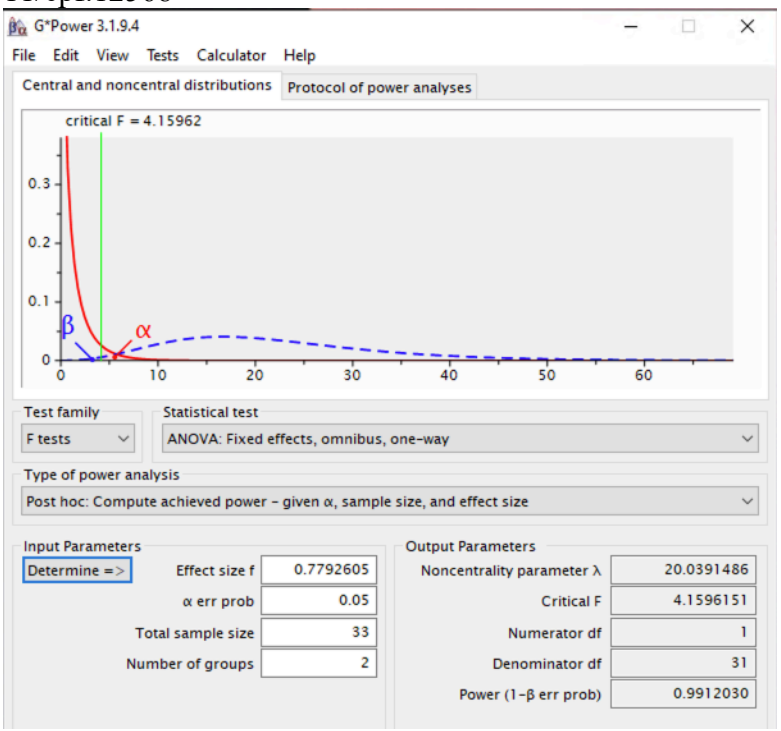

A priori analysis of sample size required for **Study 2** of the dissertation.

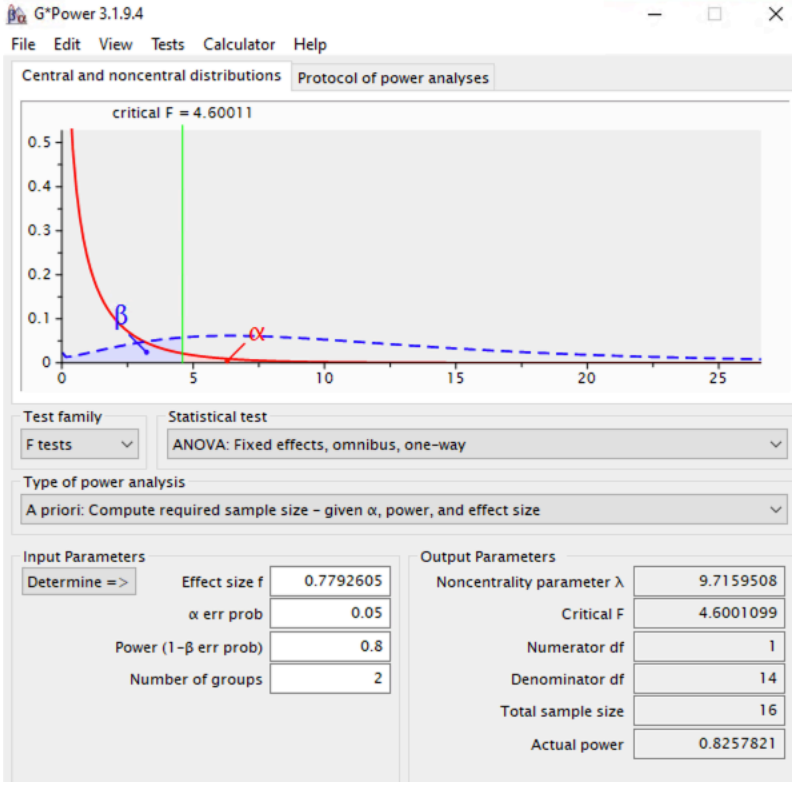

Post-hoc analysis of effect size from Warnert, E. A. H., Rodrigues, J. C. L., Burchell, A. E., Neumann, S., Ratcliffe, L. E. K., Manghat, N. E., Harris, A. D., Adams, Z., Nightingale, A. K., Wise, R. G., Paton, J. F. R., & Hart, E. C. (2016). Is High Blood Pressure Self-Protection for the Brain? *Circulation Research*, *119*(12), e140–e151.

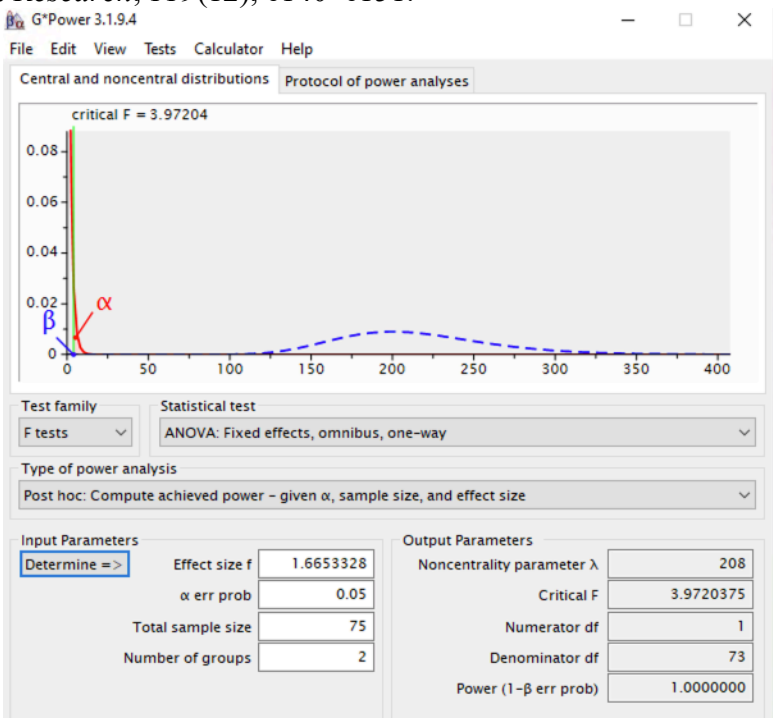

A priori analysis of sample size required for **Study 3** of the dissertation.

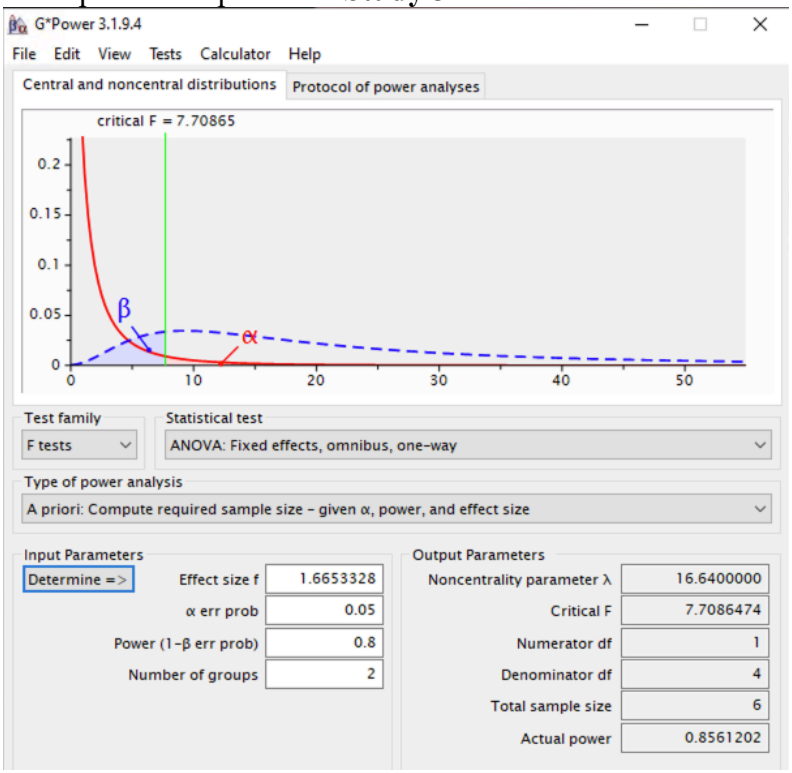

Appendix 2: Retrospective Determination of Vertebral Artery Hypoplasia